Geochemistry and Petrology of the Alkalic Igneous Complex at Magnet Cove, Arkansas

---

GEOLOGICAL SURVEY PROFESSIONAL PAPER 425

Prepared in cooperation
with the Defense Minerals
Procurement Agency

U.S. DEPARTMENT OF THE INTERIOR
March 3, 1849

Geochemistry and Petrology of the Alkalic Igneous Complex at Magnet Cove, Arkansas

By R. L. ERICKSON *and* L. V. BLADE

GEOLOGICAL SURVEY PROFESSIONAL PAPER 425

Prepared in cooperation
with the Defense Minerals
Procurement Agency

U.S. DEPARTMENT OF THE INTERIOR
March 3, 1849

UNITED STATES GOVERNMENT PRINTING OFFICE, WASHINGTON : 1963

UNITED STATES DEPARTMENT OF THE INTERIOR

STEWART L. UDALL, *Secretary*

GEOLOGICAL SURVEY

Thomas B. Nolan, *Director*

The U.S. Geological Survey Library has cataloged this publication as follows:

Erickson, Ralph Leroy, 1923—
Geochemistry and petrology of the alkalic igneous complex at Magnet Cove, Arkansas, by R. L. Erickson and L. V. Blade. Washington, U.S. Govt. Print. Off., 1963.

v, 95 p. maps (part fold., 1 col., in pocket) diagrs., tables. 29 cm. (U.S. Geological Survey. Professional paper 425)

Prepared in cooperation with the Defense Minerals Procurement Agency.

Bibliography: p. 90–91.

(Continued on next card)

Erickson, Ralph Leroy, 1923—
Geochemistry and petrology of the alkalic igneous complex at Magnet Cove, Arkansas, 1963. (Card 2)

1. Geochemistry—Arkansas—Magnet Cove. 2. Petrology—Arkansas—Magnet Cove. 3. Rocks, Igneous. 4. Rocks—Analysis. I. Blade, Lawrence Vernon, 1917– joint author. II. U.S. Defense Minerals Procurement Agency. III. Title: The alkalic igneous complex at Magnet Cove, Arkansas. (Series)

For sale by the Superintendent of Documents, U.S. Government Printing Office
Washington 25, D.C.

CONTENTS

ILLUSTRATIONS

[Plates are in pocket]

TABLES

GEOCHEMISTRY AND PETROLOGY OF THE ALKALIC IGNEOUS COMPLEX AT MAGNET COVE, ARKANSAS

By R. L. Erickson and L. V. Blade

ABSTRACT

The Magnet Cove alkalic igneous complex together with the surrounding contact zone has been mapped on a scale of 1:6,000. The complex, about 4.6 square miles in area, is composed of a series of ring dikes post-Mississippian in age that were intruded into faulted and folded Paleozoic sedimentary rocks of the Ouachita geosyncline.

The Paleozoic sedimentary rocks in the area are predominantly shale, sandstone, and novaculite, but include minor amounts of conglomerate and limestone. The rocks range in age from Ordovician to Mississippian. The contact zone ranges in width from 1,000 to 2,500 feet and is composed of Missouri Mountain shale of Silurian age, Arkansas novaculite of Devonian and Mississippian age, and Stanley shale of Mississippian age. Deformation of the sedimentary rocks by the intrusion has been slight. The shales have been changed to spotted argillite, hornfels, and gneiss. The quartz of the novaculite has been recrystallized and near the intrusion appears as a friable sandstone. Except for a slight recrystallization of the quartz, the sandstones have not been much affected.

The ring dike igneous complex has a core of ijolite and carbonatite, an intermediate ring of trachyte and phonolite, an outer ring of nepheline syenites, and two masses of jacupirangite, one on the west edge of the complex and the other on the northeast edge. Smaller dikes of tinguaite, trachyte porphyry, nepheline syenite, miscellaneous trachytes, pegmatite, aplite, gabbro, fourchite, and carbonatite, and a variety of veins are widespread. Mineralogically, the igneous rocks of the complex can be divided into two groups, those rocks containing feldspar and those virtually free of feldspar. The igneous rocks containing feldspar include: phonolite, various trachytes, tinguaite, various syenites (some pegmatitic), alkalic gabbro, and aplites. The igneous rocks that are generally free of feldspar include: jacupirangite, sphene pyroxenite, ijolite, melteigite, fourchite, and carbonatite.

The carbonatite occurs in irregularly shaped bodies in the central part of the complex. Aggregates of apatite, magnetite, pyrite, monticellite, perovskite, and kimzeyite (zirconium garnet) are scattered through a groundmass of coarse calcite. Part of the carbonatite has weathered to porous rock composed of residual apatite, magnetite, and perovskite in a matrix of secondary apatite. In contact with the ijolite, the carbonatite fluids were reactive and altered the minerals of the ijolite.

Dikes outside the complex are grouped in the following categories: pegmatite, aplite, syenite, trachyte porphyry, trachyte, tinguaite, andesite, diorite, monzonite, and lamprophyre.

Veins of various types are found both within and outside the complex: quartz-brookite-rutile veins, most common in the recrystallized novaculite on the east edge of the complex; feldspar-carbonate veins, most common in the northern two-thirds of the complex; and feldspar, quartz-feldspar, and fluorite veins. Late quartz veins are associated with the carbonatite. Molybdenite and apatite veins are found in the carbonatite and ijolite. Earthy monazite, apparently a weathering product of an apatite-pyrite vein, was found in the central part of the complex. Paramorphs of rutile after brookite are found as float throughout the complex but are most abundant in the northern two-thirds of the complex.

Rocks were analyzed chemically and spectrographically; some of the minerals separated from the analyzed rocks were chemically analyzed, and all were spectrographically analyzed. Chemically the igneous rocks are high volatile, high lime, alkalic, and subsilicic; they include intrusive carbonatite masses as well as the iron, titanium, zirconium, and phosphate minerals that characterize similar alkalic rocks throughout the world. High niobium substitution in titanium minerals and rare-earth substitution in apatite and perovskite are also typical. Compared to average igneous rocks, the Magnet Cove rocks are low in SiO_2, MgO, Cr, Ni, Co, Cu, U, and Th and high in Al_2O_3, Fe_2O_3, FeO, MnO, CaO, BaO, Na_2O, K_2O, H_2O^+, TiO_2, CO_2, P_2O_5, Cl, F, S, Be, Sr, Sc, Y, La, Zr, V, Nb, Ga, and probably SO_3. The oxide contents of the rocks were plotted against CaO in variation diagrams.

Significant quantities of niobium in the igneous rocks and in the associated titanium deposits are concentrated in rutile, brookite, perovskite, sphene, garnet, aegirine, and hornblende. The niobium content ranges from 0.11 to 6.6 percent in rutile, 0.5 to 3.2 percent in brookite, 0.37 to 4.6 percent in paramorphs of rutile after brookite, 0.2 to 9.0 percent in perovskite, 0.1 to 0.7 percent in sphene, 0 to 0.1 percent in garnet, 0 to 0.03 percent in aegirine, and 0.007 to 0.01 percent in hornblende.

The rocks of the complex were intruded during separate but closely related periods; however, the true age sequence is not clear because rock outcrops are relatively scarce and deeply weathered. The available field evidence and the writers' prejudices after 3 years of working in the area suggest the following sequence from oldest to youngest: 1. phonolite and trachyte; 2. jacupirangite; 3. alkalic syenites; 4. ijolite; 5. carbonatite, dike rocks, and veins.

The writers belive that the Magnet Cove complex of alkalic igneous rocks was derived by differentiation and fractional crystallization of a residual magma of a mafic phonolite composition rich in alkali, lime, and volatile constituents. The high concentration of volatiles is belived to be of great importance in the development of the many varieties of unusual rock types. This residual magma is believed to have been derived by fractional crystallization from a regional undersaturated olivine basalt magma.

INTRODUCTION

Recent studies on alkalic rock complexes, like that at Magnet Cove, have revealed substantial resources in such commodities as the rare earths, barite, niobium (columbium), uranium, phosphate, and agricultural lime.

In the past, the Magnet Cove Titanium Corp. deposit has been worked for rutile; the Kimzey calcite quarry for agricultural lime; and the Kimzey magnetite pit for magnetite.

Niobium, or columbium as it is called in commerce, is known to occur in the rutile and brookite of the veins and in the perovskite of the carbonatite. Its distribution in the other rocks and minerals of the Magnet Cove igneous complex, however, has not been known.

LOCATION AND SURFACE FEATURES

The Magnet Cove alkalic igneous complex and its surrounding contact zone occupy about 8 square miles in the northeastern part of Hot Spring County, Ark. This heart-shaped complex is easily accessible by U.S. Highway 270, which crosses the middle of the area in a generally east-west direction. Hot Springs is about 12 miles west and Malvern is about 7 miles southeast of the area; both are on U.S. Highway 270 (fig. 1).

The Magnet Cove complex lies at the east end of the Mazarn basin of the Ouachita Mountain physiographic province. The complex is bounded on the south by the Trap Mountains and on the north and east by the Zigzag Mountains (fig. 4). Altitudes range from slightly less than 340 feet in the central basin to slightly more than 600 feet on the surrounding ridges.

Most of the central basin and other low-lying areas are farmland or pasture. Parts of these areas are covered with alluvium and the remaining parts are saprolite from which most of the hard rock float has been removed.

Most of the ridges are covered with timber or thick brush; brambles and thorny trees are always present. Pine trees are abundant in areas of sedimentary rock, and deciduous trees in areas of igneous rock. Hard rock exposures are rare. In the central basin they are confined to one quarry, a few open pits, and a few outcrops, mostly in stream bottoms. They are more common on the ridges than in the basin, and are most abundant in valley floors and walls where streams cut the ridges. Rock float is abundant on ridges, although in some areas much of it has been removed by the early settlers to clear fields and to build stone fences. The climate is warm and humid.

PREVIOUS WORK

From 1806, when Macrery (1806) first mentioned minerals from the Magnet Cove area, to 1891 when Williams published his classic study of the area, many papers were published on the mineralogy of the region. Williams (1891) summarized this earlier work, made a detailed petrologic study of the igneous rocks, and published the first detailed map of the area. A few years later, Washington (1900) published a revised version of Williams' map. In a later paper, Washington (1901) presented additional chemical analyses and redefined several of the rock names. The most complete description of the sedimentary rocks of the region was published by Purdue and Miser in 1923. Landes (1931) presented a list of most of the minerals present, discussed the structure of the igneous rocks, and offered a theory of origin for the calcite. Parks and Branner (1932) published a map that showed the separate sedimentary rock units in contact with the Magnet Cove complex.

From 1892 to 1952 individual minerals from Magnet Cove were discussed in several papers. The minerals and authors include: natrolite, Melville (1892); anatase, Penfield (1894); monticellite, Penfield and Forbes (1896), Kouvo (1952); magnetite, Harrington (1907); catapleiite, Foshag (1923); astrophyllite, Gossner and Reindl (1934); sodalite, Glass (1937), Miser and Glass (1941); taenolite, Miser and Stevens (1938); carbonate-apatite, McConnell and Gruner (1940); molybdenite, Sleight (1941); hackmanite, Miser and Glass (1941); schorlomite, McConnell (1942); and perovskite, Murdoch (1951).

From 1938 to 1954 many papers were published on the individual rutile and brookite deposits. The several authors include: Miser and Stevens (1938); Ross (1938, 1941 Ross and Hendricks, 1945); Spencer (1946); Holbrook (1947, 1948); Reed (1949a and b); Kinney (1949); Fryklund (1949); Fryklund and Holbrook (1950); and Fryklund, Harner, and Kaiser (1954).

SCOPE AND METHODS OF WORK

This project was designed to make a detailed petrologic and geochemical study of the igneous rocks at Magnet Cove, Ark., in order to improve understanding of the origin and geochemical environment of niobium and associated elements. The bedrock geology was mapped at a scale of 1:6,000 (pl. 1) in order to gain further knowledge of the petrology, intrusive history, and structure of the igneous complex and to determine the relation of the complex to the surrounding sedimentary rocks.

Erickson and Blade mapped the igneous complex during the spring and fall of 1953 and 1954. Blade added details and mapped the contact zone during 1955 and 1956.

Mapping was on an enlarged topographic base taken from the Malvern quadrangle, and compiled by the U.S. Geological Survey. The alidade-planetable method was used in the cleared areas, and the pace and compass method was used in the brush-covered areas. Williams' isogonic chart (1891, pl. 13), transferred to a modern base and corrected for annual

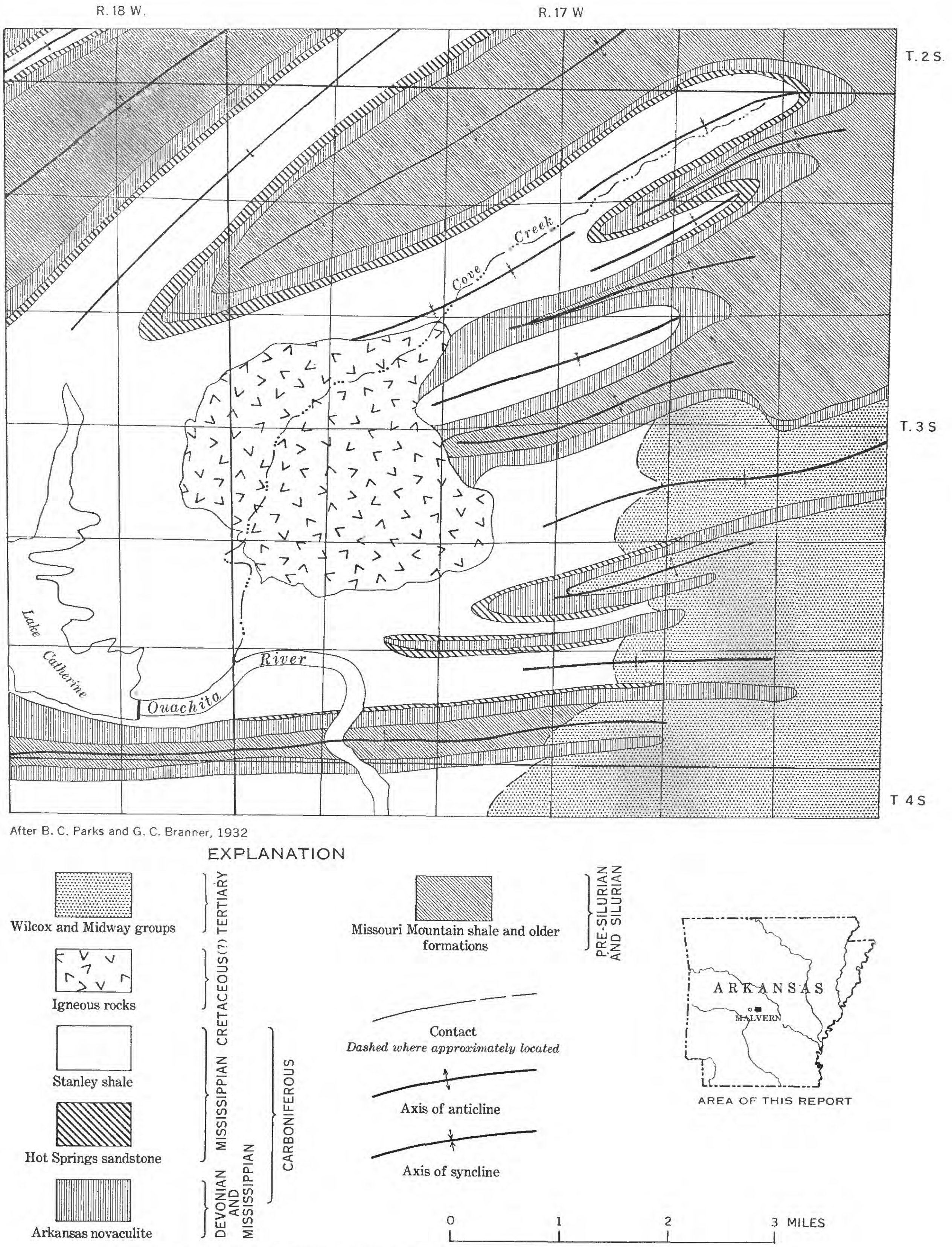

After B. C. Parks and G. C. Branner, 1932

FIGURE 1.—Index map and generalized geology of the Magnet Cove area, Hot Spring County, Ark.

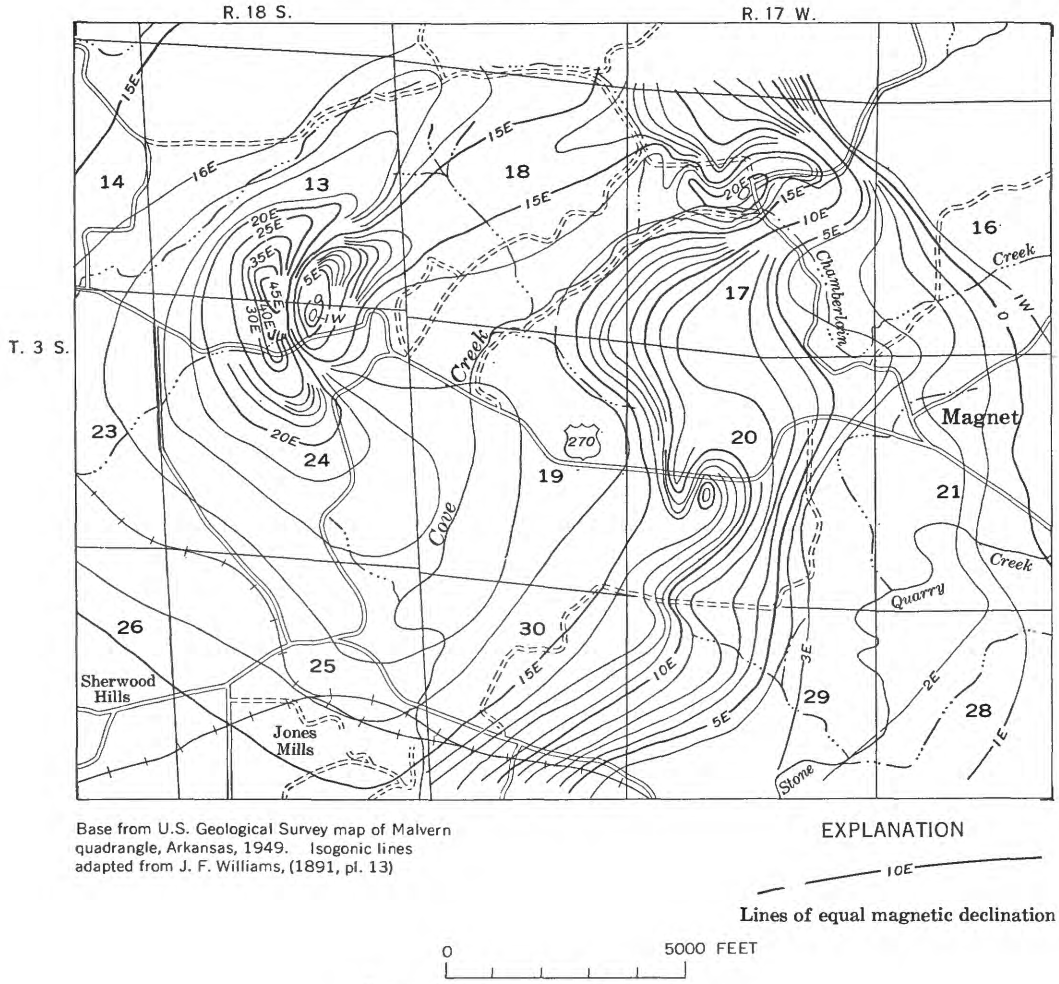

Base from U.S. Geological Survey map of Malvern quadrangle, Arkansas, 1949. Isogonic lines adapted from J. F. Williams, (1891, pl. 13)

FIGURE 2.—Isogonic chart of Magnet Cove.

change (fig. 2), proved indispensable in the pace and compass traversing. The chart was unreliable in the area of the Kimzey magnetite pit (pl. 1) probably because much of the magnetite has been mined since the chart was made.

Most of the mapping was based on the distribution of rock float, as outcrops are scarce. In areas where float was absent, saprolite was used either directly or by comparison of the heavy minerals with panned concentrates from saprolites of known origin. Samples were obtained by drilling through overburden with a power auger to the saprolite zone. In the Cove Creek valley flat just north of U.S. Highway 270 and east of the Kimzey calcite quarry (pl. 1) several auger holes were attempted but the gravel of the valley fill was too coarse to allow penetration. An unpublished magnetometer survey made for the U.S. Bureau of Mines by the Heiland Research Corp. in 1942 proved useful in two areas in outlining bodies of jacupirangite (fig. 3; pl. 1).

All the rocks were examined in thin section and analyzed spectrographically. Standard chemical analyses were made of the major rocks. Minerals were separated from the coarser grained major rocks for quantitative spectrographic analysis and a few for standard chemical analysis. Heavy liquids, the Franz Isodynamic Separator, and hand picking were the methods used in making the separation. Eighty-six rutile and brookite samples were selected for spectrographic analysis. Chemical, spectrographic, and X-ray analyses were made in both the Washington and Denver laboratories of the U.S. Geological Survey.

ACKNOWLEDGMENTS

Several U.S. Geological Survey geologists have contributed to the Magnet Cove study through field conferences, discussions, and laboratory investigations. W. R. Griffitts spent 6 weeks in the field when the project was initiated in February 1953, and made many helpful suggestions during the subsequent field work and laboratory work. Walter Danilchik mapped the sedimentary rocks adjacent to the complex (pl. 1), as a part of more extensive work in surrounding areas.

We are indebted to N. F. Williams, Director of the Arkansas Geological and Conservation Commission, and his staff for their generous cooperation in all phases of this work. The power auger and certain other equipment were provided by the State. W. A. Keith, lessee of much of the carbonatite area, allowed us to log the core from four holes drilled in the carbonatite. The cooperation of J. W. Kimzey and other residents of the Magnet Cove area is gratefully acknowledged.

This investigation, as part of the niobium program of the U.S. Geological Survey, was supported largely by funds from the Defense Minerals Procurement Agency.

GENERAL GEOLOGY

The Magnet Cove igneous complex, about 4.6 square miles in area, is but one of many silica-poor igneous complexes that intrude the folded and faulted Paleozoic sedimentary rocks of the Ouachita geosyncline (pl. 2).

The undersaturated alkaline igneous rocks studied in this investigation occur at the east end of a belt of dikes and other small intrusive bodies that extend westward to Hot Springs and intrude Ordovician to Mississippian sedimentary rocks in the east-west trending Mazarn synclinorium. This synclinorium is bounded by northeastward-trending folds of the Zigzag Mountains on the north and the east-west trending Trap Mountain anticlinorium on the south. This abrupt change in strike of the major structural elements probably influenced the localization of the igneous rocks.

The intruded sedimentary rocks are overturned and thrust to the north and northwest and include rocks ranging in age from Ordovician to Mississippian. These rocks are tabulated below from information given by Walter Danilchik (written communication, 1955):

Age	Formation	Description	Thickness (feet)
Mississippian	Stanley shale	Shale, sandstone and conglomerate.	±3, 500
	Hot Springs sandstone.	Sandstone, conglomerate, and shale.	0–200
Mississippian and Devonian.	Arkansas novaculite	Novaculite, calcareous novaculite, shale, sandstone and conglomerate.	100–800
Silurian	Missouri Mountain shale.	Shale, sandstone, quartzite and conglomerate.	50–100
	Blaylock sandstone	Sandstone and shale	0–550
Ordovician	Polk Creek shale	Shale, sandstone, and chert.	25–200
	Bigfork chert	Chert, shale, sandstone, and limestone.	700
	Womble shale	Shale, sandstone, limestone.	250–900

Tertiary deposits of the Gulf Coastal Plain occur to the east and south (fig. 1).

Stanley shale is in contact with the complex for about three-fourths of its perimeter; Arkansas novaculite, and a little Missouri Mountain shale are in contact with the eastern part of the complex. These rocks have been altered by the Magnet Cove intrusive mass for distances up to 2,500 feet from the contact.

Igneous rocks of varied composition are found as dikes and sills in the contact zone and in the Paleozoic sediments to the west. These rocks include andesite and various types of pegmatite, aplite, syenite, trachyte porphyry, trachyte, tinguaite, and lamprophyre. Quartz-brookite-rutile veins are concentrated in the recrystallized novaculite of the contact zone. Feldspar-carbonate veins are concentrated in the northern two-thirds of the complex. Quartz veins are closely associated with the carbonatite. Feldspar, apatite, and molybdenite veins are found both within and outside the complex.

AGE OF THE ROCKS

The maximum possible age for the igneous rocks of the complex is Mississippian because the youngest sedimentary rock intruded by them is the Stanley shale. The alluvium in some of the stream valleys is probably Quaternary. Inasmuch as this leaves a large gap, we must look outside the area for a reasonable age. Lead-alpha age determinations were made by Thomas W. Stern (written communication, 1958) on zircon separated from a feldspathoidal syenite pegmatite dike that occurs about 500 feet west of the igneous complex in the N½ sec. 24 (L–287, pl. 1). The zircon gave ages of 178 and 184 million years (Triassic). Unfortunately, zircon was not detected in any of the more than 300 thin sections of igneous rocks from within the complex. Thus the usefulness of this age determination in relation to the main igneous complex is questionable. Bramlette (1936) found the nepheline syenite of the bauxite area of Arkansas to be younger than the metamorphosed Paleozoic sedimentary rocks and older than the Midway group of Paleocene age. Miser (1912) found the peridotite near Murfreesboro, Ark., to be of early Late Cretaceous age. Ross, Miser, and Stephenson (1929) found phonolitic rocks similar in composition to those in the Magnet Cove complex as water-laid volcanic deposits in the lower Upper Cretaceous in southwestern Arkansas, southeastern Oklahoma, and northeastern Texas.

The evidence indicates that the igneous rocks at Magnet Cove are Mesozoic in age; igneous activity may have extended from Triassic to Cretaceous time. The igneous rocks are shown as Cretaceous(?) in age on the geologic map (pl. 1). A more positive dating of these rocks may be achieved by K/Ar or Rb/Sr age determinations on biotite.

STRUCTURE

The Magnet Cove igneous area is an elliptically shaped ring dike complex with a small central core that may be a stock or an undecapitated ring dike. The complex has been emplaced in a tightly folded, westward-plunging group of Paleozoic anticlines and synclines that appear to be subsidiary features on a major southwest plunging anticlinal nose.

In general terms the complex can be divided into three parts: the central part of the area, a topographic basin, is occupied by mineralogic and textural varieties of ijolite and carbonatite. Fine-grained rocks of phonolitic composition as well as calcareous intrusive breccias surround the ijolotic core and form the second part of the complex. The third part of the complex is the outside ring of topographic ridges composed of several types of feldspathoidal syenites.

As the contacts were mapped predominantly from float, the attitudes of the contacts are not accurately known. However, a study of the outcrop trends in relation to topography suggests that most contacts are vertical or dip steeply away from the center of the complex.

Plate 3 shows the relationship of the igneous complex to total intensity aeromagnetic contours in the Magnet Cove area. L. C. Pakiser, Jr., of the U.S. Geological Survey (oral communication, 1959) made the following observations from inspection of this figure.

> Comparison of the magnetic field over Magnet Cove with prismatic models in a similar magnetic latitude (Vacquier and others, 1951, p. 123) and of roughly comparable horizontal dimensions indicates that the magnetic body is vertical or near vertical and extends to a depth many times greater than its horizontal dimensions. The peak of the magnetic high lies near the southern edge as would be expected for a vertical body; and the absence of flanking magnetic lows corresponds to what would be expected from a body of large vertical extent.

The two magnetic highs shown in the northern part of the map reflect bodies of jacupirangite, a magnetite-rich pyroxenite.

The gross structural elements shown on plates 1 and 3 indicate that the intrusive complex is nearly vertical and that the thrust planes and overturned folds in the Paleozoic sediments dip south. These south-dipping zones of weakness may have tapped a deep-seated magma reservoir. Note also (fig 1) the abrupt change in regional trend of the major structures from northeast to east-west. It seems very probable that a major east-west fault zone may occur in the area of the change in structural trends.

Miser (1934) noted that "the Ouachita belt in which the igneous rocks reached the surface apparently contained zones of structural weakness in the deformed Paleozoic rocks where the molten and fragmental material could move upward most readily."

The Magnet Cove igneous area is interpreted to be a ring-dike complex. This conclusion is based upon the arcuate dikelike relation of the exposed rock bodies, and their similarity to such ring complexes in other parts of the world. It is interesting to note that in many localities of the world, strongly alkaline undersaturated rocks occur in continental volcanic areas as ring dikes and cone-sheet complexes. The importance of this association will be discussed in the section on origin of the igneous rocks.

The most widely accepted theory for the formation of ring dikes requires a period of cauldron subsidence into a relatively steep-sided magma reservior. Howel Williams (1941) attributes subsidence to lack of support of the roof caused by removal of material from the magma chamber along vertical or steep outward dipping fractures. While the central block subsides, magma rises from the reservoir into the circular fracture that bounds the sinking block. These fractures may extend to the surface and give rise to explosive volcanic activity or they might be exposed only through deep erosion. It is the writers' belief that the intermediate ring of fine-grained rocks and breccias of phonolitic composition represents the earliest period of igneous activity in the area. The abundance of volatile constituents, particularly CO_2, and the presence of miarolitic cavities and amygdaloidal textures in these fine-grained rocks strongly suggest a period of explosive volcanic activity at Magnet Cove. The abundance of volcanic tuffs of phonolitic composition in nearby Cretaceous rocks supports this conclusion. This phase of activity was attended and immediately followed by cauldron subsidence or sinking of the central block. Erosion to the present level has removed all traces of the volcanic superstructure. It may be postulated that the upper part of the sinking block was composed of volcanic tuff and agglomerates which had accumulated around the volcano.

IGNEOUS COMPLEX

The feldspathoidal igneous complex may be conveniently subdivided for purposes of rock description as outlined in the previous section: a core of ijolite, an intermediate ring of trachyte and phonolite, and an outer ring of nepheline syenite. Two masses of jacupirangite, one on the west edge of the complex and the other on the northeast edge are described with the outer ring. The minor rock units are described last. Most of the mapped units are arcuate bodies, but one of them, garnet-pseudoleucite syenite, forms a nearly complete ring.

Topographically, syenite and trachyte form the ridges, and ijolite, melteigite, and jacupirangite form the basins. Carbonatite appears as low hills in the ijolite.

Mineralogically, the rocks can be divided into two groups—those containing feldspar (syenite group) and those virtually free of feldspar (ijolite group and carbonatite). Those containing feldspar form the intermediate and outer rings and have been classified in accordance with Wahlstrom (1947). They include altered phonolite, undivided trachyte, sodalite trachyte, trachyte porphyry, tinguaite (dike phonolite), feldspathoidal leucosyenite, garnet-pseudoleucite syenite, garnet-nepheline syenite, sphene-nepheline syenite, sphene-garnet-nepheline syenite, sphene-cancrinite syenite, analcime-olivine melagabbro, nepheline syenite pegmatite, eudialyte-nepheline syenite pegmatite, and aplite. Rocks that are practically free of feldspar occupy the central basin area (jacupirangite excepted) and have been classified after Johannsen (1938).

They are chiefly nepheline pyroxene rocks and may be subdivided into four groups on the basis of percentage of their feldspathoids: urtite, more than 70 percent nepheline or its alteration products; ijolite, nepheline between 50 and 70 percent; melteigite, nepheline between 5 and 50 percent; jacupirangite-magnetite pyroxenite with less than 5 percent nepheline.

In the following pages, the rocks are described in order of their position on the geologic map (pl. 1): outer ring, intermediate ring, inner core, and miscellaneous dike rocks. The location and field number of described or analyzed samples are plotted on plate 1. Spectrographic sensitivities of the elements for this investigation are shown in table 1. Tin, unless otherwise noted, is not reliable in the spectrographic analyses of the mineral separates because metallic tin was used to stabilize the methylene iodide used in separating the minerals.

TABLE 1.—*Spectrographic sensitivities of the elements*

Spectral limits when the standard exposure is made for the ultraviolet region

Element	Weight percent	Element	Weight percent
Ag	0.0001	Na	0.1
Al	.001	Nb	.005
As	.05	Nd	.01
Au	.003	Ni	.0005
B	.001	P	.1
Ba	.001	Pb	.001
Be	.0001	Pd	.0003
Bi	.001	Pr	.07
Ca	.0001	Pt	.001
Cd	.005	Rb	10.0
Ce	.02	Re	.005
Co	.0005	Rh	.0003
Cr	.0001	Ru	.008
Cs	1.0	Sb	.01
Cu	.0001	Sc	.0001
Dy	.003	Si	.001
Er	.001	Sm	.003
Eu	.003	Sn	.002
Fe	.001	Sr	.001
Ga	.001	Ta	.04
Gd	.003	Tb	.004
Ge	.001	Te	.1
Hf	.03	Th	.05
Hg	.1	Ti	.0005
Ho	.003	Tl	.005
In	.001	Tm	.001
Ir	.01	U	.05
K	.5	V	.001
La	.003	W	.05
Li	.05	Y	.001
Lu	.003	Yb	.0001
Mg	.0001	Zn	.02
Mo	.0005	Zr	.001
Mn	.001		

Spectral limits when a special exposure is made for the visible region

Cs	0.005	Li	0.0001
F	.1	Na	.0001
K	.0005	Rb	.001

OUTER RING

The outer ring of igneous rocks occurs as topographic ridges and is composed chiefly of mineralogic and textural varieties of feldspathoidal syenites. Two masses of jacupirangite and one mass of melteigite occur in the outer ring, and although they have no mineralogic or chemical similarity to the syenites, they will be included in the description of outer ring rocks.

Five rock groups are described: sphene-nepheline syenite, garnet-pseudoleucite syenite, miscellaneous syenites, jacupirangite, and garnet-biotite melteigite. The location of analyzed and described rocks is shown on the geologic map (pl. 1).

SPHENE-NEPHELINE SYENITE

DISTRIBUTION AND DESCRIPTION

Sphene-nepheline syenite, about 7 percent of the exposed igneous rocks of the complex, is best exposed in the road cut in the NE¼ sec. 25 and SE¼ sec. 13. The top of the ridge consists of coarse-grained sphene-nepheline syenite; downslope to the west the rock is medium grained, and downslope to the east it is fine grained. This arcuate-shaped body of rock is about 7,500 feet long and ranges in width from a few feet to about 1,300 feet. The western contact is with the Stanley shale, and in sec. 25 it surrounds an older body of jacupirangite. The eastern contact is largely with younger(?) pseudoleucite syenite and the ends of the body pinch out against the garnet-pseudoleucite syenite-Stanley shale contact (pl. 1). The joint system follows the elongate trend of the body and dips both east and west.

A smaller body of sphene-nepheline syenite is exposed along Cove Creek in the SE¼ sec. 19. The only other known outcrop of this rock is in the SE¼ sec. 21 where it makes a small isolated knob in the surrounding sedimentary rocks.

Called fine-grained eleolite syenite by Williams (1891) and covite by Washington (1901), the rock is typically a fine- to medium-grained light-gray to gray phanerite that weathers to a reddish-brown or mottled (reddish-brown, tan, and brownish-green) saprolite. Feldspar, pyroxene, nepheline, and sphene are readily visible. Although the mineralogy of the textural varieties is almost identical, the contacts are sharp and suggest separate intrusions. In general the fine-grained varieties cut coarser grained syenite.

In thin section the phanerites have a hypautomorphic granular texture. Minerals in the rock include (in approximate order of abundance): subhedral laths of kaolinized sodic orthoclase (some perthite) with minor sericite alteration; anhedral nepheline partly altered to cancrinite; corroded and zoned crystals of neutral or very pale reddish-brown diopside-hedenbergite rimmed with green aegirine-diopside partly altered to green and bluish-green hornblende and green or brown biotite. The accessory minerals include euhedral sphene, apatite, magnetite, sodalite or analcime, and pale-brown garnet; plagioclase (andesine) is found in the coarser grained phases. In contrast to the garnet-nepheline syenite, sphene but not garnet is macroscopic in this rock.

The analyzed sample (MC–1, table 2) is a light-gray medium-grained syenite. In thin section the texture is hypautomorphic granular. The chief minerals are sodic orthoclase (53 percent), nepheline (25 percent), and pyroxene (9 percent). Although the sodic orthoclase tends to be elongated (average about 2 mm), the sides of the laths are generally not well developed. Carlsbad twinning is present though not common and all the laths are moderately kaolinized.

Nepheline occurs as unusually fresh blocky subhedral grains averaging 1mm across. Rows of colorless inclusions are common. Although sodic orthoclase and nepheline have mutual boundary textures, the nepheline is better crystallized, and in places appears to be older than the orthoclase.

Three ages of pyroxene minerals are present as shown in a few crystals which have three zones: an inner core of colorless diopside-hedenbergite rimmed by purple titanaugite which in turn is rimmed by green aegirine-diopside. The diopside-hedenbergite occurs as well-formed crystals but their sodic rims are irregular and in some cases, altered to sodic amphibole. The average length of the crystals is 0.8 mm. The late pyroxene crystals are small and have formed directly as titanaugite or aegirine-diopside.

Hornblende occurs as lath-shaped or anhedral grains (up to 1 mm in length) that are clearly younger than the pyroxene. Pleochroism ranges from pale greenish brown to deep bluish green. The extinction angle ranges from 20° to 40° and at the position of maximum extinction the mineral has an anomalous deep copper color.

Sphene, as euhedral crystals up to 1 mm across, is the most abundant accessory mineral. Sodalite occurs as blocky subhedral and anhedral grains and appears to be a late stage magmatic or deuteric mineral. Other accessory minerals are apatite, magnetite, and pyrite.

The coarse-grained syenite on top of the ridge in sec. 13 contains more amphibole and less nepheline; andesine (Ab_6An_4) occurs as early formed laths included in larger sodic orthoclase grains. In some thin sections the andesine is mantled with sodic orthoclase. One other local variety of the coarse-grained nepheline syenite occurs on the small knob in the SE¼ sec. 21 where the rock contains about 20 percent andesine and about 50 percent pyroxene so that the rock is closer to a camptonite.

In the fine-grained sphene-nepheline syenite only a few pyroxene grains show original diopside-hedenbergite and titanaugite cores; most of the grains are completely altered to sodic varieties. The groundmass is an equigranular mosaic of nepheline (20 percent) and sodic orthoclase (50 percent) in which larger anhedral to euhedral grains of mafic minerals (25 percent) are present.

The dike of sphene-nepheline syenite (L–286) that cuts jacupirangite in the northern part of sec. 24 is also fine grained. The texture in thin section is trachytic and the rock is composed of subhedral sodic orthoclase (some perthite)—about 74 percent; anhedral plagioclase (trace); anhedral nepheline partly altered to cancrinite (about 8 percent); anhedral sodalite or analcime (late) (about 2 percent); and anhedral to subhedral dark brownish-green hornblende, needles of green aegirine and colorless acmite, sphene, apatite, magnetite, and green biotite (about 15 percent).

The presence of plagioclase in the coarse-grained variety and its virtual absence in the finer grained nepheline syenite suggest that part of the magma cooled slowly so that plagioclase crystals formed with the early pyroxene crystals. The late minerals followed an orderly sequence giving amphibole and sodic orthoclase. In the younger, finer grained rocks, which cut medium- and coarse-grained bodies, the magma not only cooled quickly but was probably somewhat deficient in lime so that plagioclase crystals did not form and most of the calcium went into pyroxene. The amphibole also tended to form chiefly as alteration rims on pyroxene crystals rather than as separate grains.

Panned concentrates of saprolite of sphene-nepheline syenite contain magnetite, clay aggregates, sphene, apatite, and mica. Rutile in the panned concentrates indicates weathered rutile veinlets not apparent when the sample was taken. A. J. Gude 3d, (written communication, 1956) reported major kaolinite and trace illite in an X-ray analysis of the clay and silt parts of the saprolite.

CHEMISTRY

Chemical and spectrographic analyses, norms and modes of the analyzed rocks, table 2, show a typical nepheline syenite composition; SiO_2 is low and Al_2O_3 and the alkalies are high. The nepheline is potassic, orthoclase is very sodic, and K_2O is about the same in both minerals. This suggests considerable solid solu-

TABLE 2.—*Analyses, norm, and modes of sphene-nepheline syenite, in percent*

Standard chemical analyses [1]

	Sample No.			
	MC-1	MC-1-11	MC-1-9	MC-1-10
SiO_2	51.27	43.27	46.2	57.9
Al_2O_3	20.42	8.10	32.0	23.1
Fe_2O_3	2.12	5.02	n.d.	n.d.
FeO	2.60	9.54	n.d.	n.d.
MnO	.20	.76	n.d.	n.d.
MgO	1.22	8.27	n.d.	n.d.
CaO	4.69	18.14	n.d.	n.d.
BaO	.18	n.d.	n.d.	n.d.
Na_2O	8.05	1.91	14.2	9.0
K_2O	6.10	.96	6.1	7.0
H_2O-	.06	.03	n.d.	n.d.
H_2O+	.94	n.d.	n.d.	n.d.
TiO_2	1.21	2.80	n.d.	n.d.
CO_2	.11	n.d.	n.d.	n.d.
P_2O_5	.20	n.d.	n.d.	n.d.
SO_3	.00	n.d.	n.d.	n.d.
Cl	.46	n.d.	n.d.	n.d.
F	.29	n.d.	n.d.	n.d.
S	.18	n.d.	n.d.	n.d.
Ignition loss	n.d.	n.d.	1.0	2.2
Total	100.30	98.80	99.5	99.2
Less O	.31	----------	----------	----------
	99.99	----------	----------	----------

Spectrographic analyses [2]

	Sample No.		
	MC-1	L-27	L-24
Be	0.0004	0.0002	0.0002
Mg	n.d.	.3	.2
Ca	n.d.	.07	.03
Sr	.065	.01	.01
Ba	.40	.2	.1
B	0	0	0
Sc	.0005	.001	.003
Y	.0036	0	.003
La	.024	.009	.03
Yb	.0003	0	.0009
Ti	n.d.	1	4
Zr	.040	.04	.04
V	.018	.02	.04
Nb	.0087	.02	.05
Cr	.013	.002	.001
Mo	.0006	0	0
Mn	.13	.08	.04
Fe	n.d.	4	<10
Co	.0012	.002	.001
Ni	.0012	.001	.002
Cu	.0021	.002	.005
Ga	.0022	.002	.004
Pb	0	.001	.005

Norm

	Sample No.
	MC-1
or	36.14
ab	12.58
an	3.61
ne	27.83
hl	.70
nc	.21
di	8.68
wo	2.55
mt	3.02
il	2.28
ap	.34
fr	.62
pr	.36

Mode [3]

	Sample No.		
	MC-1	L-24	L-27
Sodic orthoclase (perthite).	53	58	72
Nepheline (cancrinite)	25	5	15
Andesine	----------	15	----------
Sodalite and analcime	2	2	3
Diopside-hedenbergite	9	20	10
Aegirine-diopside			
Hornblende	6		
Sphene	3		
Apatite	----------		
Magnetite	2		
Pyrite-pyrrhotite	----------		
Biotite	----------		
Garnet	----------		

Colorimetric analyses [4]

	MC-1	L-24	L-27
As	0.002	0.001	<0.001
Sb	.0002	.0002	.0002
W	.001	n.d.	n.d.
Zn	.010	.010	.010

Radiometric analyses [5]

	MC-1	L-24	L-27
eU	0.004	0.001	<0.001

Low-level chemical analyses [6]

	MC-1	L-24	L-27
U	0.00027	n.d.	n.d.
Th	.00100	n.d.	n.d.

[1] Analyses: MC-1 by L. M. Kehl; MC-1-11 by L. N. Tarrant; MC-1-9 and MC-1-10 by P. L. D. Elmore and K. E. White.

[2] Looked (spectrographically) for but not found: Ce, Hf, Th, P, Ta, W, Re, Ru, Rh, Pd, Os, Ir, Pt, Ag, Au, Zn, Cd, Hg, In, Tl, Ge, Sn, As, Sb, Bi, and Te. Analyses: MC-1 by H. J. Rose; L-27 and L-24 by Sol Berman.

[3] Modes by L. V. Blade.

[4] Analyses by H. E. Crowe and A. P. Marranzino.

[5] Analyses by B. A. McCall.

[6] Analyses by J. C. Antweiler.

n.d.=not determined.

MC-1. Sphene-nepheline syenite, SE¼ sec. 13.
MC-1-9. Nepheline separate from MC-1.
MC-1-10. Sodic orthoclase separate from MC-1.
MC-1-11. Pyroxene-amphibole composite from MC-1.
L-24. Sphene-nepheline syenite, NE¼ sec. 24. Mode on fresh rock, analyses on saprolite.
L-27. Sphene-nepheline syenite, NE¼ sec. 24. Mode on fresh rock, analyses on saprolite.

tion of kalisilite in nepheline and albite in orthoclase (some of the modal sodic orthoclase is perthitic). Excess Na_2O occurs in aegirine-diopside as indicated by chemical analysis of the pyroxene-amphibole composite.

The abundant chlorine makes sodalite the logical choice for the bulk of the colorless low-index isotropic mineral in the rock. No fluorite was detected in thin section so the fluorine must be found in apatite, biotite and perhaps minor amounts in hornblende (although none was detected in the composite) and sphene. The titanium occurs in sphene, magnetite, and pyroxene.

Spectrographic analyses show a higher barium content than the chemical analyses. Distribution of barium in the mineral separates (table 3) suggests that the spectrographic analyses for barium in the rock are probably high.

Trace elements in the rock that are equal to or exceed 0.01 percent and in order of abundance include: Sr, Zr, La, V, Cr, and Nb. The distribution of the trace elements is shown by the spectrographic analyses of minerals separated from the analyzed rock (table 3).

Discrepancies in the results on like mineral phases such as nepheline, sodic orthoclase, and diopside-hedenbergite may be due to several factors which include: nonuniform distribution of trace elements within the minerals, different methods of separation, and different analysts. Any or all of these factors may be operative here, since the like phases were separated at different times and analyzed by different analysts.

Of all the trace elements reported in table 3, only Ba and Ga are higher in the felsic minerals than in mafic minerals. Strontium occurs in felsic minerals at about the same level of concentration as Ba, but is three to four times more abundant in the mafic minerals. Ba^{+2} (1.34 A) is a large cation and tends to concentrate in the late fractions of the magma, and may replace K^{+1} (1.33 A) in the sodic orthoclase as long as the charge is balanced by Al^{+3} in tetrahedral coordination. The size of the Sr^{+2} ion (1.13 A) is similar to Ca^{+2} (0.99 A) and substitutes for Ca in the pyroxene and apatite.

Following are some further observations on the trace-element distribution in sphene nepheline syenite.

TABLE 3.—*Spectrographic analyses, in percent, of mineral separates of sphene-nepheline syenite*

	L-24-1	MC-1-c	MC-1-b	MC-1-6	MC-1-5	MC-1-8	MC-1-9	MC-1-2	MC-1-10	MC-1-1
Be	0.001	0	0.001	0	0.0006	0.0003	0	0.0001	0	0.0001
Mg	.2	.03	>10	>10	>10	>10	.04	.02	.06	.02
Ca	n.d.	>10	>10	n.d.	n.d.	n.d.	.44	n.d.	.28	------------
Sr	.01	.3	.4	.05	.2	.3	.12	.2	.14	.3
Ba	.0006	.1	.01	0	.006	.02	.2	.3	.3	.4
Sc	0	.0002	.006	.01	.004	.0006	0	0.	0	0
Y	0	.04	.02	0	.008	.008	0	0	0	0
La	.02	.04	0	0	.02	.04	0	0	0	0
Yb	n.d.	.0008	.001	n.d.	n.d.	n.d.	0	n.d.	0	n.d.
Ti	2.2	1-10	1-10	1.8	1.5	1.3	.06	.03	.02	.03
Zr	.006	.05	.05	.007	.04	.08	.002	0	.003	0
V	.5	.04	.02	.06	.08	.1	.001	.01	.001	.01
Nb	0	.7	0	0	0	.01	0	0	0	0
Cr	.009	.0002	.08	.1	.0009	.0007	0	.0007	0	.0005
Mo	0	.0006	0	0	0	0	0	0	0	0
Mn	.5	.001	.08	.08	.7	.9	.001	.006	.003	.01
Fe	>10	.4	1-10	>10	>10	>10	.40	.5	.24	.3
Co	.008	.0008	.004	.003	.002	.003	0	0	0	0
Ni	.007	.01	.01	.01	.002	.003	0	0	0	0
Cu	.01	.005	.001	.002	.002	.002	.0001	.001	.002	.001
Zn	.1	0	0	0	0	0	0	0	0	0
Ga	.005	0	.002	.0007	.003	.004	.011	.004	.005	.002
Sn	0	n.d.	n.d.	.005	.006	.007	0	0	0	0
Pb	0	.005	0	0	0	0	002	0	.002	.006
Specific gravity				3.35±.05	3.4±.1	3.24±.05	------------	2.65±.05	------------	2.55±.02

Indices of refraction [1]

α	=1.697±.005
β	=1.708±.005
γ	=1.730±.005

[1] Determined by D. J. Jameson.

n.d. =not determined.
Looked for but not found: B, Th, P, Ta, W, U, Re, Pd, Ir, Pt, Ag, Au, Cd, Hg, In, Ge, As, Sb, Bi.

EXPLANATION OF SAMPLES

	Sample	X-ray	Analyst	
			X-ray	Spectrographic
L-24-1	Magnetite	n.d.		H. J. Rose.
MC-1-c	Sphene	n.d.		J. D. Fletcher.
MC-1-b	Diopside-hedenbergite	n.d.		Do.
MC-1-6	do	Monoclinic pyroxene prob. intermediate between diopside and augite.	F. A. Hildebrand	H. J. Rose.
MC-1-5	Aegirine-diopside	do	do	Do.
MC-1-8	Green hornblende	Amphibole probably hornblende	do	Do.
MC-1-9	Nepheline	n.d.		Harry Bastron.
MC-1-2	do	Nepheline and minor analcime(?)	F. A. Hildebrand	H. J. Rose.
MC-1-10	Sodic orthoclase	n.d.		Harry Bastron.
MC-1-1	do	n.d.		H. J. Rose.

1. Zirconium occurs in amphibole (0.08 percent), pyroxene 0.007–0.05 percent) and sphene (0.05 percent).
2. Most of the lanthanum is in early formed sphene and in the late forming mafics, aegirine-diopside and hornblende.
3. Vanadium is concentrated chiefly in magnetite (0.5 percent) and also occurs in the other mafic minerals in concentration ranging from 0.02 percent to 0.1 percent. Late formed pyroxene contains more vanadium (0.08–0.1 percent) than early more titaniferous pyroxene (0.02–0.06 percent).
4. Most of the chromium is in early pyroxene.
5. Niobium is concentrated almost exclusively in sphene. Some was detected in hornblende.
6. Most of the copper, cobalt, and zinc are in magnetite, whereas most of the nickel is in sphene and early pyroxene.
7. Scandium occurs in pyroxene and amphibole and is most abundant in sodic pyroxene (0.01 percent).

By comparing the trace-element content of the saprolite, L–24, with that of the fresh rock, MC–1, we can get some idea of the effects of weathering on the trace elements. Ti, Nb, Sc, Yb, and Pb are enriched in the saprolite, whereas Sr, Mn, and Cr are decreased. Resistant sphene probably is responsible for the concentration of Yb, Nb, Pb, and part of the Ti. Resistant magnetite probably is responsible for concentration of part of the Ti.

GARNET-PSEUDOLEUCITE SYENITE

DISTRIBUTION AND DESCRIPTION

The garnet-pseudoleucite syenite, the most abundant rock type, represents about 21 percent of the igneous rock exposed in the complex. It forms a nearly complete ring ranging from a few to nearly 2,000 feet in width (pl. 1).

Good exposures include: The Diamond Jo quarry in the western part of sec. 29, the creekbeds of secs. 29 and 30, the creekbed in the northwestern part of sec. 18, and the highway cut in the northeastern part of sec. 24. The latter exposure is saprolite but the porphyritic texture of the original rock is preserved and a few residual boulders with a fresh rock core can be found.

Several mineralogic and textural varieties of this rock can be found but the typical fresh rock is light gray, medium grained, and composed of pseudoleucite, feldspar, black titanium garnet, pyroxene, and nepheline. Nepheline is much more abundant than in the sphene-nepheline syenite. Weathered surfaces are rough due to the protuberance of sodic orthoclase laths. The white pseudoleucite crystals are the most conspicuous criteria for defining this rock type but they are not always present, whereas the consistent occurrence of black garnet and absence of visible sphene in all varieties are diagnostic. Black titanium garnet is abundant in ijolite also, but the ijolite contains no feldspar.

Inclusions in the rock are abundant and include metamorphosed sediments and fine- to coarse-grained ijolite and melteigite fragments. These inclusions up to 10 feet across are most easily seen and studied in the north face of the Diamond Jo quarry but they are also found in the float throughout the mapped unit.

Miarolitic cavities up to 3 inches across are common in the rock in the Diamond Jo quarry. The minerals that partly fill these cavities are generally automorphic and include: tabular white orthoclase, needles of green aegirine, needles of colorless pseudowavellite, and short prisms of colorless apophyllite.

Color variations in the fresh rock include light gray, light greenish gray, and gray. The saprolite is generally some shade of brown but is sometimes gray and if the original rock was porphyritic the residual phenocrysts of pseudoleucite stand out as white spots.

A coarser grained more slowly cooled phase of the garnet-pseudoleucite syenite was mapped separately as garnet nepheline syenite and comprises about 3.5 percent of the exposed igneous rocks. The best exposures of this rock are in the NE¼ sec. 18 where it occupies the top of the ridge and is surrounded by the more typical garnet-pseudoleucite syenite. Earlier workers mapped this rock as part of the sphene-nepheline syenite, but the presence of macroscopic garnet, absence of macroscopic sphene and gradational contact with garnet pseudoleucite syenite mark it as a coarser grained phase of garnet pseudoleucite syenite. The early formed leucite crystals must have reacted with the magma and were completely eliminated. In the more rapidly cooled medium-grained rock, the early leucite crystals were not resorbed but adjusted to stability conditions by exsolution of fine-grained masses of nepheline and orthoclase but preserving the outward crystal form of leucite—hence, pseudoleucite. The chemical analyses of the two garnet syenites are very similar and they differ from the sphene-bearing nepheline syenite.

A well-developed major joint system strikes parallel to the ring-dike outcrop pattern. The major set dips about 55° SE.; the minor set dips northwest. A second minor system strikes at right angles to the major system and dips range from 75° to vertical.

In most thin sections, nepheline occurs in two generations: as unusually clear, blocky subhedral to euhedral crystals or phenocrysts up to 10 mm across that appear to be earlier than the sodic orthoclase, and as late, potash-rich, anhedral equigranular grains in the groundmass. Phenocrystic nepheline poikilitically includes aegirine laths. The borders of the crystals are commonly altered to analcime, sodalite group, cancrinite and calcite. Nepheline is more abundant in this rock than in the sphene-bearing nepheline syenite and ranges from 20 to 60 percent of the rock. In the coarse-grained variety, nepheline comprises only 15 to 25 percent of the rock and is probably younger than the feldspar.

Sodic orthoclase as elongate tabular crystals as much as 5 mm long comprises 5 to 40 percent of the pseudoleucite phase and 40 to 60 percent of the coarse-grained phase. In some rocks the potash feldspar is microperthite; in others, anorthoclase. In one thin section anorthoclase forms large optically continuous areas that poikilitically include all other minerals. In a few samples potash feldspar occurs as phenocrysts up to 4 mm long.

Early diopside-hedenbergite, late aegirine-augite and aegirine are the chief pyroxene minerals. In some areas the diopside-hedenbergite is tinted purple due to the presence of titanium in the structure. The relative proportions of the pyroxenes vary widely but together they average 15 percent of the rock. The diopside-hedenbergite occurs as colorless ravaged euhedral crystals that are rimmed with green aegirine-diopside. Aegirine occurs as very late formed small euhedral crystals. Rarely pyroxene is altered to green biotite; no amphibole has been observed in the 18 to 20 thin sections studied.

A black titanium garnet that ranges in composition from titanium-bearing andradite to melanite is one of the most diagnostic minerals of the garnet-pseudoleucite syenite. The proportion of garnet ranges from an accessory mineral to a major constituent status. In thin section the garnet is a deep brown, late-formed mineral, commonly subhedral, and poikilitically includes early-formed minerals. Pale-yellow, highly birefringent alteration masses of the garnet may be sphene formed by release of iron from the garnet leaving calcium, titanium, and silica, the components of sphene. Perhaps some of the released iron goes into deuteric green biotite.

White pseudoleucite crystals ranging from ¼ to 2 inches across are also diagnostic of the garnet-pseudoleucite syenite, but their proportion in the rock is extremely variable ranging from 0 to 60 percent. On weathered surfaces they stand out in positive relief and almost perfect crystals may be picked up in grus accumulations. Pseudoleucite is rarely present in the coarse-grained phase of the rock which suggests complete reaction of early leucite crystals with magma. The pseudoleucite crystals are composed of fine-grained masses of orthoclase and nepheline that have the trapezohedron form of the original leucite crystals. One thin section of pseudoleucite showed a myrmekitic-like intergrowth of sodic orthoclase and nepheline. Commonly the nepheline is altered to cancrinite.

A brief description of each of the analyzed samples follows:

MC-111 (NE¼ sec. 18).—Gray, porphyritic, medium-grained garnet-pseudoleucite syenite (table 4). Phenocrysts of pseudoleucite up to 7 mm, and black garnet as much as 6 mm make up about 3 percent of the rock. In thin section the minerals are subhedral to anhedral nepheline partly altered to analcime, sodalite group, and cancrinite; subhedral to anhedral sodic-orthoclase partially altered to analcime, sodalite group, and cancrinite (some of the feldspar crystals poikilitically include nepheline, diopside-hedenbergite, garnet, sphene, aegirine and magnetite); subhedral to anhedral diopside-hedenbergite rimmed with aegirine-diopside and the whole partly altered to biotite and magnetite; euhedral to anhedral aegirine partly altered to biotite; anhedral garnets, some of which are zoned from brown in the center to colorless on the borders and partly altered to sphene; anhedral sphene; anhedral perovskite; and anhedral fluorite generally intergrown with sphene. No apatite was detected in thin section but the P_2O_5 in the analysis indicated some was probably present in the rock.

MC-121 (west edge, sec. 29).—Gray porphyritic medium-grained garnet-pseudoleucite syenite (table 4). In thin section the rock is composed of subhedral nepheline (early) and anhedral nepheline (late) both partly altered to analcime, sodalite-group minerals, and cancrinite; subhedral to anhedral sodic orthoclase partly altered to analcime, sodalite-group minerals, and cancrinite; euhedral to anhedral diopside-hedenbergite, rimmed with aegirine-diopside and aegirine and partly altered to biotite and magnetite; euhedral to anhedral aegirine-diopside rimmed with aegirine and partly altered to biotite and magnetite; euhedral to anhedral aegirine partly altered to biotite and magnetite; euhedral to anhedral garnet some of which is zoned, brown in the center to colorless borders, and partly altered to sphene;

TABLE 4.—*Analyses, norms, and modes of garnet-pseudoleucite syenite, in percent*

	Sample No.	
	MC-111	MC-121
Standard chemical analyses [1]		
SiO_2	49.43	47.31
Al_2O_3	20.17	20.10
Fe_2O_3	4.00	3.57
FeO	1.71	2.62
MnO	.32	.30
MgO	.64	.89
CaO	5.08	6.67
BaO	.27	.36
Na_2O	8.30	7.98
K_2O	6.19	6.50
H_2O-	.10	.10
H_2O+	1.73	1.42
TiO_2	.63	.88
CO_2	.96	1.07
P_2O_5	.13	.21
SO_3	.13	.01
Cl	.08	.04
F	.20	.19
S	.03	.06
Total	100.10	100.28
Less O	.12	.12
	99.98	100.16

	Sample No.			
	MC-111	MC-121	L-21	L-50
Spectrographic analyses [2]				
Be	0.0007	0.0004	0.0005	0.0005
Mg	n.d.	n.d.	.7	.2
Ca	n.d.	n.d.	>5	.02
Sr	.014	.044	.2	.05
Ba	.26	.48	.3	.3
B	0	0	.002	.001
Sc	.0003	.0003	0	0
Y	.0024	.0038	.003	0
La	.027	.018	.006	.03
Ce	n.d.	n.d.	0	0
Yb	.0002	.0002	.0008	0
Ti	n.d.	n.d.	1	.5
Zr	.022	.021	.03	.03
V	.046	.045	.06	.03
Nb	.0096	.0074	.03	.03
Cr	.0034	.0005	.0004	.001
Mn	.26	.22	.5	.1
Fe	n.d.	n.d.	4	4
Co	.0008	.0009	.0008	.0008
Ni	0	.0006	0	0
Cu	.0010	.0008	.02	.0003
Ga	.0027	.0027	.003	.003
Pb	0	0	0	.001

	Sample No.	
	MC-111	MC-121
Norms		
or	36.70	38.36
ab	11.00	
an	6.39	6.39
--------	--------	--------
ne	24.99	29.82
hl	.12	
th	.28	
nc	2.33	2.54
di	3.46	6.24
wo	5.34	7.31
mt	4.64	5.10
hm	.80	
il	1.22	1.67
ap	.34	.34
fr	.39	.39
pr	--------	.12

	Sample No.				
	MC-111	MC-121	L-21	L-50	MC-64
Modes [3]					
Orthoclase	30	25	35	35	
Nepheline (cancrinite).	40	40	41	41	
Analcime (or sodalite group).	3	1	3	3	
Monoclinic pyroxene:					
Diopside-hedenbergite.	5	2	1	2	
Aegirine-diopside. Aegirine	12	16	7	9	
Biotite (magnetite).	4	3	6	7	
Garnet (sphene)	5	11	6	2	
Apatite Calcite Clinozoisite Fluorite Magnetite Perovskite Pyrite	1	2	1	1	
Colorimetric analyses [4]					
As	<0.001	0.003	<0.001	0.002	n.d.
Sb	.0001	<.0001	.0001	.0002	n.d.
W	.001	<.001	n.d.	n.d.	n.d.
Zn	.015	.012	.015	.013	n.d.
Radiometric analyses [5]					
eU	0.003	0.002	<0.001	0.003	
Chemical analyses [6]					
U	0.00020	0.00020	n.d.	n.d.	0.00017
Th	n.d.	.00055	n.d.	n.d.	.00069

[1] Standard chemical analyses. MC-111 and MC-121 by L. M. Kehl; MC-111-1 by L. N. Tarrant.

[2] Spectrographic analyses. MC-111 and MC-121 by H. J. Rose; L-21 and L-50 by Sol Berman.

[3] Modes by L. V. Blade.

[4] Colorimetric analyses by H. E. Crowe and A. P. Marranzino.

[5] Radiometric analyses by B. A. McCall.

[6] Low-level chemical analyses of uranium and thorium by J. C. Antweiler.

n.d.—not determined.

Looked for (spectrographically) but not found: Hf, Th, P, Ta, Mo, W, U, Re, Ru, Rh, Pd, Os, Ir, Pt, Ag, Au, Zn, Cd, Hg, In, Tl, Ge, Sn, As, Sb, Bi, Te.

MC-111. Porphyritic garnet pseudoleucite syenite, NE¼ sec. 18.
MC-121. Porphyritic garnet pseudoleucite syenite, SW¼ sec. 29.
MC-111-1. Pyroxene composite from MC-111.
L-21. Porphyritic garnet pseudoleucite syenite, NE¼ sec. 24. Mode of fresh rock, analyses of saprolite.
L-50. Porphyritic garnet pseudoleucite syenite, NE¼ sec. 24. Mode of fresh rock, analyses of saprolite.
MC-64. Porphyritic garnet pseudoleucite syenite, NE¼ sec. 18.

TABLE 5.—*Analyses, norm, and modes of garnet-nepheline syenite, in percent*

	Sample No.	
	MC-112	MC-112-6
Standard chemical analyses[1]		
SiO_2	48.88	46.65
Al_2O_3	19.77	4.51
Fe_2O_3	4.20	15.38
FeO	1.72	7.04
MnO	.31	1.26
MgO	.72	2.81
CaO	5.38	12.13
BaO	.32	n.d.
Na_2O	7.95	6.21
K_2O	6.80	.98
H_2O-	.30	.09
H_2O+	1.39	.59
TiO_2	.76	1.12
CO_2	1.09	n.d.
P_2O_5	.14	n.d.
SO_3	.00	n.d.
Cl	.07	n.d.
F	.28	.66
S	.04	n.d.
Total	100.12	99.43
Less O	.16	.28
	99.96	99.15

	Sample No.		
	MC-112	L-54	L-84
Spectrographic analyses[2]			
Be	0.0007	0.0003	0.0003
Mg	n.d.	.1	.2
Ca	n.d.	.04	.07
Sr	.054	.1	.05
Ba	.33	.5	.5
B	0	0	.001
Sc	.0003	0	0
Y	0	.002	0
La	.024	0	0
Ti	n.d.	.3	.3
Zr	.03	.02	.03
V	.052	.009	.05
Nb	.0099	.02	.04
Cr	.002	.0005	.001
Mo	0	.0008	.001
Mn	.28	.2	.2
Fe	n.d.	1	4
Co	.0008	.0005	.001
Ni	0	.0007	.0008
Cu	.0009	.0009	.001
Ga	.0033	.002	.003
Pb	0	.01	.001

	Sample No.
	MC-112
Norm	
or	40.03
ab	7.34
an	5.56
ne	24.99
hl	.12
nc	2.65
di	4.47
wo	5.68
mt	4.18
hm	1.28
il	1.52
ap	.34
fr	.62

	Sample No.		
	MC-112	L-54	L-84
Modes[3]			
Sodic orthoclase	27	42	36
Nepheline (cancrinite and zeolite).	43	42	33
Sodalite and (or) analcime	1	2	5
Diopside-hedenbergite	2	11	
Aegirine-diopside	16		19
Aegirine			
Garnet	6	3	6
Sphene	3		1
Calcite	2		
Fluorite			
Apatite			
Magnetite			
Biotite			
Pyrite			
Clinozoisite			
Colorimetric analyses[4]			
As	<0.001	0.004	0.001
Sb	<.0001	.0002	.0002
W	<.001	n.d.	n.d.
Zn	.015	.05	.013
Radiometric analyses[5]			
eU	0.005	0.006	0.005
Chemical analyses[6]			
U	0.00027	n.d.	n.d.
Th	.00045	n.d.	n.d.

[1] Standard chemical analyses. MC-112 by L. M. Kehl and MC-112-6 by L. N. Tarrant.
[2] Spectrographic analyses. MC-112 by H. J. Rose, L-54, L-84 by Sol Berman.
[3] Modes by L. V. Blade.
[4] Colorimetric analyses. MC-112, L-54, L-84 by H. E. Crowe and A. P. Marranzino.
[5] Radiometric analyses by B. A. McCall.
[6] Low-level chemical analyses of uranium and thorium by J. C. Antweiler.

n.d.—not determined.

Looked for (spectrographically) but not found: Ce, Yb, Hf, Th, P, Ta, W, Re, Ru, Rh, Pd, Os, Ir, Pt, Ag, Au, Zn, Cd, Hg, In, Ge, Sn, As, Sb, Bi, Te.

MC-112. Garnet-nepheline syenite, NW¼ sec. 17.
MC-112-6. Pyroxene composite from MC-112.
L-54. Garnet-nepheline syenite, NW¼ sec. 17. Mode on fresh rock, analyses on saprolite.
L-84. Garnet-nepheline syenite, NE¼ sec. 20. Mode on fresh rock, analyses on saprolite.

and euhedral apatite. No fluorite was detected in thin section but it is probably present in the sample.

L-21 (*NE1/4 sec. 24*).—Light-gray medium-grained garnet-pseudoleucite syenite (table 4). The fresh rock in thin section is composed of subhedral to anhedral sodic orthoclase partly altered to analcime or sodalite group, cancrinite, and calcite; nepheline as corroded crystals (earlier than the feldspar) partly altered to analcime or sodalite group, cancrinite and calcite; corroded crystals of very pale brown diopside-hedenbergite rimmed with green aegirine-diopside and aegirine; subhedral to anhedral green aegirine-diopside rimmed with green aegirine and partly altered to green biotite and magnetite; euhedral to anhedral crystals of green aegirine some partly altered to biotite and magnetite; euhedral to anhedral zoned garnet with brown centers (melanite) and colorless rims (andradite) partly altered to sphene, green biotite, magnetite, and calcite; subhedral crystals of magnetite some rimmed with biotite; and euhedral apatite. Material in the concentrate of the panned saprolite occurs in about the following order of abundance: feldspar, nepheline (some pink), garnet, pale-brown mica, green pyroxene, magnetite, pyrite, and apatite. A spectrographic analysis of the saprolite and the mode of the fresh rock are shown in table 4.

L-50 (*NE1/4 sec. 24*).—Light gray, porphyritic, medium-grained garnet-pseudoleucite syenite (table 4). Phenocrysts of pseudoleucite as much as 10 mm, sodic orthoclase 10 mm long, nepheline 10 mm, black garnet 5 mm, respectively, and agglomerates of fine-grained pyroxene and sodic orthoclase make up about 5 percent of the fresh rock. In thin section the minerals are: subhedral nepheline earlier than the feldspar and anhedral nepheline later than the feldspar both partly altered to analcime or sodalite group and cancrinite; subhedral to anhedral sodic orthoclase partly altered to analcime or sodalite group and cancrinite; subhedral diopside-hedenbergite altered on the borders to aegirine diopside; euhedral to anhedral aegirine-diopside partly altered to biotite and magnetite; anhedral brown- to brownish-yellow zoned garnet partly altered to sphene and fluorite; and euhedral apatite as inclusions in the diopside-hedenbergite. Material in the concentrate of the panned saprolite occurs in about the following order of abundance: feldspar, nepheline, pale-brown mica, garnet, pyroxene, pyrite, apatite, and magnetite. From an X-ray analysis of the clay- and silt-size part of the saprolite sample, A. J. Gude 3d, (written communication, 1956) reported major kaolinite and minor illite. A spectrographic analysis of the saprolite and the mode of the fresh rock are given in table 4.

CHEMISTRY

Chemical and spectrographic analyses, norms, and modes of garnet-pseudoleucite syenite and garnet-nepheline syenite (tables 4 and 5) show that these rocks are typical nepheline syenites but distinctly different from the previously described sphene-nepheline syenite, particularly in silica and in volatile content. Silica is lower, but the alkali is the same resulting in a much higher nepheline content. CO_2 is uniformly high and occurs in cancrinite; the high Cl (in sodalite) characteristic of sphene-nepheline syenite is negligible in these rocks. The TiO_2 content is lower and is chiefly in garnet, whereas the higher TiO_2 content of sphene-nepheline syenite occurs in sphene.

The amount of modal nepheline is much greater than normative nepheline. However, the nepheline deficiency in the norm can be ascribed to the use of much of the sodium in normative albite and some of the potassium in normative orthoclase. The excess silica would combine with normative anorthite, wollastonite, ilmenite and part of the iron oxides to make the modal pyroxenes and titanium garnet which comprise 22 to 29 percent of the rock.

The high Fe_2O_3 and Na_2O in the analyzed pyroxene composite reflect the aegirine-diopside and aegirine alteration of early diopside hedenbergite; the K_2O is probably in minor biotite alteration products.

Trace elements equal to or greater than 0.01 percent include, in order of abundance, Ba, Sr, V, La, Zr, and Nb. The distribution of most of the trace elements within these rocks is shown in the spectrographic analyses of minerals separated from the analyzed rocks (tables 6 and 7).

1. Most of the manganese in the rock is in magnetite, sodic pyroxene, and garnet.
2. Most of the nickel is in garnet.
3. Vanadium has its highest concentration in magnetite, garnet, and perovskite but is also present in the pyroxenes, particularly sodic pyroxene.
4. Yttrium is concentrated in perovskite and garnet with lesser amounts in the diopside hedenbergite. Lanthanum, however, is not present in the pyroxenes, but occurs in the garnet and perovskite in concentrations up to 0.06 percent. The high lanthanum content of the rocks (0.018 to 0.027 percent) suggests that not all of the lanthanum is accounted for by the minerals so far analyzed in this study.

TABLE 6.—*Spectrographic analyses, in percent, of mineral separates of garnet-pseudoleucite syenite*

	MC-121-1	MC-121-c	MC-121-b	MC-111-c	MC-111-d	MC-111-10	MC-111-a	MC-121-a	MC-111-9	MC-111-b	MC-111-11
Be	0	0	0	0	0	0	0	0	0	0.001	0.00008
Mg	.3	.02	1	1	.1	>10	>10	>10	>10	1	.01
Ca	n.d.	>10	>10	10	>10	n.d.	>10	>10	n.d.	>10	n.d.
Sr	.0009	.3	.2	.7	1	.2	.4	.4	.3	.6	.02
Ba	.005	.002	.02	.05	.1	.003	.009	.02	.002	.08	.003
Sc	0	0	0	0	0	.0004	.001	.002	.0003	0	0
Y	0	.1	.1	.05	.06	.006	.02	.02	0	0	0
La	0	.05	.01	.02	.06	0	0	0	0	0	0
Yb	n.d.	n.d.	n.d.	n.d.	.002	n.d.	.0008	.0005	n.d.	0	n.d.
Ti	3.4	>10	1-10	1-10	1-10	1.5	1-10	1-10	.5	.4	.008
Zr	0	0	.2	.08	.2	.04	.06	.002	.01	.02	.02
V	.5	.1	.3	.2	.2	.1	.04	.03	.2	.06	.007
Nb	0	.3	.009	.02	.1	0	0	0	0	0	0
Cr	.004	.0008	.0002	.0002	.0002	.0007	.003	.003	.0007	.0002	.0007
Mn	1	.04	.2	.3	.6	.09	.1	.06	.7	.5	.001
Fe	>10	>10	>10	>10	1-10	>10	1-10	1-10	>10	>10	.03
Co	.008	.003	.001	.003	0	.0008	.003	.002	.0006	.001	0
Ni	.007	0	.004	.001	.004	.002	0	0	.003	0	0
Cu	.002	.009	.002	.002	.003	.003	.002	.001	.003	.001	.0006
Ag	0	0	0	0	0	0	0	0	0	.0001	0
Zn	.2	0	0	0	0	0	0	0	0	0	0
Ga	.003	0	.0002	0	.003	.0009	.002	.002	.001	.001	.003
Sn	0	n.d.	n.d.	n.d.	n.d.	0	n.d.	n.d.	.008	n.d.	0
Specific gravity						3.35±.05			3.55±.05		2.25±.05

Indices of refraction [1]

	MC-121-1	MC-121-c	MC-121-b	MC-111-c	MC-111-d	MC-111-10	MC-111-a	MC-121-a	MC-111-9	MC-111-b	MC-111-11
α						1.725±.005			1.712±.005		
β						1.737±.005			1.738±.005		
γ						1.750±.005			1.785±.005		

[1] Determined by D. J. Jameson.

n.d.—not determined.

Looked for but not found: B, Th, P, Ta, Mo, W, U, Re, Rh, Pd, Ir, Pt, Au, Cd, Hg, In, Ge, Pb, As, Sb, Bi.

EXPLANATION OF SAMPLES

	Analyst	Sample	X-ray	Analyst
MC-121-1	H. J. Rose, Jr.	Magnetite		
MC-121-c	J. D. Fletcher	Perovskite		
MC-121-b	do	Garnet (melanite)		
MC-111-c	do	do		
MC-111-d	do	Garnet (pale-brown andradite)	Andradite	W. F. Outerbridge.
MC-111-10	H. J. Rose, Jr.	Diopside-hedenbergite	Monoclinic pyroxene, probably augite and minor biotite.	F. A. Hildebrand.
MC-111-a	J. D. Fletcher	do		
MC-121-a	do	do		
MC-111-9	H. J. Rose, Jr.	Aegirine-diopside	Monoclinic pyroxene, probably intermediate between diopside and augite.	Do.
MC-111-b	J. D. Fletcher	Aegirine		
MC-111-11	H. J. Rose, Jr.	Analcime	Analcime	Do.

TABLE 7.—*Spectrographic analyses of mineral separates of garnet-nepheline syenite, in percent*

	MC-112a	MC-112b	MC-112-1	MC-112-2	MC-112-3	MC-112-4	MC-112-5
Be	0	0	0	0.0001	0.0001	0	0.0001
Mg	.4	>10	>10	>10	>10	.02	.04
Ca	>10	>10	n.d.	n.d.	n.d.	n.d.	n.d.
Sr	.3	.4	.1	.4	.4	.5	.1
Ba	.04	.008	.001	.002	.001	9.5	.009
Sc	0	.002	.003	0	0	0	0
Y	.02	.03	.008	.004	.004	0	0
La	0	0	0	.0009	.0009	0	0
Yb	n.d.	.001	n.d.	n.d.	n.d.	n.d.	n.d.
Ti	1–10	1–10	2.4	.5	.6	.03	.01
Zr	.04	.05	.03	.02	.05	.04	.01
V	.2	.03	.03	.2	.2	.01	.01
Nb	.06	0	0	0	0	0	0
Cr	.0001	.0002	.0007	.0007	.007	.0007	.002
Mn	.18	.06	.04	1.1	1.0	.001	.005
Fe	>10	1–10	>10	>10	>10	.9	.2
Co	.0005	.003	.002	.001	0	0	0
Ni	.0006	0	0	.003	.004	0	0
Cu	.002	.002	.0009	.002	.001	.0008	.0008
Ag	0	0	0	.0003	.0004	0	0
Ga	.0002	.004	.001	.002	.001	.003	.008
Sn	n.d.	n.d.	.002	.004	.002	0	0
Specific gravity	------------	------------	3.35±.05	3.35±.05	3.55±.05	2.75±.05	2.3
Indices of refraction[1]							
α	------------	------------	1.713±0.005	1.693±0.005			
β	------------	------------	1.721± .005	1.719± .005			
γ	------------	------------	1.745± .005	1.779± .005			

[1] Determined by D. J. Jameson.

n.d.=not determined.

Looked for but not found: B, Hf, Th, P, Ta, Mo, W, U, Re, Pd, Ir, Pt, Au, Zn, Cd, Hg, In, Ge, Pb, As, Sb, Bi.

EXPLANATION OF SAMPLES

	Sample	X-ray	Analyst	
			X-ray	Spectrographic
MC-112a	Dark garnet			J. D. Fletcher.
MC-112b	Diopside-hedenbergite			Do.
MC-112-1	do	Monoclinic pyroxene probably augite	F. A. Hildebrand	H. J. Rose.
MC-112-2	Aegirine	Monoclinic pyroxene probably aegirine and minor biotite.	do	Do.
MC-112-3	do	Monoclinic pyroxene probably aegirine	do	Do.
MC-112-4	Barian feldspar			Do.
MC-112-5	Zeolite	Natrolite and minor sodalite	do	Do.

5. Zirconium occurs chiefly in the garnet and diopside-hedenbergite, with lesser amounts in sodic pyroxene and felsic minerals.
6. Niobium is concentrated in perovskite and garnet.
7. Strontium is concentrated in the mafic minerals. The quantity of barium found in the analyzed minerals is insufficient to account for the barium content of the rock. Most of the barium probably is present in feldspar with lesser amounts in the garnet. The high barium content of the barian feldspar of the garnet nepheline syenite is particularly noteworthy.
8. Gallium is not concentrated to any great extent in any mineral but is highest in the zeolite.

MISCELLANEOUS SYENITES

Scattered about the complex are gray medium-grained syenites that are not readily classified with any of the foregoing syenites nor with each other. These rocks are chemically similar to the previously described rocks, but small mineralogic differences in isolated bodies permit differentiation of these units on the geologic map.

FELDSPATHOIDAL LEUCOSYENITE

A unit mapped as feldspathoidal leucosyenite occurs in the southeastern of the complex and represents about 0.7 percent of the exposed part of the igneous complex (pl. 1). Good exposures are rare.

The rock is a light-gray fine- to medium-grained phanerite that ranges in composition from alkalic to nepheline syenite. In thin section the texture is hypautomorphic-trachitoid. Felsic minerals include sodic orthoclase, analcime or sodalite, perthite, plagioclase, and nepheline. Other minerals (usually not abundant) include aegirine-diopside, biotite, muscovite, hornblende, colorless to brown garnet, apatite, sphene, fluorite, magnetite-ilmenite, pyrite, and pyrrhotite. Alterations include sodic orthoclase to kaolinite, sericite, or cancrinite; nepheline to cancrinite, and pyroxene to biotite. Analcime or sodalite and calcite (where present) are late.

Some of the variants are briefly described below:

MC–146.—Light-gray, medium-grained feldspathoidal leucosyenite, southwestern part of sec. 21. In thin section the rock has a hypautomorphic-trachitoid texture and is composed of analcime or sodalite, about 2 percent; nepheline partially altered to cancrinite, about 4 percent; plagioclase probably albite, about 2 percent; kaolinized sodic orthoclase and perthite, about 82 percent; and neutral diopside-hedenbergite almost completely altered to brownish-green biotite, sphene (some euhedral), and pyrrhotite, about 10 percent.

MC–233.—Light-gray fine-grained nepheline syenite; southeastern part of sec. 20. The rock has a hypautomorphic-trachitoid texture and contains analcime or sodalite, about 2 percent; nepheline partly altered to cancrinite, about 15 percent; sodic orthoclase partly altered to cancrinite, about 71 percent; and aegirine-diopside, fluorite, pyrrhotite, and clinozoisite(?), about 12 percent.

MC–234.—Light-gray medium-grained feldspathoidal leucosyenite, same locality as MC–233. The rock has a hypautomorphic-trachitoid texture and contains analcime or sodalite, about 4 percent; nepheline partly altered to cancrinite, about 6 percent; kaolinized sodic orthoclase and perthite partly altered to sericite, about 85 percent; and sphene, brown to colorless garnet, brownish-green biotite, brownish-green hornblende, and pyrrhotite, about 5 percent.

L–325.—Light-gray, medium-grained alkalic syenite, same locality as MC–233 and MC–234. The rock has a hypautomorphic trachitoid texture and contains late calcite associated with garnet, analcime, kaolinized sodic orthoclase partly altered to sericite, yellowish-green biotite, muscovite, colorless garnet intergrown with sphene, apatite, magnetite-ilmenite, pyrite, and pyrrhotite.

Chemical and spectrographic analyses, the norm, and the mode of feldspathoidal leucosyenite (table 8) are distinctly different from the previously described nepheline syenites. The K_2O is higher than Na_2O—a rarity in Magnet Cove rocks. This relationship is brought out in the mode by the high content of sodic orthoclase. Nepheline (21.3 percent) appears in the norm but not in the mode because sericite alteration and biotite and muscovite (low-silica minerals) occur in the mode whereas this silica deficiency shows in the norm as nepheline. The FeO/Fe_2O_3 ratio of the chemical analysis is not reliable because a soluble sulfide, pyrrhotite, is present in the mode. The isotropic mineral in the mode is interpreted to be analcime, since SO_3 and Cl are low in the analysis.

Trace elements equal to or greater than 0.01 and in order of abundance include Sr, Ba, Zr, V, Nb, and La.

TABLE 8.—*Analyses, norm, and mode of feldspathoidal leucosyenite, in percent*

Chemical		Spectrographic		Norm		Mode	
SiO_2	54.67	Be	0.0002	C	0.31	Soda orthoclase (sericite).	82
Al_2O_3	20.83	Mg	n.d.	or	49.48	Analcime	3
Fe_2O_3	.20	Ca	n.d.	ab	5.24	Calcite	1
Feo	3.69	Sr	.6	an	7.51	Garnet	4
MnO	.32	Ba	.2	ne	21.30	Sphene	1
MgO	.20	La	.009	ol	3.14	Biotite	2
CaO	2.59	Ti	n.d.	mt	.23	Muscovite	4
BaO	.20	Zr	.03	il	.61	Magnetite-ilmenite	3
Na_2O	5.27	P	n.d.	fr	.47	Pyrite-pyrrhotite	
K_2O	8.43	V	.03	pr	2.76	Apatite (tr.)	
H_2O-	.09	Nb	.03	cc	1.40		
H_2O+	1.60	Mn	n.d.				
TiO_2	.35	Fe	n.d.				
CO_2	.60	Cu	.001				
P_2O_5	.03	Ga	.004				
SO_3	.01	Pb	.002				
Cl	.01						
F	.23						
S	1.48						
Total	100.80						
Less O	.84						
	99.96						

n.d.=not determined.
Looked for (spectrographically) but not found: B, Se, Y, Ce, Yb, Hf, Th, Ta, Cr, Mo, W, U, Re, Co, Ni, Ru, Rh, Pd, Os, Ir, Pt, Ag, Au, Zn, Cd, Hg, In, Ti, Ge, Sn, As, Sb, Bi, Te.
L–325, Alkalic syenite, SE¼ sec. 20.
Standard chemical analysis by M. K. Balazs.
Spectrographic analysis by Sol Berman.
Mode by L. V. Blade.

SPHENE-CANCRINITE SYENITE

A sphene-cancrinite syenite, at least 0.04 percent of the exposed igneous rocks of the complex, is found in the northeastern part of sec. 17 as a small dike in jacupirangite and in the eastern half of sec. 24 as small irregular shaped bodies.

The rock is a gray- to dark-gray fine- to medium-grained phanerite. In thin section the texture is holocrystalline hypautomorphic-granular and the minerals include: anhedral sodic orthoclase partly altered to cancrinite, calcite, and analcime or sodalite, 50 to 70 percent; anhedral cancrinite (late interstitial and alteration product), 10 to 25 percent; and corroded diopside-hedenbergite partly to completely altered to brown and green biotite and leucoxene. Other minerals include sphene, pyrite, pyrrhotite, apatite, and fluorite, 20 to 25 percent.

SPHENE-GARNET-NEPHELINE SYENITE

Sphene-garnet-nepheline syenite, less than 0.1 percent of the exposed igneous rocks of the complex, occurs as small dikes in jacupirangite or sphene pyroxenite. The samples taken for thin section all came from sec. 17.

The rock is a light- gray to gray, fine, to medium-grained phanerite. In thin section the texture is holocrystalline hypautomorphic-granular and the minerals include: anhedral sodic orthoclase partly altered to calcite, cancrinite, and sodalite or analcime, 30 to 80 percent; anhedral to euhedral nepheline partly altered to calcite, cancrinite, and sodalite or analcine, 12 to 40 percent; and anhedral to euhedral green aegirine. Accessory minerals include sphene, anhedral zoned (brown to colorless) garnet, biotite (reddish-brown and green), apatite, magnetite, pyrite, pyrrhotite.

A few minor syenite units are mapped as miscellaneous syenites. Rocks from two of these bodies are described below:

MC–154.—Altered, gray medium-grained alkalic syenite (NE¼ sec. 17). This rock apparently intrudes jacupirangite and sphene pyroxenite. In thin section the texture is holocrystalline hypautomorphic trachitoid, and the minerals include: sodic orthoclase partly altered to sericite, cancrinite, and calcite, about 92 percent; and colorless to brown garnet, brown and green biotite, and pyrite, about 8 percent.

MC–212.—Altered, gray medium-grained alkalic syenite (NW¼ sec. 19). This rock occurs as a mappable body in contact with several rock types. However, all contacts are float contacts so relative ages are unknown. In thin section the texture is holocrystalline hypautomorphic-trachitoid, and the minerals include: sodic orthoclase and some perthite partly altered to cancrinite, calcite, and analcime or sodalite, about 80 percent; and green biotite, apatite, yellowish-brown acmite, green aegirine, pyrite, and magnetite-ilmenite, about 20 percent.

JACUPIRANGITE AND SPHENE PYROXENITE

DISTRIBUTION AND DESCRIPTION

Jacupirangite, a magnetite pyroxenite that may contain a few percent of feldspathoids, constitutes about 10 percent of the exposed igneous rocks of the complex. It crops out at two localities in Magnet Cove and forms magnetic highs which are helpful in delimiting the boundaries of the unit on the map (pl. 1).

The largest body of jacupirangite occurs in sec. 17 and ranges in composition from sphene pyroxenite (by reaction with novaculite along the contact) to melteigite. Swarms of light-colored, vertical dikes of nepheline syenite, ijolite, and melteigite ranging from less than 1 inch to 3 feet in width cut the jacupirangite and stand out in bold relief on weathered surfaces.

The second and smaller body of jacupirangite makes the magnetic high and topographic low on the west side of Magnet Cove in secs. 24 and 13. No fresh rock is exposed but banks of highly magnetic saprolite cut by resistant dikes and stringers of nepheline syenite indicate the character of the rock. One residual knot of moderately fresh rock in the saprolite was composed almost entirely of pyroxene and magnetite. The limits of this rock mass were determined from magnetometer readings (fig. 3) and from panned concentrates of saprolite.

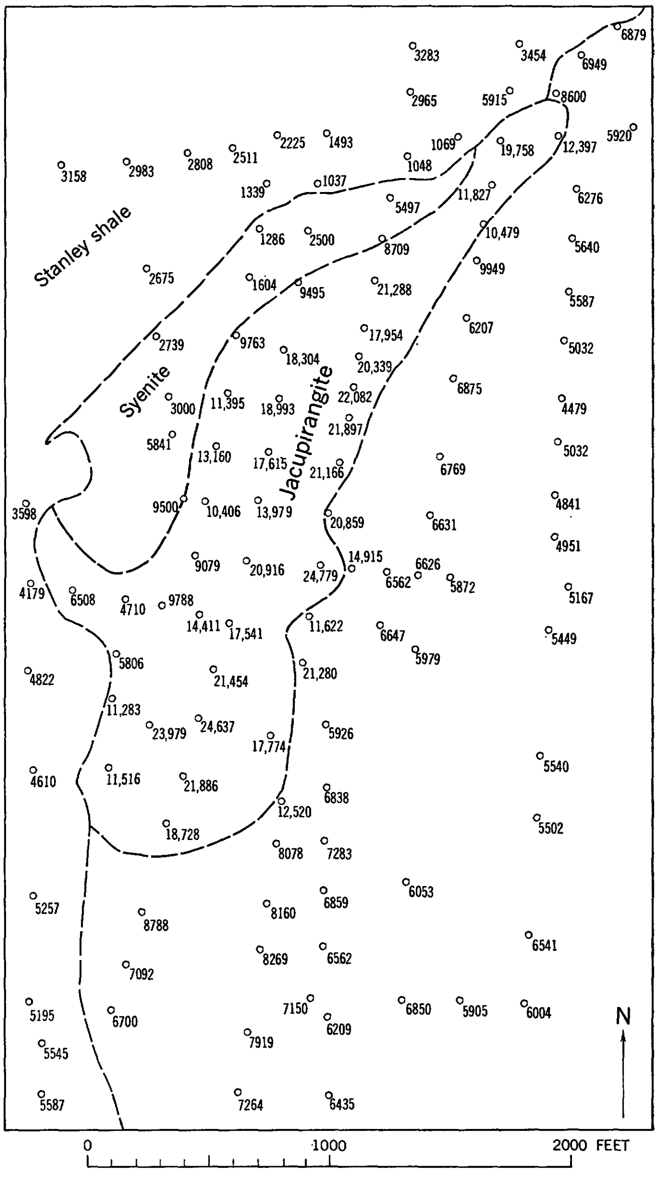

FIGURE 3.—Map showing distribution of jacupirangite inferred from high magnetometer readings, in gammas. After magnetometer survey map made by Heiland Research Corp. for U.S. Bureau of Mines (written communication, 1942).

Called eleolite mica syenite (cove type) by Williams (1891) and jacupirangite by Washington (1901), the rock is typically a dark-gray fine- to medium-grained phanerite that weathers to a dark-brown or mottled reddish-brown and olive-green saprolite. Pyroxene is the chief constituent and always comprises more than 50 percent of the rock. Magnetite is abundant. Apatite, biotite, sphene, garnet, and perovskite are always present, sometimes in proportions greater than 10 percent. Zeolite formed from the alteration of nepheline, calcite, and cancrinite is common. Other accessory minerals include pyrite and pyrrhotite.

The pyroxene crystals (salite) up to 10 mm long appear to have formed an early crystal mush. Many of the grains have a light-green to colorless core that is rimmed by pink-tinted titanaugite; other grains have ravaged edges marked by formation of sodic pyroxene or biotite. Inclusions of magnetite, perovskite, and apatite are common.

Magnetite-ilmenite in grains as much as 6 mm across comprise about 2 to 25 percent of the rock. Some of the grains are rimmed with perovskite and have apatite inclusions. In some thin sections this assemblage plus brown to colorless garnet, aegirine-diopside, sphene, pyrite, biotite, and apatite occur in veinlets cutting the rock and appears to be a late introduction. Small rods of ilmenite (?) occur as minor inclusions in the pyroxene.

The panned concentrate of saprolite of jacupirangite contains magnetite, pyroxene, sphene, apatite, perovskite and (or) garnet, mica, and clay aggregates. From an X-ray analysis of the clay- and silt-size portion of the saprolite, A. J. Gude 3d (written communication, 1956) reported major chlorite, minor montmorillonite, and a trace of kaolinite (?).

Two noteworthy varieties of the jacupirangite are produced by reaction with sedimentary rocks. A small body of sphene pyroxenite in the northeastern part of the complex has formed from the reaction of jacupirangite and Arkansas novaculite. Exposures are poor and the contact with novaculite is covered with colluvium.

The color of the rock in hand specimen depends on the amount of sphene present, but this fine- to medium-grained phanerite is typically dark gray with reddish-gray and greenish-gray variations. In thin section the texture is hypautomorphic-granular, and mineralogically there are two types represented by MC–151 and MC–172 described below:

MC–151.—Sphene pyroxenite composed of faintly pleochroic (pale yellowish-brown to pale bluish-green) diopside-hedenbergite, about 67 percent; anhedral to euhedral sphene, about 8 percent; apatite, about 4 percent; anhedral brownish-violet perovskite rimmed with sphene, about 1 percent; pyrite, about 1 percent; and a late interstitial mixture of birefringent zeolite and analcime or sodalite group minerals which replaces pyroxene in part, about 19 percent.

MC–172.—Quartz sphene pyroxenite composed of very pale green diopside rimmed with green aegirine-diopside; euhedral and anhedral sphene; apatite; pyrite; pyrrhotite. Orthoclase, perthite, plagioclase probably albite, quartz, calcite, and myrmekitic intergrowths of quartz and orthoclase occur as late introduced minerals in the interstices between pyroxene grains. The lack of perovskite suggests that silica from the novaculite combined with titanium and iron to form silicate (sphene) rather than the oxide (perovskite).

At the contact with Stanley shale, the rock is a meladiorite consisting of pyroxene (50 percent), plagioclase (30 percent), biotite (5 percent), with accessory magnetite, sphene, and apatite. The plagioclase, oligoclase-andesine (Ab_7An_3), occurs as large, late-forming, optically continuous areas that poikilitically include pyroxene crystals. It seems probable that

TABLE 9.—*Analyses, norm, and modes of jacupinangite, in percent*

	MC–173	L–81–2	(1)
Chemical analyses [2]			
SiO_2	35.42		38.38
Al_2O_3	9.21		6.15
Fe_2O_3	8.94		11.70
FeO	7.17		8.14
MnO	.29		.16
MgO	7.77		11.47
CaO	20.83		18.60
BaO	.00		n.d.
Na_2O	1.47		.78
K_2O	.62		.13
H_2O-	.11		.18
H_2O+	1.05		.54
TiO_2	4.05		4.32
CO_2	.11		.00
P_2O_5	2.23		.17
SO_3	.12		n.d.
Cl	.02	.01	n.d.
F	.17	2.19	n.d.
S	.38		n.d.
Total	99.96		100.72
Less O	.26		
	99.70		

	MC–173	L–81	L–124
Spectrographic analyses [3]			
Be	0.0008	0.0001	0.0002
Sr	.5	.2	.2
Ba	.05	.05	.1
B	0	0	.003
Sc	.002	.006	.006
Y	.008	.008	.01
La	.03	.03	.05
Ce	n.d.	.09	n.d.
Yb	.001	.0005	.001
Zr	.04	.04	.04
V	.07	.04	.05
Nb	.002	.03	.04
Cr	.0001	.001	.002
Mo	.001	0	.002
Mn	.2	.2	.2
Fe	>10	4	>10
Co	.005	.002	.005
Ni	.001	.002	.0005
Cu	.02	.03	.01
Ga	.002	.002	.002

	MC–173
Norm	
an	16.96
lc	2.62
ne	6.53
th	.14
di	37.15
ol	1.54
cs	7.40
mt	11.14
hm	1.28
il	7.60
ap	5.04
pr	.72
cc	.20

	MC–173	L–81	L–124
Modes [4]			
Diopside-hedenbergite (salite).	78	78	
Magnetite-ilmenite Pyrite-pyrrhotite	5	10	
Perovskite	3	5	
Sphene	2		
Apatite	6	5	
Biotite	1	2	
Calcite Zeolite Analcime and (or) sodalite group.	4		
Garnet	1		
Colorimetric analyses [5]			
As	0.001	0.001	0.001
Sb	.0001	.0001	.0001
Zn	.013	.013	.015
Radiometric analyses [6]			
eU	0.001	0.001	0.001
Chemical analyses [7]			
U	0.00049	n.d.	n.d.
Th	.00339	n.d.	n.d.

[1] Type jacupirangite from Brazil, Washington (1901).

[2] Standard chemical analyses. MC–173 by S. M. Berthold; L–81–2 by L. N Tarrant.

[3] Spectrographic analyses. MC–173 by J. D. Fletcher; L–81 and L–124 by Sol Berman.

[4] Modes by L. V. Blade.

[5] Colorimetric analyses by H. E. Crowe and A. P. Marranzino.

[6] Radiometric analyses by B. A. McCall.

[7] Low-level chemical analyses for uranium and thorium by J. C. r.Antweile

n.d.—not determined.

Looked for (spectrograghically)but not found: Hf, Th, Ta, W, U, Re, Ru, Rh, Pd, Os, Ir, Pt, Ag, Pb, Au, Zn, Cd, Hg, In, Tl, Ge, As, Sb, Bi, Sn.

MC–173. Jacupirangite, NE¼ sec. 17.

L–81. Jacupirangite, near center of sec. 17. Mode on fresh rock, analyses on saprolite.

L–81–2. Apatite from L–81.

L–124. Saprolite of jacupirangite, NE¼ sec. 17.

sufficient silica was added from the shale to make plagioclase; sodic orthoclase would not be developed since the potassium content of the original magma was very low and is used in biotite.

CHEMISTRY

Chemical and spectrographic analyses, norms, and modes of jacupirangite and sphene pyroexnite are given in tables 9 and 10.

The presence of an acid-soluble sulfide, pyrrhotite, renders the FeO/Fe_2O_3 ratio of the analyses unreliable.

The analyzed rock (table 9) is similar to the type jacupirangite from Brazil, but is lower in SiO_2, total iron oxides, and MgO and higher in Al_2O_3, Na_2O, K_2O, and P_2O_5.

Felsic minerals occur in the norm calculation but not in the mode. The CaO and Al_2O_3 of normative anorthite is in modal pyroxene; K_2O of normative leucite is in biotite; Na_2O of normative nepheline is in zeolite and analcime.

It is noteworthy that although jacupirangite has the highest content of magnesia (7.77 percent) of all rock types in the complex, the pyroxene (salite), which makes up 78 percent of the rock, does not have the highest content of magnesia of all pyroxenes (table 56). This is partly explained by the high magnesia content of more than 10 percent in early crystallized magnetite (magnesioferrite) and partly by the abundance of pyroxene in jacupirangite.

The sphene pyroxenite has a higher SiO_2 and lower Al_2O_3 and total iron content than the jacupirangite and reflects the reaction of typical jacupirangite with novaculite.

Trace elements that exceed or are equal to 0.01 percent include Sr, Ba, V, Zr, La, Cu, and Y. Distribution of the trace elements within the rocks is shown by the analyses of minerals separated from the analyzed rocks (tables 11 and 12).

1. Strontium occurs mainly in apatite (>1 percent), perovskite, sphene, and pyroxene.
2. The bulk of the zirconium is in sphene (0.1 to 0.19 percent) with lesser amounts in apatite and pyroxene.
3. Vanadium occurs in all mineral separates but is particularly enriched in magnetite (0.2 percent), pyroxene, and apatite.
4. Niobium is concentrated in perovskite (0.3 percent) and sphene (0.1 to 0.15 percent).
5. Lanthanum and yttrium are concentrated chiefly in perovskite, sphene, and apatite.
6. Copper was detected in all separates but is most abundant in pyrite, perovskite, magnetite, and apatite.
7. Cobalt and nickel are concentrated chiefly in pyrite with lesser amounts in magnetite.
8. Molybdenum was detected only in zeolites.

TABLE 10.—*Analyses, norms, and modes of sphene pyroxenite, in percent*

	Sample No.	
	MC-172	L-326
Standard chemical analyses [1]		
SiO_2	49.10	46.01
Al_2O_3	3.11	1.92
Fe_2O_3	3.21	3.80
FeO	6.52	9.66
MnO	.30	.50
MgO	7.35	6.35
CaO	19.63	21.76
BaO	0	.03
Na_2O	1.60	1.25
K_2O	1.04	.60
H_2O-	.18	.06
H_2O+	.26	.11
TiO_2	5.21	5.10
CO_2	.32	.91
P_2O_5	1.68	1.38
SO_3	.59	0
Cl	.08	.02
F	.16	.20
S	.55	1.06
Total	100.89	100.72
Less O	.36	.61
	100.53	100.11

	Sample No.	
	MC-172	L-326
Spectrographic analyses [2]		
Be	0	0.0001
Sr	.5	.4
Ba	.05	.001
B	0	0
Sc	.002	.003
Y	.008	.004
La	.02	.009
Ce	n.d.	0
Yb	.0006	.0005
Ti	7.0	n.d.
Zr	.02	.03
P	0	n.d.
V	.058	.3
Nb	.008	.03
Cr	.0004	.002
Mo	.003	.001
Mn	.2	n.d.
Co	.005	.004
Ni	.003	.001
Cu	0	.03
Ga	0	0
Pb	.002	0

	Sample No.	
	MC-172	L-326
Norms		
Q	7.38	5.94
or	6.12	3.34
ab	9.96	1.57
ac	3.23	7.85
di	39.99	47.74
wo	13.57	13.92
mt	3.02	1.62
il	9.88	9.73
ap	4.03	3.36
fr	.07	.16
pr	1.35	1.96
cc	.70	2.00

	Sample No.	
	MC-172	L-326
Modes [3]		
Diopside-hedenbergite and aegirine-diopside.	73	85
Sphene	20	8
Apatite	1	3
Pyrite-pyrrhotite	1	1
Orthoclase Perthite Albite Quartz Calcite	5	3
Colorimetric analyses [4]		
As	<0.001	n.d.
Sb	.0001	n.d.
Zn	.005	n.d.
Radiometric analyses [5]		
eU	<0.001	0.001
Chemical analyses [6]		
U	0.00020	n.d.
Th	.00048	n.d.

[1] Standard chemical analyses. MC-172 by S. M. Berthold and L-326 by M. K. Balazs.

[2] Spectrographic analyses. MC-172 by J. D. Fletcher and L-326 by Sol Berman.

[3] Modes: MC-172, R. L. Erickson; L-326, L. V. Blade.

[4] Colorimetric analyses by H. E. Crowe and A. P. Marranzino.

[5] Radiometric analyses. MC-172 by B. A. McCall and L-326 by D. L. Schafer.

[6] Low-level chemical analyses of uranium and thorium by J. C. Antweiler.

N.d.=not determined.

Looked for (spectrographically) but not found: Hf, Th, Ta, W, U, Re, Ru, Rh, Pd, Os, Ir, Pt, Ag, Au, Zn, Cd, Hg, In, Ti, As, Bi, Sn.

MC-172. Sphene pyroxenite, NE¼ sec. 17.
L-326. Sphene pyroxenite, NW¼ sec. 16.

TABLE 11.—*Spectrographic analyses, in percent, of mineral separates of jacupirangite*

	MC-173-10	L-81-9	MC-173-4	MC-173-5	L-81-10	MC-173-6	L-81-8	MC-173-1	MC-173-2	L-81-11	MC-173-3	MC-173-7	MC-173-8	L-81-1	L-81-2	MC-173-9	L-81-4	L-81-5
Be	0	0	0	0	0	0	0	0.0003	0.0003	0	0	0	0	0	0	0.0003	0.005	0.0005
Mg	>10	>10	n.d.	n.d.	.04	n.d.	.02	n.d.	n.d.	>10	n.d.	.01	.005	.02	.03	.05	.04	.08
Sr	.007	.02	.2	.2	.4	.05	.8	.5	.4	.01	.04	1.1	.95	1-5	1-5	.01	.7	.01
Ba	.002	.002	0	0	.001	0	.02	.06	.01	.004	.09	.004	.003	.03	.02	.002	.1	.008
B	0	0	0	0	0	0	0	0	0	0	0	.005	.002	.0007	.0007	.005	0	.004
Al	n.d.	n.d.	n.d.	n.d.	n.d.	n.d.	n.d.	n.d.	n.d.	n.d.	n.d.	.05	.03	n.d.	n.d.	>10	n.d.	>10
Sc	0	.0003	.0004	.0004	.003	.0004	0	.007	.007	.004	.0002	0	0	0	0	0	0	0
Y	.006	.006	.057	.050	.04	.029	.02	.002	.002	.008	.002	.02	.02	.03	.03	0	0	0
La	0	0	.1	.1	.4	.04	.04	.002	.002	0	0	.09	.01	.01	.02	0	0	0
Yb	0	n.d.	0	0	n.d.	0	n.d.	0	0	n.d.	0	0	0	.0009	.0008	0	0	0
Ti	3.4	4.0	>10	>10	>10	>10	>10	2.8	2.8	2.2	5.0	.02	.01	.03	.08	.02	.02	.02
Zr	0	0	0	0	0	.19	1	.03	.03	.02	0	0	0	0	0	0	0	0
P	0	0	0	0	0	0	0	0	0	0	0	>10	>10	n.d.	n.d.	0	n.d.	0
V	.2	.2	.045	.039	.04	.070	.07	.2	.1	.04	.02	.04	.04	.06	.08	.009	.0008	.004
Nb	0	0	.27	.30	.2	.15	.1	0	0	0	0	0	0	0	0	0	0	0
Cr	.0005	.0003	0	0	.0005	0	0007	.0003	.0003	.0007	0	0	0	0	0	0	.00009	0
Mo	0	0	0	0	0	0	0	0	0	0	0	0	0	0	0	.007	.001	0
Mn	1.1	1.1	.03	.03	.02	.009	.008	.07	.07	.05	.2	.01	.01	.006	.006	.003	.003	.004
Fe	>10	>10	n.d.	n.d.	1.4	n.d.	.8	n.d.	n.d.	>10	n.d.	.2	.1	.09	.2	.3	.2	.2
Co	.01	.02	0	0	.002	0	.002	.003	.002	.002	.01	0	0	0	0	0	0	0
Ni	.008	.009	0	0	0	0	.002	.002	.001	.002	.004	0	0	0	0	0	0	0
Cu	.008	.01	.012	.033	.007	.0075	.004	.008	.001	.01	.003	.0007	.0004	.005	.009	.01	.005	.007
Ga	.004	.006	0	0	0	0	0	.002	.0005	.001	.002	0	0	0	0	.002	.0006	.003
Tl	n.d.	n.d.	n.d.	n.d.	n.d.	n.d.	n.d.	n.d.	n.d.	n.d.	n.d.	n.d.	n.d.	.x	0	n.d.	0	n.d.
Sn	0	0	0	0	0	0	.001	.04	.04	.007	.09	.008	.008	0	0	0	0	0
Pb	0	0	0	0	.002	0	0	0	0	0	0	0	0	.002	0	0	0	0
Specific gravity	---------	---------	<4.0	4.±.07	4.±.07	3.4±.1	3.4±.1	3.35±.05	3.35±.05	3.35±.05	3.1±.3	3.02±.12	3.22±.07	3.35±.05	3.05±.25		2.35±.05	2.25±.05
								Indices of refraction[1]										
α	---------	---------	---------	---------	---------	---------	---------	1.707±.005	1.707±.005	1.705±.005								
β	---------	---------	---------	---------	---------	---------	---------	1.719±.005	1.712±.005	1.718±.005								
γ	---------	---------	---------	---------	---------	---------	---------	1.739±.005	1.737±.005	1.740±.005								

[1] Determined by D. J. Jameson.

n.d.=not determined.
Looked for but not found: Ce, Th, Ta, W, U, Re, Pd, Ir, Pt, Ag, Au, Zn, Cd, Hg, In, Ge, As, Sb, Bi.

EXPLANATION OF SAMPLES

	Sample	X-ray	Analyst			Sample	X-ray	Analyst	
			X-ray	Spectrographic				X-ray	Spectrographic
MC-173-10	Magnetite-ilmenite	Magnetite and moderate amount of ilmenite.	F. A. Hildebrand	H. J. Rose.	MC-173-2	Salite	Monoclinic pyroxene, probably augite and minor biotite.	F. A. Hildebrand	H. J. Rose.
L-81-9	do	Magnetite and moderate amount of ilmenite, trace of hematite.	do	Do.	L-81-11	Diopside-hedenbergite.	Monoclinic pyroxene, probably augite.	do	Do.
MC-173-4	Perovskite			Do.	MC-173-3	Biotite	Biotite-phlogopite type mica	do	Do.
MC-173-5	do			Do.	MC-173-7	Apatite			Do.
L-81-10	do			Do.	MC-173-8	do			Do.
MC-173-6	Sphene			Do.	L-81-1	do			J. D. Fletcher.
L-81-8	do			Do.	L-81-2	do			Do.
MC-173-1	Salite	Monoclinic pyroxene, probably augite and minor biotite.	F. A. Hildebrand	Do.	MC-173-9	Zeolite			H. J. Rose.
					L-81-4	do	Thomsonite-gonnardite type zeolite.	do	J. D. Fletcher.
					L-81-5	do			H. J. Rose.

TABLE 12.—*Spectrographic analyses, in percent, of mineral separates of sphene pyroxenite*

	MC-172-5	MC-176	MC-177	MC-172-4	MC-172-3	MC-172-1	MC-172-2
Be	0	0	0	0	0.0002	0	0
Mg	n.d.	.00x	.00x	n.d.	n.d.	n.d.	n.d.
Sr	.002	.x	.x	.05	.4	.07	.003
Ba	.004	.00x	.00x	.002	.02	.09	.01
Sc	0	0	0	.0004	.002	0	0
Y	0	.0x	.0x	.037	.001	0	0
La	0	.0x	.x	.02	0	0	.005
Yb	0	.00x	.00x	0	0	0	0
Ti	.2	>10	>10	>10	.2	.03	.02
Zr	0	.0x	.0x	.14	0	0	0
V	0	.29	.12	.15	.2	.001	0
Nb	0	.22	.20	.12	0	0	0
Cr	0	.000x	.000x	0	.0004	0	0
Mn	.02	.0x	.0x	.01	.2	.003	.002
Fe	n.d.	2.5	2.0	n.d.	n.d.	n.d.	n.d.
Co	.22	0	0	0	.007	0	0
Ni	.12	0	0	.006	.004	0	0
Cu	.09	.00x	.00x	.01	.01	.002	.001
Ga	0	0	0	0	0	.002	0
Sn	0	.00x	.00x	0	0	0	0
Pb	.007	0	0	0	0	0	0
Specific gravity	----------	----------	----------	3.4±.1	3.±.3	2.55±.05	2.65±.05
					Indices of refraction [1]		
α					=1.693±.005		
β					=1.699±.005		
γ					=1.712±.005		

[1] Determined by D. J. Jameson.

n.d. = not determined.

x = found but quantity not determined.

Looked for but not found: B, Ce, Th, P, Ta, Mo, W, Re, Pd, Ir, Pt, Ag, Au, Zn, Cd, Hg, In, Ge, As, Sb, Bi.

EXPLANATION OF SAMPLES

	Sample	X-ray	Analyst	
			X-ray	Spectrographic
MC-172-5	Pyrite			H. J. Rose.
MC-176	Sphene			J. D. Fletcher.
MC-177	do			Do.
MC-172-4	do			H. J. Rose.
MC-172-3	Diopside	Monoclinic pyroxene probably diopside	F. A. Hildebrand	Do.
MC-172-1	Orthoclase	Feldspar probably microcline or sanidine	do	Do.
MC-172-2	Quartz			Do.

9. The greatest concentration of beryllium (0.005 percent) is in a thomsonite-gonnardite type of zeolite.
10. Most of the scandium is in pyroxene.

Comparison of the content of trace-elements of the saprolites with the content of the fresh rock indicates that Nb, Sc, and Cr are concentrated during weathering and Be and Sr are lost. Resistant magnetite probably accounts for most of the concentration of chromium and a part of the scandium, and resistant perovskite, sphene, and garnet probably account for most of the concentration of niobium and a part of the scandium.

GARNET-BIOTITE MELTEIGITE

DISTRIBUTION AND DESCRIPTION

A small area of melteigite, about 0.4 percent of the exposed igneous rocks of the complex, was mapped in the northeastern part of sec. 18 and the northwestern part of sec. 17 (pl. 1). Good exposures are rare and most of the area was delimited by means of float and saprolite.

The rock contains rounded phenocrysts of brown biotite set in a dark-gray groundmass. Occasionally irregular inclusions of ijolite are found. In thin section the fine- to medium-grained groundmass has a holocrystalline xenomorphic-granular texture and is composed of very pale brown diopside-hedenbergite rimmed with pale-green diopside and partly altered to brown biotite; pale-green diopside, pale-brown to greenish-brown biotite, brownish-violet perovskite rimmed with sphene and some rimmed with brown garnet; brown to colorless garnet some intergrown with sphene; apatite; magnetite-ilmenite; pyrrhotite; and nepheline partly

TABLE 13.—*Analyses, norm, and mode of garnet-biotite melteigite, in percent*

Chemical		Spectrographic			Colorimetric			Norm		Mode [1]	
	MC-113		MC-113	L-86		MC-113	L-86		MC-113		MC-113
SiO_2	40.08	Be	0.0004	0.0001	As	0.002	0.003	an	4.73	Nepheline	21
Al_2O_3	11.74	Sr	.044	.08	Sb	.0001	.0003	lc	16.13	Sodalite group	5
Fe_2O_3	7.19	Ba	.18	.2	W	<.001	n.d.	ne	17.32	Orthoclase-nepheline intergrowth	6
FeO	4.76	Sc	.0009	.002	Zn	.018	.050	th	.28	Diopside-hedenbergite	30
MnO	.32	Y	.0022	.004	Pb	<.0005	n.d.	di	34.99	Biotite	9
MgO	6.72	La	.037	.02				ol	.42	Garnet	22
CaO	15.69	Yb	0	.0003				cs	6.19	Sphene	5
BaO	.14	Zr	.062	.02	eU [2]	.002	.001	mt	3.94	Apatite	.5
Na_2O	3.89	V	.096	.05				hm	4.48	Pyrrhotite	1
K_2O	3.47	Nb	.014	.03				il	6.54	Magnetite	
H_2O-	.06	Cr	.018	.002				ap	2.02	Calcite	.5
H_2O+	.87	Mo	0	.001	U [3]	.00019	n.d.	fr	.31		
TiO_2	3.44	Mn	.14	.4	Th [3]	.00055	n.d.	pr	1.20		
CO_2	.18	Co	.0045	.005				cc	.50		
P_2O_5	.87	Ni	.0065	.001							
SO_3	.13	Cu	.024	.004							
Cl	.04	Ga	.003	.003							
F	.24										
S	.65										
Total	100.48										
Less O	.44										
	100.04										

[1] Mode by D. J. Jameson.
[2] Radiometric analyses.
[3] Chemical analyses.

n.d.=not determined.
Looked for (spectrographically) but not found: B, Ce, Hf, Th, P, Ta, W, U, Re, Rh, Pd, Os, Ir, Pt, Ag, Au, Zn, Cd, Hg, In, Tl, Ge, Sn, Pb, As, Sb, Bi, Te.

Standard chemical analyses by L. M. Kehl.

Spectrographic analyses. MC-113 by H. J. Rose; L-86 by Sol Berman.
Colorimetric analyses by H. E. Crowe and A. P. Marranzino.
Radiometric analyses by B. A. McCall.
Low-level chemical analyses for uranium and thorium by J. C. Antweiler.
MC-113. Garnet-biotite melteigite, NW¼ sec. 17.
L-86. Saprolite of garnet-biotite melteigite, NW¼ sec. 17.

altered to cancrinite, sodalite group minerals or analcime, and calcite. A calcite veinlet and an intergrowth of sodic orthoclase and nepheline were found in the analyzed rock.

CHEMISTRY

Chemical and spectrographic analyses, norm, and mode of the garnet-biotite melteigite, table 13, emphasize the feldspathoidal character of this rock type and its close association to the ijolite group. Thenardite in the norm probably appears in the mode as a member of the sodalite group. Fluorine in the analysis is in biotite and apatite.

Compared with Nockolds' average melteigite (table 18), the analyzed rock is lower in SiO_2, CaO, Na_2O, CO_2, and P_2O_5; and higher in Fe_2O_3, MgO, K_2O, and TiO_2.

Trace elements in the rock that are equal to or exceed 0. 01 percent include Mn, Sr, Ba, La, Zr, V, Nb, Cr, Ni, and Cu. Spectrographic analyses of minerals separated from the analyzed rock show the distribution of the trace elements (table 14).

1. Strontium occurs chiefly in apatite and pyroxene.
2. Barium occurs in biotite (0. 4 percent) probably as potassium replacement. The bulk of the barium, however, is probably in felsic minerals, none of which could be separated for analysis.
3. Lanthanum and yttrium are chiefly in perovskite and apatite with lesser amounts in garnet.
4. Zirconium is concentrated in garnet and sphene.
5. Most of the vanadium is in magnetite, garnet, and sphene.
6. Niobium is concentrated in perovskite and sphene.
7. Chromium and copper are detected in all analyzed minerals but chromium is concentrated chiefly in magnetite and biotite and copper in magnetite and apatite.
8. Most of the nickel occurs in biotite (0. 02 percent).

TABLE 14.—*Spectrographic analyses of mineral separates of garnet-biotite melteigite, in percent*

	MC-113-1	MC-113-d	MC-113-2	MC-113-3	MC-113-a	MC-113-c	MC-113-e	MC-113-b
Be	0	0	0	0	0	0	0.0007	0
Mg	.2	.002	.5	.1	.04	1-10	>10	1-10
Sr	.002	.1	.03	.3	1.	.4	.9	.2
Ba	.005	.002	.008	.009	.08	.03	.01	.4
B	n.d.	0	n.d.	n.d.	.002	0	0	0
Sc	0	.001	.006	0	.0005	.006	.001	.0008
Y	0	.04	.02	0	.03	0	0	0
La	0	.2	.03	.06	.2	0	0	0
Yb	n.d.	n.d.	n.d.	n.d.	.0007	0	0	0
Ti	2.8	>10	>10	>10	.05	1-10	.6	1-10
Zr	0	0	.2	.08	0	.02	.002	.002
V	.3	.04	.2	.1	.04	.01	.01	.01
Nb	0	.3	.01	.2	0	0	.02	0
Cr	.2	.001	.01	.02	.0001	.02	.003	.06
Mn	1.0	.04	.3	.03	.008	.05	.09	.1
Fe	>10	>10	>10	1.7	.07	1-10	1-10	1-10
Co	.008	.003	0	0	0	.002	.003	.004
Ni	.001	0	0	0	0	.004	.006	.02
Cu	.02	.01	.002	.003	.02	.006	.003	.003
Ga	.004	0	.004	0	0	.003	0	.002
Sn	0	n.d.	0	.002	n.d.	n.d.	n.d.	n.d.
Zn	.2	0	0	0	0	0	0	0

n.d.=not determined.
Looked for but not found: Ce, Th, Ta, Mo, W, U, Re, Rh, Pd, Ir, Pt, Ag, Au, Cd, Hg, In, Ge, Pb, As, Sb, Bi.

EXPLANATION OF SAMPLES

	Sample	X-ray	Analyst	
			X-ray	Spectrographic
MC-113-1	Magnetite			H. J. Rose.
MC-113-d	Perovskite	Dysanalyte (columbian perovskite)	W. F. Outerbridge.	J. D. Fletcher.
MC-113-2	Dark-colored garnet.			H. J. Rose.
MC-113-3	Sphene			Do.
MC-113-a	Apatite			J. D. Fletcher
MC-113-c	Diopside-hedenbergite.	Monoclinic pyroxene.	W. F. Outerbridge.	Do.
MC-113-e	Diopside	Diopside-sphene.	do	Do.
MC-113-b	Biotite			Do.

Spectrographic analysis of the saprolite, L–86, indicates that Sr, Sc, Y, Yb, Nb, and Mn are concentrated and Be, Zr, V, Cr, Ni, and Cu are lost during weathering.

Resistant perovskite accounts for part of the concentration of Sr, Y, and Nb; resistant garnet accounts for part of the concentration of Sc, Y, and Mn; resistant apatite accounts for part of the concentration of Sr and Nb.

INTERMEDIATE RING

The intermediate ring of igneous rocks is composed chiefly of fine-grained rocks and breccias of trachytic and phonolitic composition, which the writers believe represents the earliest phase of intrusive activity at Magnet Cove. Although the complex has been deeply eroded, the fineness of grain, abundance of breccia, and high volatile content of these rocks suggest that the intermediate fracture ring was the original channelway to the surface and supplied explosive volcanic material to the surrounding area.

Rutile-bearing veins and irregular masses of metamorphosed sedimentary rocks are most abundant in this unit.

The rocks described in this section include altered phonolite and undivided trachyte-phonolite.

ALTERED PHONOLITE

DISTRIBUTION AND DESCRIPTION

The altered phonolite unit, about 7 percent of the exposed igneous complex, is a dark-gray aphanite that weathers to a mottled greenish-gray and reddish-brown saprolite with a fine-grained texture. The unit is most abundant in the western half of the intermediate ring.

Good exposures of the altered phonolite occur in the western part of sec. 18 where the contact with the fine-grained chilled border phase of younger garnet pseudoleucite syenite is exposed in the stream that cuts through the ridge.

In thin section the rock is porphyritic with a trachytic or xenomorphic-granular groundmass and ranges in composition from alkalic trachyte to nepheline trachyte or phonolite. The chief minerals are pyroxene phenocrysts up to 2 mm long that are altered to green biotite, calcite, and magnetite; hexagonal outlines of former nepheline phenocrysts replaced by calcite, biotite, and fine-grained anhedral nepheline; and pyrite cubes in a fine-grained groundmass of calcite, nepheline, orthoclase, and green biotite shreds. Apatite prisms up to 1 mm long appear as phenocrysts. Sodalite, fluorite, and sphene are accessory. Both pyrite and calcite are particularly abundant in and near the breccia.

One of the most interesting features of this rock is the uniform abundance of calcite (15 to 20 percent) throughout the mapped phonolite bodies. It occurs chiefly as small grains, 0.02 mm, disseminated in the groundmass, and sometimes as coarse-grained anhedral patches that suggest recrystallization of the calcite. It is clearly a late-forming mineral because together with biotite and magnetite, it replaces early formed pyroxene and nepheline crystals.

In many samples of the phonolite, fine-grained green biotite (0.015 mm) comprises more than half the rock; it ranges from 20 to 60 percent. Biotite, like calcite, is a deuteric mineral formed at the expense of early-formed mafic minerals which were the source of magnesium and iron.

Fresh pyroxene is very rare in the phonolite; a few remnants of diopside-hedenbergite mantled with aegirine-augite are present in some thin sections. Lath-shaped relics of former phenocrysts up to 2 mm long are outlined by rims of fine granular magnetite. The interior of the grains consists of fine-grained calcite, biotite, and magnetite.

Hexagonal aggregates of calcite, biotite, and fine granular nepheline(?), outlined by fine granular magnetite indicate the presence of former euhedral nepheline phenocrysts. For the most part, the felsic minerals occur with biotite and calcite in the groundmass as a fine-grained composite and are difficult to identify. Some of the rock was treated with dilute HCl which produced abundant silica gel indicative of feldspathoids.

Euhedral pyrite in crystals up to 0.5 mm across is a late-forming mineral and poikilitically includes parts of the groundmass. Locally pyrite exceeds 10 percent of the rock.

Locally the rock is a breccia containing fragments that include pieces of metamorphosed sedimentary rocks, altered pyroxene-rich rocks, and fragments similar to the interstitial altered phonolite. In some places phonolite fragments are predominant, and the brecciated character of the rock is not readily apparent except on weathered surfaces. Good exposures of breccia in the southwestern part of sec. 19 on the west side of Cove Creek contain abundant angular fragments averaging 1 inch in diameter that are composed of the same material as the groundmass. This suggests that the rock is an intrusive breccia formed by repeated pulses of phonolitic magma into previously partly cooled rock in the conduit of a volcano. One inclusion of light-colored syenite about 4 inches across indicates that at least some of the syenites are older than the altered phonolite. Upstream the breccia is very coarse, contains boulders as much as 3 feet across, and is cut by a pseudoleucite tinguaite dike. The predominant pieces are metamorphosed shale and novaculite. The included igneous types are chiefly pyroxene-rich por-

TABLE 15.—*Analyses and norms of altered phonolite, in percent*

	MC-114	MC-229
Chemical analyses [1]		
SiO_2	40.93	39.77
Al_2O_3	15.13	15.76
Fe_2O_3	1.32	1.53
FeO	6.86	7.85
Mno	.29	.31
MgO	1.74	2.40
CaO	10.71	8.88
BaO	.17	.16
Na_2O	7.19	7.32
K_2O	2.82	3.63
H_2O-	.04	.07
H_2O+	.84	1.25
TiO_2	2.23	2.76
CO_2	7.85	4.46
P_2O_5	.48	.68
SO_3	.22	.58
Cl	.42	.71
F	.24	.39
S	.88	2.46
Total	100.36	100.97
Less O	.42	.94
	99.94	100.03
Colorimetric analyses [3]		
As	0.004	n.d.
Sb	.0002	n.d.
W	.001	n.d.
Zn	.018	n.d.
Radiometric analyses [4]		
eU	0.003	0.005
Chemical analyses [5]		
U	0.00033	0.00040
Th	.00043	.00110

	MC-114	MC-229	MC-114a	MC-114b	MC-114c
Spectrographic analyses [2]					
Be	0.0005	0	0	0.002	0.001
Mg	n.d.	n.d.	.03	.8	1.0
Ca	n.d.	n.d.	.2	1-10	1-10
Sr	.071	.08	.0003	.3	.4
Ba	.29	.1	.07	.1	.2
B	0	0	0	0	0
Sc	.0005	0	0	0	.0002
Y	.0030	.008	0	0	.02
La	.032	.02	0	.01	.02
Yb	.0002	.0004	0	0	n.d.
Ti	n.d.	1.8	.06	1-10	1-10
Zr	.056	.04	.01	.03	.01
V	.052	.06	0	.07	.03
Nb	.015	.01	0	.02	.05
Cr	.0007	.001	0	.004	.0005
Mo	0	.003	0	0	0
Mn	.19	.1	.02	.4	.2
Co	.0021	.002	.02	.01	.009
Ni	.0009	0	.002	.02	.002
Cu	.0074	.005	.006	.03	.01
Ga	.0036	.002	.0003	.001	.001

	MC-114	MC-229
Norm		
C	1.53	
or	16.68	21.13
ab	32.49	16.77
an		4.45
ne	11.64	19.60
hl	.70	1.17
th	.43	.99
nc	.42	
di		3.86
ol	7.98	4.58
mt	1.86	2.09
il	4.26	5.32
ap	1.34	1.68
fr	.39	.62
pr	1.68	4.58
cc	17.40	10.20

[1] Standard chemical analysis. MC-114 by L. M. Kehl and MC-229 by L. N. Tarrant.

[2] Spectrographic analyses. MC-114 by H. J. Rose; MC-114a, b, c, by J. D. Fletcher; and MC-229 by Harry Bastron.

[3] Colorimetric analyses by H. E. Crowe and A. P. Marranzino.

[4] Radiometric analyses by B. A. McCall.

[5] Low-level uranium and thorium analyses by J. C. Antweiler.

n.d.=not determined.

Looked for (spectrographically) but not found: Li, Cs, Ce, Hf, Th, P, Ta, W, U, Re, Ru, Rh, Pd, Os, Ir, Pt, Au, Zn, Cd, Hg, In, Tl, Ge, Sn, As, Sb, Bi, Te.

MC-114. Altered phonolite, W½ sec. 18.
MC-229. Altered phonolite, NE¼ sec. 29.
MC-114a. Pyrite separate from MC-114.
MC-114b. Magnetic (hand magnet) fraction of heavy concentrate.
MC-114c. Nonmagnetic fraction of heavy concentrate.

phyritic basic rocks. The coarse breccia at this locality may be a contact breccia not related to the intrusive breccia described above.

Following is a description of the analyzed samples (table 15):

MC-114.—Altered phonolite. In thin section the rock has a microporphyritic texture. Lath-shaped relics of pyroxene(?) crystals up to 2 mm long are outlined by rims of fine-grained magnetite surrounding an aggregate of fine-grained green biotite, calcite, magnetite, and leucoxene. The fine-grained xenomorphic granular groundmass consists of green biotite, pyrite, magnetite or ilmenite, and sodic orthoclase and nepheline partly altered to calcite, cancrinite, and a sodalite group mineral. Euhedral apatite and late cubes of pyrite are scattered throughout the groundmass. Visual estimates of mineral percentages are: sodic orthoclase, nepheline, cancrinite, sodalite, 30; calcite, 15; biotite, 44; magnetite-ilmenite, 6; pyrite, 3; apatite, 2; leucoxene, trace.

MC-229.—Altered phonolite breccia. The breccia fragments average less than 1 inch in diameter and are composed of the same material as the groundmass, altered feldspathoidal trachyte. In the trachytic groundmass, euhedral apatite, anhedral sphene, anhedral magnetite, and anhedral green biotite are disseminated in sodic orthoclase, sodalite group minerals, plagioclase, and nepheline all partially replaced by calcite, sodalite group minerals, and cancrinite. Euhedral and anhedral pyrite is late. A visually estimated mode follows: calcite, 10; sodic orthoclase, plagioclase and nepheline, 55; sodalite group minerals, 5; biotite, 20; pyrite and magnetite, 5; apatite and sphene, 5.

CHEMISTRY

Chemical and spectrographic analyses and norms of this rock type are given in table 15. The chemical analyses most closely resemble that of ijolite, particularly in the K_2O–Na_2O ratio and silica content. Silica is much too low for a normal phonolite and it seems doubtful that it would escape during deuteric alteration in a quick-cooling rock. However, if the analysis is recalculated omitting the CO_2 the silica content would more closely approximate that expectable in a phonolite.

There is little agreement between the chemical analyses and the estimated mode. There is not sufficient K_2O and MgO to make a rock containing more than 40 percent common biotite. This suggests that the green mica is a biotite of unusual composition in which sodium probably substitutes for potassium and ferrous iron for magnesium. If so, normative corundum, olivine, and a portion of albite and nepheline appear in the mode as biotite. Thus the salic portions of the norm are reduced to a more reasonable agreement with the mode. The fluorine is probably also in the modal biotite. The isotropic mineral of the mode is interpreted from the high Cl and SO_3 in the analysis to be a member of the sodalite group.

In general, the rock was too fine grained to separate the various minerals but a pyrite separate was hand picked for spectrographic analysis (table 15). Iron, cobalt, nickel, and lead are concentrated in the pyrite. Two separates of that portion of the rock greater in specific gravity than 3.3 were made with the hand magnet. The most magnetic fraction is dominantly magnetite-ilmentite, and the other fraction is a mixture of pyrite, pyroxene, and leucoxene (table 15).

Trace elements in the whole rock that exceed or are equal to 0.01 percent include Sr, B, La, Ti, Zr, V, Nb, and Mn. Of these Sr, Ti, V, Nb, and Mn seem to be concentrated in the heavy fraction of the rock.

ORIGIN

The uniform distribution and abundance of calcite in the altered phonolite suggest that the alteration of this rock is not due to local hydrothermal activity but is a product of deuteric reactions. The magma, heavily charged with CO_2, water, Cl, and F, cooled quickly so that all the gases did not escape but reacted with the early formed mafic minerals to form calcite, biotite, and magnetite, but still preserving the crystal outline of the mafic minerals. The feldspar and to some extent, the nepheline, appear to have been less subject to deuteric alteration. This interpretation agrees with our concept of volcanic activity at Magnet Cove. Thus, this rock represents the portion of phonolitic magma trapped in parts of the ring conduit during the waning stages of volcanic eruption.

Local hydrothermal activity associated with the emplacement of feldspar-carbonate-rutile veins in the fractured and brecciated phonolite introduced additional carbonate to this rock unit, particularly in sec. 18.

UNDIVIDED TRACHYTE-PHONOLITE

DISTRIBUTION AND DESCRIPTION

The undivided trachyte-phonolite unit, about 20 percent of the exposed igneous complex, forms the horseshoe-shaped ridge that separates the garnet ijolite from the garnet-pseudoleucite syenite in the eastern half of the complex. These are the rocks that Williams (1891) mapped as metamorphosed sandstones and shales.

The trachytes-phonolites are all holocrystalline aphanites that range in color from light gray to greenish gray and dark gray and include alkalic trachyte, calci-alkalic trachyte, and nepheline trachyte or phonolite. Porphyritic, microporphyritic, trachytic, subtrachytic, xenomorphic granular, and amygdaloidal textures are represented. They weather to a fine-grained gray to brown saprolite. Locally the rocks are brecciated and contain abundant calcite and pyrite. A coarser grained foliated rock that occurs in contact with garnet ijolite has been mapped separately as banded trachyte.

Mineralogically the rocks contain such felsic minerals as sodic orthoclase, plagioclase (albite or andesine), nepheline, analcime, and sodalite group minerals. Mafic minerals are diopside-hedenbergite, biotite, garnet, hornblende, aegirine, and aegirine-diopside. Sphene, magnetite-ilmenite, pyrite, pyrrhotite, apatite, and fluorite are accessory minerals. There are no extensive exposures of the trachyte-phonolite but fresh rock is readily available from the abundant float and intermittent outcrops.

Abundant breccia float is found just south and east of the center of sec. 19. The angular breccia fragments average less than 1 inch in diameter, and are similar in composition and grain size to the groundmass trachyte except for a higher percentage of dark minerals. A few very dense and light-colored fragments may be pieces of sedimentary rocks.

In the southwestern part of sec. 19, a breccia is well exposed on the east bank of Cove Creek. Angular fragments of metamorphosed sediments up to several feet across and smaller, less abundant fragments of fine- to coarse-grained pyroxene-rich rocks are found in a matrix of altered melaphonolite.

The undivided trachyte-phonolite grades into a banded trachyte that becomes progressively more foliated and coarser grained toward the garnet ijolite contact (pl. 1). The nearly vertical foliation banding trends parallel to the garnet ijolite contact and the ring structure of the trachyte. In thin section the foliation consists of layers of anhedral equidimensional crystals of light- and dark-colored minerals alternating with discontinuous layers of predominantly dark-colored minerals. The layers bend around the inclusions of dark-colored pyroxene-rich rocks that are locally present in the foliated zone.

Some of the variants of the undivided trachyte are described below:

MC-138 (*NW1/4 sec. 19*).—Altered phonolite with amygdaloidal texture. The groundmass is composed of plagioclase, sodic-orthoclase, and nepheline all partly replaced by zeolites (about 50 percent of the rock); ragged brownish-green hornblende; anhedral green biotite; apatite; sphene; pyrite; and magnetite rimmed with sphene. The edge of the amygdules is usually rimmed with pale-brown to colorless garnet (andradite?)

and the centers contain calcite, colorless diopside, pyrite, zeolite, garnet and wollastonite.

MC–170 (*NE1/4 sec. 20*).—Phonolite (table 16). The texture is xenomorphic granular. About 80 percent of the minerals in the rock are felsic and include nepheline, minor albite, and sodic orthoclase slightly altered to sericite. The remaining minerals are brownish-green hornblende (about 15 percent) and the accessory minerals—sphene, brown garnet, pyrite, pyrrhotite, apatite, colorless fluorite and rare calcite.

MC–227 (*SW¼ sec. 20*).—Altered alkalic trachyte (table 16). In thin section aggregates of pale-brown biotite and anhedral magnetite appear to have replaced early phenocrysts of pyroxene(?). These together with the disseminated darker minerals, pale-brown biotite, magnetite, sphene, apatite, pyrite, and green hornblende occur in a subtrachytic groundmass of sodic orthoclase and albite. Melilite(?), colorless to brown garnet, colorless diopside, and calcite appear to have been introduced as small irregular veinlets. An estimated mode of the rock shows the following proportions: 55 percent sodic orthoclase and albite, 30 percent biotite and the remaining minerals in accessory amounts.

L–122 (*NE¼ sec. 20*).—Saprolite of calci-alkalic trachyte (table 16). In thin sections of hard rock, corroded phenocrysts of anorthoclase or sanidine are scattered through a subtrachytic groundmass of sodic orthoclase, andesine, greenish-brown biotite, magnetite, pyrite, and pyrrhotite. There is a minor sericite alteration of the anorthoclase and sodic orthoclase. Material in the concentrate panned from the saprolite occurs in the following order of abundance: clay aggregates, feldspar, and magnetite. From an X-ray analysis of the clay minerals in the clay- and silt-size portion of the saprolite, A. J. Gude 3d (written communication, 1956) reported major illite and minor montmorillonite.

L–162 (*NE¼ sec. 24*).—Microporphyritic alkalic trachyte. Corroded phenocrysts of diopside-hedenbergite and magnetite with sphene are set in a subtrachytic groundmass of sodic orthoclase that forms subhedral laths and equidimensional anhedra. The sodic orthoclase is partly altered to deuteric analcime(?), cancrinite, and calcite. The diopside-hedenbergite is altered to aegirine-diopside and brown biotite. Sphene forms a reaction border on the magnetite. Pyrrhotite is rare.

L–152a (*central part of sec. 19*).—Phonolite. The rock has a xenomorphic granular texture, and consists of about 15 percent nepheline and analcime or sodalite group, and about 77 percent sodic orthoclase. The remainder consists of brownish-green biotite and less abundant pyrite, magnetite, and sphene.

L–85 (*NW¼ sec. 20*).—Saprolite of banded alkalic syenite (table 16). In thin section the rock appears as an equigranular mosaic of orthoclase (about 68 percent), plagioclase (about 5 percent), sodalite or analcime (about 3 percent), and dark-colored minerals (about 25 percent) including olive-green hornblende, green aegirine-diopside and accessory apatite, sphene, magnetite, and pyrite. Some of the orthoclase and hornblende crystals contain poikilitic inclusions of other minerals. Magnetite crystals are commonly rimmed with sphene. Material in the panned concentrate occurs in about the following order of abundance: clay aggregates, orthoclase, weathered pyrite, magnetite, sphene, and apatite. From an X-ray analysis for the clay minerals on the clay- and silt-size portion of the saprolite, A. J. Gude 3d (written communication, 1956) reported major kaolinite and minor montmorillonite.

MC–171 (*NW¼ sec. 20*).—Banded nepheline syenite (table 16). In thin section a few ravaged and cloudy phenocrysts of orthoclase remain in an equigranular mosaic of orthoclase (clear), nepheline, cancrinite, sodalite, green hornblende, green aegirine-diopside, sphene, apatite, colorless to pale-green biotite, pyrrhotite, and zoisite(?).

L–159 (*SW¼ sec. 20*).—Dark-gray, very fine-grained foliated melaphonolite. The texture is xenomorphic granular with the dark-colored minerals in slightly smaller equant crystals than the light-colored minerals. The minerals include orthoclase, albite, nepheline partly altered to cancrinite, neutral to very pale green diopside, and the accessories—sphene, pale-brown biotite, pyrrhotite, and apatite.

L–101 (*central part of sec. 19*).—Calci-alkalic trachyte. The texture in most of the thin sections is xenomorphic equigranular but in some subhedral orthoclase laths lie with the long dimension roughly parallel to the foliation. Estimated mineral percentages are: orthoclase, 58; andesine, 20; perthite, 2; and the dark minerals (about 20 percent) which include green hornblende and accessory amounts of sphene, apatite, biotite and magnetite.

In general, the contact between banded trachyte and garnet ijolite is poorly exposed. However, in the central part of sec. 19 (L–153, pl. 1) a fair exposure of garnet ijolite near the contact has a crude foliation caused by an imperfect segregation of light- and dark-colored minerals. In thin section the rock shows a xenomorphic granular texture and is composed of nepheline (about 40 percent), a micrographic intergrowth of orthoclase and nepheline (about 40 percent), zoned brown to colorless garnet, pale-green diopside partly altered to pale-red and pale-green biotite, and accessory apatite, pyrite, magnetite, and sphene. The ratio of orthoclase to nepheline in the intergrowth is about 2 to 1. This is probably a contaminated garnet ijolite. Sample L–161, from a poor exposure in central part of sec. 20, appears to be the same rock in the same relationship to the contact as that described above. In thin section, however, there is only about 8 percent orthoclase and no intergrowth with nepheline. This rock is even closer to the feldspar-free garnet ijolite. The interpretation is that younger garnet ijolite near the contact has reacted with the more silica-rich trachyte producing some orthoclase in the garnet ijolite.

CHEMISTRY

The chemical and spectrographic analysis and norms, table 16, of the undivided trachyte-phonolite and banded trachyte show the phonolitic composition of these rocks; however, CaO and total Fe are higher and silica is lower than in average phonolite.

The analyses also show a wide composition range for these rocks, particularly in CaO and alkali. High Cl and SO_3 in the banded trachyte (MC–171) suggests a member of the sodalite group in the mode. Fluorine occurs in the apatite and biotite.

In the altered alkalic trachyte, MC–227, not enough K_2O was reported to make the abundant orthoclase and biotite, and the amount of MgO reported is also insufficient to make a rock containing 30 percent of normal biotite. Sodium and perhaps some calcium probably substitute for potassium and ferrous iron for magnesium.

TABLE 16.—*Analyses, norms, and mode of the undivided trachyte-phonolite, in percent*

	MC-170	MC-227	MC-171	(1)
	Standard chemical analyses [2]			
SiO_2	52.60	50.48	49.62	56.90
Al_2O_3	22.18	20.98	19.13	20.17
Fe_2O_3	.29	2.29	1.04	2.26
FeO	3.83	5.16	5.59	1.85
MnO	.27	.29	.23	.19
MgO	.33	1.65	1.68	.58
CaO	3.67	5.11	6.52	1.88
BaO	.29	.18	.14	
Na_2O	5.61	5.96	6.93	8.72
K_2O	7.41	3.39	4.81	5.42
H_2O-	.10	.11	.07	
H_2O+	1.61	.99	.63	.96
TiO_2	.71	2.21	1.97	.59
CO_2	.00	.31	.05	
P_2O_5	.07	.37	.38	.17
SO_3	.11	.01	.10	.13
Cl	<.01	.00	.25	.23
F	.36	.35	.22	
S	1.02	.36	1.57	
Total	100.46	100.20	100.93	
Less O	.66	.24	.93	
	99.80	99.96	100.00	

	MC-170	MC-227	L-122	MC-171	MC-171-1	L-85
	Spectrographic analyses [3]					
Be	0.002	0	0.0002	0.001	0	0.0009
Mg	.2	n.d.	.1	1-10	n.d.	.4
Ca	>10	n.d.	.2	>10	n.d.	.5
Sr	.5	.08	.07	.5	.05	.08
Ba	.2	.1	.2	.2	.002	.3
B	0	0	.004	0	0	.002
Sc	0	0	0	.0003	.0004	.002
Y	0	.007	0	.007	.04	.002
La	.02	.02	.009	.02	.04	0
Yb	0	.0002	0	.0004	n.d.	.0005
Ti	.50	1.1	.2	1.9	>10	1
Zr	.02	.04	.05	.03	.4	.05
V	.021	.02	.008	.029	.2	.04
Nb	.01	.01	.01	.02	.3	.02
Cr	.0004	.001	.002	.001	.0008	.002
Mo	0	0	0	.0007	0	.001
Mn	.3	.1	.09	.2	.07	.2
Fe	1-10	n.d.	3.0	1-10	n.d.	5
Co	0	.001	.002	.002	0	.002
Ni	0	0	.001	.001	.006	.0009
Cu	.0008	0	.001	.003	.02	.002
Ga	.001	.002	.004	.001	0	.005
Sn	0	0	0	0	.003	n.d.
Pb	.002	0	.001	0	0	.001
	Colorimetric analyses [5]					
As	<0.001		0.001	<0.001		<0.001
Sb	.0001		.0002	.0003		.0002
Zn	.01		.01	<.002		.013
	Radiometric analyses [6]					
eU	0.006	0.003	0.005	0.004		0.002
	Chemical analyses [7]					
U	0.00043	0.00025		0.00029		
Th	.00101	.00069		.00053		

	MC-170	MC-227	MC-171
	Norms		
C		.61	
or	43.92	20.02	28.36
ab	12.58	34.58	14.15
an	13.62	18.63	8.06
ne	18.74	8.52	22.72
hl			.35
th			.14
nc			.11
di	1.43		15.52
ol	3.07	5.66	
mt	.46	3.25	1.39
il	1.37	4.26	3.80
ap	.34	1.01	1.01
fr	.78	.62	.39
pr	1.95	.69	2.91
cc		.70	
wo			.58

	MC-171
Mode [4]	
Orthoclase	37
Nepheline	21
Cancrinite	1
Sodalite group	6
Aegirine-diopside.	21
Hornblende	5
Biotite	1
Sphene	1
Apatite	1
Pyrrhotite	6

[1] Average phonolite (Nockolds, 1954).

[2] Standard chemical analysis. MC-170, MC-171 by S. M. Berthold; MC-227 by L. N. Tarrant.

[3] Spectrographic analyses. MC-170, MC-171 by J. D. Fletcher; MC-227 by Harry Bastron; L-122, L-85 by Sol Berman; MC-171-1 by H. J. Rose.

[4] Mode by D. J. Jameson.

[5] Colorimetric analyses by H. E. Crowe and A. P. Marranzino.

[6] Radiometric analyses by B. A. McCall.

[7] Low-level uranium and thorium chemical analyses by J. C. Antweiler.

n.d.—not determined.

Looked for (spectrographically) but not found: Li, Cs, Ce, Hf, Th, P, Ta, W, U, Re, Ru, Rh, Pd, Os, Ir, Pt, Ag, Au, Zn, Cd, Hg, In, Tl, Ge, As, Sb, Bi, Te.

MC-170. Phonolite, NE¼ sec. 20.
MC-171. Banded nepheline syenite, NW¼ sec. 20.
MC-171-1. Sphene from MC-171.
L-85. Saprolite of banded alkalic syenite, NW¼ sec. 20.
L-122. Saprolite of calci-alkalic trachyte, NE¼ sec. 20.

Compared with the average of the analyses of the igneous rocks in the Magnet Cove complex (table 46) the trachytes are lower in MgO, total iron, MnO, CaO, CO_2, P_2O_5, SO_3, and higher in SiO_2 and Al_2O_3.

Trace elements that exceed 0.01 percent include Sr, Ba, La, Zr, V, and Nb. Spectrographic analysis of sphene from the banded trachyte show that Zr, Nb, V, and Cu, are concentrated in this mineral.

ORIGIN

As mentioned previously these rocks were mapped by Williams (1891) as metamorphosed sandstones and shales and his interpretation has been followed by later workers in the area. However, the field and laboratory evidence indicates an igneous origin for these rocks. Following are the observations that led us to this conclusion:

1. Trachytic and phonolitic composition, mineralogically and chemically.
2. Lack of any residual sedimentary structures or bedding throughout the entire width of exposure—up to 2,500 feet. Paleozoic units cannot be traced through this unit.
3. Trace element distribution is about the same as in other igneous rocks of the area.
4. Local development of breccia with trachyte matrix.
5. Projection of the sedimentary section from outside the complex would put novaculite in position as one of the units to be metamorphosed. It is not reasonable that metamorphism of novaculite would produce a subsilicic rock.
6. Arcuate shape of the rock body, discordant to the folds in the sedimentary rocks but similar to those of other intrusive bodies.

INNER CORE

The inner core rocks occupy a topographic basin and consist chiefly of mineralogic and textural varieties of ijolite, carbonatite, and lime-silicate rocks.

IJOLITE

DISTRIBUTION AND DESCRIPTION

Ijolite, a feldspar-free rock composed chiefly of nepheline, pyroxene, titanium garnet, biotite and magnetite, occupies a topographic low in the central part of the complex and has been divided—on the basis of grain size, and the proportion of biotite—into two map units, biotite-garnet ijolite and garnet ijolite.

Biotite-garnet ijolite, about 7 percent of the exposed igneous rocks of the complex, occupies the central part of the basin and is well exposed in the creekbed in front of the Magnet Cove church on U.S. Highway 270. It is surrounded by garnet ijolite and the contact appears to be gradational. Colluvium and alluvium are thick over parts of the area particularly at the lower altitudes and outcrops of fresh rock are very scarce. The samples for chemical analyses were taken from resistant boulders in saprolite.

Biotite-garnet ijolite ranges from a medium grained to a very coarse grained phanerite (pegmatitic). Masses of nepheline, garnet, and magnetite as much as 4 inches across and mica plates that reach 6 inches across occur as local segregation pods and stringers. The color of the fresh rock is a mottled mixture of the white and pink of nepheline, white of zeolites, brown and black of garnet, green of diopside, green and black of biotite, and some yellow of pyrite. The unit shows increasing intensity of alteration on approaching the lime silicate mass exposed in the Kimzey magnetite pit in the NW¼ sec. 20.

Garnet ijolite ranges in composition from a dark-gray fine-grained phanerite to a meuium-grained mottled phanerite. Both rock types weather to a saprolite mottled in gray, brown, pink, and black.

Although the grain size and relative proportions of the minerals of the ijolitic rocks vary widely (urtite to melteigite), the absence of feldspar and abundance of black titanium garnet is diagnostic. In thin section these rocks have a holocrystalline hypautomorphic-granular texture. The chief minerals are nepheline, black titanium garnet, pyroxene, and biotite partly altered to phlogopite. Apatite, pyrrhotite, perovskite, sphene, and primary calcite are accessory minerals. Thomsonite is abundant as an alteration product of nepheline particularly around the periphery of the magnetite pit area in sec. 20, and on Cove Creek where the ijolite is in contact with carbonatite. Cancrinite and calcite are other common alteration products; late-forming biotite is sometimes developed at the expense of pyroxene.

The largest single crystals and masses of nepheline are found in the ijolite and range from less than 1 mm to several inches in diameter. The color ranges from greasy grayish white to brown to deep pink. Commonly the large crystals have only a residual core of nepheline and are replaced by white birefringent zeolite, calcite, cancrinite, idocrase, colorless garnet, pectolite, and tremolite. Nepheline (10 to 95 percent of the rock) is older than garnet or biotite but probably later than pyroxene.

A light-green diopsidic pyroxene with high birefringence is generally the earliest formed mineral and comprises from less than 5 to more than 50 percent of the rock. Many of the grains have a mottled appearance under crossed nicols, caused by patches of slightly greener pyroxene that go to extinction at a different position from the almost colorless material. The green patches appear to be early and residual, have slightly lower birefringence and are most abundant in the interior of the grains. No pyroxene crystals larger than 1 inch in diameter have been observed whereas some crystals of garnet, mica, and nepheline are several inches in diameter.

Garnet is a late-forming mineral that occurs both as irregular anhedral masses and as euhedral crystals. Poikilitic inclusions of altered nepheline and pyroxene are common. The color of the garnet in thin section ranges from light brown to very dark brown which probably is a reflection of the titanium content. In some thin sections of the biotite-garnet ijolite, the garnet contains residual cores of purple perovskite.

Biotite, probably closer to phlogopite, is pleochroic in shades of light green. A few residual brown patches suggest that original dark-brown biotite has been altered to a pale phlogopite mica. The mica, like garnet, is a late-forming mineral and commonly occurs as mica-rich stringers or dikelets in the ijolite.

CHEMISTRY

Chemical and spectrographic analyses, norms, and modes of garnet ijolite and biotite-garnet ijolite, table 17 are similar to Nockolds' average ijolite (table 18). The only appreciable consistent difference is the lower Na_2O and higher CaO in the Magnet Cove rocks. The Magnet Cove ijolites are characterized by high CaO, high alkali and low silica. Individual rocks show appreciable differences in SiO_2, Fe_2O_3, P_2O_5, and TiO_2 which are a reflection of the relative proportions of the chief constituent minerals. The high H_2O^+ reflects zeolite alteration of nepheline.

A member of the sodalite group in the mode is deduced from the sulfur trioxide in the analyses; fluorine in the analysis is probably in biotite.

Trace elements in the ijolites that are equal to or exceed 0.01 percent include: Sr, Ba, Zr, and V.

Spectrographic analyses of minerals separated from the ijolite group (tables 19 and 20) show the distribution of the trace elements.

TABLE 17.—*Analyses, norms, and modes of biotite-garnet ijolite and garnet ijolite, in percent*

Standard chemical analyses [1]

	Sample No. MC-216	L-17	L-123
SiO_2	35.46	41.19	43.36
Al_2O_3	18.60	17.99	19.12
Fe_2O_3	7.90	5.63	2.85
FeO	3.27	1.76	1.44
MnO	.25	.30	.25
MgO	4.16	3.06	5.21
CaO	12.66	14.61	12.62
BaO	.10	.06	.01
Na_2O	6.34	6.85	7.88
K_2O	3.07	2.38	2.82
H_2O-	.33	.40	.58
H_2O+	3.46	3.13	2.56
TiO_2	2.47	1.67	.56
CO_2	.17	.46	.66
P_2O_5	1.08	.41	.05
SO_3	.03	.07	.06
Cl	.00	.01	.00
F	.16	.04	.03
S	.97	.41	.16
Total	100.48	100.43	100.22
Less O	.31	.23	.05
	100.17	100.20	100.17

Spectrographic analyses [2]

	Sample No. MC-216	L-17	L-123	L-125	L-93	L-123-b
Be	0.0008	0.002	0.004	0.0005	0.0002	0.001
Sr	.5	.08	.6	.04	.01	.01
Ba	.1	.02	.03	.3	.2	.2
B	0	.002	0	.002	0	.002
Sc	.0003	0	.001	.002	.003	.006
Y	.004	.003	0	.006	.004	.02
La	0	.005	0	0	0	0
Ce	n.d.	n.d.	n.d.	0	.03	0
Yb	.0002	.0008	0	.0005	.0004	.002
Ti	n.d.	n.d.	n.d.	1	1	5
Zr	.01	.03	.02	.007	.06	.08
V	.04	.1	.02	.03	.02	.1
Nb	.005	.002	0	.01	0	.04
Cr	0	0	.0004	.002	.0009	.007
Mo	0	0	0	0	0	.001
Mn	.1	.2	.1	.1	.2	.6
Co	.003	.0005	.001	.003	.0006	.009
Ni	0	0	0	.0005	0	.001
Cu	.004	.003	.0009	.01	.002	.002
Ga	.003	.003	.003	.002	.001	.004

Colorimetric analyses [4]

	MC-216	L-17	L-123	L-125	L-93	L-123-b
As	<0.001	<0.001	<0.001	<0.001	<0.001	<0.001
Sb	.0002	.0001	.0003	.0002	.0002	.0001
Zn	.020	<.002	<.002	.010	.013	.005

Radiometric analyses [5]

	MC-216	L-17	L-123	L-125	L-93	L-123-b
eU	0.002	<0.001	<0.001	<0.001	0.003	<0.001

Chemical analyses [6]

	MC-216	L-17	L-123	L-125	L-93	L-123-b
U	0.00021	0.00038	----------	----------	----------	----------
Th	.00028	.00063	----------	----------	----------	----------

Norms

	Sample No. MC-216	L-17	L-123
or		1.11	
an	13.07	11.40	8.62
lc	14.39	10.46	13.08
ne	28.97	30.96	35.78
th		.14	.14
di	7.56	16.42	28.08
wo		14.50	1.39
ol	4.90		
cs	9.63		3.10
mt	.70	.46	3.02
hm	7.36	5.28	.80
il	4.71	3.19	1.06
ap	2.69	1.01	
fr	.07		.07
pr	1.80	.75	.27
cc	.40	1.00	1.50

Modes [3]

	Sample No. MC-216	L-17	L-123	L-93
Nepheline	60	29	62	30
Cancrinite				
Zeolite (birefringent)		33		10
Calcite		2	2	Tr.
Tremolite(?)		1		
Sodalite group and (or) analcime.		2	2	
Diopside	2	12	24	30
Biotite	10	4		
Perovskite	2	2	8	Tr.
Garnet	20	12		30
Sphene		Tr.	Tr.	Tr.
Apatite	2	2	Tr.	
Pyrite	2	1	Tr.	
Magnetite	2	Tr.	2	Tr.

[1] Standard chemical analyses. MC-216 by L. N. Tarrant;L-17 by L. M. Kehl; L-123 by L. N. Tarrant.
[2] Spectrographic analyses. MC-216, L-17, L-123 by J. D. Fletcher; L-125, L-93, L-123 by Sol Berman.
[3] Modes. MC-216, L-93, L-123, by R. L. Erickson; L-17 by L. V. Blade.
[4] Colorimetric analyses by H. E. Crowe and A. P. Marranzino.
[5] Radiometric analyses by B. A. McCall.
[6] Low level chemical analyses of uranium and thorium by J. C. Antweiler.

n.d.=not determined.
Looked for (spectrographically) but not found: Hf, Th, P, Ta, W, U, Re, Ru, Rh, Pd, Os, Ir, Pt, Ag, Au, Zn, Cd, Hg, In, Tl, Ge, Sn, Pb, As, Sb, Bi, Te.

MC-216. Biotite garnet ijolite, E½ sec. 19.
L-17. Garnet ijolite, NE¼ sec. 19.
L-123. Garnet ijolite, NW¼ sec. 20.
L-125. Saprolite of biotite garnet ijolite, W½ sec. 20.
L-93. Garnet ijolite, mode on fresh rock, spectrographic analyses on saprolite, NW¼ sec. 20.
L-123b. Saprolite of garnet ijolite, NW¼ sec. 20.

TABLE 18.—*Average and type urtite, ijolite, and melteigite*

	Chemical analyses (percent)					
	1	2	3	4	5	6
SiO_2	42. 59	42. 58	41. 90	45. 43	42. 79	40. 64
Al_2O_3	27. 42	18. 46	12. 20	28. 77	19. 89	10. 58
Fe_2O_3	2. 49	4. 01	6. 41	3. 10	4. 39	4. 18
FeO	1. 89	4. 19	4. 32	. 40	2. 33	4. 18
MnO	. 09	. 20	. 22		. 41	. 28
MgO	. 69	3. 22	5. 45	. 22	1. 87	6. 47
CaO	4. 38	11. 38	16. 60	1. 86	11. 76	19. 91
BaO						. 11
Na_2O	14. 12	9. 55	5. 10	16. 16	9. 31	4. 75
K_2O	3. 82	2. 55	2. 66	3. 38	1. 67	1. 86
H_2O					. 99	. 14
H_2O+	. 42	. 55	. 87			. 27
TiO_2	. 35	1. 41	2. 21		1. 10	2. 24
CO_2	1. 30	. 38	. 82			2. 08
P_2O_5	. 44	1. 52	1. 24		1. 70	1. 91
Cl						. 03
F						. 12
S						. 05
ZrO_2						. 10
Total	--------	--------	--------	99. 32	99. 81	99. 90

	Modes (percent		
	4	5	6
Nepheline	85. 72	49. 41	20. 86
Cancrinite			4. 83
Muscovite			1. 23
Apatite	1. 97	4. 02	4. 53
Biotite			6. 16
Pyroxene	11. 96	41. 86	47. 14
Garnet		2. 15	4. 43
Sphene		1. 67	4. 23
Microlith			. 86
Magnetite			. 61
Calcite			5. 50

1. Nockolds' average urtite (1954).
2. Nockolds' average ijolite (1954).
3. Nockolds' average melteigite (1954).
4. Type urtite—Lujavr-Urt, Kola Peninsula—Ramsay, 1896, from Johannsen (1938)
5. Type ijolite—Iiwaara, Finland-Ramsay and Berghell, 1891, from Johannsen (1938).
6. Type melteigite—Fen District, Norway—Brogger, 1921, from Johannsen (1938).

1. Strontium is concentrated in apatite, calcite, and pyroxene.
2. Beryllium and molybdenum are concentrated almost exclusively in zeolite (up to 0. 02 percent Be and 0. 003 percent Mo).
3. Lanthanum and yttrium are in perovskite and apatite.
4. Scandium occurs chiefly in diopside.
5. Zirconium is concentrated in sphene (0. 6 percent) and dark garnet.
6. Vanadium occurs chiefly in garnet, diopside, sphene, and apatite.
7. Niobium is concentrated in perovskite and sphene with lesser amounts in dark garnet.
8. Cobalt, nickel, and copper occur chiefly in pyrite and to a lesser extent, in garnet. Copper also occurs in concentration up to 0. 01 percent in perovskite.
9. Gallium occurs chiefly in the felsic minerals but is also detected in biotite and garnet.

Spectrographic analyses of the saprolites show the following effects of weathering on the trace elements: a loss of Be and Sr; and a gain of Ba, Sc,Y, Zr,Nb, Cr, Ni, and Cu. Resistant perovskite accounts for a part of the concentration of Sc, Y, Nb, and Cu; resistant garnet accounts for the concentration of Zr and a part of the Sc, Y, Nb, Cr, Ni, and Cu; resistant biotite accounts for a part of the concentration of Ba, resistant apatite accounts for a part of the concentration of Y and Cr; resistant magnetite probably accounts for a part of the Cr, Ni, and Cu.

FINE-GRAINED IJOLITE

DISTRIBUTION AND DESCRIPTION

Fine-grained ijolite, about 5 percent of the exposed igneous rocks of the complex, is found as a topographic low in the west-central part of the complex. Fresh rock exposures are rare, but saprolite is abundant. The concealed contact between altered phonolite and fine-grained ijolite was delimited by samples of saprolite taken with a power auger, but the alluvium in Cove Creek valley, which conceals the contact between fine-grained ijolite and garnet ijolite, could not be penetrated with the auger.

The rock ranges in composition from melteigite to ijolite; in grain size from a dense aphanite to medium-grained phanerite; and in color from gray and greenish gray to dark gray. It weathers to a saprolite colored various shades of brown and gray and often mottled in these colors. The dense aphanite is easily confused with the dark trachytes except that when the garnet content of this ijolite is high the rock has a distinctive resinous luster. The chief minerals are pyroxene, biotite, nepheline, and garnet. The textures include porphyritic, glomero-porphyritic, xenomorphic-granular, micro-porphyritic, amygdaloidal, and fine-grained breccia; all are holocrystalline.

Some of the variants are described below:

MC-217 (*NW¼ NW¼ sec. 19*).—A dark-gray aphanite with a few fragments of grayish-green altered alkalic trachyte. The aphanitic groundmass has a xenomorphic-granular texture and is composed of calcite, sodalite group, and nepheline partly altered to cancrinite—about 15 percent; pale brownish-green biotite, brown garnet (melanite), pale-green diopside, sphene, apatite, magnetite-ilmenite, and pyrite—about 85 percent. The altered alkalic trachyte fragments are composed of about 68 percent sodic orthoclase; 2 percent calcite and analcime and (or) sodalite group; and 30 percent brown biotite, sphene, apatite, and pyrite.

TABLE 19.—*Spectrographic analyses of mineral separates of biotite-garnet ijolite, in percent*

[Spectrographic analyses by H. J. Rose]

	L-133-1	MC-216-10	MC-216-7	MC-216-8	MC-216-9	MC-216-5	MC-216-4	MC-216-6	MC-216-3	MC-216-1	MC-216-2
Be	0	0	0	0	0	0.0003	0	0	0.0005	0.0005	0.0006
Mg	n.d.	n.d.	n.d.	n.d.	n.d.	n.d.	n.d.	.01	n.d.	.3	.3
Sr	.1	.2	.05	.05	.01	.5	.006	.84	.4	.01	.06
Ba	0	.002	0	0	.002	.003	.1	.02	.06	.001	.001
B	0	n.d.	0	0	0	0	.002	.002	.001	.01	.02
Al	n.d.	n.d.	n.d.	n.d.	n.d.	n.d.	n.d.	.04	n.d.	>10	>10
Sc	.0004	.0004	.0009	.0009	0	0	0	0	0	0	0
Y	.069	.02	.03	.03	0	0	.002	.02	0	0	0
La	.04	.1	0	0	0	0	0	.04	0	0	0
Ti	>10	>10	>10	>10	.6	.05	1.1	.006	.01	.009	.008
Zr	0	0	.1	.1	0	0	0	0	0	0	0
P	0	0	0	0	0	0	0	>10	0	0	0
V	.07	.04	.2	.2	.09	.03	.009	.1	.03	.005	.008
Nb	.36	.9	.03	.03	0	0	0	0	0	0	0
Cr	0	0	0	0	0	.0003	0	.0009	.0004	0	0
Mo	0	0	0	0	0	0	0	0	.0004	.002	.003
Mn	.03	.04	.005	.3	.2	.3	.3	.01	.007	.01	.005
Fe	n.d.	n.d.	n.d.	n.d.	n.d.	n.d.	n.d.	.04	n.d.	.3	.3
Co	0	0	.002	.002	0	.0005	.005	0	0	0	0
Ni	0	0	.009	.009	.005	0	0	0	0	0	0
Cu	.011	.01	.003	.01	.0005	.0002	.001	.0002	.0004	.0002	.0006
Ga	0	0	.001	.0009	.001	.0003	.003	0	.003	.002	.002
Sn	0	.003	.003	.003	.002	.1	0	.004	0	0	0
Specific gravity		4±.1	3.5±.1	3.8±.1	3.8±.1	3.1±.2	----------	3.1±.2	2.65±.05	2.25±.05	2.35±.05
Indices of refraction[1]											
						$\alpha=1.677\pm.005$ $\beta=1.682\pm.005$ $\gamma=1.699\pm.005$	----------	----------	$\epsilon=1.539\pm.002$ $\omega=1.545\pm.002$	----------	----------

[1] Determined by D. J. Jameson.

n.d.=not determined.

Looked for but not found: Ce, Yb, Th, Ta, W, Re, Pd, Ir, Pt, Ag, Au, Zn, Cd, Hg, In, Ge, Pb, As, Sb, Bi.

EXPLANATION OF SAMPLES

	Sample	X-ray	Analyst
L-133-1	Perovskite		
MC-216-10	do		
MC-216-7	Dark garnet		
MC-216-8	do	Andradite(?) slightly larger unit cell.	F. A. Hildebrand.
MC-216-9	Yellow garnet	Andradite	Do.
MC-216-5	Diopside		
MC-216-4	Phlogopite		
MC-216-6	Apatite		
MC-216-3	Nepheline		
MC-216-1	Zeolite	Natrolite	Do.
MC-216-2	do	do	Do.

L-327 (*SW¼ sec. 17.*)—Porphyritic micromelteigite composed of corroded phenocrysts of very pale reddish-brown diopside-hedenbergite rimmed with pale-green diopside and partly altered to pale greenish-brown biotite, calcite, sphene, and brown garnet; pale-green diopside; greenish-brown biotite; anhedral to euhedral brown to colorless garnet; sphene; apatite; pyrrhotite; late anhedral nepheline; late anhedral member of the sodalite group; and late calcite.

L-3 (*SW¼ sec. 18*).—Gray, fine-grained ijolite with xenomorphic-granular texture and composed of pale greenish-brown biotite, brown to colorless garnet, green aegirine, sphene, apatite, pyrite—about 30 percent; and zeolite(?) which poikilitically includes all of the above minerals—about 70 percent. The mineral tentatively identified as a zeolite is colorless, uniaxial positive, birefringence about 0.008, and index less than 1.537. It probably is an alteration product of nepheline. From an X-ray analysis of the silt- and clay-size portion of the saprolite, A. J. Gude 3d (written communication, 1956) reported major montmorillonite and minor chlorite.

L-19 (*NW¼ sec. 19*).—Greenish-gray ijolite with xenomorphic-granular texture and composed of pale-green diopside, brown to colorless garnet, pale greenish-brown biotite, sphene, apatite, pyrite and magnetite—about 45 percent; an interstitial sodalite group mineral or analcime and late calcite—about 55 percent.

L-92 (*SW¼ sec. 17*).—Dark-gray ijolite with xenomorphic-granular texture composed of sphene, brown to colorless garnet, pale greenish-brown biotite, pale-green diopside, euhedral apatite, and pyrrhotite—about 42 percent; interstitial nepheline and sodalite group mineral or analcime—about 52 percent; and late calcite—about 6 percent.

L-157 (*SE¼ sec. 19*).—This dark-gray aphanite has a fine-grained amygdaloidal texture. The amygdules (up to 1 mm in diam) are irregular in shape and are intermittently connected to form chains that are crudely parallel and give a lineated appearance to the rock. In thin section the amygdules are filled by anhedral calcite and rimmed with brown to colorless garnet. Minerals in the rock are pale-bluish-green hornblende, brown to colorless garnet, brown biotite, sphene, colorless to pale-green diopside, apatite, pyrite, pyrrhotite, and magnetite—about 55 percent; and nepheline partly altered to calcite and analcime or sodalite group mineral—about 45 percent.

Along Cove Creek north of the bridge on U.S. 270, the fine-grained ijolite has been altered by the later

TABLE 20.—*Spectrographic analyses of mineral separates of garnet ijolite, in percent*

	L-123-9	L-17-11	L-123-8	L-17-9	L-17-10	L-17-8	L-17-7	L-123-6	L-123-7	L-17-6	L-17-1	L-123-5	L-123-4	L-17-5	L-17-4	L-123-3	L-123-1	L-123-2	L-17-2	L-17-3
Be	0	0	0	0	0	0	0.0005	0.0003	0.0003	0.0003	0	0	0	0.0003	0.0005	0.0003	0.0005	0.0005	0.02	0.01
Mg	n.d.	n.d.	n.d.	n.d.	n.d.	n.d.	n.d.	n.d.	n.d.	n.d.	.002	.01	.05	.03	n.d.	n.d.	.2	.1	.04	.03
Sr	0	0	.01	.08	.06	.07	.5	.4	.3	.3	1-5	.84	.84	.84	.2	.2	.004	.01	1-5	.8
Ba	.002	.004	.004	.003	0	0	.003	.003	.002	.005	.02	.009	.1	.1	.04	.01	.01	.01	.2	.06
B	0	0	0	0	0	0	0	0	0	0	0	0	.001	.001	.003	0	.006	.004	.002	0
Al	n.d.	n.d.	n.d.	n.d.	n.d.	n.d.	n.d.	n.d.	n.d.	n.d.	n.d.	.05	.08	.09	n.d.	n.d.	>10	>10	n.d.	n.d.
Sc	0	0	.007	.0003	0	.0001	.01	.001	0	0	0	0	0	0	0	.001	0	0	0	0
Y	0	0	.03	.02	.005	.009	.001	0	0	0	.01	.004	0	0	0	0	0	0	0	0
La	0	0	0	0	0	.01	.002	0	0	0	.01	.05	.002	.002	0	0	0	0	0	0
Yb	0	n.d.	0	n.d.	n.d.	n.d.	n.d.	0	0	n.d.	.0002	0	0	0	n.d.	0	0	0	0	0
Ti	.004	.004	>10	>10	1.2	>10	.05	.0004	.0003	.04	0	.003	.002	.007	.007	.006	.004	.005	.009	.004
Zr	0	0	.3	.2	.01	.6	.02	0	0	0	0	0	0	0	0	0	0	0	0	0
P	0	0	0	0	0	0	0	0	0	0	n.d.	>10	0	0	0	0	0	0	n.d.	n.d.
V	0	0	.2	.3	.3	.4	.2	.08	.05	.1	.1	.1	.003	.003	.02	.03	.007	.004	.001	.001
Nb	0	0	.01	.01	0	.2	0	0	0	0	0	0	0	0	0	0	0	0	0	0
Cr	0	0	.002	0	0	0	.0003	.001	.0008	.0003	0	0	0	0	.0004	.0004	0	0	0	.00009
Mo	0	0	0	0	0	0	0	0	0	0	0	0	0	0	0	0	.001	.002	.0005	.0006
Mn	.005	.02	.2	.2	.2	.01	.4	.2	.2	.2	.02	.01	.04	.03	.01	.004	.01	.008	.004	.003
Fe	n.d.	n.d.	n.d.	n.d.	n.d.	n.d.	n.d.	n.d.	n.d.	n.d.	.02	.03	.1	.1	n.d.	n.d.	.07	.1	.07	.05
Co	.03	.1	.001	.001	.0008	0	.002	.0003	.0003	.0003	0	0	0	0	0	0	0	0	0	0
Ni	.01	.004	.007	.02	.02	.01	.002	0	0	0	0	0	0	0	0	0	0	0	0	0
Cu	.02	.02	.004	.002	.0004	.001	.0003	.0004	.0004	.0002	.0003	.0002	.0003	.0004	.0002	0	.0003	.0003	.0007	.0005
Ga	0	0	.001	.001	.004	0	.0004	0	0	.0004	0	0	0	0	.006	.004	.007	.003	.0007	.0007
Sn	0	0	.003	.001	0	.002	0	.03	.06	0	.003	0	0	0	0	0	0	0	0	0
Pb	.002	0	0	0	0	0	0	0	0	0	0	0	0	0	0	0	0	0	0	0
Specific gravity	--------	--------	3.8±.1	3.8±.1	3.8±.1	3.55±.05	3.1±.2	3.1±.2	3.1±.2	3.1±.2	3.1±.2	3.1±.2	2.8±.1	2.8±.1	2.65±.05	2.65±.05	2.25±.05	2.35±.05	2.5±.1	2.35±.05

Indices of refraction[1]

	L-17-7	L-123-6	L-123-7	L-17-6	L-17-4
α	1.695 ±.005	1.680 ±.005	1.673 ±.005	1.675 ±.005	
β	1.703 ±.005	1.685 ±.005	1.684 ±.005	1.683 ±.005	ϵ=1.543±0.002 ω=1.548±0.002
γ	1.719 ±.005	1.701 ±.005	1.703 ±.005	1.703 ±.005	

[1] Determined by D. J. Jameson.

n.d.=not determined.
Looked for but not found: Ce, Th, Ta, W, U, Re, Pd, Ir, Pt, Ag, Au, Zn, Cd, Hg, In, Tl, Ge, As, Sb, Bi.

EXPLANATION OF SAMPLES

	Sample	X-ray	Analyst	
			X-ray	Spectrographic
L-123-9	Pyrite			H. J. Rose.
L-17-11	do			Do.
L-123-8	Dark garnet			Do.
L-17-9	do			Do.
L-17-10	Yellow garnet			Do.
L-17-8	Sphene			Do.
L-17-7	Diopside			Do.
L-123-6	do	Monoclinic pyroxene probably diopside.	F. A. Hildebrand	Do.
L-123-7	do			Do.
L-17-6	do			J. D. Fletcher.
L-17-1	Apatite			H. J. Rose.
L-123-5	do			Do.
L-123-4	Calcite			Do.
L-17-5	do			Do.
L-17-4	Nepheline			Do.
L-123-3	do	Nepheline	F. A. Hildebrand	Do.
L-123-1	Zeolite	Natrolite	do	Do.
L-123-2	do	do	do	Do.
L-17-2	do	Thomsonite-gonnardite type.	do	J. D. Fletcher.
L-17-3	do	Zeolite-gonnardite	do	Do.

TABLE 21.—*Analyses, norms, and mode of fine-grained ijolite, in percent*

Standard chemical analyses[1]	MC-217	L-327
SiO_2	36.89	37.29
Al_2O_3	13.28	14.41
Fe_2O_3	7.58	4.23
FeO	3.71	6.10
MnO	.33	.32
MgO	4.22	4.15
CaO	14.80	13.69
BaO	.18	.14
Na_2O	5.29	5.61
K_2O	4.62	4.22
H_2O-	.14	.04
H_2O+	1.11	.69
TiO_2	3.32	3.46
CO_2	1.54	3.29
P_2O_5	.99	.77
SO_3	.80	.19
Cl	.41	.33
F	.40	.32
S	.95	2.43
Total	100.56	101.68
Less O	.50	1.43
	100.06	100.25

Spectrographic analyses[2]	MC-217	L-327	L-3	L-19	L-92	L-157	MC-217-1
Be	0.004	0.0002	0.0006	0.0004	0.0002	0.0003	0
Mg	n.d.	n.d.	2	2	3	.9	n.d.
Ca	n.d.	n.d.	>10	>5	>5	.1	n.d.
Sr	.5	.9	.03	.02	.06	.02	.08
Ba	.2	.2	.4	.2	.2	.3	.03
B	0	0	.001	0	0	.003	0
Sc	.0009	.002	.003	.002	.003	.002	.0009
Y	.005	.003	.01	.005	.006	.004	.01
La	.01	.009	.03	.006	.01	.02	0
Ce	n.d.	0	0	0	.06	0	n.d.
Yb	.0003	.0003	.0007	.001	.0005	.0005	n.d.
Ti	n.d.	n.d.	3	2	2	2	4.8
Zr	.03	.04	.03	.04	.04	.04	.06
V	.05	.1	.06	.08	.03	.04	.1
Nb	.01	.02	.02	.03	.02	.009	0
Cr	.0007	.003	.005	.002	.002	.004	.002
Mo	0	.0008	0	0	0	0	0
Mn	.2	n.d.	.3	.4	.2	.07	.2
Fe	n.d.	n.d.	5	>5	3	>10	n.d.
Co	.002	.002	.004	.002	.001	.003	.0008
Ni	.001	.0007	.002	.001	.001	.0007	.005
Cu	.005	.01	.01	.007	.01	.004	.006
Ga	.003	.003	.003	.003	.002	.004	.001
Sn	0	0	0	0	0	0	.001
Pb	0	0	.001	0	.004	.001	0
Colorimetric analyses[4]							
As	<0.001	n.d.	0.003	0.002	0.001	n.d.	
Sb	.0001	n.d.	.0004	.0004	.0002	n.d.	
Zn	.015	n.d.	.025	.015	.010	n.d.	
Radiometric analyses[5]							
eU	0.003	0.002	0.003	<0.001	0.002	<0.001	
Chemical analyses[6]							
U	0.00041	n.d.	n.d.	n.d.	n.d.	n.d.	
Th	.00060	n.d.	n.d.	n.d.	n.d.	n.d.	

Norms	MC-217	L-327
or	--------	3.89
an	3.34	3.89
lc	21.36	16.57
ne	19.60	23.28
hl	.70	.59
th	1.42	.43
di	22.90	22.46
wo	1.04	3.13
cs	5.04	
mt		1.86
hm	7.68	2.88
pf	0.14	
il	6.08	6.54
ap	2.35	2.02
fr	.62	.47
pr	1.80	4.48
cc	3.40	7.50

Mode[3]	L-327
Nepheline	14
Analcime or sodalite group.	7
Diopside-hedenbergite	40
Biotite	14
Garnet	4
Sphene	6
Apatite	3
Pyrrhotite	6
Calcite	6

[1] Standard chemical analyses. MC-217 by L. N. Tarrant and L-327 by M. K. Balazs.

[2] Spectrographic analyses. MC-217 by J. D. Fletcher; L-327, L-3, L-19, L-92, L-157 by Sol Berman; MC-217-1 by H. J. Rose.

[3] Mode by L. V. Blade.

[4] Colorimetric analyses by H. E. Crowe and A. P. Marranzino.

[5] Radiometric analyses. MC-217, L-3, L-19, L-92, L-157 by B. A. McCall; L-327 by J. P. Schafer.

[6] Low-level chemical analyses for uranium and thorium by J. C. Antweiler.

n.d.=not determined.

Looked for (spectrographically) but not found: Hf, Th, P, Ta, W, U, Re, Ru, Rh, Pd, Os, Ir, Pt, Ag, Au, Zn, Cd, Hg, In, Tl, Ge, As, Sb, Bi, Te.

MC-217. Micromelteigite breccia, NW¼ sec. 19.
L-327. Porphyritic micromelteigite, SW¼ sec. 17.
MC-217-1. Garnet (melanite) from MC-217.
L-3. Saprolite of fine-grained ijolite, NW¼ sec. 19.
L-19. Saprolite of fine-grained ijolite, NW¼ sec. 19.
L-92. Saprolite of fine-grained ijolite, SW¼ sec. 17.
L-157. Saprolite of micromelteigite, SE¼ sec. 19.

carbonatite. Nepheline is replaced by zeolite (probably thomsonite), brown garnet is partly altered to colorless garnet and idocrase, biotite and diopside are bleached, and a little tremolite (?) has formed. Abundant pale-green biotite has formed along calcite veinlets in the ijolite.

CHEMISTRY

The analyzed rocks (table 21) have a melteigite composition and are very similar to Nockolds' average melteigite (table 18); SiO_2, MgO, CaO, and P_2O_5 are lower, total iron oxides and Na_2O are about the same and Al_2O_3, MnO, K_2O, TiO_2, and CO_2 are higher. K_2O and TiO_2 are higher in these rocks than in the coarser grained ijolite. H_2O^+ is low, reflecting less zeolitic alteration in fine-grained rocks than in the more easily attacked coarse-grained ijolite.

From the abundant Cl and SO_3 in the analyses, the isotropic low index mineral in the mode is inferred to be some member of the sodalite group. Apatite and biotite probably account for the abundant fluorine.

Trace elements in the rock that exceed or are equal to 0.01 percent include: Sr, Ba, La, Ti, Zr, V, Nb, and Mn.

Spectrographic analysis of a dark-colored garnet separated from MC-217 (table 21) show that Ti, Zr, V, Ni, and Y are concentrated in the garnet.

Spectrographic analyses of saprolite compared with those of the fresh rock indicate that La, Y, Yb, and Pb are slightly concentrated and that Sr is lost during weathering. Resistant garnet would account for the concentration of Y and resistant sphene for the concentration of La. The concentration of Yb and Pb is not explainable on the available evidence.

CARBONATITE

DISTRIBUTION AND DESCRIPTION

Masses of coarse-grained calcite (carbonatite) that contain unusual accessory minerals including niobium-bearing perovskite and zirconium garnet (kimzeyite) are one of the most interesting rock types that occur at Magnet Cove. The carbonatite, about 1.8 percent of the exposed igneous rocks of the complex, is divided into two map units—carbonatite and residual phosphate. Residual phosphate is characterized by abundant float of a porous rock composed of apatite, magnetite, and perovskite in matrix of secondary apatite, whereas the carbonatite is characterized by calcite outcrops or residual apatite, magnetite, and perovskite in the saprolite. Core drilling by W. A. Keith established the presence of carbonatite under the areas mapped as residual phosphate. Logs and locations of the core holes are given in table 22. The carbonatite mapped in secs. 18, 19, and 20, represents the mappable bodies of this rock type but small stringers of calcite in the surrounding ijolite and reports of calcite found in several wells and drill holes in the immediate vicinity suggest that concealed bodies of carbonatite may exist. Although the carbonatite is more resistant than the surrounding ijolite, good exposures are rare; the best occur along Cove Creek and in the Kimzey calcite quarry in the northwestern part of sec. 19 (Fryklund, Harner, and Kaiser, 1954).

TABLE 22.—*Descriptive logs of core holes*

[All holes were drilled by W. A. Keith, lessee of much of the carbonatite area, with a Cooper rig using a wire-line core barrel. The cores were logged by L. V. Blade. Except where noted all descriptions are of recovered core; minerals are listed in decreasing order of abundance]

Hole L-130

Location: NW1/4 sec. 19.
Date drilled: August 23–28, 1954.

Depth (feet)	*Description*
0–37	Cuttings taken at surface, 10, 12, and 20 ft. Ijolite saprolite, weathered mica, garnet, apatite, clay.
37–72	Cavernous section, no samples taken. Probably carbonatite.
72–74	Vuggy carbonatite, coarse-grained calcite (75 percent), apatite, clay, pyrite, rutile, magnetite partly altered to hematite, fine-grained calcite, perovskite, mica, wavellite.
74–78	Vuggy carbonatite, coarse-grained calcite (80 percent), apatite, clay, magnetite, partly altered to hematite, pyrite, rutile, wavellite, chalcedony(?).
84–94	Vuggy carbonatite, coarse-grained calcite (80 percent), apatite, clay, pyrite, magnetite partly altered to hematite and limonite, rutile, biotite, perovskite, pale yellow mica, wavellite.
94–111	Cuttings, no core. Carbonatite, coarse calcite (90 percent), apatite, pyrite, magnetite, rutile.
111–115	No sample. Driller's log shows that hard rock (probably ijolite) was cut at 113 ft.
115–129	Cuttings, 60 to 90 percent ijolite, 40 to 10 percent carbonatite.
129–139	Ijolite cut by calcite veins.
139–145¼	Cuttings. Calcite.
145¼–146½	Ijolite and calcite with abundant biotite along the contact between the two.
146½–152	Ijolite with small stringers of calcite.
152–155	Ijolite.
155–156.7	Ijolite with pyrite-rich stringers at base of core.

Hole L-132

Location: NW¼ sec. 20
Date drilled: August 30–September 17, 1954

Depth (feet)	*Description*
0–22	Gossan composed of limonite, and minor hematite, mica, pyrite, apatite and magnetite.
22–28	Transition zone composed of partly weathered apatite-pyrite vein of grayish-green color and limonite.
28–44	Partly weathered grayish-green apatite-pyrite vein.
44–52	White clay. Minerals include pyrite, apatite, rutile, perovskite(?). Probably a rutile vein.
52–90	Partly weathered grayish-green, apatite-pyrite vein, and magnetite.
90–96	Apatite-magnetite rock. Magnetite up to 25 percent of rock.
96–106	Apatite-green biotite-magnetite rock. Apatite 85 to 90 percent.
106–116	Transition zone, apatite, biotite, magnetite, calcite. Apatite 85 to 90 percent.
116–139	Carbonatite cuttings, calcite 75 percent, apatite, biotite, magnetite.
139–221	Vuggy carbonatite, coarse-grained calcite 75 to 95 percent; apatite, biotite, magnetite and pyrite.
221–226	Upper 0.9 ft carbonatite, coarse-grained yellow calcite (90 percent), apatite, pyrite, biotite. Lower 1.2 ft vuggy carbonatite, coarse- and medium-grained calcite (60 percent), pyrite, montmorillonite(?), clay, apatite, biotite, minor garnet, rutile.
226–236	Soft interval, 227 to 230. Carbonatite, coarse- and medium-grained calcite (some white, black, and yellow, 90 percent), apatite, pyrite, biotite, minor magnetite, pyroxene.
236–242	Upper half: carbonatite, coarse- and medium-grained calcite (60 percent), pale-brown mica (phlogopite(?)), biotite, pyrite, apatite. Lower half: carbonatite, coarse- and medium-grained calcite (90 percent), pyrite, biotite, minor pale brown phlogopite(?), apatite.
242–244	No sample.
244–254	Carbonatite, coarse-grained calcite (75 percent), fine-grained calcite, biotite, phlogopite(?), pyrite, minor apatite, garnet.
254–254.7	Carbonatite, coarse-grained calcite (80 percent), apatite, biotite, minor monticellite, pyroxene, magnetite.
254.7–256	Carbonatite, coarse-grained calcite (60 percent), monticellite, magnetite, apatite, minor lemon yellow pyroxene, perovskite.
256–266	Carbonatite, coarse-grained calcite (80 to 95 percent), monticellite, apatite, pyroxene, magnetite, biotite.
266–289	Carbonatite, coarse-grained calcite (55 to 95 percent), apatite, biotite, magnetite, pyrite, pyroxene, amphibole.
289–294	Carbonatite, coarse-grained calcite (90 percent), apatite, cryptocrystalline green material, monticellite, magnetite, biotite, pyroxene, cryptocrystalline red material.
294–299	Carbonatite, coarse- and medium-grained calcite (60 percent), light-green cryptocrystalline material (a mixture of calcite and probably amphibole), apatite, biotite, magnetite, minor green amphibole, monticellite, pyrite, fine-grained purple calcite.

TABLE 22.—*Descriptive logs of core holes*—Continued

Hole L-132—Continued

Depth (feet)	*Description*
299–311	Carbonatite, coarse- and medium-grained calcite (80 percent), fine-grained green material, apatite, pyrite, biotite, magnetite, monticellite, amphibole, pyroxene, perovskite.
311–417	Carbonatite, coarse- and medium-grained calcite (70 to 95 percent), magnetite, apatite, biotite, monticellite, fine-grained brown material, fine-grained green material, pyroxene, fine-grained red material, pyrite, garnet(?), and fine-grained white material. Perovskite detected in interval from 311–321 ft.

Hole L-135

Location: Perovskite Hill NW1/4 sec. 19.
Date drilled: September 26–30, 1954.

Depth (feet)	*Description*
1–7	Mixture of alluvium and carbonatite saprolite. Alluvium in the slush pit 2 to 4 ft thick.
7–8	Magnetite (50 percent), coarse calcite, apatite, perovskite.
8–19	Carbonatite, calcite (90 percent), magnetite, apatite, perovskite, pyrite.

TABLE 22.—*Descriptive logs of core holes*—Continued

Hole L-135—Continued

Depth (feet)	*Description*
19–135	Very poor core recovery. Carbonatite-coarse-grained calcite (50 to 95 percent), apatite. monticellite, magnetite (some altered to hematite), fine-grained calcite (red, brown, and green), perovskite, amphibole(?), pyrite, chalcedony(?), blue clay, rutile.

Hole L-134

Location: NE1/4 sec. 19.
Date drilled: September 19–25, 1954.

Depth (feet)	*Description*
0–10	Mixture of carbonatite saprolite and alluvium. In the slush pit 10 feet north of the hole, alluvium is 2 to 3 ft thick lying on carbonatite saprolite.
10–106	Carbonatite, calcite ranges from 90 to 95 percent, apatite, biotite, magnetite, limonite, hematite, manganese oxides(?), pyrite. Minor rutile detected in following intervals: 39–71 and 84–101 ft.

The rock is composed chiefly of white to light-gray medium- to coarse-grained calcite with scattered irreg-

TABLE 23.—*Analyses of carbonatite, in percent*

														Colorimetric	
	L-304	L-166-2		L-304	L-12	L-166-a	L-117	L-135	L-170-a	L-170-b	L-131-a	L-131-b	L-131-c		L-117
	Standard chemical analyses			**Spectrographic analyses**										**Colorimetric analyses**	
SiO_2	1.90		Be	0.0001	0	0.002	0.0004	0.0005	0	0	0.0008	0.0005	[0.0002	As	0.0004
Al_2O_3	.33		Mg	n.d.	.2	3	.5	.5	1	.3	.03	.03	.08	Sb	.0004
Fe_2O_3	.42		Sr	.5	.5	.9	.9	.9	.9	.9	.2	.2	.1	Zn	.02
FeO	.32		Ba	.1	.2	.009	.3	.2	.02	.009	.2	.2	.05		
MnO	.26		B	0	0	.001	.001	.001	0	.001	.001	.001	.001		
MgO	1.05		Sc	0	.004	.002	.007	.007	.007	.007	.002	.002	.002		
CaO	53.37		Y	.004	.01	.009	.04	.03	.05	.04	.01	.01	.006		
BaO	.00		La	.03	.06	.04	.08	.08	.2	.2	.02	.08	.02		
Na_2O	.00		Ce	0	.3	.04	.3	.09	.5	.5	.02	.02	.02		
K_2O	.16		Yb	.0005	.002	.0004	.003	.003	.002	.002	.001	.0007	.0003		
H_2O-	.04		Ti	n.d.	.08	.6	.2	.6	1	1	.1	.07	.04		
H_2O+	.12		Zr	.001	.002	.03	.006	.02	.2	.2	.003	.002	.003		
TiO_2	.10		P	n.d.	.x	.x	xx	x	x	xx	xx	xx	xx		
CO_2	39.41		V	.02	.03	.004	.05	.06	.1	.1	.06	.04	.03		
P_2O_5	2.00		Nb	0	.05	.06	.02	.01	.2	.4	.02	0	.009		
SO_3	.02		Cr	0	.0007	.0004	.002	.002	.0008	.001	.001	.0008	.0008		
Cl	.00	.01	Mo	.001	0	.003	0	.004	0	0	.007	.009	0		
F	.15	.67	Mn	n.d.	.5	.1	.8	2	.5	.09	.5	.6	.1		
S	.09		Fe	n.d.	2	2	4	3	>5	1	2	1	1		
Total	99.74		Co	0	0	.002	.003	.001	.003	.002	0	0	0		
Less O	.11		Ni	0	0	0	.002	.001	.003	.004	.003	.003	.0006		
	99.63														
			Cu	.001	.004	.03	.07	.01	.001	.001	.01	.01	.004		
			Ga	0	0	.002	.001	.002	.002	0	0	0	0		
			Pb	0	0	0	.008	.003	0	0	0	0	0		
			Radiometric analyses												
eU				<0.001	<0.001	<0.001	0.004	0.001	0.004	0.007	<0.001	0.002	<0.001		
			Chemical analysis												
U				<0.001	n.d.	n.d.	n.d.	n.d.	n.d.	n.d.	n.d.	n.d.	n.d.		

n.d.=not determined.
Looked for (spectrographically) but not found: Hf, Th, Ta, W, U, Re, Ru, Rh, Pd, Os, Ir, Pt, Ag, Au, Zn, Cd, Hg, In, Tl, Ge, Sn, As, Sb, Bi, Te.

Standard chemical analyses. L-304 by M. K. Balazs; L-166-2 by L.N. Tarrant.
Spectrographic analyses by Sol Berman.
Radiometric analyses. L-304, by D. L. Schafer; all others by B. A. McCall.
Chemical analysis for uranium by J. P. Schuch.
Colorimetric analyses by H. E. Crowe and A. P. Marranzino.

L-304. Carbonatite, NW¼ sec. 19.
L-12. Black carbonatite, SW¼ sec. 18.
L-166-a. Altered inclusion in carbonatite, NW¼ sec. 19.
L-117. Carbonatite saprolite, NW¼ sec. 19.
L-135. Carbonatite saprolite, NW¼ sec. 19.
L-170-a. Carbonatite saprolite minus clay, NW¼ sec. 19.
L-170-b. Carbonatite saprolite minus clay, and hand magnetic fraction, NW¼ sec. 19.
L-131-a. Residual and secondary apatite, NW¼ sec. 19.
L-131-b. Residual and secondary apatite, NW¼ sec. 19.
L-131-c. Residual and secondary apatite, NW¼ sec. 19.
L-166-2. Apatite from carbonatite.

ular areas enriched in apatite, brown monticellite, magnetite, black perovskite, black zirconium garnet (kimzeyite), green biotite, and pyrite. Minute irregularly shaped black inclusions agglomerated and disseminated in the calcite have produced a black medium-grained variant found in contact with the analcime-olivine melagabbro in the southern part of sec. 18.

Inclusions of ijolite a few inches to more than 50 feet across occur in the carbonatite. The larger blocks in the quarry have reaction rims of varying thickness. Fryklund, Harner, and Kaiser (1954) have described a typical rim composed of three zones:

1. A narrow outer zone, usually less than 1 inch wide, of magnetite and pyrrhotite lying in a medium-grained calcite matrix.
2. An intermediate zone rich in green biotite. Some biotite grains may reach 1 centimeter in diameter.
3. A fine-grained idocrase-rich inner zone of variable width, in some cases including the whole block. A few large idocrase crystals, reaching 3 to 4 centimeters in length, are present in these zones.

The alteration of the ijolite inclusions is similar to the alteration along the contact of the carbonatite and ijolite and involved thorough replacement of nepheline by zeolite (probably thomsonite), partial to complete alteration of brown garnet to colorless garnet and idocrase, bleaching of the biotite, and the formation of tremolite(?) and pectolite(?).

Weathering of the carbonatite yields two products—a black or brown saprolite and the porous rock composed of both residual and secondary apatite. The latter rock was called tufa by Williams (1891), but Fryklund, Harner, and Kaiser (1954) suggested it was a product of weathering, and we concur. Near the Kimzey calcite quarry the secondary apatite can be seen on the surface of the fresh rock. Several apatite samples were analyzed (tables 23 and 24). The samples are described below:

L–131, 131a, 131b, and 131c.—These samples are composed of residual apatite, magnetite, and perovskite in a matrix of sec-

TABLE 24.—*Analyses of saprolite of carbonatite, in percent*

	L–117	L–117–a	L–117–b	L–131	L–135	L–135–a	L–135–b	L–170–a	L–170–b
Standard phosphate analyses [Analysts. G. Edgington and E. Y. Campbell]									
Al_2O_3	11.4	1.1	0.8	2.1	15.2	3.7	3.0	2.7	2.7
Fe_1O_3	8.0	3.3	1.0	1.4	8.8	4.0	3.4	12.2	1.8
CaO	24.9	47.9	51.5	50.4	16.1	40.3	41.7	43.9	48.5
P_2O_5	19.7	37.2	40.4	36.8	14.7	31.6	32.2	29.2	31.6
F	.31	.43	.35	1.9	.93	1.5	1.5	.26	.27
Acid insoluble	25.3	9.1	4.8	1.7	31.9	11.3	10.9	17.4	14.6
Radiometric analyses [Analyst. B. A. McCall]									
eU	0.007	0.006	0.005	0.002	0.003	0.004	0.004	0.006	0.007
Chemical analyses [Analysts. A. Sweeney and Wendell Tucker]									
U	0.003	0.005	0.004	0.002	0.001	0.002	0.005	0.005	0.007

Semiquantitative spectrographic analyses
[Analyst. K. E. Valentine]

Sample (percent)	L–117	L–117–a	L–117–b	L–131	L–135	L–135–a	L–135–b	L–170–a	L–170–b
>10	Al	Ca, P	Ca, P	Ca, P	Al	Ca, P	Ca, P	Ca, P	Ca, P.
5–10	Ca, P, Si				Ca, P, Si				Ti
1–5	Fe	Si, Fe	Si	Al, Fe	Fe, Mg	Si, Al, Mg, Fe	Si, Al, K, Fe	Ti, Fe, Al	Si, Al, Fe
0.5–1	Sr, Mg	Al, Sr	Sr	Si, Sr	Mn, K, Sr, Ti	Mn, K, La, Sr	Mg, Sr, La	Mg, Sr, La, Si	Sr, La, Mg
0.1–0.5	K, La, Mn, Ti, Ba, Pb, Ce, Na	La, Mg, Ce, Y, Na, Mn, V	Fe, La, Ce, Al, Na, Mg	Mn, Ba, Mg	La, Ce, Y, Li	Ce, Na, Y, Ti, Li	Mn, Ti, Ce, Na, Y, Li	Zr, Na, Ce, Mn	Ce, V, Y, Zr, Mn, Na
0.05–0.1	Nd, V, Y, Li	Nd, Li	Mn, V, Y, Nd, Li	Na, Ti, Li, V, K	Ba, V, Na	Ba, V, Nd	Nd, Ba, V	Nd, V, Y	Nd, Ba
0.01–0.05	Cu, B, Pr	B, Pr, Ba, K, Ti, Pb, Cu	Ti, Pr, K, Ba	Ce, La, Y, B, Nd	Nd, Pr, Yb	Pr, Yb	Pr	Nb, Li, K, Ba, Pr	Nb, Li, K, Pr
0.005–0.01	Zr, Nb, Yb, Ga, Dy	Nb, Gd, Dy, Yb	Pb, Gd, Yb, B, Cu, Dy Er	Cu	B, Ga, Dy, Cu, Pb	B, Gd, Er, Dy, Pb	B, Er, Gd, Dy, Yb	B	
0.001–0.005	Er, Ni, Sc	Er, Zr, Ni, Sc.	Ni, Zr, Nb, Co, Sc	Ni, Zr, Mo, Nb, Yb	Zr, Er, Ni, Sc, Mo, Nb	Sc, Nb, Zr, Ni, Cu, Mo	Cu, Nb, Pb, Mo, Sc, Ni, Zr	Sn, Yb, Ni, Sc	Dy, Yb, Ni, Sc
0.0005–0.001	Cr, Be	Cr	Cr	Cr, Sc	Cr	Cr	Cr	Cu, Cr	Cu, Cr
0.0001–0.0005	Ag	Ag		Be	Be	Be	Be		
0.00005–0.0001		Be	Ag	Ag					
0.00001–0.00005			Be					Be	

L–117. Carbonatite saprolite, NW¼ sec. 19.
L–117–a. Carbonatite saprolite minus clay, NW¼ sec. 19.
L–117–b. Carbonatite saprolite minus clay and hand magnetic fraction, NW¼ sec. 19.
L–131. Residual and secondary apatite, NW¼ sec. 19.
L–135. Carbonatite saprolite, NW¼ sec. 19.
L–135–a. Carbonatite saprolite minus clay, NW¼ sec. 19.
L–135–b. Carbonatite saprolite minus clay and hand magnetic fraction, NW¼ sec. 19.
L–170–a. Carbonatite saprolite minus clay, NW¼ sec. 19.
L–170–b. Carbonatite saprolite minus clay and hand magnetic fraction NW¼ sec. 19.

ondary apatite. The secondary apatite occurs in cryptocrystalline granular masses and as radiating fibers in colloform crusts.

L–117 and L–135.—Saprolite. From X-ray analyses of the clay- and silt-size portion of these saprolites, A. J. Gude 3d, (written communication, 1956) reported major montmorillonite and minor kaolinite in L–117 and major kaolinite, and traces of montmorillonite and chlorite in L–135.

L–117a, 135a, and 170a.—Panned concentrates of the saprolite. Of the saprolite, L–117-a represents about 40 percent and L–135a represents about 26 percent.

L–117b, 135b, and 170b.—Panned concentrates with the hand magnetic fraction (mostly magnetite) removed. Visual estimates of the composition of these fractions are as follows: L–117b (39 percent of the saprolite) apatite 90 percent, and the remainder—iron-stained clay aggregates, weathered pyrite, rutile, perovskite, and anatase. L–135b (25.5 percent of the saprolite) apatite 70 percent, and the remainder—iron-stained clay aggregates, weathered pyrite, rutile, perovskite and anatase. L–170b apatite 90 percent, and the remainder—perovskite, anatase, kimzeyite, and mica.

CHEMISTRY

Chemical and spectrographic analyses of a composite of the carbonatite in the quarry, table 23, show that the carbonatite is a relatively pure calcite rock. Phosphate, silica, and magnesia are the only other oxides greater than 1 percent. The magnesia occurs chiefly in magnetite (magnesioferrite) and monticellite; phosphate occurs in light-green acicular crystals of apatite. The early crystallization of these minerals as well as perovskite and kimzeyite provided for the capture of most of the trace elements and explains the high purity of the late crystallizing calcite.

Trace elements in the rock that are equal to or exceed 0.01 percent and in order of abundance include: Sr, Mn, Ba, Ti, and V. The difficulty of getting a representative sample of the carbonatite is illustrated by the content of niobium in the carbonatite. Fryklund, Harner, and Kaiser (1954) cut 21 channel samples of the carbonatite for Nb, TiO_2, V_2O_5, Y, and La analysis. Niobium was detected in only 6 of the samples, but a simple average yields a value of 0.01 percent niobium for the carbonatite.

From the standard phosphate analyses (table 24) of the concentrates of the saprolite, it is obvious that the grade is adequate for commercial phosphate. How-

TABLE 25.—*Spectrographic analyses of mineral separates from carbonatite, in percent*

	L–166–1	L–166–2	L–166–3	L–166–4	L–166–5	L–166–6	L–135–a	L–129–c	L–129–d
Be	0.003	0	0	0	0	0	0.001	0	0
Mg	>10	.03	.1	>10	>10	.5	n.d.	.0x	.0x
Ca	n.d.	n.d.	n.d.	n.d.	n.d.	n.d.	n.d.	>10	>10
Sr	.1	.1	.5	.008	0	.01	.02	.x	.x
Ba	.002	.002	.02	0	0	.002	.005	.0x	.0x
Sc	.0004	.0006	0	0	.001	.02	.001	.00x	.00x
Y	.004	.02	0	.02	0	.1	.19	.0x	.0x
La	.04	.1	0	0	0	.04	.2	x	x
Ti	.5	.005	.005	.01	1.0	3.2	>10	n.d.	n.d.
Zr	.06	0	0	0	.03	>10	.63	0	0
P	0	>10	0	0	0	0	2.0	0	0
V	.04	.2	.03	.006	.07	.01	.92	.025	.025
Nb	.02	0	0	0	.03	.2	6.8	8.2	9.2
Cr	.002	.0007	.003	.002	.0007	.001	.0002	.000x	.000x
Mn	.02	.002	.01	1.2	2.7	.05	.13	.0x	.0x
Co	0	0	0	.004	.01	0	0	0	0
Ni	0	.002	0	0	0	0	.006	.00x	.00x
Cu	.0009	.0004	.0006	.0009	.001	.0006	.018	.00x	.00x
Ga	.004	0	0	0	.009	.008	0	0	0
Sn	0	0	0	0	0	.02	0	0	0
Pb	0	0	0	0	0	0	.004	0	0

n.d.—not determined.
Looked for but not found: B, Yb, Hf, Th, Ta, Mo, W, U, Re, Rh, Pd, Ir, Pt, Ag, Au, Zn, Cd, Hg, In, Tl, Ge, As, Sb, Bi.

EXPLANATION OF SAMPLES

	Sample	X-ray	X-ray analyst	Spectrographic analyst
L–166–1	Idocrase			H. J. Rose.
L–166–2	Apatite			Do.
L–166–3	Calcite			Do.
L–166–4	Monticellite			Do.
L–166–5	Magnetite			Do.
L–166–6	Kimzeyite			Do.
L–135–a	Anatase	Anatase and small amount of apatite.	F. A. Hildebrand	Do.
L–129–c	Perovskite			J. D. Fletcher.
L–129–d	Perovskite			Do.

ever, more drilling and sampling must be done to determine the size of the deposit.

Several minerals were separated from the carbonatite in the quarry for spectrographic analyses (table 25). The anatase and perovskite are float crystals found south of the quarry on Perovskite Hill. The fine-grained pale-brown anatase occurs as an alteration product of perovskite with the replacement varying from partial to complete. Anatase in this rock has been observed only in the saprolite and thus it may be a product of weathering as suggested by Williams (1891).

The zirconium garnet is a new mineral, and has been named kimzeyite (Milton and Blade, 1958). Individual crystals as much as 2 mm across are black and where euhedral have the crystal habit of garnet, the dodecahedron in combination with the trapezohedron. X-ray work by J. M. Axelrod and F. A. Hildebrand indicates that the mineral is isotypic with garnet; the cell edge $(a_0)=12.46A$. In thin section, it is isotropic, light brown, and has an index of refraction near 1.95. The computed oxide percentages from spectrographic analyses by Harry Bastron (table 26) show relatively high Nb, Sc, and Sn content. The total is low; however, P_2O_5, H_2O, F, S, and CO_2 were not tested. Further work on this mineral is in progress by Charles Milton.

TABLE 26.—*Composition of kimzeyite*

[Data from Milton and Blade (1958)]

Element	Amount (percent)	Computed as oxide	
		Oxide	Percent
Si	10	SiO_2	21.4
Al	6	Al_2O_3	11.4
Ca	12	CaO	16.8
Fe	11.5	Fe_2O_3	16.45
Ti	3.5	TiO_2	5.8
Zr	15	ZrO_2	20.25
Nb	.5	Nb_2O_5	.72
Mg	.3	MgO	.5
Mn	.1	MnO	.13
Sn	.07	SnO_2	.09
Sc	.06	Sc_2O_3	.09
Cu, Ba, Sr	Tr.		
Total			94

Looked for but found: Ag, Au, Hg, Ru, Rh, Pd, Ce, Ir, Ge, Pb, As, Sb, Pt, Mo, W, Re, Bi, Zn, Cd, Te, In, Co, Ni, Ga, Cr, V, Y, La, Hf, Th, Ta, Be, Li, Na, K, B.

The distribution of the trace elements within the carbonatite is shown by the spectrographic analyses of the separated minerals.

1. The calcite is relatively pure; Sr is the most abundant trace element (0.5 percent) followed by V, Ba, and Mn, in order of abundance.
2. The high magnesium content of magnetite indicates that it is more properly called magnesioferrite.
3. Strontium occurs in calcite, perovskite, apatite and idocrase.
4. Scandium is in kimzeyite.
5. Lanthanum is particularly concentrated in perovskite (greater than 1 percent) and to a lesser extent in anatase and apatite.
6. Zirconium occurs as a major constituent in kimzeyite and is also found in anatase (0.63 percent) with lesser amounts in idocrase.
7. Vanadium is in anatase (0.92 percent), apatite and magnetite.
8. Niobium is highly concentrated in perovskite and anatase (up to 9.2 percent).
9. Cobalt and gallium occur in magnetite; gallium is in kimzeyite.
10. Nickel and copper are most abundant in anatase.
11. Yttrium is most abundant in anatase and kimzeyite.

The trace-element content of the carbonatite saprolite shows that Be, Sr, Ba, Sc, Y, La, Ce, Yb, Ti, Zr, P, V, Nb, Cr, Mn, Co, Ni, Cu, Ga, and Pb, are concentrated during weathering. Resistant minerals account for most of the concentration of these elements particularly because the easily weathered calcite is poor in trace elements.

ORIGIN

The origin of similar carbonate bodies from other localities has been ascribed to sedimentary limestone xenoliths, hydrothermal replacement bodies, and magmatic intrusions. Reexamination of these various modes of origin as well as detailed studies of alkalic rock complexes have been stimulated recently by the economic potential of carbonatite deposits for commodities such as niobium, rare earths, apatite, uranium, and agricultural lime.

Pecora (1956) reviewed the carbonatite problem and listed 32 worldwide occurrences which appear to have originated "from a hot carbonatic fluid genetically derived through some magmatic process." He concludes from his review that "carbonatites were deposited by carbonatic solutions having a wide range of temperature, pressure, and concentration and derived from alkalic magmas during the process of silicate crystallization." And further that "a carbonate magma in the normal sense is less likely to exist than carbonate-rich solutions which at elevated temperature and pressure can have a higher concentration of dissolved ingredients than normally believed for hydrothermal solutions."

The field observation and laboratory work on the Magnet Cove carbonatite indicate that it is an intrusive mass and probably was deposited from late-stage heavily gas charged, magmatic solutions. Some of the observations are listed below:

1. Virtual absence of limestone in the known Paleozoic section of this region of Arkansas.
2. Abundance of inclusions of syenitic and possibly ijolitic type rocks in the carbonate body. These inclusions range in size from a few inches to blocks 7 to 8 feet long and

have a strong reaction zone characterized by an outer rim of pyrrhotite, magnetite, green biotite, and idocrase. Many of the inclusions are completely altered to mica, zoisite(?), and an impure aggregate that may be zeolitic alteration of nepheline. The inclusions attest to the introduced, mobile, and reactive character of the carbonate and indicate that the carbonate body is younger than most of the igneous rocks and probably represents a late stage in the development of the Magnet Cove complex.

3. Absence of any structure or layering in the coarsely crystalline mass of calcite.
4. Abundance of carbonate as a major constituent of the feldspar-carbonate pyrite-rutile veins and dikes that cut the igneous rocks and are so abundant in the Magnet Cove area.
5. Abundance of coarsely crystalline calcite dikes that cut ijolite in the basin of the Cove area.
6. The abundance of rare earths, niobium, titanium, and zirconium in the silicate minerals in the carbonatite that could not be supplied by a normal sedimentary limestone, nor by reaction with the included blocks of igneous rock. These elements must have been a part of the carbonate mass as it moved into its present position.
7. The presence of primary calcite in coarse-grained ijolite rocks that occupy most of the Cove basin. Fine-grained calcite is a major constituent of the altered phonolite and phonolite breccia which we believe is produced by reaction of trapped CO_2 with early-formed minerals in quick-cooling magma.
8. Calcite-pyroxene-nepheline pegmatite also testify to primary nature of calcite.

These observations indicate that the carbonatite bodies at Magnet Cove are not sedimentary limestone xenoliths. The mobile introduced nature of the carbonate has been firmly established but whether this introduction is hydrothermal or magmatic is not so easily resolved. However, primary calcite in many of the rocks even to the extent of being a major constituent of the altered phonolite and one of the pegmatites suggests that the carbonate is a late stage differentiate—pegmatitelike—on the borderline between magmatic and hydrothermal, greatly enriched in CO_2, Ti, Nb, and rare earths. The origin of the carbonatite is further discussed in the section on origin of the rocks.

LIME-SILICATE ROCK

A complex body of lime-silicate rock, about 0.4 percent of the exposed igneous rocks in the complex, occurs in the northwestern part of sec. 20. Like the surrounding ijolite it is deeply weathered, and therefore age relations with the ijolite are not determinable. Small areas of fresh rock are exposed in a pit opened to mine residual magnetite.

The bulk of the rock is a fine- to medium-grained intergrowth of anhedral idocrase and colorless diopside with a few euhedral crystal of apatite. Abundant miarolitic cavities are lined with euhedral crystals of diopside, aegirine, apatite, idocrase, and andradite. A few large crystals of melilite, some more than 18 inches across, are partly replaced by a fine- to coarse-grained mixture of idocrase, diopside, tremolite, pale brownish-green biotite, perovskite, brown to colorless garnet, calcite, and zeolite. Irregular but rounded masses of magnetite, up to 1 foot across, are found, some alined like beads on a string in the idocrase-diopside matrix. Pieces of fine-grained zeolite with miarolitic cavities containing euhedral crystals of natrolite were found on the waste-rock dump but none were seen in place. The melilite with its alteration products looks similar to the uncompahgrite of the Iron Hill complex in Colorado. It seems most probable that the rock type is a basic crystal differentiate of magnetite, melilite, and minor feldspathoid from the ijolite magma and that its contact with the surrounding ijolite is gradational. Late introduction of the high-volatile carbonatite fluids probably caused the intense alteration of melilite. Carbonatite occurs within 500 feet to the northwest of the lime-silicate body.

Spectrographic analyses of several handpicked minerals, table 27, show that:

1. Magnetite is both titaniferous and magnesian probably close to magnesioferrite. The trace elements in this magnetite in order of abundance are: Mn, V, Co, Zr, Zn, Ga, and Sc.
2. The three analyzed garnets show the direct relationship between dark color and high titanium content. V, Zr, Nb, and Y are concentrated only in the dark garnet.
3. Aegirine captures the greatest amount and variety of trace elements of the analyzed minerals. In order of abundance these include: Zr, Sr, Nb, Mn, V, Y, Ba, Cu, Be, Co, Sc, Ga, Cr, Ag. Concentration ranges from 0.2 percent Zr to 0.0003 percent Ag.
4. The bulk of the Sc is in colorless diopside (0.01 percent).
5. Sr is particularly high in apatite, idocrase, and melilite; barium is in biotite.

DIKES

Although the entire Magnet Cove igneous area is a dike complex, the rocks described in this section are clearly late stage, of minor areal extent, and show cross-cutting relationships to the major ring dike rock units.

These dike rocks will be described in two sections: dikes within the complex and dikes outside the complex.

DIKES WITHIN THE COMPLEX

Dike rocks within the complex include in approximate order of abundance: tinguaite, analcime olivine melagabbro, nepheline syenite pegmatite, trachyte porphyry, aplite, eudialyte nepheline pegmatite, and garnet fourchite.

TINGUAITE

DISTRIBUTION AND DESCRIPTION

Tinguaite (dike phonolite), the most abundant dike rock exclusive of ring dikes in the Magnet Cove igneous complex, occurs as narrow, fine-grained, green to black dikes and irregular or oval-shaped bodies that cut all other igneous rock types. Some of the tinguaites are porphyritic and contain pseudoleucite and (or) nephe-

TABLE 27.—*Spectrographic analyses, in percent, of mineral separates of lime-silicate rock*

	L-168-2	L-168-5	L-168-6	L-168-11	L-168-7	L-168-13	L-168-14	L-168-10	L-168-8	L-168-4	L-168-12	L-168-3	L-168-1	L-168-9
Be	0	0	0	0.0004	0.0004	0.0009	0.004	0.002	0.004	0	0	0	0.002	0.0009
Mg	>1	.4	.2	.09	>1	>1	>1	>1	>1	1	.1	.02	>1	.06
Sr	0	.002	.002	.005	.1	.1	.04	1.2	.6	.005	1	.2	.6	.007
Ba	0	.002	0	.002	.01	.002	.007	.04	.004	1.2	.005	.02	.01	.007
Sc	.004	.006	0	0	0	.01	.001	0	0	.004	0	0	0	0
Y	0	.02	0	0	0	0	.01	0	0	0	.01	0	0	0
La	0	0	0	0	0	0	0	0	0	0	.01	0	0	0
Ti	3.6	4.2	.4	.03	.01	.03	.004	.02	.04	.6	.004	.002	.02	.005
Zr	.02	.2	0	0	0	.006	.2	0	0	.008	.004	0	0	0
P	0	0	0	0	0	.9	0	0	0	0	>10	0	0	0
V	.2	.3	.2	.006	.005	.005	.02	.005	.02	.02	.1	.009	.01	.004
Nb	0	.04	0	0	0	0	.03	0	0	0	0	0	0	0
Cr	.0009	.001	.0009	.0009	.002	.0009	.0006	.0009	.0006	.0006	.0009	.003	.001	.0006
Mn	.8	.2	.04	.02	.03	.06	.02	.02	.01	.1	.002	.01	.08	.001
Fe	>10	>10	>10	>10	1.5	.4	>10	3.2	4.4	4	.01	.001	2.4	.08
Co	.02	0	0	0	0	.003	.003	.003	0	.001	0	0	.002	0
Ni	.002	.002	.002	0	0	0	0	0	0	0	0	0	0	0
Cu	.001	.001	.0008	.001	.0006	.0006	.005	.002	.0008	.002	.0006	.0008	.001	.0007
Ag	0	0	0	0	0	0	.0003	0	0	.0001	0	0	0	.0001
Zn	.01	0	0	0	0	0	0	0	0	0	0	0	0	0
Ga	.004	.001	.004	0	0	0	.001	.003	.002	.003	0	0	.001	.002
Indices of refraction [1]														
α					1.671±0.005	1.662±0.005								
β					1.679± .005	1.669± .005								
γ					1.707± .005	1.693± .005								

[1] Determinations by D. J. Jameson.

Spectrographic analyses by H. J. Rose.
X-ray analyses by F. A. Hildebrand.

Looked for but not found: Ce, Hf, Th, Ta, Mo, W, U, Re, Pd, Ir, Pt, Au, Cd, Hg, In, Ge, Sn, Pb, As, Sb, Bi.

EXPLANATION OF SAMPLES

	Sample	X-ray analyses
L-168-2	Magnetite	
L-168-5	Dark garnet	
L-168-6	Brownish-yellow garnet	
L-168-11	Pale greenish-yellow andradite	Garnet type mineral unit cell-melanite.
L-168-7	Pale-green diopside	
L-168-13	Colorless diopside	
L-168-14	Aegirine	Monoclinic pyroxene probably aegirine.
L-168-10	Idocrase-diopside mixture	Idocrase plus moderate amount of monoclinic pyroxene.
L-168-8	Idocrase	Idocrase.
L-168-4	Brown and green biotite	
L-168-12	Apatite	
L-168-3	Calcite	
L-168-1	Melilite	
L-168-9	Natrolite	

line phenocrysts. Many of the nonporphyritic tinguaite outcrops are easily mistaken for fine-grained metamorphic rocks, but the green color and uniform texture are characteristic.

The pseudoleucite tinguaite porphyry, the most striking of the tinguaitic rocks, is best exposed about 1,000 feet south of U.S. Highway 270 in sec. 21. White pseudoleucite phenocrysts up to 1 inch across are abundant in a fine-grained green matrix.

In thin section, the texture of the rock ranges from tinguaitic to pilotaxitic. The fine-grained, holocrystalline groundmass consists of a mesh of rod-shaped sodic pyroxene microlites with equigranular nepheline and sodic orthoclase in the interstices (tinguaitic texture). In some of the rocks the sodic orthoclase occurs as a felt of lath-shaped microlites in flow lines (pilotaxitic texture).

The proportion of phenocrysts in the tinguaites ranges from 0 to 50 percent. Pseudoleucite phenocrysts are most abundant; nepheline and pyroxene phenocrysts are common. The pseudoleucite crystals are hexagonal in part and composed of clear fresh nepheline and dirty, partly kaolinized sodic orthoclase. Some of the nepheline is altered to cancrinite. Sodic pyroxene rods tend to concentrate around the edges of the pseudoleucite crystals. Some of the larger, almost euhedral early formed pyroxene crystals are zoned and have a core which is near normal augite. Fluorite, sphene, magnetite, apatite, sodalite and plagioclase are accessory minerals. Calcite, cancrinite, and kaolinite are alteration products.

Brief descriptions of some of the variants are given below:

MC-152.—Grayish-green tinguaite porphyry cuts sphene pyroxenite and the contact zone sediments in the NE¼ sec. 17 and the NW¼ sec. 16. Phenocrysts of sodic orthoclase up to 3 inches long and nepheline up to 3 mm across make up about 25 percent of the rock. In thin section the minerals are: sodic orthoclase as phenocrysts and groundmass anhedra plus minor perthite and albite—about 45 percent, nepheline as phenocrysts and groundmass anhedra both altered to cancrinite and sodalite (?)—about 20 percent, and green aegirine as stubby phenocrysts and groundmass needles—about 35 percent.

L–23.—Grayish-green porphyritic tinguaite cuts fine-grained ijolite, analcime-olivine melagabbro, garnet fourchite, and altered phonolite in the SW¼ sec. 18. Phenocrysts of nepheline up to 2 mm across and pseudoleucite of about the same size make up about 10 percent of the rock. In thin section the minerals are: sodic orthoclase as phenocrysts and minute laths—about 40 percent, nepheline as phenocrysts partly to completely altered to sodalite(?) and minor cancrinite—about 20 percent, green aegirine as phenocrysts and minute needles plus accessory anhedral magnetite—about 40 percent. The saprolite of this rock was analyzed spectrographically (table 28). Material in the panned concentrate occurs in the following order of abundance: clay aggregates, feldspar, weathered pyrite, magnetite, and a trace of rutile. The presence of rutile and perhaps pyrite indicates contamination by weathered rutile veinlets not apparent when the sample was taken. From an X-ray analysis of the clay- and silt-size portion of this sample, A. J. Gude 3d (written communication, 1956) reported halloysite(?) and chlorite(?).

MC–115.—Greenish-gray porphyritic tinguaite dike cuts garnet-pseudoleucite syenite in the NE¼ sec. 24. Phenocrysts of pseudoleucite up to 5 mm across make up about 5 percent of the rock. In thin section the minerals are: pseudoleucite phenocrysts composed of kaolinized orthoclase and partly altered nepheline, kaolinized orthoclase phenocrysts, nepheline phenocrysts partially altered to sodalite(?) and cancrinite—about 65 percent; green aegirine in elongated prisms—about 35 percent; and accessory anhedral fluorite.

CHEMISTRY

Chemical and spectrographic analyses and norm, table 28, show the highly alkaline character of the tinguaite and its similarity to Daly's average tinguaite. The total alkali content is greater (16.83 percent) than in any of the other analyzed rocks from Magnet Cove. Sodalite and fluorite were not seen in the rock, but the

TABLE 28.—*Analyses and norm of tinguaite, in percent*

	MC–115	(1)		MC–115	MC–115a	MC–115b	MC–115c	L–23	MC–152–1		MC–115
Standard chemical analyses [2]				**Spectrographic analyses** [3]							**Norm**
SiO_2	52.85	55.02	Be	0.0005	0.0007	0.002	0.001	0.0005	0	or	47.26
Al_2O_3	19.44	20.42	Mg	n.d.	.07	.2	.7	.2	.004	ab	1.05
Fe_2O_3	4.82	3.06	Ca	n.d.	.3	1–10	1–10	.08	n.d.	ne	29.25
FeO	.57	1.82	Sr	.066	.3	.7	.8	.005	.4	hl	.94
MnO	.37	.22	Ba	.48	.07	.4	.08	.3	.2	nc	.32
MgO	.13	.59	B	0	0	0	0	.002	n.d.	ac	12.47
CaO	2.53	1.67	Sc	0	0	0	0	.001	0	di	2.13
BaO	.35		Y	0	0	0	0	.004	0	wo	3.13
Na_2O	8.87	8.63	La	.021	0	.04	.02	.07	0	mt	.70
K_2O	7.96	5.38	Ce	n.d.	n.d.	n.d.	n.d.	0	n.d.	il	.61
H_2O-	.07	2.77	Yb	0	0	0	0	.0007	n.d.	fr	.86
H_2O+	.78		Ti	n.d.	.06	.5	.6	3	.01		
TiO_2	.33	.36	Zr	.027	.01	.009	.02	.07	0		
CO_2	.13		V	.014	.007	.01	.07	.02	.007		
P_2O_5	.04	.06	Nb	.022	0	.05	.03	.03	0		
SO_3	.03		Cr	.0007	.05	.0002	.00008	.002	.0006		
Cl	.60		Mo	0	n.d.	.002	0	.001	.02		
F	.42		Mn	.23	.8	.4	1	.2	.002		
S	.04		Fe	n.d.	>10	1–10	>10	3	.3		
Total	100.36		Co	0	.004	0	0	0	0		
Less O	.42		Ni	0	.03	0	0	.003	0		
	99.94		Cu	.0006	.01	.008	.002	.003	.0009		
			Ga	.0045	.0008	.003	.0008	.004	.004		
			Pb	.0072	0	.02	.04	.005	0		
			Ag	0	0	0	0	0	.0001		
				Colorimetric analyses [4]							
			As	<0.001				0.001			
			Sb	<.001				.0002			
			W	.004				n.d.			
			Zn	.25				.15			
				Radiometric analyses [5]							
			eU	0.006				0.004			
				Chemical analyses [6]							
			U	0.00043				n.d.			
			Th	.00054				n.d.			

[1] Average tinguaite (Daly, 1933).
[2] Quantitative chemical analyses by L. M. Kehl.
[3] Spectrographic analyses: MC–115, MC–152–1 by H. J. Rose; MC–115a, 115–b, 115–c by J. D. Fletcher; L–23 by Sol Berman.
[4] Colorimetric analyses by H. E. Crowe and A. P. Marranzino.
[5] Radiometric analyses by B. A. McCall.
[6] Low-level uranium and thorium chemical analyses by J. C. Antweiler.

n.d.=not determined.
Looked for (spectrographically) but not found: Hf, Th, P, Ta, W, U, Re, Rh, Pd, Os, Ir, Pt, Au, Zn, Cd, Hg, In, Tl, Ge, Sn, As, Sb, Bi, Te.

MC–115. Tinguaite, NE¼ sec. 24.
MC–115a. Magnetic (hand magnet) fraction of heavy concentrate.
MC–115b. Nonmagnetic fraction of heavy concentrate.
MC–115c. Aegirine separate from MC–115.
L–23. Saprolite from tinguaite, SW¼ sec. 18.
MC–152–1. Sodic orthoclase separate from tinguaite porphyry, MC–152, NW¼ sec. 16.

high chlorine and fluorine content suggests that they could be found.

Compared with the average of analyses of the rocks in the complex (table 46) the tinguaite is lower in MgO, FeO, CaO, H_2O^+, TiO_2, CO_2, P_2O_5, SO_3, S, and higher in SiO_2, Al_2O_3, Fe_2O_3, MnO, BaO, Na_2O, K_2O, Cl, and F. BaO is unusually high and suggests that the feldspar is barian orthoclase.

Trace elements equal to or exceeding 0.01 percent include Sr, Ba, La, Zr, V, Nb, and Zn. Pb approaches this value (0.007 percent) and Be is unusually high (0.0005 percent). Sr, La, Ti, V, Mn, Nb, and Pb are concentrated in the heavier fraction of the rock. Mn, Ti, Sr, V, Pb, Nb, and Be are concentrated in aegirine.

The high Mo content (0.02 percent) of sodic orthoclase deserves special attention and will be discussed further in the section on geochemistry.

SODALITE TRACHYTE

Sodalite trachyte, about 3.5 percent of the exposed igneous rocks, is widely distributed in the complex, but the bulk of these rocks is found in the garnet-pseudoleucite syenite in the southern part of the area.

The trachytes are all holocrystalline, greenish-gray to dark-gray aphanites. Light-gray to greenish-gray and dark-gray breccia is closely associated with the trachyte.

A good exposure of sodalite trachyte occurs on the south bank of Stone Quarry Creek in the northeastern part of sec. 29. Irregular patches of aegirine (20 percent), pleochroic in green and brownish yellow, are scattered through a groundmass of sodic orthoclase (70 percent) and sodalite (10 percent). Anhedral sphene is an accessory mineral. Microscopic veinlets of cancrinite, sodic orthoclase, plagioclase, and calcite cut the rock.

The chemical analysis of sodalite trachyte (table 29) shows a phonolitic composition and is almost identical with the analysis of tinguaite (table 28).

The isotropic mineral in the mode is assumed to be sodalite because of the abundant chlorine in the rock.

Trace elements equal to or greater than 0.01 percent include Sr, Ba, La, Zr, Nb, and V.

ANALCIME-OLIVINE MELAGABBRO

DISTRIBUTION AND DESCRIPTION

Analcime-olivine melagabbro, about 0.7 percent of the exposed igneous rocks of the complex, forms an elongated dikelike mass about one-half mile long and up to 500 feet wide that cuts fine-grained ijolite in the SW1/4 sec. 18. A much smaller dike but with similar orientation is exposed in the Magnet Cove Titanium Corp. pit. The rock is easily weathered and good exposures are rare.

Williams (1891) and Fryklund and Holbrook (1950) called the rock a monchiquite. One sample was found which could be called a monchiquite but abundant lab-

TABLE 29.—*Analyses and norm of sodalite trachyte, in percent*

[Sample MC-228, sodalite trachyte, NE1/4 sec. 29]

	Chemical	Spectrographic		Radiometric		Chemical		Norm	
SiO	53.61	Be	0	eU	0.010	U	0.00066	or	45.59
Al_2O_3	20.32					Th	.00077	ab	11.53
Fe_2O_3	2.84								
FeO	1.98	Sr	0.08					ne	26.98
MnO	.36	Ba	.1					hl	.82
MgO	.15	B	0						
CaO	2.49	Sc	0					nc	.32
BaO	.19	Y	0					ac	2.31
Na_2O	8.20	La	.01					di	4.83
K_2O	7.66	Yb	0					wo	2.09
H_2O-	.06	Ti	.2						
H_2O+	1.12	Zr	.03					mt	3.02
TiO_2	.31	V	.008					il	.61
CO_2	.14	Nb	.02					ap	.34
P_2O_5	.10	Cr	.001					fr	.39
SO_3	.02	Mo	.002						
Cl	.52	Mn	.2						
F	.19								
S	.03								
Total	100.99								
Less O	.22	Ni	0						
	100.07								
		Cu	.001						
		Ga	.003						

Standard chemical analyses by L. N. Tarrant.
Spectrographic analyses by Harry Bastron.
Radiometric analyses by B. A. McCall.
Low-level chemical analyses for uranium and thorium by J. C. Antweiler.

Looked for (spectrographically) but not found: Li, Cs, Ce, Th, P, Ta, W, U, Re, Ru, Rh, Pd, Pt, Ag, Au, Zn, Cd, Hg, In, Tl, Ge, Sn, Pb, As, Sb, Bi, Te.

radorite in most of the thin sections makes gabbro a better name.

The rock is dark gray, fine grained to medium grained, and weathers to mottled (brown and green) saprolite. Altered olivine appears as minute light-colored spots against a dark background. In thin section the texture is holocrystalline hypautomorphic-granular.

Subhedral pyroxene up to 3 mm long with pale-lavender tints, probably titanaugite, is the most abundant mineral—40 to 60 percent of the rock. Colorless olivine, near forsterite, makes up as much as 20 percent and is remarkably fresh in the fine-grained rocks but almost completely altered to yellow-green and green serpentine and calcite in the coarser grained rocks. Labradorite (An_{52}) occurs as anhedral grains, up to 2 mm long, in the interstices between pyroxene and olivine crystals and comprises 5 to 20 percent of the rock. Late-forming orange-brown hornblende, near lamprobolite (5 to 10 percent) occurs as anhedral grains less than 1 mm long. Apatite, as crystals up to 2 mm long, and deuteric analcime occur in quantities approaching 5 percent. Magnetite and pyrite are accessory minerals.

Panned concentrates of two samples, L–22 and L–95, of saprolite show the following minerals in order of abundance: L–22, apatite, rutile and brookite, clay aggregates, mica, and magnetite-ilmenite; L–95, magnetite, clay aggregates, weathered pyrite, pyroxene, apatite, rutile and brookite, mica, ilmenite, and garnet. Rutile and brookite in the concentrates indicate contamination by rutile and brookite veins and garnet indicates contamination by garnet fourchite or ijolite.

CHEMISTRY

Chemical and spectrographic analyses, norm, and mode of analcime-olivine melagabbro, L–11a, are given in table 30. Discrepancies between the mode and the norm indicate that the one thin section taken of the coarse-grained rock is not representative.

Normative albite is present in the mode in analcime and labradorite. Much of normative ilmenite, magnetite and a part of anorthite is probably in modal olivine, titanaugite, and hornblende.

Trace elements in the rock that exceed or are equal to 0.01 percent include: Sr, Ba, Cr, V, and Ni. Cu and Sc approach 0.01 percent.

Spectrographic analyses of minerals separated from the analyzed rock (table 31) indicate the distribution of trace elements within the rock. Of the two pyroxenes analyzed, sample L–11a–2a is slightly more magnetic than L–11a–1a.

TABLE 30.—*Analyses, norm, and mode of analcime-olivine melagabbro*

	L–11a
Standard chemical analyses[1]	
SiO_2	34.51
Al_2O_3	10.24
Fe_2O_3	5.58
FeO	8.48
MnO	.22
MgO	8.26
CaO	15.62
BaO	.14
Na_2O	1.62
K_2O	.70
H_2O-	.51
H_2O+	1.06
TiO_2	4.88
CO_2	5.36
P_2O_5	2.72
SO_3	.03
Cl	.02
F	.18
S	.26
Total	100.39
Less O	.21
	100.18

	L–11a	L–22	L–95
Spectrographic analyses[2]			
Be	0	0.0005	0.0003
Mg	n.d.	5	1
Ca	n.d.	>5	.3
Sr	.2	.1	.004
Ba	.1	.2	.2
B	0	.003	.001
Sc	.007	.003	.009
Y	.003	.004	.02
La	.005	.02	.1
Ce	n.d.	0	.09
Yb	.0002	.001	.002
Ti	n.d.	4	4
Zr	.007	.03	.03
P	n.d.	0	0
V	.04	.09	.01
Nb	.002	.02	.02
Cr	.05	.02	.07
Mo	0	0	.001
Mn	.1	.6	.4
Fe	n.d.	>5	>5
Co	.004	.003	.009
Ni	.02	.0009	.03
Cu	.008	.01	.01
Ga	.002	.002	.003
Pb	0	0	.01
Zn	0	0	.05

	L–11a	L–22	L–95
Colorimetric analyses[3]			
As	<0.001	n.d.	<0.001
Sb	.0001	n.d.	.0001
Zn	.010	n.d.	.150
Radiometric analyses[4]			
eU	0.001	0.004	0.001
Chemical analyses[5]			
U	0.00004	n.d.	n.d.
Th	.00038	n.d.	n.d.

	L–11a
Norm	
or	3.89
ab	13.62
an	18.63
di	6.36
hy	17.71
ol	2.09
mt	8.12
il	9.27
ap	6.38
pr	.48
cc	12.20
Mode[6]	
Analcime	3
Labradorite	18
Olivine (serpentine).	5
Augite	49
Hornblende	3
Biotite	1
Apatite	4
Magnetite-ilmenite.	11
Calcite	3
Zeolite	3

[1] Standard chemical analyses by L. M. Kehl.

[2] Spectrographic analyses. L–11a by J. D. Fletcher; L–22, L–95 by Sol Berman.

[3] Colorimetric analyses by H. E. Crowe and A. P. Marranzino.

[4] Radiometric analyses by B. A. McCall.

[5] Low-level chemical analyses for uranium and thorium by J. C. Antweiler.

[6] Mode by L. V. Blade.

n.d.=not determined.

Looked for (spectrographically) but not found: Hf, Th, Ta, W, U, Re, Ru, Rh, Pd, Os, Ir, Pt, Ag, Au, Cd, In, Tl, Ge, Sn, Pd, As, Sb, Bi, Te.

L–11a. Analcime-olivine melagabbro, SW¼ sec. 18.

L–22. Saprolite of analcime-olivine melagabbro, SW¼ sec. 18.

L–95. Saprolite of analcime-olivine melagabbro, SW¼ sec. 18.

1. Strontium is most abundant in apatite and labradorite and to a lesser extent in pyroxene and hornblende.
2. Scandium and chromium are concentrated in the pyroxene.
3. Vanadium is concentrated in pyroxene and ilmenite.
4. Zirconium occurs chiefly in hornblende.
5. Cobalt, nickel, and copper are concentrated in ilmenite.
6. Niobium occurs only in the hornblende.
7. A surprisingly high amount of silver (0.004 percent) was detected in one of the pyroxenes.
8. None of the analyzed minerals contained as much gallium as indicated for the rock. It is probably concentrated in unanalyzed zeolite.

TABLE 31.—*Spectrographic analyses of mineral separates of analcime-olivine melagabbro, in percent*

	L–11a–4	L–11a–1a	L–11a 2a	L–11a–3a	L–11a–1	L–11a–2	L–11a–3
Mg	n.d.	n.d.	n.d.	n.d.	0.1	0.05	0.03
Sr	0.002	0.3	0.3	0.22	1–5	1–5	.1
Ba	.002	.009	.01	.09	.01	.5	.3
Sc	.0001	.01	.01	.001	0	0	0
Y	0	.001	.003	.009	.03	0	0
La	0	0	.002	.01	.009	0	0
Yb	n.d.	0	0	n.d.	.0008	0	0
Ti	>10	1.9	2.4	6.8	.008	.1	.05
Zr	0	0	.009	.02	0	0	.004
V	.08	.1	.1	.02	.02	0	0
Nb	0	0	0	.007	0	0	0
Cr	.0004	.08	.05	.002	0	.0002	0
Mn	1.1	.03	.3	.1	.04	.003	.002
Fe	n.d.	n.d.	n.d.	n.d.	.2	.2	.06
Co	.03	.002	.002	.004	0	0	0
Ni	.04	.01	.008	.007	0	0	0
Cu	.011	.001	.004	.004	.0008	.009	.001
Ag	0	0	.004	0	0	0	0
Ga	0	.0004	.0005	.0008	0	.0003	.0007
Sn	0	.003	.005	.03	.002	0	0
Specific gravity		3.1±.2	3.1±.2	3.1±.2	3.1±.2	2.75±.15	2.25±.05

n.d.=not determined.
Looked for but not found: Be, B, Ce, Th, P, Ta, Mo, W, U, Re, Pd, Ir, Pt, Au, Zn, Cd, Hg, In, Ge, Pb, As, Sb, Bi.

EXPLANATION OF SAMPLES

	X-ray		X-ray analyst	Spectrographic analyst
L–11a–4	Ilmenite	Ilmenite	F. A. Hildebrand	H. J. Rose
L–11a–1a	Augite	Monoclinic pyroxene probably augite.	do	Do.
L–11a–2a	do	do	do	Do.
L–11a–3a	Hornblende	Amphibole probably hornblende.	do	Do.
L–11a–1	Apatite			J. D. Fletcher
L–11a–2	Labradorite			Do.
L–11a–3	Analcime	Analcime	do	Do.

NEPHELINE SYENITE PEGMATITE

DISTRIBUTION AND DESCRIPTION

Nepheline syenite pegmatite, about 0.2 percent of the exposed igneous rocks of the complex, occurs in small irregular bodies, particularly along the outer contact of the complex with sedimentary rock. Good exposures are found all along the south edge of the garnet-pseudoleucite syenite in secs. 28, 29, and 30; in the eastern part of sec. 24; and along the north edge of the garnet-pseudoleucite syenite in sec. 18. Williams (1891), and later geologists who adapted his rock names, named this rock Diamond Jo syenite and included other medium- and fine-grained syenites in this type. However, the chemistry and mineralogy of the pegmatite set it apart from any other. Most of the rocks previously mapped as Diamond Jo syenite in the northern two-thirds of the area are a coarse-grained chemical equivalent of the garnet-pseudoleucite syenite.

The best exposure of nepheline syenite pegmatite is in the quarry at the west edge of sec. 29 where it is in contact with garnet-pseudoleucite syenite. The contact strikes east-west across the quarry parallel to the north face.

Light-colored minerals, chiefly barian sodic orthoclase with minor nepheline and cancrinite, make up 70 to 90 percent of the pegmatite. Black titanium garnet and zoned pyroxene are the chief mafic minerals and tend to be segregated in patches. Pyrite, calcite, and magnetite are accessory constituents. Blue sodalite and purple fluorite occur as thin skins, one-eighth inch thick, on vertical joint planes.

Barian sodic orthoclase, the most abundant mineral in the rock (70–80 percent), occurs as very light gray, lustrous, tabular crystals as much as 30 mm long. A fine network of kaolinite formed along cleavage planes gives the crystals the appearance of perthite. In thin section, these crystals have a faint suggestion of microcline structure and a moderately low 2*V*.

Nepheline, 10 to 15 percent of the rock, occurs as greasy gray grains in the interstices between feldspar crystals. Much of the nepheline is altered to cancrinite. Sodalite is common on joint surfaces. The pyroxene, chiefly green aegirine-diopside and aegirine-acmite, occurs as elongate prisms up to 15 mm in length that have low birefringence and a reaction rim which is composed of fine-grained green biotite and granular magnetite.

In the southern part of sec. 13 on the west border of the complex (MC–198), the pegmatite is light gray and has a holocrystalline xenomorphic-granular texture. The minerals in thin section are: nepheline partly altered to cancrinite, sericite, analcime and (or) sodalite group minerals—about 20 percent; sodic orthoclase plus microperthite—about 75 percent; and brown and green biotite, colorless to purple fluorite some intergrown with sphene, pyrite, and magnetite—about 5 percent.

A panned concentrate of the saprolite taken adjacent to the analyzed sample (MC–120) contains the following minerals in order of abundance: feldspar, clay aggregates, nepheline, pyroxene, hematite, magnetite, and mica. From an X-ray analysis of clay- and silt-size portion of the saprolite, A. J. Gude 3d (written communication, 1956) reported major kaolinite and traces of montmorillonite and chlorite.

CHEMISTRY

Chemical and spectrographic analyses and norms of nepheline syenite pegmatite, table 32, show that chemical composition is very similar to the analyzed tinguaite, table 28. It contains more K_2O than Na_2O; BaO content is unusually high (1.5 percent); CaO, P_2O_5, and TiO_2 contents are low. V and Zr are low in comparison to the other analyzed rocks; Co, Ni, Y, and Yb were not detected; Sr is high.

Comparison of the norm and mode indicates that part of the sodium in normative albite is probably in the barian sodic orthoclase and part in sodic pyroxene. BaO which is in the modal sodic orthoclase was combined with CaO in calculating normative anorthite and wollastonite. High CO_2, SO_3, and Cl in the analysis appear as normative sodium carbonate and halite, and are present in the mode in cancrinite and sodalite.

Trace elements in the rock that equal or exceed 0.01 percent are Sr, Ba, La, Zr, and V. Niobium contents of 0.01 percent were detected in 2 of the analyzed samples.

Spectrographic analyses of minerals separated from the analyzed rock (table 33) show the distribution of trace elements within the rocks. Nb, V, and Zr occur chiefly in titanium garnet; part of the Nb is in aegirine. The iron content of the sodic pyroxene suggests that it is probably closer to acmite than aegirine. La, Cr, Mo,

TABLE 32.—*Analyses and norm of nepheline syenite pegmatite, in percent*

	MC-120		MC-120	MC-198	L-154	L-155	MC-120-b	MC-120-a	MC-120-c	MC-120-d		MC-120
Standard chemical analysis[1]		**Spectrographic analyses**									**Norm**	
SiO_2	52.00	Be	0.0004	0.0004	0.0002	0.0001	0	0	0.0007	0	or	48.37
Al_2O_3	20.80	Mg	n.d.	.07	.1	.09	.2	1-10	1-10	.01	ab	8.91
Fe_2O_3	2.36	Ca	n.d.	.8	2	.1	>10	>10	>10	.13	an	6.12
FeO	1.15	Sr	.091	.07	.6	.08	.4	.6	.6	.61	ne	22.15
MnO	.22	Ba	1.5	.001	.4	.5	.02	.5	.06	2.4	hl	.47
MgO	.28	B	0	.004	0	.003	0	0	0	0	th	.43
CaO	2.86	Sc	0	0	0	0	.0002	0	0	0	nc	2.65
BaO	1.52	Y	0	0	0	0	0	0	0	0		
Na_2O	7.87	La	.011	.01	.02	0	0	0	0	0	di	1.51
K_2O	8.18	Yb	0	0	0	0	0	0	0	0	wo	3.48
H_2O-	.04	Ti	n.d.	.06	.3	.2	1-10	.2	.7	.01	mt	3.36
H_2O+	1.00	Zr	.0082	.06	.02	.01	.08	.01	.02	.001	il	.46
TiO_2	.24	V	.016	.004	.04	.02	.2	.04	.05	0	fr	.23
CO_2	1.10	Nb	.0053	.01	.01	.005	.04	0	.02	0	pr	.11
P_2O_5	.05	Cr	.0004	0	0	.002	0	.0001	.00008	0		
SO_3	.17	Mo	.0007	0	0	0	0	0	0	0		
Cl	.32	Mn	.14	.07	.2	.1	.4	.6	2	.005		
F	.13	Fe	n.d.	.9	3	2	>10	>10	>10	.26		
S	.05	Co	0	0	0	0	0	.001	.002	0		
		Ni	0	0	0	.0005	.0008	0	0	0		
Total	100.34	Cu	.0005	.0007	.0004	.0001	.001	.0009	.001	.0001		
Less O	.15	Ga	.0030	.004	.002	.003	.002	0	.001	.003		
	100.19	Pb	0	.006	0	.001	0	0	0	0		
		Colorimetric analyses[2]										
		As	0.002	n.d.	n.d.	n.d.						
		Sb	.0002	n.d.	n.d.	n.d.						
		W	<.001	n.d.	n.d.	n.d.						
		Zn	.010	n.d.	n.d.	n.d.						
		Pb	<.0005	n.d.	n.d.	n.d.						
		Radiometric analyses[3]										
		eU	0.004	0.005	0.006	0.006						
		Chemical analyses[4]										
		U	0.00010	0.00164	n.d.	n.d.						
		Th	.00044	.00097	n.d.	n.d.						

[1] Standard chemical analysis MC-120 by L. M. Kehl.
[2] Colorimetric analyses by H. E. Crowe and A. P. Marranzino.
[3] Radiometric analyses by B. A. McCall.
[4] Low-level chemical analyses for uranium and thorium by J. C. Antweiler.

n.d.=not determined.
Looked for (spectrographically) but not found: Li, Cs, Ce, Hf, Th, P, Ta, Cr, W, U, Re, Ru, Rh, Pd, Os, Ir, Pt, Ag, Au, Zn, Cd, Hg, In, Tl, Ge, Sn, As, Sb, Bi, Te.

EXPLANATION OF SAMPLES

		X-ray	X-ray analyst	Spectrographic analyst
MC-120	Nepheline syenite pegmatite			H. J. Rose.
MC-198	do			Sol Berman.
L-154	do			Do.
L-155	Saprolite of MC-120			Do.
MC-120-b	Dark garnet			J. D. Fletcher.
MC-120-a	Aegirine-diopside	Acmite	W. F. Outerbridge	Do.
MC-120-c	Aegirine	do	do	Do.
MC-120-d	Sodic orthoclase			Harry Bastron.

TABLE 33.—*Analyses and norm of trachyte porphyry, in percent*

Chemical analyses		Spectrographic analyses		Radiometric analyses		Chemical analyses		Norm	
	L-324		L-324	L-324	MC-193	L-324	MC-193	X	L-324
SiO_2	53.89	Be	0.0002	eU 0.004	n.d.	U n.d.	0.00069	or	46.15
Al_2O_3	21.63	Sr	.2			Th n.d.	.00136	ab	14.67
Fe_2O_3	1.74	Ba	.2					an	8.34
FeO	1.82	Y	.001					ne	20.16
MnO	.15	La	.007					hl	.12
MgO	.43	Yb	.0002					nc	.64
CaO	3.08	Ti	n.d.					di	2.87
BaO	.08	Zr	.03					wo	.23
Na_2O	6.62	P	n.d.					mt	2.55
K_2O	7.80	V	.02					il	1.22
H_2O-	.10	Nb	.009					ap	.34
H_2O+	1.09	Mn	n.d.					fr	.62
TiO_2	.60	Fe	n.d.					pr	.72
CO_2	.26	Cu	.001						
P_2O_5	.08	Ga	.002						
SO_3	.07	Pb	.002						
Cl	.09								
F	.32								
S	.35								
Total	100.20								
Less O	.33								
	99.87								

n.d.=not determined.
Looked for (spectrographically) but not found: B, Sc, Ce Th, Ta, Cr, Mo, W, U, Re, Co, Ni Ru, Rh, Pd, Os, Ir, Pt, Ag, Au, Zn, Cd, Hg, In, Tl, Ge, Sn, As, Sb, Bi, Te.

Standard chemical analysis by M. K. Balazs.

Spectrographic analysis by Sol Berman.
Radiometric analysis by B. A. McCall.
Low-level chemical analysis for uranium and thorium by J. C. Antweiler.
L-324. Trachyte porphyry, S½ sec. 19.
MC-193. Trachyte prophyry, SE¼ sec. 19.

and Ga are not concentrated in any of the minerals analyzed. These elements can perhaps be accounted for by the unanalyzed minerals: biotite, magnetite, calcite, nepheline, cancrinite, and sodalite group minerals.

TRACHYTE PORPHYRY

DISTRIBUTION AND DESCRIPTION

Narrow dikes and small irregular-shaped bodies of porphyritic rocks with sodic orthoclase phenocrysts in a light- to dark-gray trachytic or tinguaitic groundmass are scattered throughout the complex.

Sodic orthoclase phenocrysts comprise 0 to 40 percent of the rock and are in a groundmass of equigranular nepheline and sodic amphibole and pyroxene. The accessory minerals are sphene, apatite, magnetite, pyrrhotite, pyrite, and fluorite.

Some of the variants are briefly described below:

MC-61.—In the northeastern part of sec. 18 a small irregular-shaped body of gray prophyritic alkalic trachyte cuts pseudoleucite syenite. Corroded phenocrysts of perthite and sodic orthoclase, and rare corroded phenocrysts of plagioclase make up 5 percent of the rock. Aggregates of these feldspar crystals up to 5 mm across occur with a purple mineral that makes up about 2 percent of the rock. The anhedral purple mineral, probably a member of the sodalite group, is isotropic and colorless to reddish violet with the color irregularly distributed. Groundmass sodic orthoclase as narrow laths—all partly altered to sericite—comprises about 78 percent of the rock. The remaining 15 percent consists of anhedral sodalite(?) diopside-hedenbergite rimmed with aegirine-diopside with minor calcite alteration, aegirine-diopside, green biotite, sphene, colorless garnet, and magnetite.

MC-193.—A narrow dike of light-gray phonolite porphyry cuts undivided trachyte and banded trachyte in the southeastern part of sec. 19. Phenocrysts of tabular sodic orthoclase and perthite up to 10 mm long make up about 20 percent of the rock. The groundmass is composed of sodic orthoclase, about 55 percent of the rock; plagioclase probably oligoclase, about 5 percent; nepheline and analcime or sodalite both with cancrinite alteration, about 10 percent; and late anhedral green hornblende, sphene, apatite, pyrite, pyrrhotite(?), and magnetite, about 10 percent.

L-97.—A narrow dike of dark-gray alkalic trachyte porphyry cuts sphene-nepheline syenite and undivided trachyte breccia in the south-central part of sec. 19. In the hand specimen, phenocrysts of tabular sodic orthoclase up to 8 mm long make up about 20 percent of the rock. In thin section, corroded phenocrysts of sodic orthoclase and perthite plus groundmass sodic orthoclase, all with sericite alteration, comprise about 83 percent; phenocrysts of andesine, about 2 percent; and brownish-green biotite, pyrite, pyrrhotite(?), and magnetite, about 15 percent.

L-324.—In the south-central part of sec. 19, the undivided trachyte is cut by a light-gray phonolite porphyry. In the hand specimen, phenocrysts of tabular sodic orthoclase up to 8 mm long make up about 20 percent of the rock. In thin section, corroded phenocrysts of sodic orthoclase and perthite, both kaolinized, and groundmass laths of sodic orthoclase partially altered to sericite, about 70 percent; anhedral nepheline partly altered to cancrinite, about 10 percent; and green hornblende, pale-brown biotite, colorless to brown garnet, colorless mica (uniaxial negative), apatite, pyrrhotite, fluorite, and rare magnetite—about 20 percent.

CHEMISTRY

Chemical and spectrographic analyses and norm, of trachyte porphyry, table 33, show the similarity of this rock to tinguaite and nepheline syenite pegmatite. The most distinctive characteristic of all these dike rocks is that K_2O is higher than Na_2O.

The presence of pyrrhotite in the mode renders the FeO/Fe_2O_3 ratio unreliable.

Trace elements equal to or greater than 0.01 percent include Sr, Ba, Zr, V, and Nb.

MISCELLANEOUS TRACHYTES

Fine-grained dikes generally too small to be mappable and not readily classified with the major types are found in various parts of the complex. A few of these are described below:

L–25.—In the northeastern part of sec. 24 on the north side of U.S. Highway 270, sphene-nepheline syenite is cut by a light-gray phonolite. The rock has a hypautomorphic granular texture and is composed of analcime or sodalite, about 2 percent; nepheline (clear), about 25 percent; sodic orthoclase and minor perthite both with slight sericite alteration, about 65 percent; green aegirine-diopside, pale-brown to colorless garnet, sphene, magnetite, and rare pyrrhotite, 8 percent.

MC–27.—About 100 feet west of L–25, the sphene-nepheline syenite is cut by gray phonolite. In thin section corroded phenocrysts of green aegirine-diopside and subhedral olive-green hornblende crystals are set in an equigranular groundmass of nepheline, sodic orthoclase and sodalite or analcime. Apatite, sphene, and anhedral pale-brown garnet are the accessories.

MC–147.—In the southwestern part of sec. 21, feldspathoidal leucosyenite is cut by a dark-gray porphyritic phonolite composed of phenocrysts and anhedra of nepheline partly altered to cancrinite, analcime, or sodalite, and calcite, about 20 percent; anhedral plagioclase, probably albite, about 1 percent; anhedral sodic orthoclase partly altered to cancrinite and calcite, about 39 percent; corroded phenocrysts of diopside-hedenbergite partly altered to aegirine, needles and anhedral grains of aegirine and acmite, brown to colorless garnet intergrown with sphene, and yellowish-green biotite, about 40 percent.

MC–155.—In the northeast part of sec. 17, the jacupirangite is cut by a dark-gray feldspathoidal trachyte. Phenocrysts of pyroxene up to 2 mm long make up about 5 percent of the rock. In thin section the groundmass is trachytic and is composed of analcime or sodalite, about 10 percent; subhedral laths of sodic orthoclase with some calcite alteration, about 60 percent; zoned hornblende (brown centers rimmed with green) partly altered to green biotite; very pale brown phenocrysts of diopside-hedenbergite(?) partly altered to green biotite; apatite; sphene partially intergrown with colorless garnet; magnetite; pyrite, about 30 percent.

L–317.—Another sample, taken of the same mapped unit and in the vicinity of MC–155, is somewhat different from MC–155. This dark-gray feldspathoidal melatrachyte, is porphyritic with macroscopic phenocrysts of pyroxene forming about 10 percent of the rock. In thin section the minerals are: analcime or sodalite, about 5 percent; sodic orthoclase and perthite partially altered to zeolite and calcite, about 35 percent; and phenocrysts of very pale brown diopside-hedenbergite partially altered to green biotite, green biotite, sphene, apatite, magnetite, pyrite, and brown biotite, about 60 percent. An inclusion of novaculite in the rock has a reaction rim of plagioclase and aegirine.

APLITE

Scattered about the complex, as occasional pieces of light-gray to gray aphanite or fine-grained phanerite float, are the aplites. Usually the float is not abundant so the bedrock units must be small. They all are holocrystalline with a xenomorphic granular texture and mineralogically they are variable. Some of the variants are described below:

MC–40 (SW¼ sec. 18).—Feldspathoidal syenite aplite composed of sodic orthoclase (about 80 percent) deuterically altered to calcite and analcime and (or) sodalite group (about 10 percent) and acmite, green biotite, fluorite, apatite, magnetite, and pyrite (about 10 percent).

MC–44 (SE¼ sec. 13).—Nepheline syenite aplite composed of nepheline partly altered to analcime and/or sodalite group, about 15 percent; sodic orthoclase and perthite, about 80 percent; and aegirine magnetite and pyrrhotite (?), about 5 percent.

L–30 (SW¼ sec. 18).—Alkalic syenite aplite composed of sodic orthoclase and perthite partly altered to sericite (about 80 percent) and colorless to purple fluorite, green biotite, muscovite, ilmenite partly altered to leucoxene, and pyrite partially weathered to hematite, about 20 percent.

L–318 (NE¼ sec. 17).—Alkalic syenite aplite composed of sodic orthoclase and perthite (about 80 percent) and pale-green diopside-hedenbergite, sphene, magnetite, and pyrite—about 20 percent.

EUDIALYTE-NEPHELINE SYENITE PEGMATITE

DISTRIBUTION AND DESCRIPTION

Eudialyte-nepheline syenite pegmatite comprises less than 0.1 percent of the exposed igneous rocks of the complex and occurs in two localities—both in the northern part of sec. 19. A poorly exposed pegmatite with very coarse aegirine cuts fine-grained ijolite in the southeastern part of sec. 18 on Cove Creek. No eudialyte has been observed in this pegmatite but for mapping purposes it has been lumped with eudialyte-nepheline syenite pegmatite.

The eudialyte-bearing pegmatite varies in texture from a fine-grained to very coarse grained phanerite. The coarse-grained parts are well known for beautiful specimens of aegirine crystals up to 6 inches long, and ruby-colored eudialyte crystals up to 1 inch across. Williams (1891) has described in detail the mineralogy of the coarse-grained part. He mentions garnet, ilmenite, magnetite, nepheline, orthoclase, thomsonite, and wollastonite, and describes aegirine, astrophyllite, brucite, eucolite, eudialyte, manganopectolite, microcline, natrolite, and sphene.

In thin section the fine- to medium-grained parts of the dikes have a hypautomorphic-granular texture and are composed of aegirine; anhedral sodic orthoclase and (or) microcline partly altered to cancrinite, calcite, pectolite, zeolite, and sodalite group; nepheline partly altered to cancrinite and usually poikilitically included in the feldspar; euhedral to anhedral sphene some partially altered to leucoxene; apatite; magnetite; euhedral eudialyte; pyrite; pyrrhotite.

CHEMISTRY

Chemical and spectrographic analyses, norm, and mode of the fine-grained part, table 34, are very similar to normal nepheline syenite except that K_2O is unusually high.

Halite and thenardite of the norm appear in the mode as a member of the sodalite group. Much of the Na_2O in normative nepheline occurs as aegirine in the mode.

Material in the pegmatite that looked like chert was identified from an X-ray analysis by F. A. Hildebrand as tobermorite, a hydrated lime silicate. Chemical analysis of tobermorite is given in table 35.

TABLE 35.—*Chemical analysis of tobermorite from eudialyte-nepheline syenite pegmatite*

[Sample L-167-7. Standard chemical analysis by L. N. Tarrant]

Constituents	*Percent*
SiO_2	45.41
Al_2O_3	4.77
Fe_2O_3	.05
FeO	.00
MnO	.05
MgO	0
CaO	35.75
Na_2O	.32
K_2O	.81
H_2O-	3.23
H_2O+	9.48
TiO_2	.01
P_2O_5	0
Cl	0
F	0
Total	99.88

TABLE 34.—*Analyses, norm, and mode of eudialyte-nepheline syenite pegmatite, in percent*

Chemical[1]		Spectrographic[2]									Radiometric[3]		Chemical[4]		Norm		Mode[5]	
	L-303		L-303	L-167-1	L-167-2	L-167-3	L-167-4	L-167-5	L-167-6	L-167-7		L-303	L-303			L-303		L-303
SiO_2	52.18	Be	0.0002	0	0	0	0	0	0.002	0.002	eU	0.006	U	0.002	or	42.81	Nepheline	5
Al_2O_3	19.28	Mg	n.d.	.05	>10	.02	.006	.03	.02	.009					ab	9.43	Sodic orthoclase	47
Fe_2O_3	2.89														ne	26.70	Sodalite group	1
FeO	1.97	Sr	.2	.8	.04	.01	.0009	.2	.05	.01					hl	.12	Zeolite (birefringent).	15
MnO	.19	Ba	.1	.2	0	.07	.06	.01	.02	.04					th	.28	Cancrinite	
MgO	.91	Sc	0	.0004	0	0	0	0	0	0					ac	2.77	Calcite	
CaO	4.17	Y	.002	.009	0	0	0	.003	0	0					di	5.72	Aegirine	27
BaO	.10	La	.009	.04	0	0	0	.02	0	.02					wo	3.94	Sphene	4
Na_2O	7.43	Yb	.0003	n.d.	n.d.	n.d.	n.d.	n.d.	n.d.	n.d.					mt	2.78	Apatite	1
K_2O	7.21	Ti	n.d.	.4	.5	.006	.006	.04	.02	.003					il	1.98	Magnetite	Tr.
H_2O^-	.08	Zr	.04	>10	.07	0	0	0	0	0					ap	.34		
H_2O^+	1.64	V	.03	.01	.1	.01	.009	.02	.006	.009					fr	.07		
TiO_2	1.02	Nb	.01	.09	0	0	0	0	0	0					pr	.24		
CO_2	.47	Cr	.001	.002	.001	.001	.0009	.001	.002	.002					cc	1.10		
P_2O_5	.19	Mo	0	n.d.	n.d.	n.d.	n.d.	n.d.	n.d.	n.d.								
SO_3	.17	Mn	n.d.	.48	.48	.007	0	.5	.005	.05								
Cl	.06	Fe	n.d.	2.2	>10	.4	.09	.2	.02	.002								
F	.05	Co	.0006	0	0	0	0	0	0	0								
S	.12																	
Total	100.13	Cu	.002	.002	.0007	.001	.0009	.001	.0009	.0008								
Less O	.10	Ga	.003	0	0	.004	.004	0	.002	0								
	100.03	Sn	0	.09	0	0	0	0	0	0								
		Pb	0	.008	0	0	0	.003	0	0								

[1] Standard chemical analyses by M. K. Balazs.
[2] Spectrographic analysis: L-303 by Sol Berman; all other samples by H. J. Rose.
[3] Radiometric analyses by D. L. Schafer.
[4] Chemical analysis for uranium by J. P. Schuch.
[5] Mode by L. V. Blade.

0=looked for but not found.
n.d.=not determined.
Looked for (spectrographically) but not found: Ce, Hf, Th, P, Ta, W, U, Re, Ni, Pt, Ir, Pd, Ag, Au, Zn, Cd, Hg, In, Tl, Ge, As, Sb, Bi, Te, B.

EXPLANATION OF SAMPLES

	Sample	X-ray	Analyst
L-167-1	Eudialyte		
L-167-2	Aegirine		
L-167-3	Microcline	Microcline	F. A. Hildebrand.
L-167-4	Microcline	do	Do.
L-167-5	Pectolite		
L-167-6	Natrolite		
L-167-7	Tobermorite	Tobermorite	Do.

L-303. Eudialyte-nepheline syenite pegmatite, NW¼ sec. 19.
L-167-1. Eudialyte from coarse-grained part of pegmatite, NE¼ sec. 19.
L-167-2. Aegirine from coarse-grained part of pegmatite, NE¼, sec. 19.
L-167-3. Microcline from coarse-grained part of pegmatite, NE¼ sec. 19.
L-167-4. Microcline from coarse-grained part of pegmatite, NE¼ sec. 19.
L-167-5. Pectolite from coarse-grained part of pegmatite, NE¼ sec. 19.
L-167-6. Natrolite from coarse-grained part of pegmatite, NE¼ sec. 19.
L-167-7. Tobermorite from coarse-grained part of pegmatite, NE¼ sec. 19.

Compared with the average of analyses of igneous rocks in the complex (table 46), the analyzed rock is lower in MgO, Fe_2O_3, FeO, MnO, CaO, BaO, TiO_2, CO_2, P_2O_5, Cl, F, S, and higher in SiO_2, Al_2O_3, Na_2O, K_2O, SO_3.

Trace elements in the rock that are equal to or exceed 0.01 percent include: Sr, Ba, La, Zr, V, Nb, and Mn.

Spectrographic analyses of several minerals hand picked from the coarse to very coarse pegmatite, table 34, show that Sr, Ba, Sn, Pb, Nb, and La are concentrated in eudialyte. La also occurs in pectolite and tobermorite; V and Zr occur chiefly in aegirine; Ga is in microcline.

GARNET FOURCHITE

Garnet fourchite occurs in the southwestern part of sec. 18, where the saprolite and float pattern suggest a small dike that cuts fine-grained ijolite and analcime olivine melagabbro.

The rock is a dark-gray porphyritic aphanite in which phenocrysts of pyroxene comprise 20 to 40 percent of the rock. It weathers to a light greenish-brown saprolite with black spots. In thin section the augite phenocrysts are a very pale brown in color and appear zoned only under crossed nicols. They are set in a xenomorphic-granular groundmass of brown to colorless garnet—about 18 percent; magnetite-ilmenite rimmed with sphene—about 23 percent, analcime(?)—about 8 percent, nepheline partially altered to calcite—about 5 percent, and a trace of pale brownish-green biotite.

Material in the panned concentrate of the saprolite occurs in about the following order of abundance: garnet, magnetite, pyroxene, rutile, and brookite. From an X-ray analysis of the silt- and clay-size portion of the saprolite, A. J. Gude 3d (written communication, 1956) reported major montmorillonite and chlorite.

Spectrographic analyses of the fresh rock and saprolite, table 36, indicate that Cu, Co, Ni, and rare earths are unusually high in this dike rock. The repeat determinations show excellent agreement within the limit of spectrographic sensitivities for the elements detected.

TABLE 36.—*Analyses of garnet fourchite, in percent*

	L–94a	L–94a	L–94b	L–94b
Spectrographic analyses [1]				
Be	0. 0001	0. 0002	0. 0003	0. 0001
Mg	4	--------	2	3
Ca	>5	>5	>5	>5
Sr	. 2	. 5	. 04	. 04
Ba	. 1	. 1	. 3	. 3
B	0	. 001	0	. 002
Sc	. 004	. 004	. 004	. 006
Y	. 004	. 005	. 006	. 01
La	. 01	. 03	. 03	. 05
Ce	. 06	<. 1	. 09	0
Yb	0	0	. 0005	. 0009
Ti	2	3	2	>5
Zr	. 02	. 03	. 03	. 03
V	. 02	. 04	. 02	. 05
Nb	. 01	. 01	. 01	. 01
Cr	. 007	. 02	. 007	. 01
Mn	. 2	. 4	. 2	. 5
Fe	3	>5	4	>5
Co	. 002	. 004	. 002	. 005
Ni	. 002	. 004	. 003	. 004
Cu	. 02	. 02	. 02	. 03
Zn	0	. 04	0	0
Ga	. 002	. 003	. 001	. 002
Colorimetric analyses [2]				
As	n.d.	--------	0. 001	--------
Sb	n.d.	--------	. 0002	--------
Zn	n.d.	--------	. 015	--------
Radiometric analyses [3]				
eU	0. 002	--------	0. 002	--------

[1] Spectrographic analyses by Sol Berman.

[2] Colorimetric analyses by H. E. Crowe and A. P. Marranzino.

[3] Radiometric analyses by B. A. McCall. L–94a, Garnet fourchite, SW¼ sec. 18. L–94b, Saprolite of garnet fourchite, SW¼ sec. 18.

n.d.=not determined.

Looked for but not found: Hf, Th, P, Ta, W, Mo, U, Re, Rh, Pd, Os, Ir, Pt, Ag, Au, Cd, Hg, In, Tl, Ge, Sn, Pb, As, Sb, Bi, Te.

DIKES OUTSIDE THE COMPLEX

Igneous dikes, ranging in width from less than 6 inches to at least 25 feet and in length from less than 6 feet to at least 4,500 feet, are abundant in the broad valley to the west of the complex (fig. 4), and they are particularly abundant in the contact zone (pl. 1). Commonly, the dikes are revealed by float pieces and they rarely are exposed across their full width. The abundance of weathered dikes exposed in the road cut along the south side of the complex indicates that dikes probably are much more common than indicated by the float. Mineralogically, they are variable. Some can be grouped with the types within the complex but most cannot be so grouped. The rock types include pegmatite, aplite, syenite, trachyte porphyry, trachyte, tinguaite, andesite, diorite, monzonite, and lamprophyre and are described in table 37.

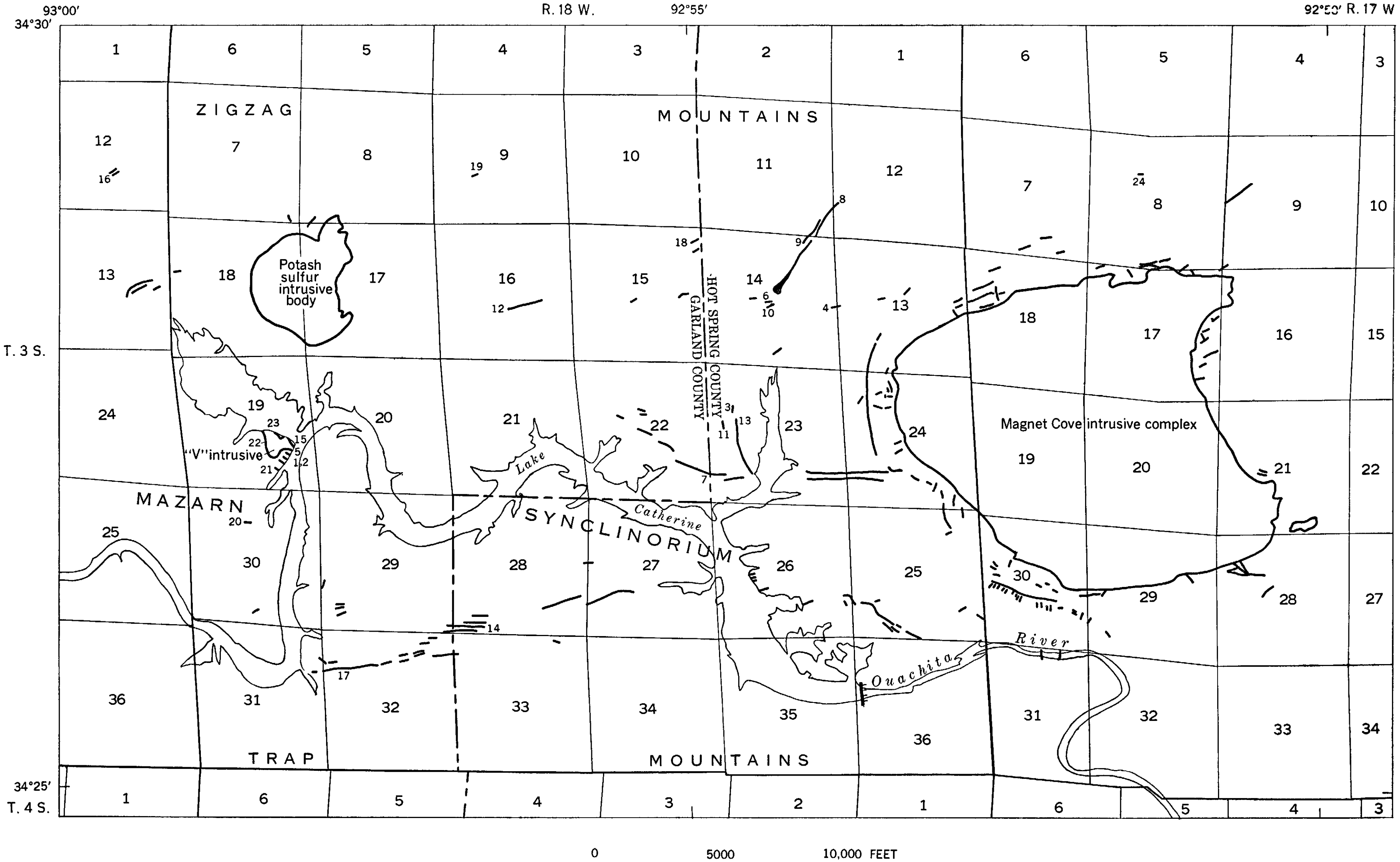

FIGURE 4.—Map showing location of igneous dikes in relation to the Magnet Cove intrusive complex, Garland and Hot Spring Counties, Ark.

TABLE 37.—*Description of dike rocks that occur outside the complex*

Sample No.	Map No.	Rock name	Texture	Mineralogy
L-53		Nepheline syenite pegmatite	Holocrystalline hypautomorphic granular.	Nepheline and sodic orthoclase partially altered to cancrinite, analcime, or sodalite group, and minor sericite; brownish-green biotite; aegirine diopside; brown garnet intergrown with sphene; and pyrite.
L-285*		do	do	Orthoclase, microcline, and microperthite (64 percent); nepheline (14 percent); analcime or sodalite group with minor calcite (12 percent); green biotite (6 percent); acmite (3 percent); and magnetite (1 percent).
L-287		do	do	Microcline, microperthite, and nepheline partially altered to cancrinite and sericite, sodalite group, brown biotite, muscovite, and zircon.
L-36*		Alkalic syenite aplite	Holocrystalline xenomorphic granular.	Orthoclase, minor microperthite, minor albite, brown biotite, brownish-green hornblende, minor aegirine, zircon, and magnetite.
L-305		do	do	Microperthite, pale green hornblende, aegirine, sphene, zircon, and hematite and limonite from pyrite(?).
L-313*		do	do	Nepheline(?) completely replaced by muscovite (1 percent); orthoclase, perthite, and minor plagioclase (62 percent); muscovite, brownish-yellow biotite, and magnetite partially weathered to limonite and hematite (37 percent).
L-283		Sphene cancrinite syenite	Holocrystalline hypautomorphic granular.	Same as described for this rock type within the igneous complex.
L-328		Garnet pseudoleucite syenite	do	Do.
L-185		Sphene garnet nepheline syenite	do	Do.
L-195		do	do	Do.
L-279		do	do	Do.
L-291		Alkalic syenite	do	Sodic orthoclase partly replaced by scapolite(?) and minor analcime or sodalite group and calcite; pale-green hornblende some with irregular bluish-green zones; sphene; brown garnet, apatite and pyrite.
V-6	[1] 1	do	do	Sodic orthoclase and nepheline partly altered to sodalite group, diopside-hedenbergite rimmed with aegirine-diopside and aegirine, aegirine, sphene, brown to colorless garnet, apatite, magnetite, and pyrite.
L-232		Nepheline syenite	do	Sodic orthoclase and nepheline partially altered to cancrinite, analcime, or sodalite group, and calcite; diopside-hedenbergite rimmed with aegirine-diopside and aegirine and partly altered to biotite, magnetite, and leucoxene; brown and green biotite; apatite; magnetite; and pyrite.
V-7	2	do	do	Sodic orthoclase and nepheline partly altered to cancrinite, zeolite, and sodalite group or analcime; aegirine-diopside rimmed with aegirine; sphene; magnetite; and pyrite.
L-223*		Alkalic leucotrachyte porphyry	Holocrystalline aphanitic	Phenocrysts of microperthite partly altered to sericite, phenocrysts of nepheline(?) completely altered to sericite, orthoclase partially altered to sericite, and hematite from pyrite(?).
MC-157*		Hornblende feldspathoidal trachyte porphyry.	do	Phenocrysts of microperthite and groundmass orthoclase plus minor plagioclase partly altered to calcite (58 percent), sodalite group or analcime (6 percent), diopside-hedenbergite and aegirine-diopside rimmed with hornblende (2 percent); brownish-green and bluish-green hornblende (30 percent); green biotite (1 percent); sphene (2 percent); and pyrite and pyrrhotite (1 percent).
L-284*		Altered alkalic trachyte porphyry.	do	Orthoclase partly altered to calcite (53 percent), phenocrysts of brown biotite (8 percent), diopside partly altered to hornblende and calcite (1 percent), yellowish-green and bluish-green hornblende partly altered to chlorite and calcite (9 percent), calcite (20 percent), pyrite (6 percent), apatite, sphene, magnetite, and chlorite (3 percent).
I-203b	3	Phonolite porphyry	do	Phenocrysts of nepheline altered to cancrinite and calcite; phenocrysts of sodic orthoclase; phenocrysts of sodalite or analcime group partly altered to calcite; groundmass sodic orthoclase, diopside-hedenbergite rimmed with aegirine-diopside, aegirine-diopside, phenocrysts of brown to colorless garnet, sphene, apatite, and magnetite.
L-220	4	Alkalic trachyte	Trachytic	Sodic orthoclase and microperthite partly altered to sericite, nepheline(?) completely altered to sericite, muscovite, and limonite and hematite weathering of pyroxene(?) and pyrite(?).
L-230		Alkalic leucotrachyte	do	Orthoclase and minor albite partly altered to sericite, sodalite group or analcime, epidote(?) and pyrite(?).
L-248*		Altered alkalic trachyte	do	Orthoclase partly replaced by scapolite(?) (21 percent), scapolite(?) partly altered to calcite (29 percent), calcite (9 percent), yellowish-brown to bluish-green hornblende partly altered to biotite (27 percent), pale-brown biotite (6.5 percent), sphene (4 percent), pyrrhotite (3 percent) and apatite.
I-174c*	5	Corundum alkalic leucotrachyte	do	Orthoclase as phenocrysts and groundmass, partly altered to sericite; corundum; reddish-brown biotite; pyrite; and magnetite.
I-199b	6	Alkalic leucotrachyte	do	Orthoclase and microperthite as phenocrysts and orthoclase as groundmass, pyrite, and calcite.
I-206b and c	7	Alkalic leucotrachyte	do	Phenocrysts of orthoclase and microperthite and groundmass orthoclase partly altered to sericite, nepheline(?) completely altered to sericite, epidote(?) introduced into vesicules.
L-221*	8	Feldspathoidal leucotrachyte	do	Phenocrysts of orthoclase and microperthite and groundmass orthoclase partly altered to analcime or sodalite group and calcite, colorless garnet and sphene intergrown, fluorite, pyrite, and leucoxene and chlorite from pyroxene(?).
L-222*	9	Leucophonolite	do	Phenocrysts of microperthite partly altered to sericite, orthoclase partly altered to sericite, nepheline(?) completely altered to sericite, and pryite.
L-199a	10	Phonolite	do	Orthoclase almost completely altered to sericite, nepheline almost completely altered to sericite and calcite, magnetite, pyrite, and leucoxene.
I-202	11	do	do	Orthoclase, nepheline partly altered to analcime and sodalite group, cancrinite and calcite; diopside-hedenbergite rimmed with aegirine-diopside, aegirine-diopside, zoned brown to colorless garnet, apatite, pyrite, and magnetite.
L-245		Altered phonolite	do	Orthoclase and nepheline partly altered to zeolite, analcime or sodalite group, and calcite; green hornblende, green biotite, sphene, diopside-hedenbergite, apatite, brown to colorless garnet, pyrite, and magnetite.
I-193	12	Tinguaite	Tinguaitic	Same as description for this rock type within the igneous complex.
I-203	13	do	do	Do.
I-203a	13	do	do	Do.
I-241	14	do	do	Do.
L-282*		Andesite	Holocrystalline hypautomorphic granular.	Orthoclase (2 percent), andesine partly altered to calcite (49 percent), colorless diopside (8 percent), brown hornblende partly altered to bluish-green hornblende (32 percent), sphene (5 percent), apatite and magnetite (3 percent).
MC-197		Diorite	do	Orthoclase and microperthite (15 percent), andesine (50 percent), and diopside partly altered to brown hornblende, brown hornblende, sphene, apatite, pyrite, and magnetite (35 percent).
L-225		Monzonite	do	Orthoclase and andesine partly to completely replaced by scapolite(?), bluish-green hornblende, brown biotite, sphene, apatite, pyrite, and pyrrhotite.

See footnotes at end of table.

TABLE 37.—*Description of dike rocks that occur outside the complex*—Continued

Sample No.	Map No.	Rock name	Texture	Mineralogy
MC-208		do	Seriate porphyritic	Orthoclase, andesine, titaniferous augite partly altered to brown hornblende and brown biotite, brown hornblende, apatite, sphene, magnetite, and pyrite.
L-255*		Feldspathoidal syenite lamprophyre.	Holocrystalline hypautomorphic granular.	Orthoclase (17 percent), analcime or sodalite group (17 percent), pale-green diopside-hedenbergite and green hornblende (39 percent), brownish-green biotite (3 percent), zoned brown to colorless garnet (12 percent), sphene (7 percent), magnetite (4 percent), apatite and pyrite.
L-270*		Altered nepheline syenite lamprophyre.	do	Orthoclase partly replaced by calcite, phenocrysts of nepheline(?) completely replaced by calcite, sphene, brown biotite partly altered to pale-green biotite, magnetite, pyrite, and apatite.
L-299		Feldspathoidal syenite lamprophyre.	do	Orthoclase, analcime or sodalite group, leucoxene from pyroxene(?), magnetite, sphene, apatite, and pyrite.
V-9	15	Nepheline syenite lamprophyre	do	Orthoclase, nepheline partly altered to zeolite, cancrinite, and analcime or sodalite group; brownish green biotite, very pale brown diopside-hedenbergite rimmed with pale-green diopside-hedenbergite and partly altered to biotite, sphene, apatite, magnetite, and pyrite.
L-292		Diorite lamprophyre	Porpyhritic	Orthoclase andesine, colorless diopside(?), brown biotite, sphene, apatite, and magnetite.
L-276*		Gabbro lamprophyre	do	Labradorite, corroded phenocrysts of augite(?) rimmed with hornblende and partially altered to biotite, colorless diopside, very pale brown hornblende, brown biotite, magnetite, and pyrite.
L-298		Altered fourchite	do	Phenocrysts of pyroxene altered to chlorite, calcite, zeolite, and leucoxene; zeolite, calcite, apatite, magnetite, and pyrite.
L-300a		Fourchite	do	Phenocrysts of diopside-hedenbergite(?), minor brown biotite, apatite, magnetite, pyrite, analcime(?), and calcite.
L-300b		Altered fourchite	do	Phenocrysts of pyroxene(?) altered to chlorite, calcite, and leucoxene; apatite, magnetite, pyrite, zeolite, and calcite.
I-161a	16	Fourchite	do	Phenocrysts of titaniferous augite(?) slightly altered to aegirine, chlorite, and biotite; magnetite, ilmenite, pyrite, apatite, and late nepheline, analcime(?) and calcite.
I-161b	16	do	do	Do.
I-247	17	do	do	Do.
L-301*		Ouachitite	do	Phenocrysts of augite(?) (18 percent), corroded phenocrysts of brown biotite (7 percent), magnetite and ilmenite (32 percent), analcime(?), nepheline, cancrinite, and calcite (40 percent), apatite and pyrite (3 percent).
L-302		Altered ouachitite	do	Pyroxene(?) altered to leucoxene, reddish-brown biotite, pyrite, and late analcime(?), calcite, and zeolite.
I-253	18	Ouachitite	do	Phenocrysts of brown augite(?) irregularly zoned with green-tinted augite(?), corroded phenocrysts of brown biotite, magnetite, pyrite, apatite, and late analcime(?), nepheline, cancrinite, zeolite, and calcite.
L-228		Alkalic syenite lamprophyre	Porphyritic	Orthoclase partly replaced by scapolite and calcite, phenocrysts of pyroxene(?), completely altered to hornblende, calcite, chlorite, and sericite, green and bluish green hornblende partially altered to biotite; sphene, apatite; magnetite, and pyrite.
L-288		do	do	Orthoclase and andesine partly altered to scapolite(?), diopsidehedenbergite(?) rimmed with hornblende, green hornblende partially altered to brown biotite, sphene, apatite, magnetite and pyrrhotite. The rock is cut by microscopic veinlets of diopside and plagioclase.
L-289*		do	do	Orthoclase with minor sericite alteration (30 percent), titaniferous augite (?) partly altered to hornblende (5 percent), brownish green hornblende (55 percent), sphene (8 percent), apatite, magnetite, and pyrrhotite (3 percent).
MC-209		Calci-alkalic syenite lamprophyre.	do	Orthoclase with minor zeolite alteration, andesine, titaniferous augite, brown hornblende, brown biotite, sphene, apatite, pyrrhotite, and magnetite-ilmenite.
L-90		Diorite lamprophyre	do	Andesine, diopside-hedenbergite(?) partially altered to hornblende, greenish brown hornblende, sphene, apatite, and pyrrhotite. The rock is cut by microscopic veinlets of orthoclase, plagioclase and magnetite.
L-231		do	do	Andesine, phenocrysts of pyroxene(?) completely altered to biotite, brown biotite, apatite, pyrite, magnetite, sphene, and hornblende. The rock is cut by microscopic veinlets of diopside and plagioclase partly altered to scapolite(?).
L-260*		do	do	Andesine (34 percent), pale green diopside-hedenbergite (7 percent), brownish green hornblende poikilitically includes sphene, apatite, magnetite, and andesine (40 percent), sphene (11 percent), apatite, magnetite, and pyrite (7 percent).
I-227*	19	Biotite monchiquite	do	Corroded phenocrysts of olivine partly altered to antigorite and chrysotile (16 percent), phenocrysts of augite(?) slightly altered to biotite and calcite (25 percent), corroded phenocrysts of brown biotite (18 percent), magnetite-ilmenite partly altered to leucoxene (21 percent), late analcime(?) and calcite (18 percent), apatite, sphene, and pyrite (2 percent).
I-172	20	Fine-grained ijolite	Hypautomorphic granular	Diopside-hedenbergite, brown garnet, brown biotite, perovskite, apatite, magnetite, pyrite, and nepheline partly altered to zeolite and calcite.
L-329		Micromelteigite	do	Diopside-hedenbergite almost completely altered to chlorite, brown biotite, sphene, magnetite, pyrite, and late zeolite and calcite.
L-277		Hornblende pyroxenite	do	Diopside-hedenbergite partly altered to hornblende and calcite, brown hornblende, brown biotite, sphene, pyrite, and late calcite and scapolite(?).
V-2a	21	Sphene-biotite pyroxenite	do	Diopside-hedenbergite, brown biotite, sphene, apatite, magnetite, pyrite; and late orthoclase, analcime or sodalite group, zeolite, and calcite.
V-3	22	Quartz feldspar vein		
V-13	23	Fluorite vein		
L-339a and b	24	Quartz-brookite-rutile vein		

---

[1] Map number refers to location of dike rock or vein shown in figure 4. Other rocks are shown on plate 1.

*Spectrographic analysis made (table 38).

TABLE 38.—*Analyses, in percent, of igneous dikes outside the complex*

	L–285	L–313	L–36	L–223	MC–157	L–284	L–221	L–222	L–248	I–174c	L–282	L–255	L–270	L–289	L–260	L–276	L–301	I–227	Range
Spectrographic analyses [Analyst, Sol Berman]																			
Be	0.0003	0.0004	0.0004	0.0004	0.0004	0.0005	0.0003	0.0004	0.0003	0.0004	0.0003	0.0002	0.0002	0.0003	0.0002	0.0002	0.0002	0.0001	.0001–0.0005
Mg	.1	.9	.3	.09	x	x	.07	.04	x	.1	x	x	x	x	x	x	x	x	.04–x
Ca	.4	.09	.6	.06	4	>5	.7	.02	>5	1	>5	>5	>5	>5	>5	>5	>5	>5	.02–>5
Sr	.08	.1	.009	.04	.2	.3	.03	.04	.2	.5	.6	.6	.5	.3	.6	.2	.2	.2	.009–.6
Ba	.007	.3	.07	.1	.09	.1	.02	.06	.1	.1	.1	.2	.1	.1	.1	.1	.09	.09	.007–.3
B	.006	.007	.02	.01	0	.001	.005	.01	.001	.001	.002	0	0	.001	.001	.004	.001	.002	0–.02
Sc	0	0	.0003	0	.001	.0003	0	0	.0006	0	.0002	.0006	.0006	.002	.0004	.003	.004	.004	0–.004
Y	0	.004	.003	.002	.004	.007	0	0	.007	0	.006	.01	.005	.006	.01	.007	.005	.004	0–.01
La	.01	0	.02	.02	.03	.02	.03	.03	.02	.02	.02	.04	.03	.02	.03	.04	.03	.02	0–.04
Ce	0	0	0	.02	.02	0	.03	.02	0	.02	<.1	<.1	<.1	0	<.1	<.1	<.1	<.1	0–.03
Yb	0	.0002	.0005	.0004	.0002	.0004	0	0	.0003	0	.0001	.0003	0	.0001	.0007	.0002	0	0	0.–0007
Ti	.09	.7	.2	.2	.9	1	.1	.08	3	.1	1	3	2	3	3	4	3	2	.08–4
Zr	.02	.06	.2	.07	.07	.05	.03	.05	.06	.02	.06	.06	.03	.04	.07	.03	.03	.02	.02–.2
V	.002	.09	.005	.004	.03	.09	.003	.008	.06	.004	.05	.08	.04	.04	.04	.04	.04	.03	.002–.09
Nb	.01	.02	.008	.009	.01	.02	.01	.01	.02	.02	.02	.02	.01	.02	.01	.01	.01	.01	.008–.02
Cr	0	0	.001	0	.0009	0	0	0	.0004	0	0	.0004	0	.0006	0	.02	.02	.08	0–.08
Mo	0	0	0	0	.0007	.001	0	0	.0008	.0005	0	.001	0	.001	0	0	0	0	0–.001
Mn	.1	.2	.06	.01	.2	.2	.09	.001	.2	.02	.2	.5	.4	.2	.4	.5	.2	.2	.001–.5
Fe	2	>5	2	1	4	>5	1	.6	5.0	1	>5	>5	5	5	>5	>5	>5	>5	.6–>5
Co	0	.0009	0	0	.001	.003	0	0	.001	0	.002	.003	.002	.003	.004	.005	.004	.004	0–.005
Ni	0	.0007	.0009	0	.0009	0	0	0	0	0	0	0	0	.0008	0	.005	.000	.02	0–.02
Cu	.0002	.0009	.0007	.0006	.006	.008	.0002	.0003	.007	.004	.001	.006	.005	.007	.01	.01	.01	.01	.0002–.01
Zn	0	0	0	0	0	0	0	0	0	0	.03	.05	.07	0	.04	.08	.04	.04	0–.08
Ga	.005	.004	.005	.005	.004	.004	.005	.004	.003	.004	.004	.003	.002	.004	.004	.003	.003	.003	.002–.005
Pb	.006	.002	.006	0	.02	.003	.01	.008	.003	.006	.003	0	0	.002	0	.002	0	0	0–.02
Radiometric analyses [Analyst, B. A. McCall]																			
eU	0.003	0.006	0.009	0.005	0.005	0.002	0.004	0.007	0.001	0.004	0.002	0.003	0.002	0.004	0.001	0.001	0.002	<0.001	
Chemical analyses [Analyst, Roosevelt Moore]																			
U	0.0008	0.0012	0.0019	0.0011	0.0012	0.0011	0.0010	0.0015	0.0011	0.0012	0.0011	0.0011	0.0010	0.0011	0.0016	0.0010	0.0010	0.0008	

x = found but quantity not determined.

Looked for (spectrographically) but not found: Hf, Th, P, Ta, W, U, Re, Ru, Rh, Pd, Os, Ir, Pt, Ag, Au, Cd, Hg, In, Tl, Ge, Sn, As, Sb, Bi, Te.

Low-level chemical analyses for uranium and thorium by J. C. Antweiler.

L–285. Nepheline syenite pegmatite, NW¼ sec. 30.
L–313. Alkalic syenite pegmatite, SE¼ sec. 30.
L–36. Alkalic syenite aplite, NW¼ sec. 18.
L–223. Alkalic leucotrachyte porphyry, SW¼ sec. 24.
MC–157. Hornblende feldspathoidal trachyte porphyry, SW¼ sec. 8.
L–284. Altered alkalic trachyte porphyry, NW¼ sec. 30.
L–221. Feldspathoidal leucotrachyte, SE¼ sec. 11, T. 3, S., R. 18, W.
L–222. Leucophonolite, NE¼ sec. 14, T. 3 S., R. 18 W.
L–248. Altered alkalic trachyte, SW¼ sec. 16.
I–174c. Corundum alkalic leucotrachyte, SE¼ sec. 19, T. 3 S., R. 18 W.
L–282. Andesite, NW¼ sec. 30.
L–255. Feldspathoidal syenite lamprophyre, SW¼ sec. 16.
L–270. Altered nepheline syenite lamprophyre, NW¼ sec. 24.
L–289. Alkalic syenite lamprophyre, NW¼ sec. 24.
L–260. Diorite lamprophyre, NE¼ sec. 17.
L–276. Gabbro lamprophyre, NW¼ sec. 29.
L–301. Ouachitite, SW¼ sec. 25.
L–227. Biotite-monchiquite, SW¼ sec. 9, T. 3 S., R. 18 W.
L–53. Nepheline syenite pegmatite, NW¼ sec. 17.

The spectrographic analyses of dike rocks (table 38) show relatively uniform high concentrations of Sr, Ti, Zr, Nb, and rare earths and emphasize the genetic relationship of these dike rocks to the Magnet Cove intrusive complex. The concentrations of individual minor elements are related to rock types. Sr, Sc, Ti, Cr, Co, Ni, Cu, and Zn are most abundant in the basic lamprophyre dikes; B and Pb are most abundant in the felsic dike rocks. Particularly notable enrichments are 0.02 percent B and 0.2 percent Zr in an alkalic syenite aplite (L–36); 0.08 percent Cr and 0.02 percent Ni in a biotite monchiquite (L–227); 0.08 percent Zn in a gabbro lamprophyre (L–276); 0.02 percent Pb in a hornblende feldspathoidal trachyte porphyry.

VEINS

Significant deposits of rutile, brookite, and molybdenite occur in veins within the igneous complex and the contact zone.

Fryklund and Holbrook (1950) made a detailed study of the veins of the Magnet Cove Titanium Corporation deposit, the Hardy-Walsh brookite deposit, and the Christy brookite deposit. Holbrook (1948) and Fryklund and Holbrook (1950) have described the veins in the Mo-Ti Corporation molybdenum-titanium prospect.

In the Magnet Cove Titanium Corp. open pit in secs. 17 and 18, Fryklund and Holbrook (1950) described six major vein types and several minor types that occur as small veinlets. The six major vein types are: sugary-textured albite-dolomite microcline-calcite, albite-ankerite, coarse-grained albite-perthite carbonate, calcite-rutile, and coarse-grained calcite which may be equivalent to the carbonatite. The minor types include: dolomite, dolomite-rutile, dolomite-pyrite, dolomite-rutile-pyrite, dolomite-rutile-pyrite-green biotite, dolomite-green biotite, fluorite, and pyrite.

The Hardy-Walsh and Christy deposits are in recrystallized novaculite of the contact zone. Fryklund and Holbrook state that the veins in these deposits are composed of recrystallized quartz (clear and smoky) and introduced rutile, brookite, taeniolite, pyrite(?), and clay minerals, kaolinite and nontronite(?). A late quartz-goethite vein cuts residual ore in the Hardy-Walsh deposit.

The range of Nb, TiO_2, Y, V, and La, in samples from the Magnet Cove Titanium Corp., Christy Brookite, and Hardy-Walsh Brookite deposits is shown in table 39. Spectrographic analyses of rutile-bearing veins outside of the major deposits are shown in tables 40 and 41.

Molybdenum-bearing veins cut jacupirangite in the Mo-Ti prospect in sec. 17; they were first described by Sleight (1941). Holbrook (1948) and Fryklund and Holbrook (1950), who described the veins in detail, found that molybdenite mineralization followed the introduction of feldspar veins composed of microcline (about 80 percent), albite, apatite, brookite, rutile, pyrite, and sphene in varying amounts.

Molybdenite also was noted in the Magnet Cove Titanium Corp. deposit by Fryklund and Holbrook (1950) and in the carbonatite at the Kimzey calcite quarry by Fryklund, Harner, and Kaiser (1954). Spectrographic analyses of a molybdenite-colorless mica veinlet in carbonatite (L–171) and material dredged from a stock pond in the western part of section 20 (L–150), composed of colorless mica—about 75 percent, molybdenite—about 15 percent, and apatite, hematite, limonite, and pyrite—about 10 percent, are given in table 40.

Other veins containing dominant quartz, quartz-feldspar, quartz-brookite-rutile, feldspar, feldspar-carbonate, or apatite were mapped and are shown on the geologic map, plate 1. Concentrations of float crystals of rutile, brookite, and paramorphs of rutile after brookite also were noted on the geologic map.

TABLE 39.—*Range, in percent, of* Nb, TiO_2, V, Y, *and* La *content in veins of the major deposits*

[From Fryklund, Harner, and Kaiser (1954)]

Deposit	Nb	TiO_2	V	Y	La
Magnet Cove Titanium Corp.	0-.12	0.25-15.8	0.013-.47	0-.31	0-.51
Christy Brookite	0-.45	2.0-26.3	.08-1.0	0-.14	----------
Hardy-Walsh Brookite	0-.46	.082-37.	.019-.34	0-.034	0-.076

Fluorite and sodalite coat the joints in the pegmatite at the Diamond Jo quarry, and Fryklund and Holbrook (1950) report small fluorite veinlets in the Magnet Cove Titanium Corporation deposit. A vein composed of colorless and purple fluorite, anhedral quartz, chalcedony, zeolite(?), and witherite(?) was found in the area known as the V-intrusive in sec. 19, T. 3 S., R. 18 W., west of the Magnet Cove complex (fig. 4).

Apatite veins composed of occasional clusters of biotite and of garnet in a matrix of subhedral apatite, cut the biotite-garnet ijolite in the NW1/4 sec. 20. Fresh material from a bulldozer cut is composed of apatite, pyrite, and zeolite(?) in varying proportions. The fresh rock is partly fine grained, L–116b, and partly medium grained L–116c. It weathers to a very fine grained mass of iron oxide rich in secondary apatite, and occasional crystals of rare earth phosphates(?), L–116 and L–116e.

L–116f is composed of resistant apatite and fine-grained limonite and hematite from partly weathered pyrite. Spectrographic analyses of these samples are given in table 42.

A very irregular vein, 2 to 8 inches wide, of earthy, very fine grained pale greenish-yellow material occurs within the extremely weathered part of the apatite-pyrite vein. As determined by X-ray the material is a mixture of monazite and a plumbogummite group mineral. The monazite is characterized according to Murata and others (1957) by a high La+Ce+Pr index, 87, and little or no thorium (no thorium was detected in the analysis, table 42).

From the following evidence it appears that the monazite is a product of the weathering of the apatite-pyrite vein:

1. No monazite was detected in the fresh rock.
2. The monazite is earthy and no remains of original crystals were detected in the smaller vein.
3. The smaller vein was observed only in the weathered portion of the apatite-pyrite vein.
4. Lack of detectable thorium in both the monazite and apatite-pyrite vein.

The spectrographic analyses of veins (tables 40, 41, 42) and vein minerals (table 43) indicate that the trace elements have a wide range of concentration but Nb, Mo, Ce, Pb, Ga, and U are more consistently enriched in the vein rock than in the major rock types. Other elements such as Co, Y, Zn, Zr, and V, show erratic, high concentrations in individual veins.

The niobium is concentrated in rutile and brookite; molybdenum is in molybdenite and feldspar; cerium is in apatite; lead and gallium are in feldspar. The highest uranium (0.058 percent) is in a monazite-plumbogummite group(?) vein; lesser concentrations (0.01 to .018 percent) occur in the clay material from brookite veins.

A lithium content of 0.03 percent was detected in the three veins analyzed for lithium. It probably occurs in a micaceous clay mineral. Similar concentrations of lithium can be anticipated for most of the other veins.

TABLE 40.—*Analyses, in percent, of veins*

	L-150	L-171	W-19	L-31	L-60a	L-74	L-76	L-78	L-112	L-278	L-310	L-310a	L-339a	L-339b	Range
Semiquantitative spectrographic analyses [Analyst, H. J. Rose]															
Li	0.03	0.03	n.d.	n.d.	n.d.	n.d.	n.d.	n.d.	0.03	n.d.	n.d.	n.d.	n.d.	n.d.	------------
Be	.0003	.0003	0.0003	0.0001	0.0003	0.0001	0.0003	0	0	0.0003	0.0003	0.0003	0.0003	0.001	0– .0003
Mg	10	10	.03	.03	.1	.3	.3	.03	.1	.03	.03	.03	.1	.01	.01–10
Ca	.1	10	.03	.01	.003	.01	.03	.003	.03	.003	1.0	.003	.1	.03	.003–10
Sr	.03	.3	.03	.03	.03	.03	.1	.003	.003	.001	.03	.003	.01	.1	.001– .3
Ba	.3	.3	.03	.3	.3	.3	.3	.03	.1	.003	.03	.03	.01	.1	.003– .3
B	0	0	0	0	0	0	.003	0	0	0	0	.001	.003	0	0– .003
Sc	0	.0003	.001	0	0	.0003	0	.0003	.0003	.0003	.003	.001	.003	.003	0– .003
Y	.003	.01	.03	.001	.001	.003	0	.003	0	.01	.03	.01	.03	.01	0– .03
La	.01	.03	.1	.003	0	.01	.03	.01	0	0	.1	.03	.003	.1	0– .1
Ce	0	0	.03	0	0	0	0	0	0	0	.3	.1	0	.1	0– .3
Ti	.1	.03	3.0	.1	.1	1.0	.1	.1	.3	10	1	.3	3.0	3.0	.03–10
Zr	0	0	.03	.03	.1	.1	.03	.01	.01	.1	.003	0	.01	.003	0– .1
P	0	1.0	0	0	0	0	0	0	0	0	3.0	0	0	.3	0– 3
V	.01	.01	.1	.01	.01	.01	.003	.3	.03	.3	.003	.003	.3	.1	.003– .3
Nb	.01	.03	.1	.01	.01	.03	.03	.03	0	.3	.1	.03	.1	.1	0– .3
Cr	.0003	.0003	.0003	.0003	.001	.0003	.0003	.003	.001	.03	.001	.001	.01	.003	.0003– .03
Mo	.3	.3	0	0	0	.003	.003	0	0	0	0	0	.003	.01	0– .3
Mn	.3	.3	.3	.03	.03	.01	.03	.3	.03	.1	.1	.03	.003	.003	.003– .3
Fe	3	1	10	3	10	3	3	10	.3	3	3	3	.3	3	.3–10
Co	.0003	0	.003	0	.0003	.0003	0	.001	0	.001	0	0	.001	.003	0– .003
Ni	0	0	0	0	.003	.003	0	0	0	0	0	0	.003	0	0– .003
Cu	.0003	.0003	.03	.003	.003	.001	.0003	.0003	.0003	.01	.003	.001	.003	.003	.0003– .03
Ag	0	0	.0003	0	0	0	0	0	0	0	0	0	0	.0001	0– .0003
Zn	0	0	0	0	0	0	0	.03	0	0	0	0	0	0	0– .03
Ga	.001	0	.003	.001	.003	.003	.003	.003	.003	0	0	0	.003	.003	0– .003
Pb	.01	.03	.003	.01	.01	0	.003	.003	0	.01	.01	.03	.03	.01	0– .03
F	.3	3.0	n.d.	n.d.	n.d.	n.d.	n.d.	n.d.	.1	n.d.	n.d.	n.d.	n.d.	n.d.	
Radiometric analyses [Analyst, B. A. McCall]															
eU	0.005	0.002	0.004	0.008	0.007	0.010	0.005	0.006	0.008	0.001	0.010	0.004	0.020	0.012	
Chemical analyses [Analyst, Roosevelt Moore]															
U	0.007	0.001	0.003	0.004	0.005	0.001	0.003	0.004	0.003	0.001	0.008	0.002	0.018	0.010	

n.d.=not determined.
Looked for (spectrographically) but not found: Hf, Th, Ta, W, U, Re, Ru, Rh, Pd, Os, Ir, Pt, Au, Cd, Hg, In, Tl, Ge, Sn, As, Sb, Bi, Te.
L-150. Weathered molybdenite, mica-bearing vein, NW¼ sec. 20.
L-171. Molybdenite-bearing vein in carbonatite, NW¼ sec. 19.
W-19. Weathered rutile-bearing vein, NE¼ sec. 19.
L-31. Weathered rutile-bearing vein, SW¼ sec. 18.
L-60a. Weathered rutile-zircon-bearing vein, NW¼ sec. 17.
L-74. Rutile-bearing vein, SE¼ sec. 17.
L-76. Weathered pyrite-bearing vein, SE¼ sec. 17.
L-78. Weathered rutile-bearing vein, SE¼ sec. 17.
L-112. Weathered rutile-bearing vein, SW¼ sec. 21.
L-278. Weathered brookite-zircon-bearing vein, SW¼ sec. 7.
L-310. Weathered rutile-apatite-bearing vein, NE¼ sec. 19.
L-310a. Weathered rutile-chalcedony-bearing vein, NE¼ sec. 19.
L-339a. Brookite and gray clay from vein, NW¼ sec. 8.
L-339b. Purple clay from vein, NW¼ sec. 8.

TABLE 41.—*Analyses, in percent, of veins*

[Spectrographic analyses by Sol Berman. Colorimetric analyses by H. E. Crowe and A. P. Marranzino]

	L-62	L-115	L-118	Mag. M.A.	L-233	Range		MC-266	MC-225	MC-218
Spectrographic analyses							**Colorimetric analyses**			
Be	0. 0001	0. 0002	0. 0006	0. 0005	0. 0004	0. 0001–0. 0006	Mn	0. 050	0. 3	0. 050
Mg	. 2	. 2	2	. 009	. 06	. 009–2	As	. 003	. 002	. 001
Ca	>5	. 2	. 5	. 02	. 2	. 02–>5	Cu	<. 002	<. 002	. 005
Sr	. 6	. 001	. 05	. 001	. 003	. 001–. 6	Sb	. 0001	. 0004	. 0002
Ba	. 1	. 02	. 1	. 003	. 06	. 003–. 1	Zn	. 04	. 013	. 005
B	0	. 001	0	. 005	. 003	0–. 005	Nb	. 02	. 045	. 014
Sc	. 003	. 001	. 007	0	0	0–. 007				
Y	. 008	. 001	. 02	0	0	0–. 02				
La	. 05	0	. 04	0	0	0–. 04				
Ce	. 2	0	. 09	0	0	0–. 2				
Yb	. 0007	0	. 002	0	0	0–. 002				
Ti	. 9	. 4	. 7	. 05	. 05	. 05–. 9				
Zr	. 02	. 006	. 006	. 004	. 01	. 006–. 02				
P	x	0	. x	0	0	0–x.				
V	. 05	. 004	. 03	. 002	. 002	. 002–. 05				
Nb	. 03	. 01	. 02	0	. 005	0–. 03				
Cr	. 0004	. 004	. 004	. 0003	. 0003	. 0003–. 004				
Mo	. 008	. 04	. 02	0	0	0–. 04				
Mn	. 01	. 2	. 5	. 03	. 1	. 03–. 5				
Fe	>5	>5	>5	. 9	1	. 9–>5				
Co	. 005	. 002	. 002	0	0	0–. 005				
Ni	. 002	. 002	. 002	0	0	0–. 002				
Cu	. 005	. 007	. 01	. 0002	. 0004	. 0002–. 01				
Zn	0	. 04	0	0	0	0–. 04				
Ga	. 001	. 002	. 004	. 003	. 003	. 001–. 004				
Pb	. 008	. 02	. 02	. 004	. 007	0–. 02				
Radiometric analyses [Analyst, B. A. McCall]										
eU	0. 006	0. 002	0. 014	0. 003	0. 003					
Chemical analyses [Analyst, Roosevelt Moore]										
U	n.d.	n.d.	n.d.	0. 0011	0. 0011					

n.d.=not determined.
x=found, quantity not determined.
Looked for (spectrographically) but not found: Hf, Th, Ta, W, U, Re, Ru, Rh, Pd, Os, Ir, Pt, Ag, Au, Cd, Hg, In, Tl, Ge, Sn, As, Sb, Bi, Te.

L-62. Weathered rutile-bearing vein, central part of sec. 17.
L-115. Weathered rutile-bearing vein, SE¼ sec. 17.
L-118. Weathered rutile-bearing vein, east-central sec. 17.
Mag. M.A. Quartz-bearing vein, N½ sec. 20.
L-233. Quartz-bearing vein, NW¼ sec. 28.
MC-226. Weathered rutile-bearing vein, NW¼ sec. 17.
MC-225. Weathered rutile-bearing vein, NE¼ sec. 18.
MC-218. Weathered rutile-bearing vein, NE¼ sec. 17.

CONTACT ZONE

A zone of metamorphosed sediments 1,000 to 2,500 feet in width and about 4.6 square miles in area surrounds the igneous complex. The formations in contact with the complex at the present erosion surface are Missouri Mountain shale, Arkansas novaculite, and Stanley shale that have been altered to gneiss, hornfels, argillite, and quartzite. Since most of the metamorphic zone is more resistant than the adjacent sediments it appears as a ridge on the north, west, and south sides of the complex. As the Missouri Mountain shale occurs along only about 500 feet of the contact with the complex, the zone of metamorphosed sediments consists very largely of the Stanley shale and Arkansas novaculite.

METAMORPHOSED ARKANSAS NOVACULITE

Metamorphism of Arkansas novaculite has resulted in recrystallization of the quartz from a chert (grain size, 0.002 to 0.025 mm) to a coarse-grained quartzite (grain size, 0.04 to 7 mm). The grain size gradually decreases away from the contact until, at a distance of 1,000 to 2,500 feet from the complex, the recrystallized character of the rock is no longer detectable with the hand lens. Some of this recrystallized novaculite, although resistant to weathering, is very friable and can be crumbled with the fingers to a sand. Outcrops east of the town of Magnet are of this nature. In thin section the recrystallized rock is composed of quartz anhedra of varying sizes; the larger crystals have sutured contacts.

The shale in the Arkansas novaculite is altered to a

TABLE 42.—*Analyses, in percent, of apatite-pyrite vein*

Spectrographic analyses

[Analyst: Sol Berman, L-116, L-116-b, L-116-c, L-116-e, L-116-f; H. J. Rose, L-116-1 and L-116-2]

	L-116	L-116-b	L-116-c	L-116-e	L-116-f	L-116-1	L-116-2
Be	0.002	0.0006	0.0008	0.002	0.0003	0.004	0
Mg	.003	.006	.005	.03	.08	0	.005
Ca	4	3	>5	>5	>5	n.d.	n.d.
Sr	.9	.2	.2	.9	.9	n.d.	.002
Ba	5	.04	.03	.2	.5	n.d.	0
B	.002	0	0	.005	0	n.d.	n.d.
Sc	.01	.01	.01	.01	.007	0	0
Y	.07	.07	.07	.3	.03	.9	0
La	1	1	.9	2	.1	24	0
Ce	1	1	1	1	.5	n.d.	n.d.
Yb	.006	.005	.006	.02	.003	n.d.	n.d.
Ti	.6	.9	.1	.6	.4	.2	.008
Zr	.03	.07	.01	.06	.2	0	0
P	xx	x	x	xx	xx	>10	0
V	.1	.04	.04	.1	.08	.08	.002
Nb	.06	.04	.02	.06	.09	0	0
Cr	.002	.002	.002	.004	.0008	0	.0004
Mo	.003	.009	.02	.002	0	0	0
Mn	.02	.002	.002	.02	.03	.08	.004
Fe	>5	>5	>5	>5	5	n.d.	>5
Co	.002	.009	.01	.003	0	0	.05
Ni	0	.002	.002	0	.003	0	0
Cu	.09	.5	.7	.2	.009	.01	.04
Ag	.0008	.0006	.002	0	0	0	.0003
Ga	.003	.02	.001	.002	.001	0	.001
Pb	.03	.02	.01	.02	.009	0	0

Radiometric analyses

[Analyst, B. A. McCall]

	L-116	L-116-b	L-116-c	L-116-e	L-116-f	L-116-1	L-116-2
eU	0.012	0.020	0.013	0.014	0.003	0.098	n.d.

Chemical analyses

[Analyst, J. Dubinsky]

	L-116	L-116-b	L-116-c	L-116-e	L-116-f	L-116-1	L-116-2
U	n.d.	n.d.	n.d.	n.d.	n.d.	.059	n.d.

n.d. = not determined.
Looked for (spectrographically) but not found: Hf, Th, Ta, W, U, Re, Ru, Rh, Pd, Os, Ir, Pt, Au, Zn, Cd, Hg, In, Tl, Ge, Sn, As, Sb, Bi, Te.

EXPLANATION OF SAMPLES

	Sample	X-ray	Analyst
L-116	Weathered apatite-pyrite vein, NW¼ sec. 20.		
L-116-b	Fresh apatite-pyrite vein, NW¼ sec. 20.		
L-116-c	do		
L-116-e	Weathered apatite-pyrite vein, NW¼ sec. 20.		
L-116-f	do		
L-116-1	Monazite and plumbogummite group(?) vein, NW¼ sec. 20.	Monazite plus plumbogummite group mineral(?)	F. A. Hildebrand.
L-116-2	Pyrite from L-116-c		

TABLE 43.—*Spectrographic analyses, in percent, of minerals from veins*

	L-75d$_1$	L-75d$_2$	L-338-1	L-165-1	MC-8-1	W-5-1	MC-162-1	MC-178-1
Mg	0.00x	0.00x	0.00x	0.01	>1	0.005	0.01	0.02
Ca	.00x	.00x	.0x	n.d.	n.d.	n.d.	n.d.	.01
Sr	n.d.	n.d.	x	0	.08	0	.004	.0008
Ba	n.d.	n.d.	>10	0	.004	.02	.6	.05
B	0	0	0	n.d.	n.d.	n.d.	n.d.	0
Sc	0	0	0	0	.004	0	0	0
Y	0	0	.0x	0	.02	0	0	0
La	0	0	.0x	0	.01	0	0	0
Yb	0	0	0	n.d.	n.d.	n.d.	n.d.	0
Ti	n.d.	n.d.	.0x	.01	.8	.004	.03	.03
V	.018	.012	0	0	.008	.003	.003	.002
Nb	.030	.035	0	0	0	0	0	0
Cr	0	0	.000x	.0007	.009	.0009	.0009	.00008
Mn	.x	.x	.00x	.0006	.1	.001	.003	.02
Fe	n.d.	n.d.	.0x	>10	>10	.09	.2	.3
Co	0	0	0	.007	0	0	0	0
Ni	0	0	0	.002	0	0	0	0
Cu	.00x	.00x	.000x	.001	.0009	.001	.002	.0007
Ag	0	0	0	0	.0002	.0001	.0001	0
Ga	0	0	0	.001	0	.002	.003	.0006

n.d. = not determined.
Looked for but not found: Be, B, Zr, Hf, Th, P, Ta, Mo, W, U, Re, Pd, Ir, Pt, Au, Zn, Cd, Hg, In, Tl, Ga, Ge, Sn, Pb, As, Sb, Bi.
Analysts: H. J. Rose—MC-8-1, W-5-1, MC-162-1, L-165-1; J. D. Fletcher—L-75d$_1$, L-75d$_2$, MC-178-1, L-338-1.

L-75d$_1$.	Ilmenite float, SE¼ sec. 17.
L-75d$_2$.	Ilmenite float, SE¼ sec. 17. Analyses from different parts of the same crystal.
L-165-1.	Pyrite, NE¼ sec. 18.
L-338-1.	Barite, NE¼ sec. 19.
MC-8-1.	Ferroan dolomite, NE¼ sec. 18.
W-5-1.	Microcline from feldspar-rich vein, NW¼ sec. 20.
MC-162-1.	Microcline from feldspar-rich vein, SW¼ sec. 17.
MC-178-1.	Microcline from feldspar-rich vein, NW¼ sec. 20.

fine-grained hornfels composed of orthoclase, perthite, brown biotite, and quartz.

METAMORPHOSED STANLEY SHALE

The Stanley shale is composed of shale and sandstone. Some of the shale is quite siliceous and the sandstones are quartzite, feldspathic quartzite, arkosite, subgraywacke, and graywacke.

The shales at the outer limit of the contact zone are characterized by black spots as much as 2 mm in diameter. In thin section the spots appear to be segregations of sericite partially altered to brown or green biotite, opaque minerals, minor recrystallized quartz, and chlorite. The groundmass is composed of recrystallized quartz, sericite partially altered to brown or green biotite, opaque minerals and chlorite. As the contact with the igneous complex is approached, the amount of biotite increases, and the grain size of both biotite and quartz increases slightly. The argillaceous portion of the sandstones is similarly affected, but in the cleaner sandstones the only effect is a minor recrystallization of the quartz.

On the north edge of the complex the narrow zone near the contact in which biotite is visible was also delimited. In the outcrop some of the rock with visible biotite is gneissic and some is massive. The mineralogy is dependent upon original material, distance from the contact, and the nature of the igneous rocks at the contact.

Good exposures of garnet-pseudoleucite syenite and garnet-nepheline syenite in contact with Stanley shale, are found in the stream that cuts the outer rim of igneous rock in the north-central part of sec. 18. In this area the metamorphosed sediments are fine grained gneisses cut by a multitude of alkalic syenite aplite dikes from ¼ to 12 inches wide. About 15 feet from the concealed contact with garnet-pseudoleucite syenite, the fine grained gneiss is composed of orthoclase, microperthite, green hornblende, brown biotite, magnetite, and pyrite. About 20 feet away from the contact the gneiss is 85 percent oligoclase, 8 percent reddish-

TABLE 44.—*Analyses, in percent, of metamorphosed sediments of the contact zone*

	L-247a	L-178	L-243	L-38	L-173	L-234	L-235	L-247b	L-149	Range
Spectrographic analyses										
Be	0.0002	0.0001	0.0003	0.0003	0.0003	0.0004	0.0002	0.0002	0.0001	0.0001–0.0004
Mg	x	x	x	.x	x	x	x	x	.x	.x–x
Ca	.2	.2	>5	.2	.2	.07	.2	x	.1	.1–>5
Sr	.02	.01	.3	.04	.1	.01	.02	.008	.01	.01–.3
Ba	.2	.07	.5	.1	.2	.09	.2	.04	.1	.04–.5
B	.02	.003	.001	.002	.003	.003	.007	.005	.002	.001–.02
Sc	.002	.0009	0	.0009	.0009	.002	.002	.0009	.0004	0–.002
Y	.005	.004	.007	.004	.006	.004	.007	.005	.004	.004–.007
La	0	.01	.02	.009	.009	.009	.01	0	0	0–.02
Yb	0	0	.0002	.0001	.0004	0	.0004	.0001	.0005	0–.0005
Ti	.4	.4	1	.4	.5	.5	.5	.3	.2	.2–1
Zr	.008	.006	.05	.04	.02	.02	.02	.03	.02	.006–.05
V	.009	.005	.07	.007	.01	.01	.008	.002	.002	.002–.07
Nb	0	0	.03	0	0	.009	0	0	0	0–.03
Cr	.01	.008	0	.007	.01	.01	.02	.004	0	0–.02
Mo	0	0	0	0	.0008	0	0	0	0	0–.0008
Mn	.04	.06	.2	.03	.03	.1	.03	.06	.01	.01–.2
Fe	4	3	>5	2	3	3	3	3	.7	.7–>5
Co	.001	.002	.002	0	.001	0	.0008	.001	0	0–.002
Ni	.003	.003	0	0	.002	.003	.005	.0009	0	0–.005
Cu	.0008	.01	.02	.0009	.002	.004	.001	.002	.0005	.0005–.02
Ag	0	0	.0001	0	0	0	0	0	0	0–.0001
Ga	.003	.002	.003	.002	.002	.002	.003	.002	.002	.002–.003
Pb	.03	0	0	0	.004	.001	0	.004	0	0–.03
Radiometric analyses [Analyst, B. A. McCall]										
eU	0.003	0.003	0.003	0.004	0.003	0.002	0.002	0.001	0.001	
Chemical analyses [Analyst, Roosevelt Moore]										
U	0.0011	0.0015	0.0012	0.0011	0.0011	0.0012	0.0014	0.0010	0.0010	

x=found, quantity not determined.

Looked for (spectrographically) but not found: Ce, Hf, Th, P, Ta, W, U, Re, Ru, Rh, Pd, Os, Ir, Pt, Au, Zn, Cd, Hg, In, Tl, Ge, Sn, As, Sb, Bi, Te.

L-247-a.	Spotted biotite-quartz argillite, SW¼ sec. 9.
L-178.	Spotted biotite-quartz argillite, NW¼ sec. 18.
L-243.	Hornblende hornfels, NE¼ sec. 17.
L-38.	Hornblende-oligoclase gneiss, NW¼ sec. 18.
L-173.	Biotite gneiss, NW¼ sec. 18.
L-234.	Acmite hornfels, NW¼ sec. 28.
L-235.	Quartz-biotite hornfels, NW¼ sec. 28.
L-247b.	Feldspathic quartzite, SW¼ sec. 9.
L-149.	Lithic tuff in Stanley shale, W½ sec. 28.

brown biotite, 4 percent pale dirty green hornblende, 1 percent aegirine, 3 percent magnetite, and a trace of pyrite. Albite, aegirine, brown biotite, greenish-brown hornblende, magnetite, and pyrite are found about 30 feet from the contact. About 40 feet from the contact the gneiss is composed of orthoclase, andesine, hornblende, sphene, apatite, and pyrite. About 125 feet from the contact the composition is 58 percent orthoclase plus minor perthite and plagioclase, 26 percent brown biotite, 7 percent sericite, 7 percent green to colorless anhedral garnet(?), 1 percent magnetite, and 0.1 percent pyrite. At the outer limit of the visible biotite zone (about 300 ft) the very fine grained gneiss is composed of quartz, brown biotite, sericite, and pyrite.

No consistent visible biotite zone was developed along the southern half of the complex, probably because the Stanley shale is more siliceous or sandy along this contact. On Stone Quarry Creek in the northwestern part of sec. 28, a medium-grained hornfels composed of orthoclase, microperthite, albite, quartz, and acmite is developed at the contact and grades into a fine-grained hornfels composed of quartz, biotite, sericite, and pyrite, about 3 feet from the contact. On a small tributary of Cove Creek in the northwestern part of sec. 30, the fine grained subgraywacke 1 foot from the contact with the pegmatite shows a partial recrystallization of the quartz and only incipient alteration of sericite to biotite.

Spectrographic analyses of several examples of the foregoing rocks, table 44, suggest that, of the trace elements, Sr, Ba, Zr, La, Nb, and V have been introduced into the sediments.

Spectrographic analyses of most of the Paleozoic formations outside of the contact metamorphic zone, table 45, show no significant additions of the trace elements that characterize the Magnet Cove igneous complex (Ti, Zr, Nb, Ba, Sr, V, and rare earths).

GEOCHEMISTRY

ROCKS

The igneous rocks of the Magnet Cove complex are high volatile, high lime, alkalic and subsilicic; they contain intrusive carbonatite masses as well as the iron, titanium, zirconium, and phosphate minerals that characterize similar alkalic rocks throughout the world. High niobium substitution in titanium minerals and rare-earth substitution in apatite and perovskite are also typical.

The weighted average of the major oxides for all the analyzed rocks from Magnet Cove (table 46) show that the average chemical composition can be expressed in rock terms as a melanocratic phonolite. It is well to remember, however, that the weighted average composition is based essentially on analyses of two very dissimilar rock groups—the mafic jacupirangite-ijolite group and the felsic phonolite-nepheline syenite group.

The most significant difference between these rocks and the average igneous rock (table 46) are the high content of soda, lime, titania phosphate, carbon dioxide, chlorine, fluorine, sulfur and sulfur trioxide, and the low content of silica. The high soda is reflected in occurrence of nepheline and sodic pyroxene and amphibole; high lime and titania produces abundant titaniferous pyroxene, melanite garnets, sphene, and perovskite; the high carbon dioxide and phosphate combine with lime to make carbonatite and apatite; chlorine and sulfur trioxide are in sodalite and cancrinite alterations of nepheline; high fluorine is in fluorite and biotite.

The trace elements which show significant concentrations in the Magnet Cove rocks as compared to average igneous rocks (table 46) are strontium (in the high lime minerals), barium (in potassic minerals), lanthanum (in apatite and perovskite), zirconium (in eudialyte and

TABLE 45.—*Analyses of sedimentary rocks in the Magnet Cove area, in percent*

Spectrographic analyses

[Analyst, Sol Berman]

	B-1	BF-209	L-332	L-316	L-315	P-278	L-333	L-309	L-331	L-224	W-780	L-295	Range
Be	0.0001	0	0	0	0.0002	0.0002	0.0002	0.0003	0.0002	0.0002	0.0001	0	0–.0003
Mg	.2	.03	.4	.005	x	.3	x	x	.6	.x	.x	.07	.0–x
Ca	<.01	<.01	x	<.01	x	<.01	.01	.4	.4	.1	.2	.03	<.01–x
Sr	.003	0	.001	0	.01	0	.001	.004	.004	.003	.002	0	0–.01
Ba	.02	.001	.001	0	.1	.06	.1	.1	.08	.09	.01	.002	0–.1
B	.01	0	0	0	.005	.01	.06	.02	.004	.009	.02	.005	0–.06
Sc	0	0	0	0	.004	.002	.006	.006	.002	.001	.0009	0	0–.006
Y	0	0	0	0	.004	.003	.006	.008	.004	.005	.006	0	0–.008
La	0	0	0	0	0	0	.01	0	0	0	0	0	0–.01
Yb	0	0	0	0	.0004	.0005	.0004	.0005	.0003	.0004	.001	0	0–.001
Ti	.1	.01	.008	0	.3	.2	.8	1	.3	.4	.5	.1	0–1
Zr	.004	0	0	0	.008	.004	.01	.02	.02	.04	.08	.02	0–.08
V	0	0	0	0	.003	.02	.008	.004	0	.002	.002	.001	0–.02
Cr	.004	.002	0	0	.006	.004	.01	.01	.004	.005	.003	.003	0–.01
Mo	0	0	0	0	0	.002	0	0	0	0	0	0	0–.002
Mn	.003	0	.02	0	.03	.004	.02	.05	.03	.02	.02	.008	0–.05
Fe	.2	.09	.07	.06	4	.3	4	>5	1	2	1	.2	.06–>5
Co	0	0	0	0	.001	0	.001	.001	.0007	.009	0	0	0–.009
Ni	0	0	0	0	.003	.003	.004	.006	.001	.001	.0005	0	0–.006
Cu	.001	.0003	.0004	.001	.007	.003	.0009	.003	.005	.0009	.0003	.0002	.0003–.005
Ga	.001	0	0	0	.001	.001	.003	.003	.002	.002	.002	0	0–.003
Pb	0	0	0	0	0	0	0	0	0	0	.006	0	0–.006

Radiometric analyses

[Analyst, B. A. McCall]

	B-1	BF-209	L-332	L-316	L-315	P-278	L-333	L-309	L-331	L-224	W-780	L-295	Range
eU	n.d.	n.d.	n.d.	n.d.	n.d.	n.d.	n.d.	n.d.	n.d.	<0.001	0.001	<0.001	

Chemical analyses

[Analysts: Grafton Daniels—B-1, BF-209, L-332, L-316, L-315, P-278, L-333, L-309, L-331; Roosevelt Moore—L-224, W-780, L-295.]

	B-1	BF-209	L-332	L-316	L-315	P-278	L-333	L-309	L-331	L-224	W-780	L-295	Range
U	<0.001	<0.001	<0.001	<0.001	<0.001	0.003	<0.001	0.001	<0.001	0.0012	0.0011	0.0010	

n.d.=not determined.

Looked for (spectrographically) but not found: Ce, Hf, Th, P, Nb, Ta, W, U, Re, Ru, Rh, Pd, Os, Ir, Pt, Ag, Au, Zn, Cd, Hg, In, Tl, Ge, Sn, As, Sb, Bi, Te.

B-1.	Bigfork chert.
BF-209.	Bigfork chert.
L-332.	Arkansas novaculite (black).
L-316.	Arkansas novaculite (white).
L-315.	Shale from the middle division of the Arkansas novaculite.
P-278.	Polk Creek shale.
L-333.	Missouri Mountain shale.
L-309.	Stanley shale.
L-331.	Sandstone from Stanley shale.
L-224.	Quartzite from Stanley shale.
W-780.	Blaylock sandstone.
L-295.	Hot Springs sandstone.

TABLE 46.—*Computed values for Magnet Cove rocks and the average igneous rock, in percent*

	Chemical			Spectrographic			Chemical	
	1	2		1	2a		1	2a
SiO_2	44.97	59.14	Be	0.0009	0.0006	U	0.00030	0.0004
Al_2O_3	17.61	15.34	Sr	.25	.03	Th	.00091	.00115
Fe_2O_3	3.74	3.08	Ba	.22	.025			
FeO	3.93	3.80	Sc	.00057	.0005			
MnO	.28	.12	Y	.0036	.00281			
MgO	2.46	3.49	La	.020	.00183			
CaO	10.06	5.08	Yb	.00029	-----			
BaO	.19	.06	Zr	.030	.022			
Na_2O	6.30	3.84	V	.044	.015			
K_2O	4.43	3.13	Nb	.009	.0024			
H_2O+	1.46	1.15	Cr	.0022	.020			
TiO_2	1.76	1.05	Mo	.0003	.00025			
CO_2	2.13	.10	-----	-----	.0015			
P_2O_5	.60	.30	Co	.0016	.0023			
SO_3	.11	-----	Ni	.0006	.0080			
Cl	.14	.05	Cu	.0044	.0070			
F	.23	.03	Ga	.0025	.0015			
S	.54	.05						

1. Bulk composition of rocks of the complex excluding sedimentary inclusions, weighted by area.
2. Average igneous rock (Clarke, 1924).
2a. Average igneous rock (Rankama and Sahama, 1950).

garnet), vanadium (in all mafic minerals), and niobium (in perovskite and sphene). Some of these elements (particularly niobium) are also concentrated in late rutile and brookite veins. Chromium, nickel, and copper show significantly less concentration in the Magnet Cove rocks than average igneous rocks.

The chemical characteristics of the igneous complex as shown in table 47 are:

1. Average silica content is low (45 percent) and ranges in the analyzed rocks from 34 percent in jacupirangite and olivine melagabbro to 54 percent in late formed tinguaitic dike rocks. The most significant break in silica content occurs between the jacupirangite-ijolite group (average, 38 percent) and the phonolite-nepheline syenite group (average, 48 percent).
2. Alumina ranges from 9 to 22 percent. It is low in jacupirangite (9.21 percent), moderate in ijolite, and high in phonolites and nepheline syenites.

TABLE 47.—*Analyses of igneous*

	Intermediate ring							Outer ring					
	Altered phonolite		Phonolite-trachyte-breccia					Syenites					Jacupirangite
			Banded trachyte	Undivided trachyte	Feldspathoidal leucotrachyte		Weighted average	Garnet pseudoleucite syenite	Garnet nepheline syenite	Garnet psuedoleucite syenite	Sphene nepheline syenite	Weighted average	
SiO_2	39.77	40.93	49.62	50.48	52.60	54.67	48.5	47.31	48.88	49.43	51.27	48.08	35.42
Al_2O_3	15.76	15.13	19.13	20.98	22.18	20.83	19.7	20.10	19.77	20.17	20.42	20.16	9.21
Fe_2O_3	1.53	1.32	1.04	2.29	.29	.20	1.31	3.57	4.20	4.00	2.12	3.45	8.94
FeO	7.85	6.86	5.59	5.16	3.83	3.69	5.33	2.62	1.72	1.71	2.60	2.21	7.17
MnO	.31	.29	.23	.29	.27	.32	.28	.30	.31	.32	.20	.28	.29
MgO	2.40	1.74	1.68	1.65	.33	.20	1.3	.89	.72	.64	1.22	.86	7.77
CaO	8.88	10.71	6.52	5.11	3.67	2.59	6.0	6.67	5.38	5.08	4.69	5.55	20.83
BaO	.16	.17	.14	.18	.29	.20	.21	.36	.32	.27	.18	.29	.00
Na_2O	7.32	7.19	6.93	5.96	5.61	5.27	6.2	7.98	7.95	8.30	8.05	8.09	1.47
K_2O	3.63	2.82	4.81	3.39	7.41	8.43	4.9	6.19	6.80	6.19	6.10	6.32	.62
H_2O+	1.25	.84	.63	.99	1.61	1.60	1.20	1.73	1.39	1.42	.94	1.11	1.05
H_2O-	.07	.04	.07	.11	.10	.09	-----	.10	.30	.10	.06	-----	.11
TiO_2	2.76	2.23	1.97	2.21	.71	.35	1.8	.88	.76	.63	1.21	.85	4.05
P_2O_5	.68	.48	.38	.37	.07	.03	.3	.21	.14	.13	.20	.17	2.23
CO_2	4.46	7.85	.05	.31	.00	.60	1.77	1.07	1.09	.96	.11	.81	.11
SO_3	.58	.22	.10	.01	.11	.01	.15	.01	.00	.13	.00	.05	.12
Cl	.71	.42	.25	.00	<.01	.01	.34	.04	.07	.08	.46	.15	.02
F	.39	.24	.22	.35	.36	.23	.34	.19	.28	.20	.29	.23	.17
S	2.46	.88	1.57	.36	1.02	1.48	1.00	.06	.04	.03	.18	.07	.38
Spectrographic analyses													
Be	0	0.0005	0.001	0	0.002	0.0002	0.0008	0.0004	0.0007	0.0007	0.0004	0.0006	0.0008
Sr	.08	.071	.5	.08	.5	.6	.24	.044	.054	.014	.065	.04	.5
Sc	0	.0005	.0003	0	0	-----	.0001	.0003	.0003	.003	.0005	.0003	.002
Y	.008	.003	.007	.007	0	-----	.004	.0038	0	.0024	.0036	.0028	.008
La	.02	.032	.02	.02	.02	.009	.02	.018	.024	.027	.024	.023	.03
Yb	.0004	.0002	.0004	.0002	0	0	.0001	.0002	-----	.0002	.0003	.0002	.001
Zr	.04	.056	.03	.04	.02	.03	.039	.021	.03	.022	.040	.027	.04
V	.06	.052	.029	.02	.021	.03	.027	.045	.052	.046	.018	.040	.07
Nb	.01	.015	.02	.01	.01	.03	.013	.0074	.0099	.0096	.0087	.0087	.002
Cr	.001	.0007	.001	.001	.0004	0	.0007	.0005	.002	.0034	.013	.0042	.0001
Mo	.003	0	.0007	0	0	0	.0003	0	0	0	.0006	.0001	.001
Co	.002	.0021	.002	.001	0	0	.001	.0009	.0008	.0008	.0012	.0009	.005
Ni	0	.0009	.001	0	0	0	.0002	.0006	0	0	.0012	.0005	.001
Cu	.005	.0074	.003	.0008	0	.001	.0023	.0008	.0009	.0010	.0021	.0012	.02
Ga	.002	.0036	.001	.002	.001	.004	.0021	.0027	.0033	.0027	.0022	.0027	.002
Pb	-----	-----	-----	-----	.002	.002	0	0	0	0	-----	-----	0
Colorimetric analyses													
As	-----	0.004	<0.001	-----	<0.001	-----	-----	0.003	<0.001	<0.001	0.002	-----	0.001
Sb	-----	.0002	.0003	-----	.0001	-----	-----	<.0001	<.0001	.0001	.0002	-----	<.0001
W	-----	.001	-----	-----	-----	-----	-----	<.001	<.001	.001	.001	-----	-----
Zn	-----	.018	<.002	-----	.01	-----	-----	.012	.015	.015	.010	-----	.013
Radiometric analyses													
eU	0.005	0.003	0.004	0.003	0.006	0.005	0.004	0.002	0.005	0.003	0.004	0.003	<0.001
U	.00040	.00033	.00029	.00025	.00043	<.001	.00034	.00020	.00027	-----	.00027	.00021	.00049
Th	.00110	.00043	.00053	.00069	.00101	-----	.00073	.00055	.00045	-----	.00100	.00070	.00339

3. Fe_2O_3 is higher than FeO except in those rocks which contain appreciable pyrite. Fersman (1937) pointed out the prevalence of high valency cations in the Khibine and Lovazero alkalic plutons.
4. Magnesia is highest in the jacupirangite and olivine melagabbro (7 to 8 percent), moderate in the ijolite group (4.2 percent, average), and low in the phonolites and nepheline syenites. The average magnesia content for the entire complex (2.46 percent), is lower than average igneous rock (3.49 percent).
5. Lime is consistently high in all the rocks and averages 10 percent for the entire complex. It ranges from 2.5 percent in tinguaite dike rocks to over 20 percent in jacupirangite. Like silica, the most significant break in lime content occurs between the ijolite group (13.49 percent) and phonolitenepheline syenite group (about 5.5 percent average).
6. Total alkali content is high in both the mafic and felsic rock groups. Twenty of the analyzed rocks contain more than 9 percent alkali. It ranges from about 2 percent in jacupirangite to almost 17 percent in tinguaite. Soda is consistently high and more abundant than potash in all analyzed rocks except two. Potash is low in the ijolite group and increases sharply in the phonolite-nepheline syenite group.
7. Titania is relatively high in all the rocks, a major constituent in jacupirangite (4.05 percent), and averages 1.76 percent for the entire complex.
8. Phosphate is high in the olivine melagabbro dike (2.72 percent), but only moderately high in the other rocks.
9. Carbon dioxide and fluorine are high in all the rocks; chlorine is high in nepheline syenites, tinguaites, and phonolite but low in psuedoleucite syenite and the ijolite group. Sulfur and sulfur trioxide are erratic but are high for the average of the entire complex.

The high lime, alkalic character of the Magnet Cove complex is well illustrated by the sum of CaO, Na_2O, and K_2O in these rocks compared to this sum in other rock types (table 48).

rocks from Magnet Cove

Inner core							Late dikes						
Ijolite group							Tinguaite			Pegmatite		Analcime olivine melagabbro	Carbonatite
Biotite-garnet ijolite	Fine-grained ijolite		Garnet ijolite		Garnet biotite melteigite	Weighted average	Tinguaite	Sodalite trachyte	Trachyte porphyry	Nepheline syenite pegmatite	Eudialyte nepheline syenite pegmatite		
35.46	36.89	37.29	41.19	43.36	40.08	38.65	52.85	53.61	53.89	52.00	52.18	34.51	1.90
18.60	13.28	14.41	17.99	19.12	11.74	17.26	19.44	20.32	21.63	20.80	19.28	10.24	.33
7.90	7.58	4.23	5.63	2.85	7.19	5.94	4.82	2.84	1.74	2.36	2.89	5.58	.42
3.27	3.71	6.10	1.76	1.44	4.76	3.06	.57	1.98	1.82	1.15	1.97	8.48	.32
.25	.33	.32	.30	.25	.32	.28	.37	.36	.15	.22	.19	.22	.26
4.16	4.22	4.15	3.06	5.21	6.72	4.20	.13	.15	.43	.28	.91	8.26	1.05
12.66	14.80	13.69	14.61	12.62	15.69	13.49	2.53	2.49	3.08	2.86	4.17	15.62	53.37
.10	.18	.14	.06	.01	.14	.09	.35	.19	.08	1.52	.10	.14	.00
6.34	5.29	5.61	6.85	7.88	3.89	6.47	8.87	8.20	6.62	7.87	7.43	1.62	.00
3.07	4.62	4.22	2.38	2.82	3.47	3.23	7.96	7.66	7.80	8.18	7.21	.70	.16
3.46	1.11	.69	3.13	2.56	.87	2.53	.78	1.12	1.09	1.00	1.64	1.06	.12
.33	.14	.04	.40	.58	.06	----------	.07	.06	.10	.04	.08	.51	.04
2.47	3.32	3.46	1.67	.56	3.44	2.20	.33	.31	.60	.24	1.02	4.88	.10
1.08	.99	.77	.41	.05	.87	.69	.04	.10	.08	.05	.19	2.72	2.00
.17	1.54	3.29	.46	.66	.18	.89	.13	.14	.26	1.10	.47	5.36	39.41
.03	.80	.19	.07	.06	.13	.16	.03	.02	.07	.17	.17	.03	.02
.00	.41	.33	.01	.00	.04	.09	.60	.52	.09	.32	.06	.02	.00
.16	.40	.32	.04	.03	.24	.17	.42	.19	.32	.13	.05	.18	.15
.97	.95	2.43	.41	.16	.65	.87	.04	.03	.35	.05	.12	.26	.09
Spectrographic analyses													
0.0008	0.004	0.0002	0.002	0.004	0.0004	0.002	0.0005	0	0.0002	0.0004	0.0002	0	0.0001
.5	.5	.9	.08	.6	.044	.33	.066	.08	.2	.091	.2	.2	.5
.0003	.0009	.002	0	.001	.0009	.0007	0	0	0	0	0	.007	0
.004	.005	.003	.003	0	.0022	.0029	0	0	.001	0	.002	.003	.004
0	.01	.009	.005	0	.037	.0042	.021	.01	.007	.011	.009	.005	.03
.0002	.0003	.0003	.0008	0	0	.0003	0	0	.0002	0	.0003	.0002	.0005
.01	.03	.04	.03	.02	.062	.022	.027	.03	.03	.0082	.04	.007	.001
.04	.05	.1	.1	.02	.096	.076	.014	.008	.02	.016	.03	.04	.02
.005	.01	.02	.002	0	.014	.007	.022	.02	.009	.0053	.01	.002	0
0	.0007	.003	0	.0004	.018	.0009	.0007	.001	0	.0004	.001	.05	0
0	0	.0008	0	0	0	.0001	0	.002	0	.0007	0	0	.001
.003	.002	.002	.0005	.001	.0045	.0019	0	0	0	0	.0006	.004	0
0	.001	.0007	0	0	.0065	.0003	0	0	0	0	0	.02	0
.004	.005	.01	.003	.0009	.024	.005	.0006	.001	.001	.005	.002	.008	.001
.003	.003	.003	.003	.003	.003	.003	.0045	.003	.002	.0030	.003	.002	0
0	0	0	0	0	0	0	.0072	----------	.002	<.0005	0	0	0
Colorimetric analyses													
<0.001	<0.001	----------	<0.001	<0.001	0.002	----------	<0.001	----------	----------	0.002	----------	<0.001	----------
.0002	.0001	----------	.0001	.0003	.0001	----------	<.0001	----------	----------	.0002	----------	.0001	----------
----------	----------	----------	----------	----------	<.001	----------	.004	----------	----------	<.001	----------	----------	----------
.020	.015	----------	<.002	<.002	.018	----------	.025	----------	----------	.010	----------	.010	----------
Radiometric analyses													
0.002	0.003	----------	<.001	<0.001	0.002	----------	0.006	0.010	0.004	0.004	0.006	<0.001	----------
.00021	.00041	----------	.00038	----------	.00019	.00032	.00043	.00066	.00069	.00010	.002(?)	.00004	----------
.00028	.00060	----------	.00063	----------	.00055	.00050	.00054	.00077	.00136	.00044	----------	.00038	----------

TABLE 48.—*Lime-alkali sums of igneous rocks compared to Magnet Cove rocks* [1]

	CaO	Na_2O	K_2O	Sum
Rhyolite	1.22	3.34	4.58	9.1
Trachyte	3.09	4.43	5.74	13.3
Andesite	5.80	3.58	2.04	11.4
Phonolite	1.50	8.84	5.23	15.6
Basalt	8.95	3.11	1.52	13.6
Olivine basalt	10.2	3.1	.9	14.2
Granite	1.99	3.48	4.11	9.6
Granodiorite	4.42	3.70	2.75	10.9
Diorite	6.74	3.39	2.12	12.2
Gabbro	10.99	2.55	.89	14.4
Average for igneous rocks	5.08	3.84	3.13	12.0
Magnet Cove complex:				
Ijolite group	13.49	6.47	3.23	23.2
Feldspathoidal syenites	5.55	8.09	6.32	20.0
Phonolites	5.94	6.34	4.91	17.2
Average for entire complex	10.06	6.30	4.43	20.8

[1] Based in part on material from Daly (1933, p. 9–28).

It is noteworthy that the alkali-lime sum from Magnet Cove rocks increases with the postulated decrease in age of the rocks. Thus, first formed rocks, phonolite-trachyte associated with volcanic activity, have the lowest alkali-lime sum. The ijolite group which is postulated to be the youngest of the major rock groups has the highest. This apparent relationship may reflect progressive desilication and increasing alkali-lime content from early to very late crystallized rocks. This possibility is discussed in the chapter on origin. In some cases the lime and alkali are separated as high lime-low alkali in jacupirangite and low lime-high alkali in tinguaite dikes.

The high alkali content of the Magnet Cove rocks is also emphasized by the high ratio of total alkali to alumina. Ussing (1911) used the term "agpaite" for nepheline syenites that have excess alkali in proportion to alumina in accordance with the equation:

$$\frac{\text{na}+\text{k}}{\text{al}}=1.2$$

where na, k, and al are the relative amounts of Na, K, and Al atoms in the rock. The average agpaitic ratio for Magnet Cove rocks is 0.91. Tinguaite is the only rock of the 29 analyzed rocks that is a true agpaite (agpaitic ratio=1.3).

Chemical analyses of the rocks (table 47) are grouped according to rock type which corresponds roughly to their position and sequence of intrusion in the complex.

The intermediate ring of phonolite-trachyte, the oldest igneous rocks in the complex, show a wide range in chemical composition particularly in SiO_2, Al_2O_3, CaO, and CO_2. This wide range, however, is caused chiefly by the high content of CO_2 and CaO as calcite and FeO and S as pyrite in the breccias. Thus, the other oxides, particularly SiO_2 and Al_2O_3, are depressed. Note also the high content of total volatiles in the breccia which will be discussed further in relation to the origin of the complex. The clean, unbrecciated trachytes and phonolites show a fairly uniform composition characterized by the lowest alkali-lime sum of any of the Magnet Cove rocks.

The weighted average composition of this rock group most closely approaches the average composition of the feldspathoidal syenites of the outer ring. However, the higher total alkalies and significantly lower strontium in the syenites set them apart.

The jacupirangite-ijolite group compared with the phonolite-nepheline syenite group is characterized by lower silica and total alkali and higher lime, magnesia, titanium, and phosphate.

The late tinguaite and pegmatite dikes are characterized by very high total alkali, and lowest lime and magnesia content of any igneous rocks in the complex.

The distribution of trace elements in the major rock groups is more erratic than the distribution of the major oxides because, for the most part, they do not form independent minerals. Distribution is controlled not only by the normal order of crystallization but also by the availability of a favorable mineral structure to accommodate the trace element. For example, niobium normally tends to concentrate in the residual magmas, however, it will enter a favorable host mineral such as perovskite that may crystallize in early differentiates.

In general, however, Be, Sr, Sc, and V are higher in the ijolite group and Ba, La, and Nb are higher in the phonolite-nepheline syenite group.

	Phonolite-nepheline syenite	*Ijolite*
Be	0.0007	0.002
Sr	.14	.33
Sc	.0002	.0007
V	.033	.076
Ba	.22	.08
La	.02	.004
Nb	.011	.007

The distribution of trace elements in the common rock-forming minerals at Magnet Cove, (table 49) is discussed in the section on "Geochemistry of minerals."

VARIATION DIAGRAMS

Several variation diagrams were constructed to determine the trends of the major elements and the chemical character of the Magnet Cove rocks. The ternary diagrams emphasize the high alkali-lime content and indicate that the lime content would provide the most significant abscissa for construction of a variation diagram.

The ternary diagram for the major elements, figure 5, shows the close grouping of the Magnet Cove rocks and emphasizes the high alkali-lime character (20 to 36 percent). The separate rock groups appear to have their own distinctive trends. The most interesting

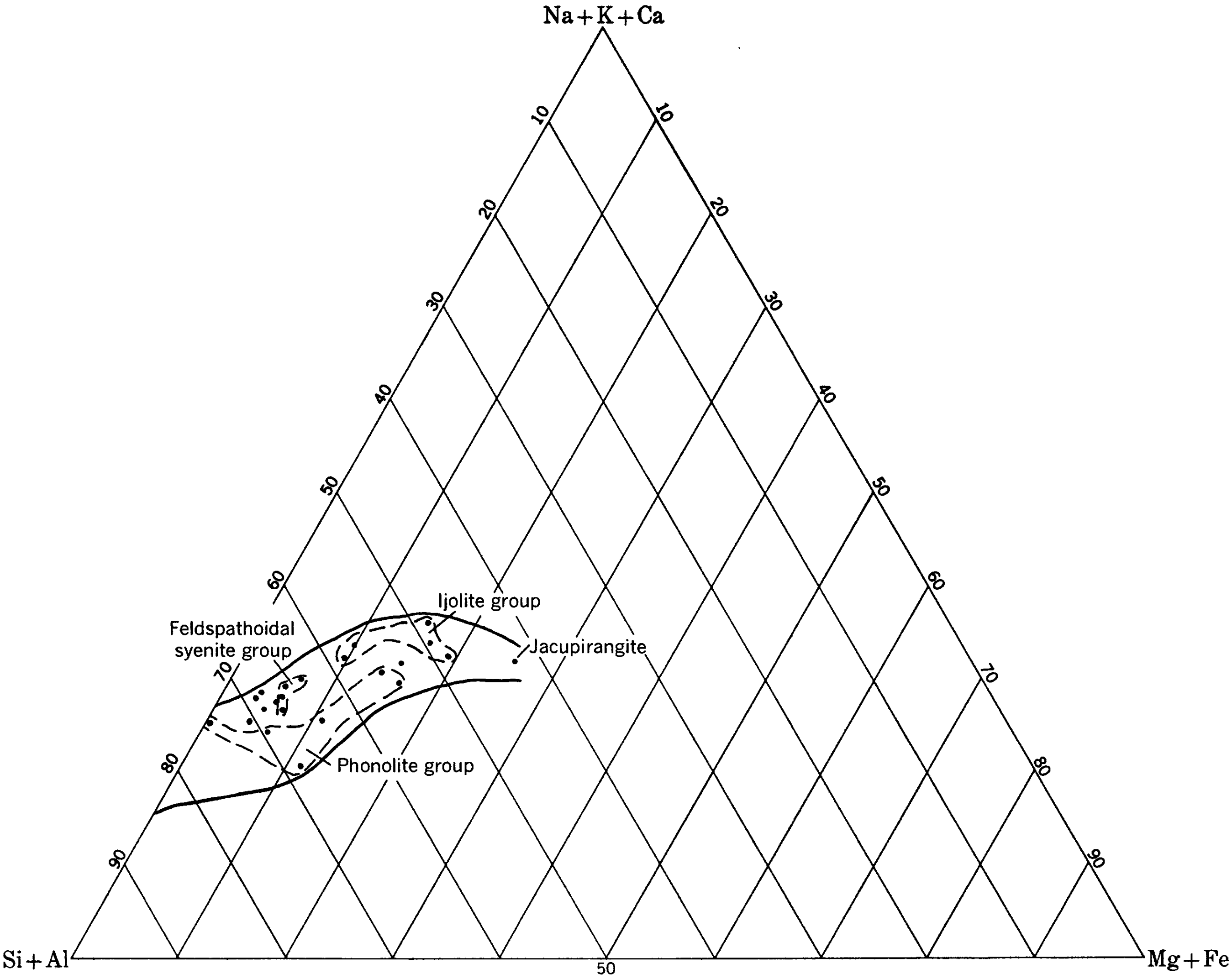

FIGURE 5.—Ternary diagram showing igneous rocks of the complex plotted against atomic proportions of the major elements.

and informative feature of all the variation diagrams is the distinctive, independent trends within each rock group. The jacupirangite-ijolite group shows greatest variation in the Mg–total Fe content with very little change in the alkali-lime total. The phonolite-trachyte group shows maximum variation toward the Si–Al apex. The nepheline syenites and late dike rocks show very close grouping.

The Si–Ca–Na+K diagram, figure 6, shows that the chief variation is toward the lime apex. Silica and alkali show only moderate changes. The greatest variation within rock groups is exhibited by the phonolite-trachyte group; however most of this variation is caused by the high calcite content of the altered phonolite and breccia. The gap from jacupirangite to ijolite is particularly noteworthy and supports our concept that jacupirangite is a crystal differentiate that was effectively separated from the rest of the magma so that gradational rock compositions could not form to fill this gap.

The K–Na–Ca diagram, figure 7, emphasizes the uniformly high total alkali content with the major trend toward the calcium apex. Again the abnormally great effect of jacupirangite in the trend is noteworthy. Both the ijolite and phonolite-trachyte groups show marked differentiation; the ijolite group moves toward the soda apex with increasing nepheline content, and the phonolite-trachyte group moves toward the potassium apex with increasing sodic orthoclase content.

The Na+K–total Fe–Mg diagram, figure 8, shows the general trend toward the alkali apex. Again jacupirangite is by itself as a crystal differentiate. The rock groups show very marked differentiation; the ijolite group trends toward total Fe apex with increasing diopside-garnet content and the phonolite-trachyte group moves toward the alkali apex.

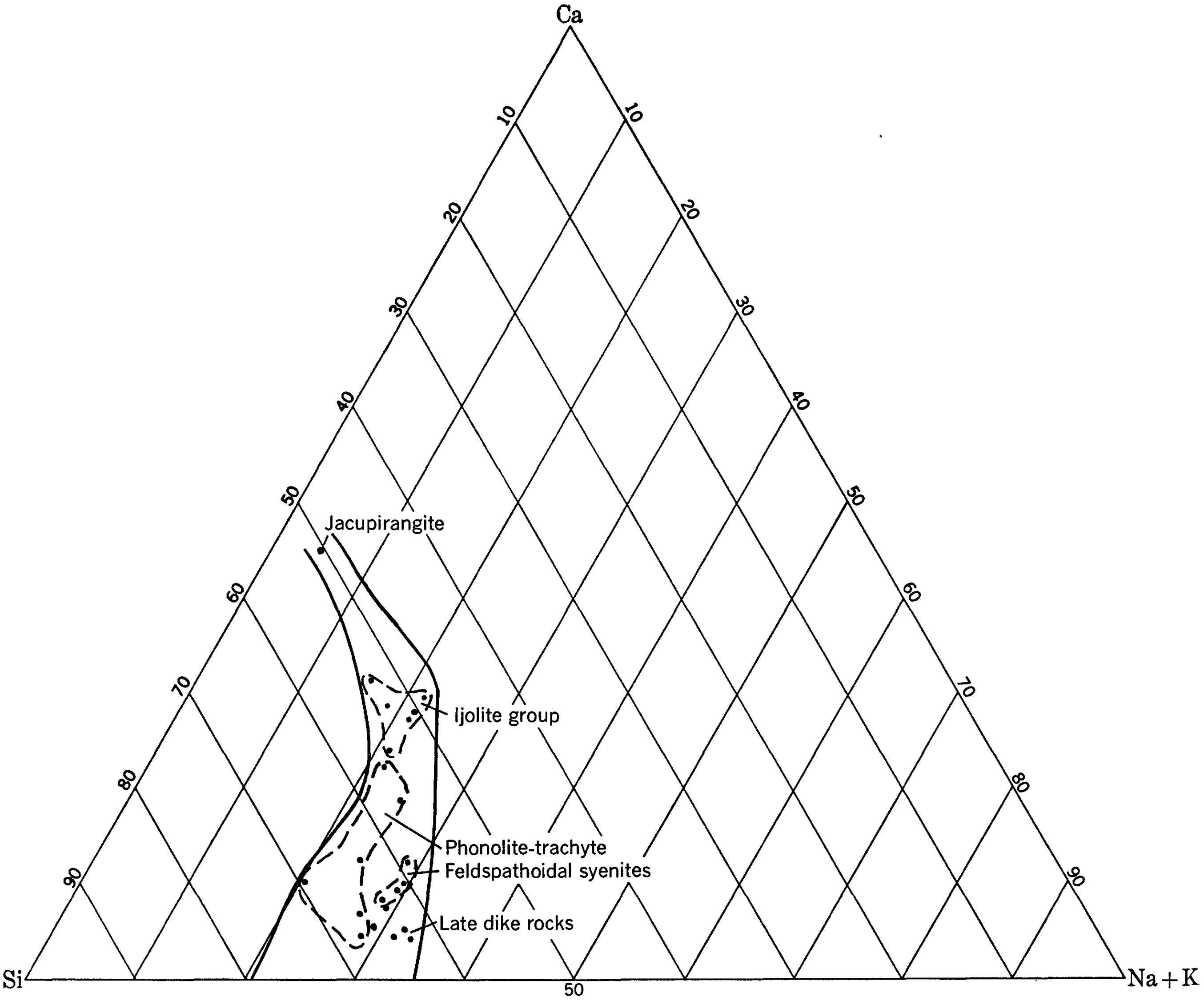

FIGURE 6.—Ternary diagram showing igneous rocks of the complex plotted against atomic proportions of Ca-Na+K-Si.

The lime variation diagram, figure 9, does not show smooth curves; however, the diagram is significant because it suggests separate periods of intrusion and differentiation within the rock groups, particularly the ijolite group. The lime content ranges from 2 to almost 21 percent; total alkali is high and Na_2O is consistently high while K_2O shows a much steeper curve. The greatest scattering of points occurs in the SiO_2, Al_2O_3, and total Fe curves. This is caused by the wide range in abundance of garnet, biotite, and nepheline in ijolite. The jacupirangite position causes the steep part of the curves.

The feldspathoidal syenite group that forms the outer ring dikes shows a much closer grouping than any other rock type. Although altered phonolite shows lower SiO_2 and Al_2O_3 and higher total Fe, it approaches the average composition of Magnet Cove rocks. If the volatile constituents are removed from the phonolite, this comparison would be closer. Note that Na_2O and K_2O offset each other so that total alkali would fall on the curve. A separate but parallel curve can be drawn for the high total iron in the phonolite-trachyte group; these rocks also have a high sulfur content (table 47).

The most significant interpretations of the variation diagrams are summarized below:

1. All the rocks are very closely related and probably formed by differentiation of a single magma.
2. Rocks were intruded at separate periods and show varying amounts of differentiation within the rock groups.
3. Total alkali and lime contents are high; soda is consistently high in all rock types, whereas potash exhibits a much steeper curve.

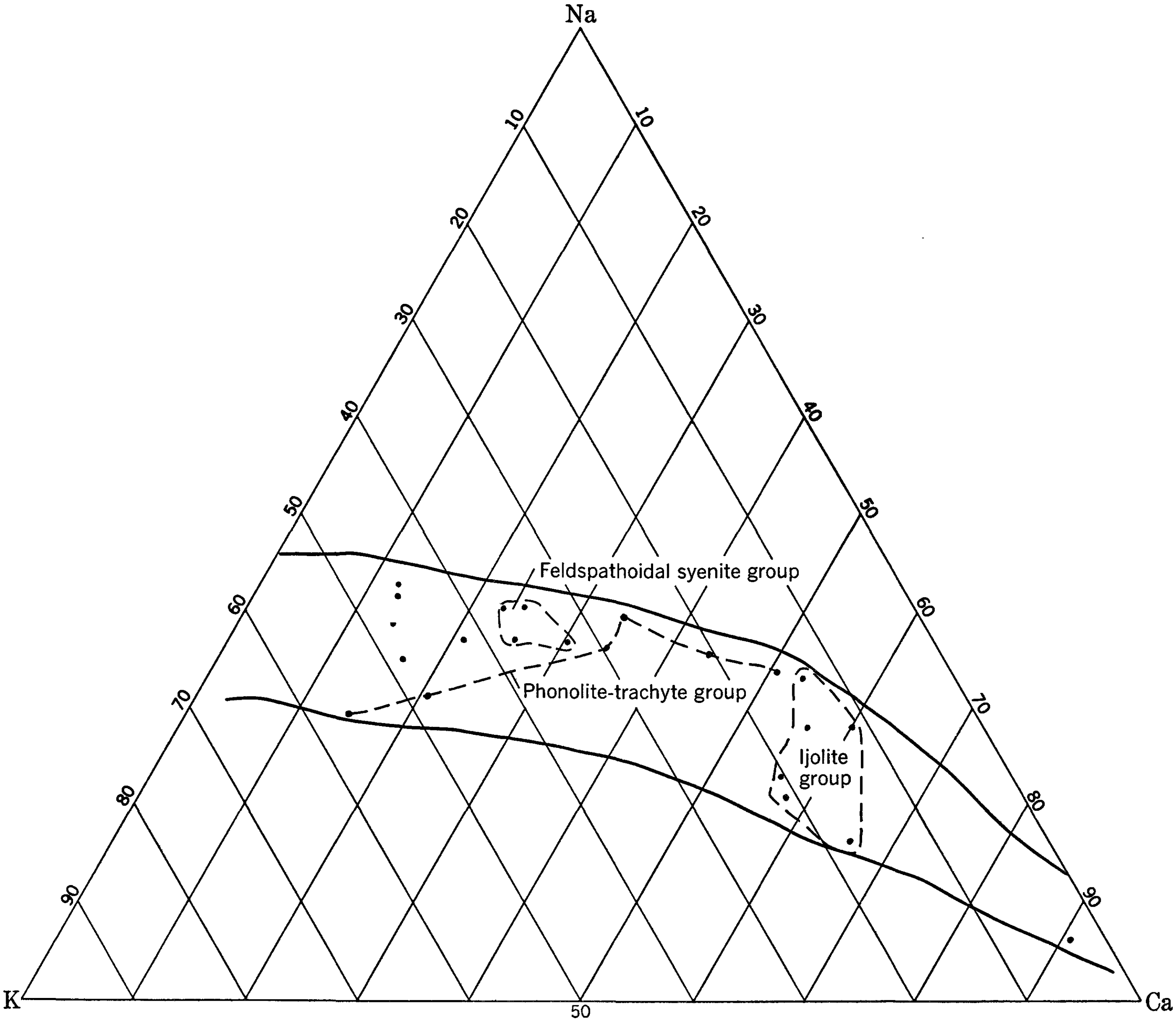

FIGURE 7.—Ternary diagram showing igneous rocks of the complex plotted against atomic proportions of Na-K-Ca.

MINERALS

The distribution of minor elements in the important rock-forming minerals and some chemical analyses of minerals are discussed in this section. The average minor-element content of each mineral is shown in table 49; variation in minor-element content within mineral species is discussed under mineral sub headings.

The following observations are made from table 49.

1. Be is concentrated in thomsonite (0.01 percent), a zeolitic alteration of nepheline, and is therefore, most abundant in the nepheline-rich ijolitic rocks (up to 0.004 percent in garnet ijolite). Be also occurs in idocrase, melilite, and tobermorite in concentration greater than 0.001 percent. It is noteworthy that all these minerals as well as thomsonite, are late cyrstallizing lime silicates; alkali feldspars, nepheline, micas, and alkali pyroxenes that commonly accumulate Be are deficient in the element. Borodin (1957) suggests that Be separated out during the early stages of rock crystallization in the Khibina alkalic rock massif in Russia because of its absence in secondary rock minerals and its constant presence in the primary rock-forming minerals. The opposite situation appears to be true at Magnet Cove. Be is chiefly in secondary lime silicate minerals that are alteration products of previously existing minerals and therefore has probably concentrated in the late residual solutions. If the Be-rich thomsonite alteration of nepheline is deuteric, it suggests that the ijolites are a late differentiate as nepheline from ijolite contains more Be than nepheline from syenite. If thomsonite alteration is hydrothermal or pneumatolytic, Be has been introduced

TABLE 49.—*Average minor element content of minerals at Magnet Cove, Ark.*

Mineral	Number of samples	Be	Mg	Sr	Ba	B	Sc	Y	La	Yb	Ti	Zr	V	Nb	Cr	Mo	Mn	Fe	Co	Ni	Cu	Ag	Zn	Ga	Pb	Sn
Felsic																										
Sodic orthoclase	3	0	0.03	0.28	*0.3	n.d.	0	0	0	0	0.02	0.001	0.006	0	0.0004	[1]*0.007	0.005	0.28	0	0	0.001	0	0	0.004	*0.003	0
Barian orthoclase	2	0	.015	*.55	*5.9	n.d.	0	0	0	0	.02	.02	.005	0	.0004	0	.003	.58	0	0	.0005	.0	0	.003	0	0
Microcline	6	0	.01	.01	.15	n.d.	0	0	0	0	.02	0	.005	0	.0006	0	.006	.21	0	0	.001	0	0	.003	0	0
Labradorite	1	0	.05	*1-5	*.5	n.d.	0	0	0	0	.1	0	0	0	.0002	0	.003	.2	0	0	.009	0	0	0	0	0
Nepheline	5	.0003	n.d.	.22	.12	.001	0	0	0	0	.02	0	[1].02	0	.0004	0	.006	n.d.	0	0	.0003	0	0	*.006	0	0
Analcime	2	0	.02	.06	.02	n.d.	0	0	0	0	[1].03	.01	.004	0	.0004	0	.002	.045	0	0	[1].0008	0	0	.002	0	0
Natrolite	9	.0007	.13	.03	.008	*.005	0	0	0	0	.01	n.d.	.006	0	n.d.	.002	.006	.2	0	0	[1]*.01	0	0	.003	0	0
Thomsonite	3	*.01	.04	*.8	.1	.001	0	0	0	0	.01	0	.001	0	.0001	.0007	.003	.1	0	0	.002	0	0	.001	0	0
Mafic																										
Diopside	9	0.0004	M	0.4	0.005	n.d.	0.003	[1]0	0	n.d.	0.1	0.003	0.07	0	0.001	0	0.2	M	0.002	0.001	[1]0.002	0	0	0	0	0
Diopside-hedenbergite	11	[1].0001	M	.3	.01	n.d.	.004	.01	0	[1].0005	2.2	.03	.06	0	*.02	0	.07	M	.002	.003	.003	0	0	.002	0	0
Aegirine-diopside	3	[1]0	M	.4	[1].15	n.d.	.001	[1]0	[1]0	n.d.	.7	.02	.10	0	.0006	0	*.7	M	.001	.002	.002	0	0	.001	0	0
Aegirine	7	[1].001	n.d.	.4	.03	n.d.	0	.003	.003	n.d.	.5	.06	.10	[1].01	.0005	0	*.9	M	.001	.001	.002	.0002	0	.001	[1]0	0
Augite	2	0	M	.3	.01	n.d.	*.01	.002	.001	0	2.1	n.d.	.10	0	*.07	0	.16	M	.002	.009	.002	[1]*.002	0	[1]0	0	0
Hornblende	2	[1]0	n.d.	.26	.06	n.d.	.0008	.009	.03	n.d.	4.1	.05	.06	.009	.0015	0	*.5	M	.004	.005	.003	0	0	.002	0	*.019
Biotite	4	0	M	.06	*.45	n.d.	.001	.001	0	0	n.d.	.002	.015	0	n.d.	0	.2	M	.005	.006	.002	0	0	.003	0	0
Garnet—light colored	4	[1]0	.13	.02	.002	n.d.	0	[1]0	[1]0	n.d.	.5	n.d.	.15	[1]0	.0009	0	.1	n.d.	0	.006	.0007	0	0	.002	0	0
Garnet—dark colored	11	0	.6	.2	.02	n.d.	.002	.03	[1].005	n.d.	M	*.15	*.2	.02	.001	0	.2	M	.001	.005	.003	0	0	.001	0	0
Apatite	11	0	.02	*.8	.02	0	[1]0	.02	.03	*.0006	.02	0	.08	0	.0002	0	.01	.09	0	0	.003	0	0	0	0	0
Sphene	9	0	n.d.	.2	.02	n.d.	.0002	.025	.04	[1].0008	M	*.22	.16	*.24	.005	0	.02	1.5	0	.004	.007	0	0	0	0	0
Perovskite:																										
(Major rocks)	6	0	n.d.	.2	.001	n.d.	.0008	.05	.15	0	M	0	.05	*.4	.0003	0	.03	n.d.	.001	0	*.013	0	0	0	0	0
(Carbonatite)	1	------	------	.X	.0X	n.d.	.00X	.0X	*X.0	------	------	0	.025	*8.7	.000X	0	.0X	3.4	0	.00X	.00X	0	0	0	0	0
Anatase	1	.001	n.d.	.02	.005	n.d.	.001	*.19	.2	0	M	*.63	*.92	*6.8	.0002	0	.13	n.d.	0	.006	*.018	0	0	0	*.004	0
Magnetite	4	0	n.d.	.004	.005	n.d.	[1]0	0	[1]0	0	3.0	.007	*.4	0	*.05	0	*.8	M	.01	.004	.008	0	.1	.004	0	0
Magnesioferrite	3	0	>10	.009	.001	n.d.	.0004	.004	0	0	2.8	[1]0	.16	[1]0	.0005	0	*.6	M	.01	.006	.006	0	0	.006	0	0
Pyrite	6	0	.015	.001	[1].01	n.d.	0	0	0	0	.05	0	0	0	.0002	0	.01	M	*.07	*.02	*.03	0	0	[1]0	[1]*.003	0
Calcite	5	0	.05	*.6	.06	.001	0	0	0	0	.004	0	.01	0	.002	0	.02	[1].05	0	0	.0005	0	0	0	0	0
Monticellite	1	0	>10	.008	0	n.d.	0	.02	0	0	.01	0	.006	0	.002	0	*1.2	n.d.	.004	0	.0009	0	0	0	0	0
Kimzeyite	1	0	.5	.01	.002	n.d.	*.02	.1	.04	0	3.2	*>10	.01	*.2	.001	0	.05	n.d.	0	0	.0006	0	0	*.008	0	*.02
Idocrase	2	.004	M	*.35	.003	n.d.	.0002	.002	.02	0	.27	.03	.03	.01	.0013	0	.02	n.d.	n.d.	0	.0009	0	0	.003	0	0
Melilite	1	.002	>1	*.6	.01	n.d.	0	0	0	0	.02	0	.01	0	.001	0	.08	2.4	.002	0	.001	0	0	.001	0	0
Pectolite	1	0	.03	.2	.01	n.d.	0	.003	.02	n.d.	.04	0	.02	0	.001	n.d.	*.5	.2	0	0	.001	0	0	0	*.003	0
Tobermorite	1	.002	.009	.01	.04	n.d.	0	0	.02	n.d.	.003	0	.009	0	.002	n.d.	.05	.002	0	0	.0008	0	0	0	0	0
Eudialyte	1	0	.05	*.8	.2	n.d.	.0004	.009	.04	n.d.	.4	*M	.01	.09	.002	n.d.	*.48	2.2	0	0	.002	0	0	0	*.008	*.09
Rutile	45	n.d.	n.d.	n.d.	n.d.	n.d.	n.d.	n.d.	n.d.	n.d.	n.d.	n.d.	*.6	*2.2	n.d.	n.d.	n.d.	1.8	n.d.	n.d.	n.d.	n.d.	n.d.	n.d.	n.d.	n.d.
Brookite	18	n.d.	n.d.	n.d.	n.d.	n.d.	n.d.	n.d.	n.d.	n.d.	n.d.	n.d.	*.18	*2.0	n.d.	n.d.	n.d.	.87	n.d.	n.d.	n.d.	n.d.	n.d.	n.d.	n.d.	n.d.
Paramorphs (rutile after brookite)	23	n.d.	n.d.	n.d.	n.d.	n.d.	n.d.	n.d.	n.d.	n.d.	n.d.	n.d.	*.36	*1.3	n.d.	n.d.	n.d.	.76	n.d.	n.d.	n.d.	n.d.	n.d.	n.d.	n.d.	n.d.

[1] Average not reliable either because the element was contained in only some of the analyzed samples or range in concentration is very large; individual mineral tables show which explanation applies.

M, major constituent; asterisk (*), most significant concentrations; n.d.=not determined.

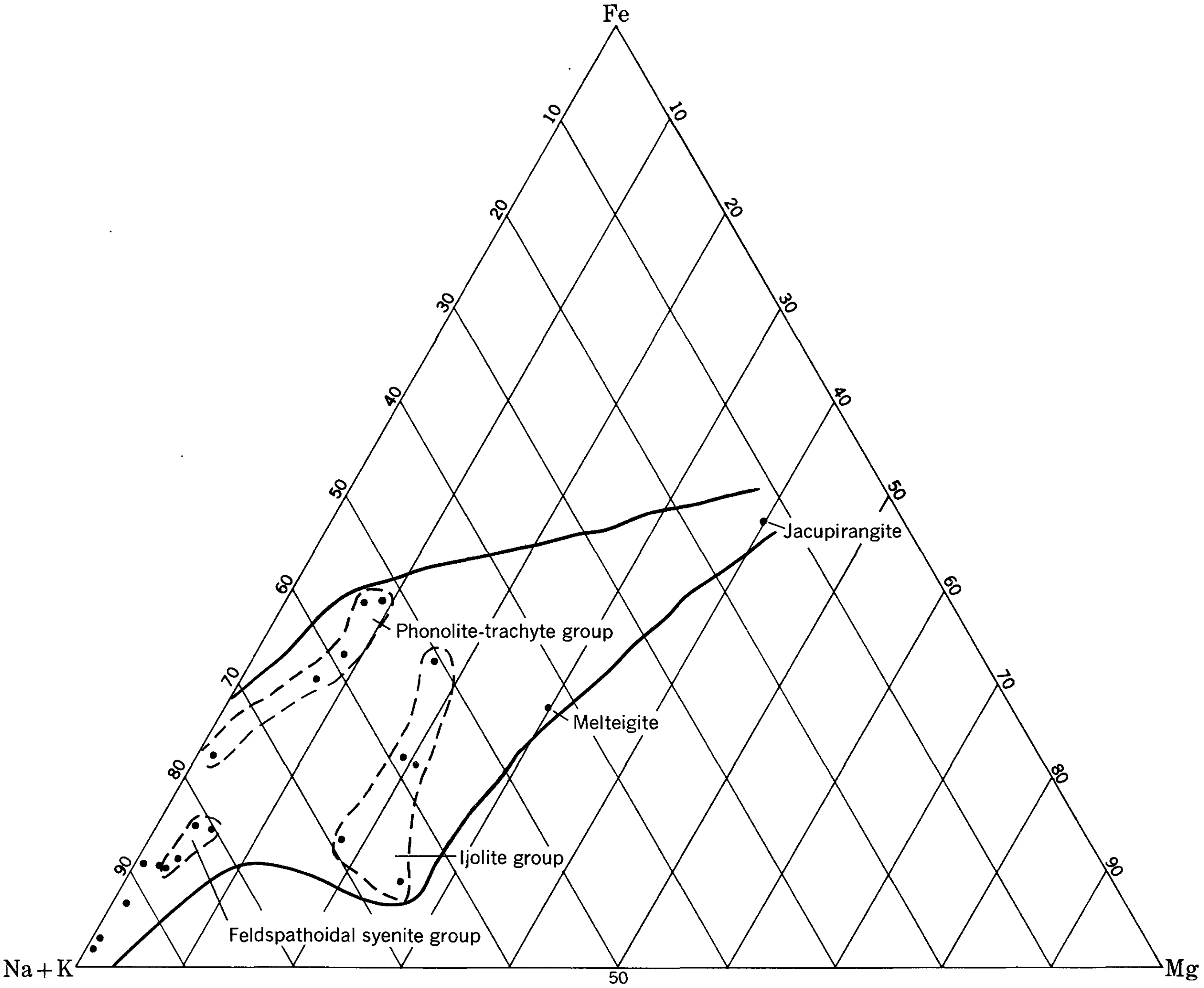

FIGURE 8.—Ternary diagram showing igneous rocks of the complex plotted against atomic proportions of Fe-Mg-Na+K.

by reaction of a residual magma of high water-high volatile content (carbonatite?) with earlier formed ijolite.

2. Strontium is one of the characteristic elements at Magnet Cove; it occurs both in felsic and mafic minerals chiefly as a substitution for Ca^{+2}. The highest concentration occurs in labradorite, apatite, thomsonite, eudialyte, melilite, calcite, and barian orthoclase.

3. Barium, like strontium, occurs in both felsic and mafic minerals but it has a much more restricted choice of host minerals because it follows potassium. It is most concentrated in feldspar and biotite.

4. Boron was detected only in natrolite (0.005 percent) and thomsonite.

5. Scandium is most abundant in kimzeyite (zirconium garnet—0.09 percent Sc_2O_5) and augite (0.01 percent). Both minerals are from late-forming rocks—carbonatite and analcime olivine melagabbro dikes, respectively.

6. Yttrium and lanthanum occur chiefly in late crystallized titanium minerals: anatase, kimzeyite, perovskite from the carbonatite. Lesser amounts occur in titanium garnet, sphene, and apatite. The concentrations of these two elements, however, do not show a direct relationship; the greater enrichment of yttrium is in anatase and the greater enrichment of lanthanum is in perovskite.

7. Ytterbium was detected only in apatite, sphene, and diopside-hedenbergite.

8. Titanium was found in all of the analyzed minerals at Magnet Cove. In addition to its occurrence in such minerals as rutile, brookite, perovskite, anatase, and sphene, it is a major constituent in titanium garnet, and kimzeyite, and appears as significant minor-element substitution in magnetite and pyroxene. Titanium is enriched in the residual solution to such an extent that the oxide minerals were formed; rutile and brookite occur

in late veins; beautiful euhedral crystals of perovskite and anatase occur in the carbonatite.

9. Vanadium follows titanium and is most abundant in anatase, rutile, brookite, magnetite, and garnet; however, the relationship is not direct. Vanadium is also consistently present in apatite (0.08 percent average) probably in the phosphate position.

10. Chromium was detected in all of the analyzed minerals but is most abundant in magnetite and pyroxene.

11. Small amounts of molybdenum are captured in the early crystallized felsic minerals, particularly sodic orthoclase, but it also concentrates in the very late residual fluids and crystallizes as molybdenite in veins.

12. Manganese is most abundant in monticellite, particularly the late-forming euhedral crystals in carbonatite. It also occurs in magnetite, sodic pyroxene, pectolite, and eudialyte. Thus manganese appears to concentrate in the residual fluids perhaps, in part, in the higher valency states.

13. Cobalt and nickel are concentrated chiefly in pyrite; however, the late formed vein pyrite is deficient in cobalt and nickel relative to early pyrite in the major rock types. Appreciable cobalt (0.01 percent) was also detected in magnetite and magnesioferrite.

14. Copper was detected in all minerals at all stages of crystallization. It is most abundant (0.03 percent average) in pyrite. The overall distribution, however, suggests that most of the copper is captured during early stages of crystallization.

15. Silver occurs in amounts up to 0.004 percent in augite from a late dike rock and in aegirine. Trace amounts (0.0001 percent) were also detected in individual samples of biotite, zeolite, feldspar, pyrite, and calcite.

16. Zinc was detected only in magnetite and is highest in the early crystallized magnetites in the major rock group; however, the lower limit of spectrographic sensitivity for zinc is 0.02 percent.

17. Gallium occurs in two unlike mineral groups: in felsic minerals (nepheline-feldspar) associated with aluminum; in magnetites, associated with Fe^{+3}.

18. Lead is concentrated in sodic orthoclase illustrating the well known relationship of lead and potassium in the crystal lattice of feldspar; however, lead also occurs in anatase, pyrite, pectolite, and eudialyte. Borodin (1957) suggested "a connection between lead and calcium and especially strontium," for the Khibina alkalic rocks because "the greatest quantity of lead is not connected with the chief rock-forming minerals, but is connected with such minerals as eudialyte, lamprophyllite, rinkolite and sphene."

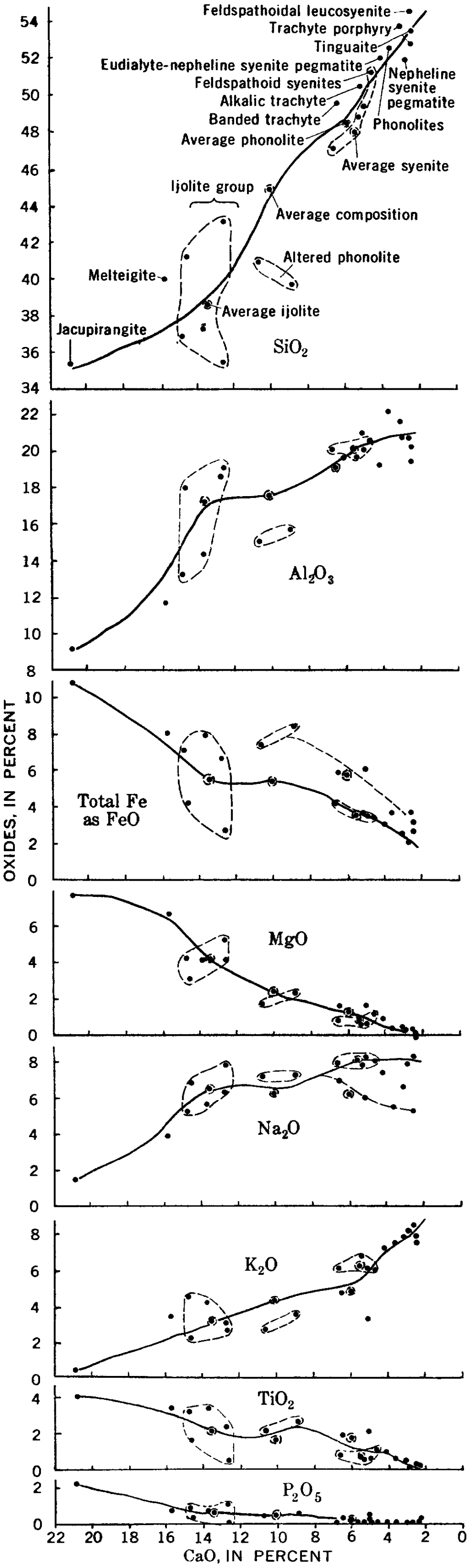

Figure 9.—Lime variation diagram.

19. Tin is chiefly in the zirconium-rich minerals, eudialyte and kimzeyite. Tin was detected also in some, but not all, rutile and brookite crystals and in sodic amphibole.

From the foregoing observations it appears that the following conclusions are justified:

1. Most of the minor elements are concentrated in either the mafic or the accessory minerals. Pb, Ga, Sr, and Ba may also be concentrated in felsic minerals; Mo is concentrated in the felsic minerals only.
2. Be, Y, La, Ti, Zr, Nb, Mn, and Sn are concentrated in the residual magma and are most abundant in the late-formed minerals in carbonatite and pegmatite.
3. Concentration of some minor elements in the residual magma became sufficiently high to produce independent minerals such as the titanium minerals perovskite, rutile, brookite, the zirconium minerals—eudialyte and kimzeyite; molybdenum and lead as molybdenite and galena in veins.
4. Co, Ni, Cu are most concentrated in the early-formed minerals; Sr, Ba, Ga, and Cu occur in all stages of crystallization.
5. The distribution of minor elements in the same minerals from different rock types emphasizes the close compositional relation of all the rocks at Magnet Cove and strongly indicates a common parent magma for the wide variety of rock types. For example, the same suite of minor elements appears in perovskite from jacupirangite, garnet pseudoleucite syenite, and carbonatite. However, the absolute amounts of some minor elements in perovskite show a progressive increase (Nb and rare earths) or decrease (V and Cu) in samples from rocks of early to very late crystallization.

FELDSPAR

Rapid chemical analyses were made on two sodic orthoclases from sphene nepheline syenite and nepheline syenite pegmatite, table 50. The orthoclase from the pegmatite has a low summation chiefly because barium was not determined. The spectrographic analysis of this feldspar (table 51) shows a barium content of 2.4 percent. The Na_2O content is equivalent to 29 percent normative albite. Feldspar from the nepheline syenite is silica deficient and has an abnormally high soda content caused by sodalite contamination and kaolinite alteration.

Spectrographic analyses of feldspar, table 51, are divided into three groups—sodic orthoclase, barium orthoclase, and microcline. All groups are poor in minor element content except for barium and strontium, both of which show a wide but systematic range in abundance; low in microcline, moderate in sodic orthoclase, and highest in barium orthoclase. Ga occurs in all feldspars; Pb was detected in two sodic orthoclases, and abnormally high concentration of Mo (0.02 percent) was detected in one sodic orthoclase. Small quantities of Fe and Ti occur in all feldspars.

TABLE 50.—*Chemical analyses of sodic orthoclase*

[Rapid chemical analyses by P. L. D. Elmore and K. E. White]

Parent rock	Sphene nepheline syenite	Nepheline syenite pegmatite
Sample No.	(MC-1-10)	(MC-120-d)
SiO_2	57.9	60.0
Al_2O_3	23.1	21.6
Na_2O	9.0	3.4
K_2O	7.0	11.6
Ignition loss	2.2	.48
Total	99.2	97.1

TABLE 51.—*Spectrographic analyses for minor elements in feldspar*

Rock type	Sample No.	Be	Mg	Ca	Sr	Ba	Ti	Zr	V	Cr	Mo	Mn	Fe	Cu	Ag	Ga	Pb
Sodic orthoclase																	
Sphene nepheline syenite	MC-1-1	0.0001	0.02	n.d.	0.3	0.4	0.03	0	0.01	0.0005	0	0.01	0.3	0.001	0	0.002	0.006
Do	MC-1-10	0	.06	.28	.14	.3	.02	.003	.001	0	0	.003	.24	.002	0	.005	.002
Tinguaite	MC-152-1	0	.004	n.d.	.4	.2	.01	0	.007	.0006	.02	.002	.3	.0009	.0001	.004	0
Average	------	0	.03	------	.28	.3	.02	------	.006	.0004	------	.005	.28	.001	------	.004	.003
Barian orthoclase																	
Pegmatite	MC-120-d	0	0.01	0.13	0.61	2.4	0.01	0.001	0	0	0	0.005	0.26	0.0001	0	0.003	0
Garnet nepheline syenite	MC-112-4	0	.02	n.d.	.5	9.5	.03	.04	.01	.0007	0	.001	.9	.0008	0	.003	0
Microcline																	
Sphene pyroxenite	MC-172-1	0	------	n.d.	0.07	0.09	0.03	0	0.001	0	0	0.003	n.d.	0.002	0	0.002	0
Pegmatite	L-167-3	0	0.02	n.d.	.01	.07	.006	0	.01	.001	0	.007	.4	.001	0	.004	0
Do	L-167-4	0	.006	n.d.	.0009	.06	.006	0	.009	.0009	0	0	.09	.0009	0	.004	0
Vein	L-162-1	0	.01	n.d.	.004	.6	.03	0	.003	.0009	0	.003	.2	.002	.0001	.003	0
Do	W-5-1	0	.005	n.d.	0	.02	.004	0	.003	.0009	0	.001	.09	.001	.0001	.002	0
Do	MC-178-1	0	.02	0.01	.0008	.05	.03	0	.002	.0001	0	.02	.3	.0007	0	.0006	0
Average	------	0	.01	------	.01	.15	.02	0	.005	.0006	0	.006	.21	.001	------	.003	0

n.d.=not determined.

NEPHELINE

Chemical analyses of nepheline, table 52, show a very similar soda-potash ratio in the nepheline from two very dissimilar rock types—nepheline syenite and ijolite. Calculation of nepheline and kaliophilite end members shows a kaliophilite content of 20 to 23 percent in the analyzed nepheline. The calculations for nepheline from the sphene nepheline syenite show an appreciable excess of silica which suggests contamination of nepheline by orthoclase, possibly present in solid solution.

Spectrographic analyses of nepheline, table 53, show moderate concentrations of Sr and Ba. Ga is high as expected, particularly in nepheline from sphene nepheline syenite (0.011 percent). Ti and V were detected in all samples; Pb was detected in one sample; and boron in two samples—probably indicating zeolitic alteration.

TABLE 52.—*Analyses of nepheline*

[Standard chemical analyses: MC-1-9 by P. L. D. Elmore and K. E. White; MC-216-3 and L-123-3 by L. N. Tarrant]

	Chemical analyses			Atomic ratios			
Parent rock	Sphene nepheline syenite	Garnet biolite ijolite	Garnet ijolite				
Sample No.	MC-1-9	MC-216-3	L-123-3	MC-216-3		L-123-3	
SiO_2	46.2	41.03	40.90	1.008		1.012	
Al_2O_3	32.0	33.74	33.37	.975	2.003	.973	2.006
Fe_2O_3	n.d.	1.10	1.12	.020		.021	
CaO	n.d.	.74	1.15	.019		.030	
Na_2O	14.2	15.09	14.37	.718		.690	
K_2O	6.1	6.89	6.82	.215	.954	.215	.935
MnO	n.d.	0	0	0		0	
MgO	n.d.	.07	.01	.002		0	
TiO_2	n.d.	.02	.02				
FeO	n.d.	0	0				
H_2O-	1.00	.22	.27				
H_2O+	n.d.	1.14	1.80				
Total	99.5	100.04	99.83				

n.d. =not determined.

TABLE 53.—*Spectrographic analyses for minor elements in nepheline*

Rock type	Sample No.	Be	Sr	Ba	B	Sc	Ti	Zr	V	Cr	Mo	Mn	Fe	Cu	Ga	Pb
Garnet biotite ijolite	MC-216-3	0.0005	0.4	0.06	0.001	0	0.01	0	0.03	0.0004	0.0004	0.007	n.d.	0.0004	0.003	0
Ijolite	L-123-3	.0003	.2	.01	0	.001	.006	0	.03	.0004	0	.004	n.d.	0	.004	0
Do	L-17-4	.0005	.2	.04	.003	0	.007	0	.02	.0004	0	.01	n.d.	.0002	.006	0
Sphene nepheline syenite	MC-1-9	0	.12	.2	0	0	.06	.002	.001	0	0	.001	.40	.0001	.011	.002
Do	MC-1-2	.0001	.2	.3	0	0	.03	0	.01	.0007	0	.006	.5	.001	.004	0
Average		.0003	.22	.12			.02		.02	.0004		.006		.0003	.006	

n.d. =not determined.

ZEOLITE

Natrolite and thomsonite occur as zeolitic alteration products of nepheline, particularly in the ijolite; analcime occurs in the groundmass of the analcime olivine melagabbro and as an alteration product of nepheline. A chemical analysis of zeolite from ijolite (table 54) was calculated after the method of Hey (1932) and fits thomsonite closely; specific gravity and refractive indices also suggest thomsonite. However, X-ray analysis of the zeolite by F. A. Hildebrand showed natrolite rather than thomsonite thus suggesting that this may be a mixture or solid solution of natrolite-thomsonite. The strontium and barium contents also suggest that the analyzed zeolite (table 55, L-123-2) belongs to the natrolite group.

Significant differences of concentrations of certain minor elements occur between the various types of zeolite. Sr, Ba, and Be are strongly concentrated in the high lime thomsonite; B and Ga are in natrolite. These differences are more marked than differences in minor element content of a single type of zeolite from unrelated rock types. However, the natrolite from jacupirangite has an unusually high concentration of Mo and Cu.

PYROXENE

The pyroxenes are all monoclinic and can be divided into four types:

1. Diopside— chiefly in ijolite group rocks.
2. Diopside-hedenbergite— chiefly in syenite and phonolite; and jacupirangite.
3. Aegirine-diopside—chiefly in syenite and phonolite as rims around a diopside-hedenbergite core. Some aegirine crystals occur in the syenite phonolite group and pegmatite.
4. Augite—found only in the late analcime olivine melagabbro dike rock.

The most characteristic features of the pyroxenes are: (1) the high lime content—the greatest proportion of the pyroxenes fall in the diopside-hedenbergite group,

TABLE 54.—*Analysis of zeolite from ijolite*

[Sample L-123-2. Standard chemical analyses by L. N. Tarrant]

	Chemical analysis (percent)	Atomic ratio	
SiO_2	38.70	20.80	
Al_2O_3	30.21	19.12	39.99
Fe_2O_3	.18	.07	
CaO	6.88	3.95	
Na_2O	10.57	11.00	
K_2O	.21	.13	15.22
MnO	.02	.01	
MgO	.16	.13	
TiO_2	.01		
FeO	.01		
H_2O-	2.13	3.80	22.52
H_2O+	10.47	18.72	
Total	99.55		

TABLE 55.—*Spectrographic analyses of zeolites*

Rock type	Sample No.	Be	Mg	Sr	Ba	B	Ti	Zr	V	Cr	Mo	Mn	Fe	Cu	Ag	Ga
Analcime																
Garnet-pseudoleucite syenite.	MC–111–1	0.00008	0.01	0.02	0.003	n.d.	0.008	0.02	0.007	0.0007	0	0.001	0.03	0.0006	0	0.003
Melagabbro	L–11a–3	0	.03	.1	.03	0	.05	.004	0	0	0	.002	.06	.001	0	.0007
Natrolite																
Jacupirangite	MC–173–9	0.0003	0.05	0.01	0.002	0.005	0.02	0	0.009	0	0.007	0.003	0.3	0.1	0	0.002
Do	L–81–5	.0005	.08	.01	.008	.004	.02	0	.004	0	0	.004	.2	.007	0	.003
Garnet biotite ijolite	MC–216–1	.0005	.3	.01	.001	.01	.009	0	.005	0	.002	.01	.3	.0002	0	.002
Do	MC–216–2	.0006	.3	.06	.001	.02	.008	0	.008	0	.003	.005	.3	.0006	0	.002
Ijolite	L–123–1	.0005	.2	.004	.01	.006	.004	0	.007	0	.001	.01	.07	.0003	0	.007
Garnet nepheline syenite	MC–112–5	.0001	.04	.1	.009	n.d.	.01	.01	.01	.002	0	.005	.2	.0008	0	.008
Pegmatite	L–167–6	.002	.02	.05	.02	n.d.	.02	0	.006	.002	0	.005	.02	.0009	0	.002
Lime silicate	L–168–9	.0009	.06	.007	.007	n.d.	.005	0	.004	.0006	0	.001	.08	.0007	.0001	.002
Ijolite	L–123–2	.0005	.1	.01	.01	.004	.005	0	.004	0	.002	.008	.1	.0003	0	.003
Average	--------	.0007	.13	.03	.008	.005	.01	--------	.006	--------	.002	.006	.2	.01	--------	.003
Thomsonite																
Jacupirangite	L–81–4	0.005	0.04	0.7	0.1	0	0.02	0	0.0008	0.00009	0.001	0.003	0.2	0.005	0	0.0006
Ijolite	L–17–2	.02	.04	1.5	.2	.002	.009	0	.001	0	.0005	.004	.07	.0007	0	.0007
Do	L–17–3	.01	.03	.8	.06	0	.004	0	.001	.00009	.0006	.003	.05	.0005	0	.0007
Average	--------	.01	.04	.8	.1	--------	.01	0	.001	.0001	.0007	.003	.1	.002	0	.0007

n.d.=not determined.

and (2) the high soda content of late-formed pyroxene. Normal augite is rare.

The analyzed pyroxenes from ijolite and jacupirangite, table 56, fit very well into the diopside and salite divisions as defined by Hess (1941, 1949). The indices of refraction, however, appear to be too high. The titanium content of the salite is also high but certainly not unexpected in salite from jacupirangite (magnetite pyroxenite).

Unfortunately the pyroxene mixtures in the nepheline syenites could not be sufficiently separated for chemical analysis. Most of the grains have a colorless to pink tinted (titaniferous) core of diopside-hedenbergite (probably salite or ferrosalite) rimmed with green aegirine-diopside and aegirine. The high ferric iron and soda in the chemical analyses of the composites support this conclusion. The high fluorine and combined water suggest that biotite or amphibole is included in the green sodic rims of the grains. The totals of the chemical analyses are particularly low; unfortunately the amount of sample available for analysis was too small to permit further analytical work. Sample MC–111–1 probably also contains substantial fluorine and combined water.

The analyzed aegirine shows the characteristic high ferric iron and soda content of this mineral. Magnesia is very low—less than titania.

Spectrographic analyses of the pyroxenes for minor elements, table 57, show some interesting relationships both for the pyroxene group as a whole and for individual types of pyroxene.

Ti, Sr, Mn, and V, show significant concentration in all pyroxenes but the degree of concentration has a wide range among the different types of pyroxene.

Titanium and manganese are diagnostic because they show significant changes from one group to another whereas Sr and V are consistently high in all pyroxene groups. However, the more sodic pyroxenes contain somewhat higher Sr and V particularly if analyses from the lime silicate and pegmatite bodies are omitted. Following is a summary of Ti and Mn concentrations relative to pyroxene groups.

	Ti	Mn
Diopside-hedenbergite	2.2	0.07
Aegirine-diopside	.7	.7
Aegirine	.5	.87
Diopside	.11	.19

Although highest Ti correlates with lowest Mn, the relationship is not exactly inverse—highest Mn does not correlate with lowest Ti. Higher Ti in aegirine than the calcic diopside reflects higher FeO content of aegirine. The marked increase in manganese content as well as ferric iron in aegirine suggests that a part of the Mn is trivalent. Fersman (1937) has noted the prevalence of highest degrees of oxidation of the elements such as Fe^{+3}, Mn^{+3}, and Mn^{+4} in the rocks of the Khibina alkalic massif in Russia.

The diopside group has captured the least amount of minor elements and is characterized by high Sr and V; most of the other elements except Mn have lower concentrations than in the other pyroxenes. Note that diopside from the lime silicate body is particularly deficient in Sr, V, and Mn. This diopside is probably a secondary mineral formed from alteration of melilite. The Nb and Ti contents of diopside from melteigite suggest possible perovskite and sphene contamination.

Diopside-hedenbergite is characterized by high Ti and low Mn relative to the other pyroxenes. Yb was detected only in this group. The high Cr, Ni, and Sc

TABLE 56.—*Analyses of pyroxene*

Chemical analyses							
Mineral	Diopside		Salite[1]		Composite pyroxene (diopside-hedenbergite rimmed with aegirine)		Aegirine
Parent rock	Ijolite		Jacupirangite		Feldspathoidal syenite		Pegmatite
Sample No.	L-123-6	L-123-7	MC-173-1	MC-173-2	MC-111-1	MC-112-6	L-167-2
SiO_2	53.17	53.50	45.04	44.55	44.53	46.65	51.20
Al_2O_2	.98	.89	6.95	7.29	5.55	4.51	1.05
TiO_2	.22	.13	2.90	3.13	.97	1.12	.82
Fe_2O_3	1.65	1.64	5.23	5.09	14.97	15.38	25.11
MgO	15.06	15.51	10.70	10.98	4.03	2.81	.43
FeO	3.24	2.52	4.53	4.05	5.83	7.04	4.97
MnO	.61	.61	.26	.22	1.29	1.26	.71
CaO	22.24	24.63	22.87	23.11	15.16	12.13	4.93
Na_2O	.52	.41	.76	.69	4.31	6.21	10.36
K_2O	.04	.04	.19	.21	1.49	.98	.02
H_2O-	.03	.02	.03	.03	.05	.09	.00
H_2O+	n.d.	n.d.	n.d.	n.d.	n.d.	.59	.04
F	n.d.	n.d.	n.d.	n.d.	n.d.	.66	n.d.
Total	99.76	99.90	99.46	99.35	98.18	99.43	99.64
Less O						.28	
						99.15	

Atomic ratios										
Mineral	Diopside				Salite				Aegirine	
Sample No.	L-123-6		L-123-7		MC-173-1		MC-173-2		L-167-2	
SiO_2	1.964	2.000	1.968	2.000	1.712	2.000	1.694	2.000	1.988	2.000
Al_2O_2	0.043 {.036		0.038 {.032		0.311 {.288		0.327 {.306		0.048 {.012	
	.007	1.007	.006	1.003	.023	1.013	.021	1.012	.036	1.002
TiO_2	.006		.003		.083		.089		.024	
Fe_2O_3	.046		.046		1.49		.144		.733	
MgO	.829		.851		.606		.622		.024	
FeO	.100		.078		1.44		.129		.161	
MnO	.019		.019		.008		.007		.024	
CaO	.958	.998	.970	1.001	.931	.995	.941	1.00	.205	.984
Na_2O	.038		.029		.055		.050		.779	
K_2O	.002		.002		.009		.009			
Ca	49.08		49.39		50.6		51.1		10.6	
Mg	42.47		43.33		33.0		33.7		1.4	
Fe+Mn	8.45		7.28		16.4		15.2		47.6	
Na									40.4	
	100.00		100.00		100.00		100.00		100.00	

[1] Salite, intermediate member of diopside-hedenbergite group. n.d.=not determined.

Standard chemical analyses. Sample L-167-2, by M. K. Balazs; all other samples by L. N. Tarrant.

TABLE 57.—*Spectrographic analyses for minor elements in pyroxene*

Rock type	Sample No.	Be	Sr	Ba	Sc	Y	La	Yb	Ti	Zr	V	Nb	Cr	Mn	Co	Ni	Cu	Ga	Ag	Pb
Diopside																				
Melteigite	MC-113-e	0.0007	0.9	0.01	0.001	0	0	0	0.6	0.002	0.01	0.02	0.003	0.09	0.003	0.006	0.003	0	0	0
Pyroxenite	MC-172-3	.0002	.4	.02	.002	.001	0	0	.2	0	.2	0	.0004	.2	.007	.004	.01	0	0	0
Ijolite	MC-216-5	.0003	.5	.003	0	0	0	0	.05	0	.03	0	.0003	.3	.0005	0	.0002	.0003	0	0
Do	L-123-6	.0003	.4	.003	.001	0	0	0	.0004	0	.08	0	.001	.2	.0003	0	.0004	0	0	0
Do	L-123-7	.0003	.3	.002	0	0	0	0	.0003	0	.05	0	.0008	.2	.0003	0	.0004	0	0	0
Do	L-17-6	.0003	.3	.005	0	0	0	0	.04	0	.1	0	.0003	.2	.0003	0	.0002	.0004	0	0
Do	L-17-7	.0005	.5	.003	.01	.001	.002	0	.05	.02	.2	0	.0003	.4	.002	.002	.0003	.0004	0	0
Lime silicate	L-168-7	.0004	.1	.01	0	0	0	n.d.	.01	0	.005	0	.002	.03	0	0	.0006	0	0	0
Do	L-168-13	.0009	.1	.002	.01	0	0	n.d.	.03	.006	.005	0	.0009	.06	.003	0	.0006	0	0	0
Average	-------	0.0004	0.4	0.005	0.003	0	0	-------	0.1	0.003	0.07	-------	0.001	0.2	0.002	0.001	0.002	0	0	0
Diopside-hedenbergite																				
Jacupirangite	MC-173-1	0.0003	0.5	0.06	0.007	0.002	0.002	0	2.8	0.03	0.2	0	0.0003	0.07	0.003	0.002	0.008	0.002	0	0
Do	MC-173-2	.0003	.4	.01	.007	.002	.002	0	2.8	.03	.1	0	.0003	.07	.002	.001	.001	.0005	0	0
Do	L-81-11	0	.01	.004	.004	.008	0	n.d.	2.2	.02	.04	0	.0007	.05	.002	.002	.01	.001	0	0
Melteigite	MC-113-c	0	.4	.03	.006	0	0	0	1-10	.02	.01	0	.02	.05	.002	.004	.006	.003	0	0
Sphene nepheline syenite.	MC-1-6	0	.05	0	.01	0	0	n.d.	1.8	.007	.06	0	.1	.08	.003	.01	.002	.0007	0	0
Do	MC-1-b	.001	.4	.01	.006	.02	0	.001	1-10	.05	.02	0	.08	.08	.004	.01	.001	.002	0	0
Pseudoleucite syenite.	MC-111-10	0	.2	.003	.0004	.006	0	n.d.	1.5	.04	.1	0	.0007	.09	.0008	.002	.003	.0009	0	0
Do	MC-111-a	0	.4	.009	.001	.02	0	.0008	1-10	.06	.04	0	.003	.1	.003	0	.002	.002	0	0
Do	MC-121-a	0	.4	.02	.002	.02	0	.0005	1-10	.002	.03	0	.003	.06	.02	0	.001	.002	0	0
Garnet nepheline syenite.	MC-112-1	0	.1	.001	.003	.008	0	n.d.	2.4	.03	.03	0	.0007	.04	.002	0	.0009	.001	0	0
Do	MC-112-b	0	.4	.008	.002	.03	0	.001	1-10	.05	.03	0	.0002	.06	.003	0	.002	.004	0	0
Average	-------	0.0001	0.3	0.01	0.004	0.01	0	0.0005	2.2	0.03	0.06	0	0.02	0.07	0.002	0.003	0.002	0.002	0	0
Aegirine-diopside																				
Sphene nepheline syenite	MC-1-5	0.0006	0.2	0.006	0.004	0.008	0.02	n.d.	1.5	0.04	0.08	0	0.0009	0.7	0.002	0.002	0.002	0.003	0	0
Garnet pseudoleucite syenite	MC-111-9	0	.3	.002	.0003	0	0	n.d.	.5	.01	.2	0	.0007	.7	.0006	.003	.003	.001	0	0
Nepheline syenite pegmatite	MC-120-a	0	.6	.5	0	0	0	0	.2	.01	.04	0	.0001	.6	.001	0	.0009	0	0	0
Average	-------	0	0.4	0.15	0.001	-------	-------	-------	0.7	0.02	0.10	0	0.0006	0.7	0.001	0.002	0.002	0.001	0	0
Aegirine																				
Garnet nepheline syenite.	MC-112-2	0.0001	0.4	0.002	0	0.004	0.0009	n.d.	0.5	0.02	0.2	0	0.0007	1.1	0.001	0.003	0.002	0.002	0.0003	0
Do	MC-112-3	.0001	.4	.001	0	.004	.0009	n.d.	.6	.05	.2	0	.0007	1.0	0	.004	.001	.001	.0004	0
Garnet pseudoleucite syenite.	MC-111-3	.001	.6	.08	0	0	0	0	.4	.02	.06	0	.0002	.5	.001	0	.001	.001	.0001	0
Tinguaite	MC-115-c	.001	.8	.08	0	0	.02	0	.6	.02	.07	.03	.00008	1.0	0	0	.002	.0008	0	.04
Nepheline syenite pegmatite.	MC-120-c	.0007	.6	.06	0	0	0	0	.7	.02	.05	.02	.00008	2.0	.002	0	.001	.001	0	0
Eudialyte pegmatite.	L-167-2	0	.04	0	0	0	0	n.d.	.5	.07	.1	0	.001	.48	0	0	.0007	0	0	0
Lime silicate	L-168-14	.004	.04	.007	.001	.01	0	n.d.	.004	.2	.02	.03	.0006	.02	.003	0	.005	.001	.0003	0
Average	-------	0.001	0.4	0.03	0	0.003	0.0003	-------	0.5	0.06	0.10	0.01	0.0005	0.9	0.001	0.001	0.002	0.001	0.0002	0
Augite																				
Analcime olivine melagabbro.	L-11a-1a	0	0.3	0.009	0.01	0.001	0	0	1.9	0	0.1	0	0.08	0.03	0.002	0.01	0.001	0.0004	0	0
Do	L-11a-2a	0	.3	.01	.01	.003	.002	0	2.4	.009	.1	0	.05	.3	.002	.008	.004	.0005	.004	0
Range and average of 32 analyzed pyroxenes																				
Range	-------	0-.004	0.01-.9	0-.5	0-.01	0-.03	0-.02	0-.001	0.0003-2.8	0-.2	0.005-.2	0-.03	0.00008-.1	0.02-2.0	0-.007	0-.01	0.0002-.01	0-.004	0-.004	0-.04
Average	-------	.0004	.35	.03	.003	.005	.002	.0002	.9	.03	.08	.003	.01	.3	.002	.002	.002	.001	.0002	-------

n.d.=not determined.

of diopside-hedenbergite from the sphene nepheline syenite is particularly noteworthy; a similar concentration of the three elements was found in the relatively rare augite from analcime olivine melagabbro. Note that the minor element content of this group is relatively uniform regardless of the parent rock type.

The most distinguishing feature of the aegirine-diopside group is the increase in Mn content as the composition of the pyroxene shifts from diopside to aegirine. The wide range in the other minor elements reflects the variation in proportions of aegirine and diopside.

Aegirine is characterized chiefly by high Mn. The occurrence of small amounts of Nb and Ag are also diagnostic. An unusual and unexplained concentration of Pb was detected in one sample (MC–115–6). Again it is interesting to note that aegirine formed as a secondary mineral in the lime silicate body contains appreciably more Y and Zr and generally lower concentrations of Sr, Ti, V, and Mn than primary aegirine; the large aegirine crystals in the late eudialyte nepheline syenite pegmatite approach concentrations of these elements similar to secondary aegirine.

Augite which occurs only in one dike rock, analcime olivine melagabbro, is characterized by high Sc, Cr, and Ni.

GARNET

Garnet is one of the common rock forming minerals in the Magnet Cove complex and ranges in composition from the light-colored andradite to dark-colored melanite (titanium garnet).

Chemical analysis of a dark-brown garnet from ijolite, table 58, shows the high TiO_2 content characteristic of melanite or schorlomite garnet. The analysis was calculated to fit the formula of andradite, $R''_3R'''_2(SiO_4)_3$, because melanite is a titaniferous andradite; however, there is only approximate agreement as can be seen from the atomic ratios. Some of the divalent cations should be brought into the R''' group to balance quadrivalent titanium. Impurities (diopside, sphene, and perovskite) were less than 3 percent.

TABLE 58.—*Analysis of dark-brown garnet from biotite-garnet ijolite*

[Sample MC–216–8. Standard chemical analysis by L. N. Tarrant]

	Chemical analysis (percent)	Atomic ratios		
SiO_2	27.89		2.352	3.000
		0.983	.648	
TiO_2	15.51		.335	1.711
Al_2O_3	2.12		.211	
Fe_2O_3	18.32		1.165	
MnO	.57		.040	3.268
FeO	2.91		.206	
CaO	31.79		2.870	
MgO	1.22		.152	
	100.33			

The spectrographic analyses of light- and dark-colored garnets, table 59, show surprisingly small differences in minor element concentrations except for significantly higher Zr, Nb, Y, and Sc in the titanium garnets. This is to be expected as these elements commonly are associated with high titanium in the Magnet Cove rocks. La occurs in four of the dark-colored garnets. Mn, V, and Sr were also detected in appreciable quantities but not as unusual enrichments.

The zirconium garnet, kimzeyite, has a relatively high Nb, Sc, and Y content compared to the other garnets. The published computed analysis (table 26) also shows appreciable Sn (0.09 percent SnO_2).

BIOTITE

Chemical analyses and atomic ratios of three biotites, table 60, show that the biotites are all of the phlogopite type; the major difference between individual samples is the FeO-MgO ratio. The high-iron biotite from jacupirangite with about equal amounts of FeO and MgO has a composition of about the midpoint in the annite-pholgopite series; it also contains the highest amount of TiO_2 and the lowest amount of fluorine. The other biotites contain less FeO and are closer to pure phlogopites.

The lime content, particularly of the biotite from jacupirangite, is due chiefly to minor amounts of apatite, sphene, pyroxene, and zeolite in the analyzed samples.

Spectrographic analyses, table 61, show that the biotites are relatively free of minor elements; Ba is most abundant (0.45 percent average) as expected in a high potash mineral but it has a wide abundance range. Mn, Sr, and V are the only other elements present in average amounts greater than 0.01 percent. High Cr and Ni were found in biotite from melteigite.

APATITE

The analyzed apatites (table 62) are relatively free of minor elements; strontium is most abundant (0.83 percent average for 11 apatites), and V, La, and Y also show significant enrichment. Yb is more consistently present and at higher amounts in apatite than any other of the analyzed minerals. B was detected in six of the nine samples.

The standard phosphate analysis of phosphate-rich saprolite from the carbonatite (table 24) show quantities of fluorine ranging from 0.26 to 1.9 percent indicating that the apatite in the saprolite is probably fluorapatite.

MAGNETITE

Spectrographic analyses of magnetite, table 63, show that some of the analyzed samples contain more than 10 percent MgO and should be called magnesioferrite. The high concentration of iron in jacupirangite magma

TABLE 59.—*Spectrographic analyses for minor elements in garnet*

Rock type	Sample No.	Be	Mg	Sr	Ba	Sc	Y	La	Yb	Ti	Zr	V	Nb	Cr	Mn	Co	Ni	Cu	Ga
								Light-colored garnets											
Ijolite	MC-216-9	0	n.d.	0.01	0.002	0	0	0	n.d.	0.6	0	0.09	0	0	0.2	0	0.005	0.0005	0.001
Do	L-17-10	0	n.d.	.06	0	0	.005	0	n.d.	1.2	.01	.3	0	0	.2	.0008	.02	.0004	.004
Lime silicate	L-168-6	0	0.2	.002	0	0	0	0	n.d.	.4	0	.2	0	.0009	.04	0	.002	.0008	.004
Do	L-168-11	.0004	.09	.005	.002	0	0	0	n.d.	.03	0	.006	0	.0009	.02	0	0	.001	0
Average	----------	--------	0.13	.02	.002	0	--------	--------	--------	.5	--------	.15	0	.0009	.1	--------	.006	.0007	.002
								Dark-colored garnets											
Melteigite	MC-113-2	0	0.5	0.03	0.008	0.006	0.02	0.03	n.d.	>10	0.2	0.2	0.01	0.01	0.3	0	0	0.002	0.004
Ijolite	MC-216-7	0	n.d.	.05	0	.0009	.03	0	n.d.	>10	.1	.2	.03	0	.005	.002	.009	.003	.001
Do	MC-216-8	0	n.d.	.05	0	.0009	.03	0	n.d.	>10	.1	.2	.03	0	.3	.002	.009	.01	.0009
Do	MC-217-1	0	n.d.	.08	.03	.0009	.01	0	n.d.	4.8	.06	.1	0	.002	.2	.0008	.005	.006	.001
Do	L-123-8	0	n.d.	.01	.004	.007	.03	0	n.d.	>10	.3	.2	.01	.002	.2	.001	.007	.004	.001
Do	L-17-9	0	n.d.	.08	.003	.0003	.02	0	n.d.	>10	.2	.3	.01	0	.2	.001	.02	.002	0
Garnet pseudoleucite syenite	MC-111-c	0	1.	.7	.05	0	.05	.02	n.d.	1-10	.08	.2	.02	.0002	.3	.003	.001	.002	.0002
Do	MC-111-d	0	.1	1.	.1	0	.06	.06	.002	1-10	.2	.2	.1	.0002	.6	0	.004	.003	.003
Do	MC-121-b	0	1.	.2	.02	0	.1	.01	n.d.	1-10	.2	.3	.009	.0002	.2	.001	.004	.002	.0002
Garnet nepheline syenite	MC-112-a	0	.4	.3	.04	0	.02	0	n.d.	1-10	.04	.2	.06	.0001	.18	.0005	.0006	.002	.0002
Pegmatite	MC-120-b	0	.2	.4	.02	.0002	0	0	0	1-10	.08	.2	.04	0	.4	0	.0008	.001	.002
Lime silicate	L-168-5	0	.4	.002	.002	.006	.02	0	n.d.	4.2	.2	.3	.04	.001	.2	0	.002	.001	.001
Average	----------	0	0.6	.2	.02	.002	.03	--------	--------	--------	.15	.2	.02	.001	.2	.001	.005	.003	.001
								Kimzeyite											
Carbonatite	----------	0	0.5	0.01	0.002	0.02	0.1	0.04	0	3.2	>10	0.01	0.2	0.001	0.05	0	0	0.0006	0.008

n.d.=not determined.

TABLE 60.—*Analyses of biotite*

[Standard chemical analyses by L. N. Tarrant]

Parent rock	Chemical analyses			Atomic ratios					
	Biotite from jacupirangite	Phlogopite from melteigite	Phlogopite from ijolite	MC-173-3		MC-113-b		MC-216-4	
Sample No.	MC-173-3	MC-113-b	MC-216-4						
SiO_2	35.06	36.38	38.67	2.71	4.00	2.69	4.00	2.81	4.00
Al_2O_3	15.70	16.26	14.11	1.43 {1.29		1.42 {1.31		1.21 {1.19	
				.14	2.97	.11	2.97	.02	2.95
Fe_2O_3	2.46	1.70	2.08	.14		.10		.11	
FeO	14.47	6.95	6.08	.94		.43		.37	
MgO	12.96	19.13	21.81	1.49		2.11		2.36	
MnO	.36	.12	.45	.02		.01		.03	
TiO_2	4.06	3.79	1.14	.24		.21		.06	
CaO	1.28	.22	.33	.11	1.06	.02	1.00	.02	1.00
Na_2O	.40	.36	.46	.06		.05		.07	
K_2O	9.05	9.88	9.76	.89		.93		.91	
H_2O+	2.68	3.08	4.08	1.38	1.44	1.52	1.74	1.98	2.18
F	.26	.95	.85						
H_2O-	----------	.52	.00	.06		.22		.20	
Total	98.74	99.34	99.82						
Less O	.11	.40	.36						
	98.63	98.94	99.46						

TABLE 61.—*Spectrographic analyses for minor elements in biotite*

Rock type	Sample No.	Sr	Ba	B	Sc	Y	Zr	V	Cr	Mn	Co	Ni	Cu	Ag	Ga
Jacupirangite	MC-173-3	0.04	0.09	0	0.0002	0.002	0	0.02	0	0.2	0.01	0.004	0.003	0	0.002
Melteigite	MC-113-b	.2	.4	0	.0008	0	.002	.01	.06	.1	.004	.02	.003	0	.002
Ijolite	MC-216-4	.006	.1	.002	0	.002	0	.009	0	.3	.005	0	.001	0	.003
Lime silicate	L-168-4	.005	1.2	n.d.	.004	0	.008	.02	.0006	.1	.001	0	.002	.0001	.003
Average		0.06	.45	--------	0.001	0.001	0.002	0.015	--------	0.2	0.005	0.006	0.002	--------	0.003

n.d.=not determined.

TABLE 62.—*Spectrographic analyses of apatite*

Rock type	Sample No.	Mg	Sr	Ba	B	Al	Sc	Y	La	Yb	Ti	Zr	V	Cr	Mn	Fe	Ni	Cu	Pb
Jacupirangite	MC-173-7	0.01	1.1	0.004	0.005	0.05	0	0.02	0.09	0	0.02	0	0.04	0	0.01	0.2	0	0.0007	0
Do	MC-173-8	.005	.95	.003	.002	.03	0	.02	.01	0	.01	0	.04	0	.01	.1	0	.0004	0
Do	L-81-1	.02	1-5	.03	.0007	n.d.	0	.03	.01	.0009	.03	0	.06	0	.006	.09	0	.005	.002
Do	L-81-2	.03	1-5	.02	.0007	n.d.	0	.03	.02	.0008	.08	0	.08	0	.006	.2	0	.009	0
Melteigite	MC-113-a	.04	1	.08	.002	n.d.	.0005	.03	.2	.0007	.05	0	.04	.0001	.008	.07	0	.02	0
Ijolite	MC-216-6	.01	.84	.02	.002	.04	0	.02	.04	0	.006	0	.1	.0009	.01	.04	0	.0002	0
Do	L-123-5	.01	.84	.009	0	.05	0	.004	.05	0	.003	0	.1	0	.01	.03	0	.0002	0
Do	L-17-1	.002	1-5	.02	0	n.d.	0	.01	.01	.0002	0	0	.1	0	.02	.02	0	.0003	0
Melagabbro	L-11a-1	.1	1-5	.01	0	n.d.	0	.03	.009	.0008	.008	0	.02	0	.04	.2	0	.0008	0
Carbonatite	L-166-2	.03	.1	.002	n.d.	n.d.	.0006	.02	.1	n.d.	.005	0	.2	.0007	.002	.002	.002	.0004	0
Lime silicate	L-168-12	.1	1.0	.005	n.d.	n.d.	0	.01	.01	n.d.	.004	.004	.1	.0009	.002	.01	0	.0006	0
Average		0.02	0.83	0.02	--------	------	--------	0.02	0.03	0.0006	0.02	-------	0.08	0.0002	0.01	0.09	-------	0.003	------

n.d. =not determined.

TABLE 63.—*Spectrographic analyses of magnetite*

Rock type	Sample No.	Be	Mg	Sr	Ba	Sc	Y	La	Ti	Zr	V	Nb	Cr	Mn	Co	Ni	Cu	Zn	Ga
Jacupirangite	MC-173-10	0	>10.0	0.007	0.002	0	0.006	0	3.4	0	0.2	0	0.0005	1.1	0.01	0.008	0.008	0	0.004
Do	L-81-9	0	>10	.02	.002	.0003	.006	0	4.0	0	.2	0	.0003	1.1	.02	.009	.01	0	.006
Melteigite	MC-113-1	0	.2	.002	.005	0	0	0	2.8	0	.3	0	.2	1.0	.008	.001	.02	.2	.004
Garnet pseudoleucite syenite.	MC-121-1	0	.3	.0009	.005	0	0	0	3.4	0	.5	0	.004	1.0	.008	.007	.002	.2	.003
Sphene nepheline syenite.	L-24-1	.001	.2	.01	.006	0	0	.02	2.2	.006	.5	0	.009	.5	.008	.007	.01	.1	.005
Carbonatite	L-166-5	0	>10	0	0	.001	0	0	1.0	.03	.07	.03	.0007	2.7	.01	0	.001	0	.009
Lime silicate	L-168-2	0	>1	0	0	.004	0	0	3.6	.02	.2	0	.0009	.8	.02	.002	.001	.01	.004
Average		------	------	0.006	0.003	0.0008	-------	------	2.9	0.008	.3	------	0.03	1.2	0.01	0.005	0.007	0.07	0.005

forced early crystallization of magnetite, and magnesia assumed the role of a minor element until sufficient iron had been deposited to lower its relative concentration with respect to magnesia and permit crystallization of magnesia-rich minerals such as pyroxene.

No significant differences in minor element content could be detected between the normal magnetite and magnesioferrite. Ti, Mn, V, Zn, Co, Ni, and Ga, in order of abundance, are concentrated in both types.

Although Ga usually accompanies aluminum in igneous rocks and is in all of the felsic minerals at Magnet Cove, its greatest concentration occurs as substitution for ferric iron in magnetite (0.009 percent) and zirconium garnet (kimzeyite-0.008 percent) from the carbonatite.

It is noteworthy that the magnetite from melteigite contains very little magnesia, yet the rock contains almost as much MgO as jacupirangite. In this case, MgO accompanies K_2O in the formation of early biotite phenocrysts in melteigite.

PEROVSKITE

Spectrographic analyses of eight perovskites ($CaTiO_3$) show significant enrichment of Fe, Nb, Sr, La, Y, V, and Cu, in this mineral (table 64). A very marked difference in concentration of Nb and La occurs between perovskite separated from the major rock types (0.38 Nb; 0.14 La) and perovskite from carbonatite (8.0 Nb; 1.0 La). This relationship demonstrates the marked tendency for Nb and rare earths to concentrate in residual magmas. However, the uniformity of the total suite of minor elements concentrated in perovskite from different rock types sharply points up the direct genetic relationship of carbonatite to the major rock types.

Sr and rare earths substitute for Ca; and Fe^{+3}, Nb, and V substitute for Ti.

SPHENE

Nine spectrographic analyses of sphene, table 65, show that Fe, Nb, Zr, Sr, and V occur in sphene in average concentrations greater than 0.1 percent. Y and La show moderate enrichment. Sr, Y, and La probably substitute for Ca; Fe, Nb, Zr, and V substitute for Ti.

All the minor elements detected in sphene show fairly uniform concentration regardless of the host rock type—except that Nb is more abundant in sphene from nepheline syenite-phonolite group than the jacupirangite-ijolite group. Mo and Pb were detected only in the sphene from sphene nepheline syenite.

PYRITE

Cobalt, nickel, and copper are concentrated in pyrite (table 66). Pyrite from the sphene pyroxenite and ijolite contains the highest concentrations of these metals whereas the vein pyrite is notably lower. This suggests that the metals enter early formed pyrite in the major rock types and are not concentrated in the residual vein-producing solutions.

The analyses of pyrite from the phonolite indicate considerable contamination from other minerals in this fine-grained rock.

CALCITE

Spectrographic analyses of four calcite samples from different host rocks, table 67, show that the calcite is unusually pure; magnesia averages only 0.05 percent

TABLE 64.—*Spectrographic analyses of perovskite*

Rock type	Sample No.	Mg	Sr	Ba	Sc	Y	La	V	Nb	Cr	Mn	Fe	Co	Ni	Cu	Pb
Jacupirangite	MC-173-4	n.d.	0.2	0	0.0004	0.057	0.1	0.045	0.27	0	0.03	n.d.	0	0	0.012	0
Do	MC-173-5	n.d.	.2	0	.0004	.050	.1	.039	.30	0	.03	n.d.	0	0	.033	0
Do	L-81-10	.04	.4	.001	.003	.04	.4	.04	.2	.0005	.02	1.4	.002	0	.007	.002
Melteigite	MC-113-d	.002	.1	.002	.001	.04	.2	.04	.3	.001	.04	>10.0	.003	0	.01	0
Ijolite	MC-216-10	n.d.	.2	.002	.0004	.02	.1	.04	.9	0	.04	n.d.	0	0	.01	0
Garnet pseudoleucite syenite	MC-121-c	.02	.3	.002	0	.1	.05	.1	.3	.0008	.04	>10.0	.003	0	.009	0
Average	------	------	.2	.001	.0008	.05	.15	.05	.4	.0003	.03	------	.001	0	.013	------
Carbonatite	L-129-c	.0x	.x	.0x	.00x	.0x	x.	.025	8.2	.000x	.0x	2.6	0	.00x	.00x	0
Do	L-129-d	.0x	.x	.0x	.00x	.0x	x.	.025	9.2	.000x	.0x	4.2	0	.00x	.00x	0

n.d.=not determined.

TABLE 65.—*Spectrographic analyses of sphene*

Rock type	Sample No.	Sr	Ba	Sc	Y	La	Yb	Zr	V	Nb	Cr	Mo	Mn	Fe	Co	Ni	Cu	Pb
Jacupirangite	L-81-8	.8	0.02	0	0.02	0.04	n.d.	0.1	0.07	0.1	0.0007	0	0.008	0.8	0.002	0.002	0.004	0
Do	MC-173-6	.05	0	.0004	.029	.04	n.d.	.19	.07	.15	0	0	.009	n.d.	0	0	.0075	0
Sphene pyroxenite	MC-176	.x	.00x	0	.0x	.0x	0.00x	.0x	.29	.22	.000x	0	.0x	2.5	0	0	.00x	0
Do	MC-177	.x	.00x	0	.0x	.x	.00x	.0x	.12	.20	.000x	0	.0x	2.0	0	0	.00x	0
Do	MC-172-4	.05	.002	.0004	.037	.02	n.d.	.14	.15	.12	0	0	.01	n.d.	0	.006	.010	0
Melteigite	MC-113-3	.3	.009	0	0	.06	n.d.	.08	.1	.2	.02	0	.03	1.7	0	0	.003	0
Ijolite	L-17-8	.07	0	.0001	.009	.01	n.d.	.6	.4	.2	0	0	.01	n.d.	0	.01	.001	0
Trachyte	MC-171-1	.05	.002	.0004	.04	.04	n.d.	.4	.2	.3	.0008	0	.07	n.d.	0	.006	.02	0
Sphene nepheline syenite	MC-1-c	.3	.1	.0002	.04	.04	.0008	.05	.04	.7	.0002	.0006	.001	.4	.0008	.01	.005	.005
Average	------	0.2	0.02	0.0002	0.025	0.04	------	0.22	0.16	0.24	0.005	------	0.02	1.5	------	0.004	0.007	------

n.d.=not determined.

TABLE 66.—*Spectrographic analyses of pyrite*

Rock type	Sample No.	Mg	Ca	Sr	Ba	Ti	Zr	V	Cr	Mn	Co	Ni	Cu	Ag	Ga	Pb
Sphene pyroxenite	MC-172-5	n.d.	n.d.	0.002	0.004	0.2	0	0	0	0.02	0.22	0.12	0.090	0	0	0.007
Ijolite	L-123-9	n.d.	n.d.	0	.002	.004	0	0	0	.005	.03	.01	.02	0	0	.002
Do	L-17-11	n.d.	n.d.	0	.004	.004	0	0	0	.02	.1	.004	.02	0	0	0
Altered phonolite	MC-114a	0.03	0.2	.0003	.07	.06	.01	0	0	.02	.02	.002	.006	0	0	.01
Vein	L-165-1	.01	n.d.	0	0	.01	0	0	.0007	.0006	.007	.002	.001	0	.001	0
Do	L-116-2	.005	n.d.	.002	0	.008	0	.002	.0004	.004	.05	0	.04	.0003	.001	0
Average		0.015		0.001	.01	0.05			0.0002	0.01	0.07	0.02	0.03			0.003

n.d.=not determined.

TABLE 67.—*Spectrographic analyses of calcite*

Rock type	Sample No.	Be	Mg	Sr	Ba	B	Al	Sc	Y	La	Ti	V	Cr	Mn	Fe	Cu	Ag
Ijolite	L-123-4	0	0.05	0.84	0.10	0.001	0.08	0	0	0.002	0.002	0.003	0	0.04	0.1	0.0003	0
Do	L-17-5	.0003	.03	.84	.1	.001	.09	0	0	.002	.007	.003	0	.03	.1	.0004	0
Lime silicate	L-168-3	0	.02	.2	.02	n.d.	n.d.	0	0	0	.002	.009	.003	.01	.001	.0008	0
Carbonatite	L-166-3	0	.1	.5	.02	n.d.	n.d.	0	0	0	.005	.03	.003	.01	.001	.0006	0
Vein	MC-8-1 [1]	0	1	.08	.004	n.d.	n.d.	.004	.02	.01	.8	.008	.009	.1	>10	.0009	.0002
Average			0.05	0.06	0.6						0.004	0.01	0.002	0.02	0.05	0.0005	

[1] Iron-rich dolomite. n.d.=not determined.

Sr is the most abundant minor element (0.2 to 0.84 percent) followed by Ba, Fe, Mn, and V. Calcite from ijolite contains 0.001 percent boron and is higher in Sr, Ba, Mn, and Fe, and lower in V, Cr, and Cu than calcite from the carbonatite and lime-silicate body.

The iron-rich dolomite, from a rutile-bearing vein, differs markedly from the analyzed calcites—particularly in its low Sr and Ba and high rare earths, Ti, and Mn content.

GEOCHEMISTRY OF NIOBIUM

Previous workers have firmly established the fact that the highest concentrations of niobium in rocks occur in alkalic rocks, particularly nepheline syenite, and that titanium minerals are the most favorable hosts for niobium. Therefore the occurrence of significant quantities of niobium (0.01 percent) in the igneous rocks of the Magnet Cove complex and (0.1 percent) in the rutile and brookite deposits associated with the complex is not surprising. In these rocks niobium is concentrated in rutile, brookite, perovskite, and sphene, and to a lesser extent in titanium garnet, aegirine, and hornblende.

RUTILE AND BROOKITE

The description and economic considerations of the rutile and brookite deposits have been discussed previously by Fryklund and Holbrook (1950) and Fryklund, Harner, and Kaiser (1954), and will not be repeated here. Spectrographic analyses of rutile, brookite, and paramorphs of rutile after brookite, tables 68, 69, and 70, show that the niobium content in these minerals ranges from less than 1 percent to more than 6 percent. The average niobium content of rutile and brookite is about 2 percent; paramorphs of rutile after brookite have an average niobium content of 1.3 percent. It is interesting to note that the highest niobium concentration in rutile occurred in cyclic twins; 6 of 7 such crystals analyzed had more than 5 percent niobium, 1 contained 1.3 percent. However, most of these crystals were from the carbonatite area on Perovskite Hill in NW¼ sec. 19. Niobium concentration is probably greater in this part of the complex. For example, perovskite from the same area contains more than 9 percent niobium.

Light-colored (red) rutile, rutile paramorphs, and brookite contain less niobium than dark-colored crystals—consistently less than 1 percent.

Light-colored (red) patches can be seen in many of the crystals, and these patches are particularly abundant in paramorphs of rutile after brookite. The contact of light- and dark-colored patches is gradational for the most part, but in a few crystals the contact appears sharp. In one thin section of a feldspar-carbonate-rutile vein, there appears to be at least two ages of rutile. The older rutile may be a paramorph after brookite. The crystal boundaries of the paramorph are encrusted with later formed rutile needles which have grown with their long axis normal to paramorph crystal faces. In transmitted light the paramorph(?) is pleochroic (yellow-orange to green) and contains purple patches. We suspect that the deep-purple, almost opaque areas are the richest in Nb and they appear to replace the highly pleochroic yellow-orange to green variety. The rutile encrustations are also purple and show rhythmic zoning in shades of purple.

The abundance of light-colored patches in paramorphs suggests that in the transformation from orthorhombic brookite to tetragonal rutile there may be some shifting of the Nb ions—perhaps tending to force them out or concentrate them in clusters. However, there is some color variation in brookite and in nonparamorph rutile but this is a more rhythmic variation. Why is Nb erratically distributed? Does it tend to cluster around particular centers in the crystal? According to Goldschmidt's capture principle, Nb, if quinquivalent, should concentrate in the earlier phases of rutile or brookite. So far, we have no evidence of this.

Correlation coefficients were determined for Nb, V, and Fe in rutile and brookite with the following results:

Nb – V = +0.60
Nb – Fe = + .72
Fe – V = + .27

For this group of 28 samples anything above +0.4 is a significant correlation. There is a moderately strong positive correlation of V and Fe with Nb but very poor correlation of Fe–V. This might be explained by the valence states of the elements concerned which are substituting for Ti^{+4} (0.68 A). Nb is probably quinquivalent (0.69 A)—thus needs a trivalent atom to balance which could be Fe^{+3} (0.64 A). If V is present as V^{+4} (0.63 A), correlation with Fe^{+3} is not expectable.

The V–Fe ratios in the rutiles (0.1 to 0.3) are probably much higher than they are in the solutions from which rutile formed. The V–Fe ratio in the rock from Magnet Cove would average 0.004. This suggests that vanadium, like niobium, moves into the rutile structure preferentially more than Fe^{+3}, and that the amount of Fe^{+3} present is directly related to the amount of Nb^{+5} that substitutes for Ti^{+4}.

Other trace elements consistently present are Mn, Ca, Mg, Cr, Cu, Sr, W—all in the 0.00x range. Mo and Sn were found in some samples in 0.00x concentration. W, Mo, Sn, and possibly Cr substitute in the Ti^{+4} position.

Semiquantitative spectrographic data for Sc, Y, and Zr are erratic and appear to vary with the analyst; however the values given are near the limit of sensitivity for the semiquantitative method. Ni was detected only by the quantitative method.

CARBONATITE

The highest niobium concentration (9.2 percent) noted in any mineral in the complex occurs in perovskite from the carbonatite. These crystals, usually octahedrons modified by a cube, have been described in detail by Williams (1891). More recently Fryklund, Harner, and Kaiser (1954) mapped the Kimzey calcite quarry geologically and analyzed perovskite crystals and channel samples of the carbonatite. They report a range of 5.1 to 8.8 percent niobium in individual perovskite crystals and a range from 0 to 0.07 percent niobium in channel samples of carbonatite. Niobium was detected in only 6 of 21 channel samples. Anatase, formed by alteration of this perovskite, contained 6.8 percent niobium. The high content of niobium in perovskite from carbonatite indicates the strong tendency for niobium to concentrate in very late residual magmas; perovskite in the igneous rocks contains less than 1 percent niobium.

IGNEOUS ROCKS AND MINERALS

The niobium content of the analyzed rocks ranges from 0 to 0.03 percent. Feldspathoidal leucosyenite and one sample of sphene pyroxenite are high, with 0.03 percent. Garnet ijolite, jacupirangite, and analcime melagabbro are all low in niobium.

Perovskite (0.2 to 0.9 percent Nb), sphene (0.1 to 0.7 percent Nb), garnet (0 to 0.1 percent Nb), aegirine (0 to 0.03 percent Nb) and hornblende (0.007 and 0.01 percent Nb) are the minerals in which niobium is concentrated. Niobium (0.1 percent) was detected in only one of the light-colored garnets whereas it was detected in all but one of the dark-colored titanium-rich garnets. Although niobium usually substitutes in titanium minerals, it may be seen from table 47 that no direct relationship exists between the niobium and titanium content of the rock. Dark basic rocks such as jacupirangite and olivine melagabbro which contain abundant titanium are low in niobium. Titanium in ijolite is principally in perovskite which apparently affords a favorable structure for niobium substitution and the tendency for niobium to stay in the residual magma is overcome. Generally the more felsic rocks such as sphene-nepheline syenite which contain small quantities of titanium have the greatest amount of niobium. These results are in accord with the general observation that niobium, because of its high valence, is concentrated in residual magmas.

Titaniferous pyroxene crystallizes very early in the igneous rocks at Magnet Cove, but although it may contain from 1 to 10 percent titanium, it does not contain niobium in detectable amounts. Late-formed sodic pyroxenes, however, which contain less than 1 percent titanium have as much as 0.02 percent niobium. On the other hand, early crystallized sphene and perovskite contain as much as 0.7 percent niobium. Thus it is apparent that at least 2 factors determine the distribution of niobium in the rocks.

1. Niobium tends to concentrate in residual magma.
2. Availability of favorable mineral structure to accommodate niobium. If perovskite or sphene crystallizes even in early differentiates such as jacupirangite, a part of the niobium will preferentially enter the structure rather than stay in residual magma. It is important, however, that niobium substitution is not as great in the minerals from early crystallized rocks as in the same minerals from late formed rocks. Sphene from sphene pyroxenite contains 0.2 percent niobium; from

Table 68—*Spectrographic*

Sample No.	V	Nb	Fe	Be	Mg	Ca	Sr	Ba	Sc	Y	Yb	Zr	Cr
L-64a	0.46	3.6	0.84	0	0.00x	0.00x	0.00x	n.d.	0	0	0	0	0.00x
L-65a	.18	.76	.45	0	.00x	.00x	.00x	n.d.	0	0	0	0	.00x
MC-74	.28	2.1	2.2	0	.00x	.00x	.00x	.00x	0	0	0	0	.00x
MC-80	.36	2.8	1.4	0	.00x	.00x	.00x	.00x	0	0	0	0	.00x
MC-96	.13	1.4	.77	0	.00x	.00x	0	0	0	0	0	0	.000x
MC-119	.40	1.7	1.3	0	.00x	.00x	.00x	.00x	0	0	0	0	.00x
MC-119a	.30	1.6	.92	0	.00x	.00x	.00x	.00x	0	0	0	0	.00x
L-56c	.46	2.3	1.5	.000x	.00x	.00x	.00x	.00x	0	0	0	0	.00x
L-66a	.29	2.2	.96	0	.00x	.00x	.00x	.00x	0	0	0	0	.00x
L-70	.23	1.4	.78	0	.00x	.00x	.000x	.00x	0	0	0	0	.00x
L-75c	.30	2.2	2.2	0	.00x	.00x	.00x	.00x	0	0	0	0	.00x
L-79b	.30	3.0	1.9	0	.0x	.00x	.00x	.00x	0	0	0	0	.00x
MC-57a	.26	3.8	1.5	0	.00x	.00x	n.d.	n.d.	0	0	0	0	.00x
MC-42	.34	2.0	.72	0	.00x	.00x	n.d.	n.d.	0	0	0	0	.00x
MC-62	.19	2.2	.94	0	.00x	.00x	n.d.	n.d.	0	0	0	0	.00x
MC-73	.18	2.2	1.1	0	.0x	.0x	n.d.	n.d.	0	0	0	0	.0x
MC-95	.36	2.2	.66	0	.00x	.00x	n.d.	n.d.	0	0	0	0	.00x
MC-100a	.054	1.0	.92	n.d.	n.d.	n.d.	n.d.	n.d.	n.d.	n.d.	n.d.	n.d.	n.d.
MC-101b	.038	.22	.72	0	.00x	.00x	n.d.	n.d.	0	0	0	0	0
L-57	.56	1.4	.92	0	.00x	.00x	.00x	.00x	0	0	0	0	.00x
L-106	2.6	5.3	1.6	0	.00x	.00x	.000x	.00x	0	0	0	0	.00x
L-113a	.48	1.3	.86	.000x	.00x	.00x	.00x	.00x	0	0	0	0	.00x
L-129a	2.4	5.6	1.5	0	.0x	.00x	.000x	.00x	0	0	0	0	.00x
MC-161b	.28	.78	.88	0	.00x	.00x	.000x	.00x	0	0	0	0	.00x
MC-180a	.27	.11	.66	.000x	.00x	.00x	0	n.d.	0	0	0	0	.0x
MC-181	.28	.90	.56	0	.00x	.00x	.00x	n.d.	0	0	0	0	.00x
MC-182a	.70	1.6	1.1	.000x	.00x	.00x	.00x	n.d.	0	0	0	0	.00x
MC-183	.42	.42	.96	.000x	.0x	.00x	.000x	.00x	0	0	0	.0x	.0x
MC-185	.26	.26	1.1	.000x	.00x	.00x	.000x	.00x	0	0	0	0	.00x
MC-188b	.42	.11	.82	.000x	.00x	.00x	.00x	n.d.	0	0	0	0	.00x
MC-189b	.80	2.0	.78	.000x	.00x	.00x	.00x	n.d.	0	0	0	0	.00x
MC-202	.13	.90	1.3	0	.00x	.00x	.000x	n.d.	0	0	0	0	.00x
MC-210	2.8	6.6	1.8	0	.00x	.00x	.000x	n.d.	.000x	0	0	0	.00x
MC-218	1.4	2.8	1.6	0	.00x	.0x	.00x	.00x	0	0	0	0	.0x
MC-75	.32	2.6	1.0	0	.00x	.00x	n.d.	n.d.	0	0	0	0	.00x
MC-88	.39	1.5	.20	0	.00x	.00x	.00x	n.d.	0	.00x	0	.00x	.0x
MC-98	.37	1.5	.28	0	.00x	.00x	.00x	n.d.	0	.00x	0	.00x	.0x
MC-99	0.42	1.5	0.08	0	0.00x	0.00x	0.00x	n.d.	0	0.00x	0	0.00x	0.0x
MC-103	.19	1.4	.18	0	.00x	.00x	.00x	n.d.	0	.00x	0	.00x	.00x
MC-106	.35	1.3	.34	0	.0x	.x	.0x	n.d.	0	.0x	.00x	.0x	.0x
L-55	.22	.8	.54	0	.0x	.00x	.00x	n.d.	0	.00x	0	.00x	.0x
L-80	.20	1.5	.24	0	.0x	.00x	.00x	n.d.	0	.00x	0	.0x	.00x
L-135b	2.3	6.0	n.d.	0	n.d.	n.d.	0	0	.0001	0	n.d.	0	.0008
L-136a	1.7	5.1	n.d.	.0003	n.d.	n.d.	0	0	.0001	0	n.d.	0	.0008
L-136b	1.7	5.6	n.d.	0	n.d.	n.d.	0	0	.0001	0	n.d.	0	.0008
Range	0.038-2.8	0.11-6.6	0.08-2.2	0-.000x	0.00x-.0x	0.00x-.0x	0-.0x	0-.00x	0-.000x	0-.00x	0-.0x	0-.0x	0-.0x
Average	.6	2.2	1.8										
Number of samples	45	45	42	44	41	41	37	21	44	44	41	44	44

[1] Tin probably introduced during separation with methylene iodide.
[2] Analyst for elements V, Nb, and Fe,R. S. Harner.

Looked for but not found: B, La, Th, Ta, U, Co, Rh, Pd, Ir, Pt, Ag, Au, Zn, Cd, Hg, Ga, In, Ge, As, Sb, Bi. n.d.=not determined.

analyses, in percent, of rutile

Mo	W	Mn	Ni	Cu	Sn	Pb	Analyst	Description
0	0.00x	0.00x	0	0.0x	0	0	J. D. Fletcher	Float. S½ sec. 17.
0	.00x	.000x	0	.0x	0	0	do	Float. Light colored. S½ sec. 17.
.00x	0	.000x	0	.00x	0	0	do.[2]	From feldspar vein. NW¼ sec. 17.
0	0	.000x	0	.00x	0	0	do.[2]	Float. NE¼ sec. 18.
0	0	.000x	0	.00x	0	0	do.[2]	Float. Center of sec. 17.
0	0	.000x	0	.00x	.00x	0	do.[2]	Float. E½ sec. 18.
0	0	.000x	0	.00x	.00x	0	do.[2]	Do.
.000x	.0x	.00x	0	.0x	.00x	0	do.[2]	Float. NW¼ sec. 17.
0	0	.000x	0	.00x	.00x	0	do.[2]	Float. SW¼ sec. 17.
0	.00x	.000x	0	.00x	0	0	do.[2]	Float. SE¼ sec. 17.
0	.00x	.00x	0	.00x	.00x	0	do.[2]	Do.
0	0	.00x	0	.00x	0	0	do.[2]	Float. NE¼ sec. 20.
0	.00x	.000x	0	.0x	.00x	0	do	Float. Geniculated twins. NE¼ sec. 18.
0	.00x	.000x	0	.0x	.00x	0	do	Float. Geniculated twins. SE¼ sec. 13.
0	.00x	.00x	0	.0x	.00x	0	do	Float. Geniculated twins. NE¼ sec. 18.
.00x	.00x	.0x	0	.0x	0	.00x	do	Float. NW¼ sec. 17.
0	.00x	.000x	0	.00x	0	0	do	From feldspar-carbonate vein NE¼ sec. 18.
n.d.	n.d.	n.d.	n.d.	n.d.	n.d.	n.d.	do	Float. Light colored. S½ sec. 17.
0	0	.000x	0	.0x	0	0	do	Do.
0	0	.00x	0	.0x	.00x[1]	0	do	Float. NW¼ sec. 17.
0	0	.0x	0	.0x	.0x[1]	0	do	Float. Cyclic twin NE¼ sec. 29.
0	0	.000x	0	.0x	0	0	do	Float. Cyclic twin S½ sec. 20.
0	0	.0x	0	.0x	.0x	0	do	Float. Cyclic twin NW¼ sec. 19.
0	0	.00x	0	.0x	0	.00x	do	From feldspar vein. Light colored. SW¼ sec. 17.
0	0	.00x	0	.0x	0	0	do	From feldspar-carbonate vein. Light-colored geniculated twins. SW¼ sec. 18.
0	0	.000x	0	.0x	0	0	do	Float. Light-colored geniculated twins. NW¼ sec. 19.
0	0	.000x	0	.0x	0	0	do	Float. NW¼ sec. 19.
0	0	.000x	0	.0x	0	.00x	do	From feldspar vein. SE¼ sec. 20.
0	0	.00x	0	.0x	0	.00x	do	From feldspar-carbonate vein. SE¼ sec. 20.
0	.x	.000x	0	.0x	0	0	do	Float. SE¼ sec. 20.
0	.x	.000x	0	.0x	0	0	do	Do.
0	0	.0x	0	.0x	0	0	do	From feldspar-carbonate veins. Geniculated twins. NE¼ sec. 24.
0	0	.0x	0	.0x	0	0	do	Float. Cyclic twin. NW¼ sec. 19.
0	0	.00x	0	.0x	.00x[1]	.00x	do	From feldspar vein. SE¼ sec. 17
0	.00x	.000x	0	.0x	.00x	0	do	Float. NW¼ sec. 17.
0	0	.00x	0	.00x	.00x[1]	.00x	Harry Bastron	From feldspar-carbonate vein. W½ sec. 17.
0	0	.00x	0	.00x	.00x[1]	0	do	From feldspar-carbonate vein. SW¼ sec. 17.
0	0	0.0x	0	0.00x	0.00x[1]	0	do	Do.
0	0	.00x	0	.00x	0	0	do	From feldspar vein. Center of sec. 17.
0	0	.00x	0	.00x	.00x[1]	.00x	do	From feldspar vein. SE¼ sec. 17. Apparently contaminated with apatite.
.00x	0	.00x	0	.00x	0	0	do	From feldspar-carbonate vein SW¼ sec. 8.
0	0	.00x		.00x	0	0	do	From feldspar vein. SW¼ sec. 17.
0	0	.03	.080	.016	.02	0	H. J. Rose	Float. Cyclic twin. NW¼ sec. 19.
0	0	.02	.052	.016	.02	0	do	Do.
0	0	.02	.065	.016	.01	0	do	Do.
0-.00x	0-.x	0.000x-.0x	0-.08	0.00x-.0x	0-.0x	0-.00x		
44	44	44	44	44	44	44		

TABLE 69.—*Spectrographic analyses, in percent, of brooklite*

Sample No.	V	Nb	Fe	Mg	Ca	Sr	Ba	Sc	Y	Yb	Zr	Cr	W	Mn	Cu	Sn	Pb	Description
L-56a(1)	0.11	2.8	1.1	0.0x	0.0x	0.000x	n.d.	0	0	0	0	0.00x	0.00x	0.00x	0.0x	0	0	Float. NW ¼ sec. 17.
L-56a(2)	.13	3.0	1.0	.0x	.00x	.000x	n.d.	0	0	0	0	.00x	.00x	.00x	.0x	0	0	Part of above crystal.
L-64b	.092	3.0	.84	.00x	.0x	.00x	n.d.	0	0	0	0	.00x	.00x	.00x	.0x	0	0	Float. S ½ sec. 17.
L-65b(1)	.078	3.2	1.6	.0x	.0x	.00x	n.d.	0	0	0	0	.00x	.00x	.00x	.0x	0	0	Do.
L-65b(2)	.078	2.8	1.3	.0x	.0x	.00x	n.d.	0	0	0	0	.00x	.00x	.00x	.0x	0	0	Do.
L-65b(3)	.074	2.8	1.4	.0x	.0x	.00x	n.d.	0	0	0	0	.00x	.00x	.00x	.0x	0	0	Do.
L-75a	.28	1.1	1.04	.00x	.0x	.00x	n.d.	0	.0x	.00x	0	.00x	.00x	.000x	.0x	0	0	Float. SE ¼ sec. 17.
MC-101a	.036	2.4	1.0	.00x	.00x	0	n.d.	0	0	0	0	0	0	.000x	.0x	0	0	Float. S ½ sec. 17.
L-96a	.20	.88	.96	.00x	.00x	0	.00x	0	0	0	0	.000x	0	.000x	.0x	0	0	Float. SW ¼ sec. 19.
MC-159	.33	2.6	1.1	.00x	.00x	.00x	.00x	0	0	0	0	.00x	0	.00x	.0x	0	0	From quartz-feldspar vein. NW ¼ sec. 17.
MC-160a	.15	2.6	.92	.00x	.00x	.00x	.00x	0	0	0	0	.00x	0	.00x	.0x	0	0	Do.
MC-161a	.12	.50	.43	.00x	.00x	0	n.d.	0	0	0	0	.00x	0	.000x	.0x	0	0	From feldspar vein. Light colored. SW ¼ sec. 17.
MC-180b	.14	.75	.66	.00x	.00x	0	n.d.	0	0	0	0	.00x	0	.000x	.0x	0	0	From fedlspar-carbonate vein. Light colored. SW ¼ sec. 18.
MC-188c	.11	1.2	.66	.00x	.00x	.00x	n.d.	0	0	0	0	.00x	0	.000x	.0x	0	0	Float. SE ¼ sec. 20.
MC-195	.45	1.8	.74	.00x	.00x	.000x	n.d.	.000x	0	0	0	.00x	.x	.00x	.0x	0	.00x	From quartz-brookite-rutile vein. W ½ sec. 21.
MC-215	.23	1.4	.48	.00x	.00x	0	n.d.	0	0	0	0	.0x	0	.000x	.0x	0	0	From feldspar vein. SW ¼ sec. 21.
MC-90	.10	1.9	.20	.00x	.00x	.00x	n.d.	0	.00x	0	.00x	0	0	.00x	.00x	0	.00x	From feldspar-carbonate vein. Center sec. 17.
MC-150a	.46	1.7	.2	.0x	.0x	.00x	0	0	0	0	0	.0x	.x	.00x	.0x	.00x	0	From quartz-feldspar vein. NE ¼ sec. 17.
Range	0.036-.45	.5-3.2	.2-1.6															
Average	0.18	2.0	.87															

Looked for but not found: Be, B, La, Th, P, Ta, Mo, U, Co, Ni, Rh, Pd, Ir, Pt, Ag, Au, Zn, Cd, Hg, Ga, In, Tl, Ge, As, Sb, Bi.
n.d.=not determined.
Analysts: Sample MC-90 by Harry Bastron; all other samples by J. D. Fletcher.

TABLE 70.—*Spectrographic analyses, in percent, of paramorphs of rutile after brookite*

Sample No.	V	Nb	Fe	Be	Mg	Ca	Sr	Ba	Sc	Y	Zr	Cr	W	Mn	Cu	Sn	Analyst	Description
L-56b	0.24	2.2	0.49	0	0.00x	0.00x	0.000x	n.d.	0	0	0	0.00x	0.00x	0.00x	0.0x	0	J. D. Fletcher	Float. NW¼ sec. 17.
L-66b	.22	1.4	.96	0	.00x	.00x	.00x	n.d.	0	0	0	.00x	.00x	.000x	.0x	0	do	Float. SW¼ sec. 17.
L-75b	.62	.68	1.06	0	.00x	.00x	.00x	n.d.	0	0	0	.00x	0	.000x	.0x	0	do	Float. Light-colored. SE¼ sec. 17.
M.C.57b	.11	.72	.96	0	.00x	.00x	.00x	0.00x	0	0	0	.00x	0	.000x	.00x	0	do [1]	Float. Light-colored. NE¼ sec. 18.
L-79a	.26	2.3	.92	0	.00x	.00x	.00x	.00x	0	0	0	.00x	.00x	.000x	.00x	0	do [1]	Float. NE¼ sec. 20.
M.C.71	.16	1.3	.64	0	.00x	.00x	n.d.	n.d.	0	0	0	.00x	.00x	.000x	.0x	0	do	Float. NW¼ sec. 17.
M.C.100	.036	.88	.66	0	.00x	.00x	n.d.	n.d.	0	0	0	.00x	0	.000x	.0x	0	do	Float. S½ sec. 17.
M.C.118	.11	1.3	.80	0	.00x	.00x	n.d.	n.d.	0	0	0	.00x	.00x	.000x	.0x	.00x	do	Float. E½ sec. 18.
M.C.118a	.15	1.3	.88	0	.00x	.00x	n.d.	n.d.	0	0	0	.00x	.00x	.000x	.0x	.00x	do	Do.
L-96b	.20	1.8	1.1	0	.00x	.00x	.000x	.00x	0	0	0	.000x	0	.000x	.0x	0	do	Float. SW¼ sec. 19.
L-102	.17	.62	.82	0	.00x	.00x	.00x	.00x	0	0	0	.000x	0	.000x	.0x	0	do	Float. Light-colored. NW¼ sec. 29.
L-105	.92	1.2	.64	0	.00x	.00x	.000x	.00x	0	0	0	.00x	0	.00x	.0x	0	do	Float. NE¼ sec. 29.
L-113b	.20	1.4	1.0	0	.00x	.00x	.000x	.00x	0	0	0	.00x	0	.00x	.0x	0	do	Float. Mottled light- and dark-colored. S½ sec 20
L-129b	.25	1.0	.96	0	.00x	.00x	.000x	.00x	0	0	0	.000x	0	.000x	.0x	0	do	Float. NW¼ sec. 19.
M.C.182b	.18	.37	.82	0	.00x	.0x	.000x	n.d.	0	0	0	.00x	0	.000x	.0x	0	do	Float. Light-colored. NW¼ sec. 19.
M.C.188a	2.4	4.6	1.1	0	.00x	.00x	.000x	n.d.	0	0	0	.00x	0	.0x	.0x	0	do	Float. SE¼ sec. 20.
M.C.189a	.44	1.5	.90	.000x	.00x	.00x	.00x	n.d.	0	0	0	.00x	0	.00x	.0x	0	do	Do.
M.C.200	.39	1.1	.64	.000x	.00x	.00x	.00x	n.d.	.000x	0	0	.0x	0	.00x	.0x	0	do	From feldspar-carbonate vein. NE¼ sec 24
M.C.160b	.80	1.2	.94	0	.00x	.00x	.00x	.00x	0	0	0	.00x	.0x	.000x	.0x	0	do	From quartz-feldspar vein. NW¼ sec. 17.
M.C.101	.054	.72	.70	0	.00x	.00x	n.d.	n.d.	0	0	0	0	0	.000x	.0x	0	do	Float. Light-colored. S½ sec. 17.
M.C.97	.15	1.4	.22	0	.00x	.00x	.00x	n.d.	0	.00x	.00x	.00x	0	.00x	.00x	0	Harry Bastron	Float. SW¼ sec. 17.
L-129e	.1	.62	.1	.0001	.005	n.d.	0	.01	0	0	0	.002	0	.001	.006	0	H. J. Rose	Float. Light-colored. NW¼ sec. 19.
L-136c	.1	.84	.1	.0001	.005	n.d.	0	.01	0	0	0	.002	0	.0009	.005	0	do	Do.
Range	0.036-2.4	.37-4.6	.1-1.1															
Average	.36	1.3	.76															

[1] Analyst for elements V, Nb, Fe—R. S. Harner.

Looked for but not found: B, La, Yb, Th, P, Ta, Mo, U, Co, Ni, Rh, Pd, Ir, Pt, Ag, Au, Zn, Cd, Ga, In, Ge, Pb, As, Sb, Bi.
n.d.=not determined.

nepheline syenite—0.7 percent niobium. Perovskite from garnet melteigite contains 0.3 percent niobium; from late-formed carbonatite—4 to 9 percent niobium.

Some interesting speculations can be made on the relative ages of Magnet Cove rocks as a function of niobium concentration in minerals. On the basis of of niobium concentration in perovskite (table 64), the relative age of perovskite bearing rocks would be from oldest to youngest:

Jacupirangite→syenite→ijolite→carbonatite.

On the basis of niobium concentration in sphene, table 65, the relative age of sphene-bearing but perovskite-free rocks would be from oldest to youngest:

{Sphene pyroxenite→sphene-nepheline syenite.
Trachyte

It seems possible that the variations in trace element concentrations in minerals common to more than one rock type may provide a useful guide in the interpretation of relative ages of closely associated rocks. Concentration in minerals would be more informative than concentration in rocks because trace element concentration is controlled not only by concentration in the magma but by the availability of favorable host minerals.

RADIOACTIVITY

Several small radioactivity anomalies of low intensity occur in the Magnet Cove area. The strongest anomaly occurs in an irregular vein, 2 to 8 inches wide, of earthy, fine-grained, pale greenish-yellow monazite, that contains 0.098 percent equivalent uranium and 0.059 percent uranium; thorium was not detected by spectrographic analysis. Other anomalies were detected in 1954 by an Atomic Energy Commission airborne radiometric reconnaissance. Field check of these anomalies by E. P. Beroni and Roger Malan showed that the highest radioactivity is in feldspar-rich rutile-bearing veins; lesser amounts were found in phosphate residuum over carbonate bodies such as the "tufa hills" in secs. 19 and 20 and at Perovskite Hill.

Thorium probably is the chief radioactive component of the veins and phosphate residuum; uranium is essentially absent. One sample contained 0.14 percent eU; none of the others contained more than 0.03 percent eU and none of the samples contained more than 0.001 percent uranium. The thorium-bearing mineral has not been identified as yet. Uranium analyses of vein material are given in tables 40, 41, and 42.

Low-level uranium and thorium determinations were made on most of the chemically analyzed rocks at Magnet Cove (table 47). For the complex as a whole, thorium (9 ppm average) is about 3 times as abundant as uranium (3 ppm average). The uranium content ranges from 2 to 7 ppm; it is highest in the late tinguaitic dike rocks and lowest in the feldspathoidal syenites (2 ppm). Thorium ranges from 2.8 to 33.9 ppm; it is highest in jacupirangite and lowest in the ijolite group (5 ppm average). Although the analytical differences are not great, uranium appears to be highest in the late-formed rock whereas thorium, with the exception of veins and weathered carbonatite, is highest in early formed rocks.

Radioactivity in the nepheline syenite body at Potash Sulfur Springs, about 6 miles west of Magnet Cove, is due chiefly to uranium and its daughter products; thorium has not been detected. Small amounts of uranian pyrochlore (about 3 percent equivalent uranium) were found in one sample, as tiny, honey-yellow octahedrons; it is isotropic, index > 2.00, specific gravity > 3.95. A black mineral in the same gravity fraction gives an X-ray pattern of rutile. The rutile probably also contains Nb.

AGE RELATIONS OF THE ROCKS

The age relations of the rocks at Magnet Cove can not be clearly established from the geologic mapping. Rock outcrops are scarce and deeply weathered. Only a few well-exposed contacts between the various rocks can be seen. However, the available field evidence together with our interpretation of a great amount of chemical work on the rock and minerals suggests the following sequence from oldest to youngest: (1) phonolite and trachyte; (2) jacupirangite; (3) alkalic syenites; (4) ijolite; (5) carbonatite, minor dike rocks and veins.

Field evidence

5. Minor dike rocks, and carbonatite, and veins. The pegmatite, tinguaite, melagabbro and related dike rocks cut all the major rock types. Carbonatite intrudes ijolite and contains large inclusions of ijolite.
4. Ijolite. No good exposure of the contact of the large mass of ijolite in the center of the igneous complex with adjacent rocks was found. However, in the northeast part of sec. 29 on the valley floor of Stone Quarry Creek, the garnet-pseudoleucite syenite is cut by a fine-grained ijolite dike (L–89), about 4 inches wide which strikes N. 50° W. and dips 85° SW. About 450 feet downstream from L–89 the garnet-pseudoleucite syenite is cut by a fine-grained ijolite porphyry dike (MC–145). This vertical dike (up to 16 inches wide) strikes N. 85° W. In the northeast part of sec. 18, a vertical, fine-grained ijolite dike (MC–85) about 4 feet wide strikes N. 55° W. in cutting the garnet-nepheline syenite. In the western part of sec. 17, another vertical, fine-grained ijolite dike (MC–91) about 10 inches wide strikes N. 80° E.

and cuts the garnet-nepheline syenite. Thus at least part of the ijolite is younger than the garnet-pseudoleucite syenite and garnet-nepheline syenite.

Field evidence to suggest that ijolite is older than garnet-pseudoleucite syenite can be found in the face of the Diamond Jo quarry, where rocks that have an ijolitic composition but different physical appearance than the main mass of ijolite occur as large inclusions in garnet-pseudoleucite syenite. Inasmuch as these inclusions do not look like the typical ijolite and were observed only in the quarry more than one-half mile from the main ijolite mass, they are of little help in determining the age relation of the principal bodies of ijolite and garnet-pseudoleucite syenite.

In the northwestern part of sec. 19 a piece of float, MC–179, was found showing a contact between altered phonolite and fine-grained ijolite. A chilled border in the ijolite at the contact indicates that the fine-grained ijolite is younger than the altered phonolite.

In the north-central part of sec. 29, a fine-grained ijolite dike, L–103, cuts the undivided trachyte. The dike is about 3 feet wide and strikes N. 25° W. and dips 75° NE.

3. Alkalic syenites. The alkalic syenites (sphene-nepheline syenite, garnet-pseudoleucite syenite and garnet-nepheline syenite) form the outer ring dike of the Magnet Cove complex and probably were all emplaced about the same time. The writers' prejudice is that sphene-nepheline syenite is slightly older than the other syenites.

In the western part of sec. 18, about 200 feet upstream from sample locality MC-114, the garnet-pseudoleucite syenite has a fine-grained chilled border in contact with the altered phonolite, and is thus interpreted to be younger than the altered phonolite. Swarms of sphene-nepheline syenite dikes ranging from 1 inch to 3 feet in width cut jacupirangite along Cove Creek in sec. 17 and thus are younger than jacupirangite.

2. Jacupirangite. Jacupirangite is older than sphene-nepheline syenite and ijolite as pointed out in no. 3 above. Its age relation to the phonolite-trachyte rocks of the intermediate ring is unknown because these rocks do not have mutual contacts.

1. Phonolite and trachyte is older than garnet-pseudoleucite syenite (no. 3 above) and ijolite (no. 4 above).

Geochemical evidence

The above age sequence of the Magnet Cove rocks is about the same sequence that would be shown if the rocks were placed in order of decreasing silica and increasing dominance of the undersaturated minerals. This general plan of gradual desilication of the rock suite from oldest to youngest has been noted by Backlund (see discussion p. 87). The distribution of niobium in the rocks also shows this same age sequence if we assume that niobium tends to concentrate in residual magmas (see discussion p. 83). If the rocks are arranged in order of increasing niobium content in perovskite separated from these rocks, the sequence is:

Jacupirangite→syenite→ijolite→carbonatite

On the basis of niobium content of sphene from sphene-bearing but perovskite-free rocks, the sequence is:

Phonolite-trachyte→syenite

Although neither the field evidence or geochemical evidence is conclusive, they mutually support each other.

ORIGIN

The origin of the igneous rocks at Magnet Cove is a part of the general problem of the origin of strongly alkaline undersaturated rocks. The origin of similar rocks in other parts of the world has been ascribed to various processes which include: (1) modification (desilication) of granitic magma by assimilation of limestone (Daly, 1910, 1918; Shand, 1945); (2) metasomatism of wall rocks, particularly migmatites, by carbonate magma (von Eckermann, 1948); (3) modification of granitic magmas by a "streaming of gases" rich in alkali (Smyth, 1913, 1927); (4) derivation from deep-seated fusion of a limy shale—evaporite sequence (Jensen, 1908); (5) differentiation of peridotite magma (Holmes, 1932, Holmes and Harwood, 1932, Strauss and Truter, 1951); (6) fractional crystallization of primary olivine basalt magma (Kennedy, 1933; Barth, 1936).

The writers believe that the Magnet Cove complex of alkalic igneous rocks was derived by differentiation and fractional crystallization of a residual melanocratic phonolite magma rich in alkali, lime, and volatiles. The high concentration of volatiles is believed to be of great importance in the development of the many varieties of unusual rock types—jacupirangite, ijolite, carbonatite, etc. This residual magma is believed to have been derived by fractional crystallization from a regional undersaturated olivine basalt magma.

Processes involving assimilation, metasomatism, or fusion may occur but they are not a necessary condition for generation of the Magnet Cove magma.

Facts that apply to alkalic undersaturated rocks in general are summarized by Turner and Verhoogen (1951):

1. "Magmas of nepheline syenite composition, though not uncommon, typically develop in volumes very much

smaller than is the case with basaltic and granitic magmas."

2. "Nepheline syenite magmas belong to the low temperature end of the evolutionary series, for in their high content of alkalies, low combined CaO, MgO and FeO, and high FeO/MgO ratio, nepheline syenites resemble both granites and the low-temperature residues of fractional crystallization recorded in laboratory investigations of silicate melts."

3. "The high content of volatile elements (P, F, Cl) and of Zr, Ti, Nb, Ta, and rare earth metals in many nepheline syenites suggests analogy with pegmatites."

From these observations comes the obvious conclusion:

Nepheline syenite magmas are residual magmas—or as stated by Turner and Verhoogen * * * "end fractions of the processes of fusion or differentiation by which magmas are generated."

The question follows: residual magmas of what parent (?) Holmes (1932) has suggested that alkali rocks are derived from parental peridotite magma by crystallization differentiation—abstraction of olivine, enstatite, and diopside. The geochemical similarities of kimberlite and ijolite are pointed out by Holmes as indicating a common peridotite parent. Strauss and Truter (1951) tentatively adopted Holmes' hypothesis for the origin of the alkali complex at Spitzkop in the Eastern Transvaal. They further point out from their review of the literature that this hypothesis finds ample support in the association of alkali rock with ultrabasic types at the Premier mine, Transvaal; Magnet Heights, Transvaal; Eastern Uganda; Southern Rhodesia; and Nyasaland.

Moor (1957) believes that alkalic basalt dikes from the northern margin of the Siberian platform are closely related to ouachitites and alnoites, and that there is a possible genetic connection between the alkalic and ultrabasic complexes and the flood basalts. Alkalic and ultrabasic rocks were formed from those portions of magma which because of depth of the chamber, richness in volatile constituents, assimilation, etc., have undergone a great deal of differentiation; whereas the common flood basalts came from shallower parts of the magmatic chamber from a magma relatively poor in volatile constituents.

The case for an olivine basalt parental magma receives support from several workers who have demonstrated in the field that undersaturated feldspathoidal rocks are characteristic of olivine basalt associations. Barth (1936) has shown that differentiation of an undersaturated olivine basalt magma will produce an undersaturated residual liquid; further he has shown that an approximately saturated parent magma can produce either a phonolitic or rhyolitic residue depending upon the extent of fractionation of early-formed olivine and pyroxene. Thus only a very slight change in the original composition of olivine basalt magma can produce widely divergent end fractions. Kennedy (1933) believes that undersaturation in parental basalt persists into the end fraction. The initially low silica content is used up in the formation of olivine and pyroxene, so that while alkalies and alumina are increasing, silica barely manages to hold its own and even may decrease slightly in the end fraction from its original concentration in the olivine basalt magma.

Turner and Verhoogen (1951, p. 340) have concluded that

> the normal course of evolution of undersaturated olivine-basalt magma commonly leads to development of a small proportion of alkaline magma which would crystallize under plutonic conditions as nepheline syenite. This can occur in an oceanic environment where, so far as we know, neither granite, limestone, nor any rock other than basalt is available for reaction with the evolving magma. The most likely mechanism is one of fractional crystallization accompanied, and perhaps modified, in the final stages by high concentration of volatiles.

How does the alkalic complex at Magnet Cove fit into this picture? Can any association with olivine basalt rock be demonstrated? The answer is an emphatic "yes." The Magnet Cove complex is not an isolated geologic curiosity but only a small part of a regional belt of strongly alkaline undersaturated rocks. This belt of igneous rocks of similar chemical composition and of similar age extends in an arc from West Texas to Central Mississippi and, as previously noted by Miser (1934), fall within or near the boundaries of the old Ouachita geosyncline (pl. 2). This Paleozoic structure provided zones of structural weakness for the intrusive and extrusive rocks.

Undersaturated rocks, many of them strongly alkalic, have been found during deep drilling in the search for oil and gas in the northern Gulf Coastal Plain (Moody, 1949). These rock types include peridotite, olivine basalt, nepheline syenite, phonolite, tinguaite, monchiquite, fourchite, and much alkalic and basaltic pyroclastics. Moody reports that

> virtually every well in western Mississippi and in eastern Louisiana which has been drilled through the Upper Cretaceous section has pierced beds which are in part, at least, composed of fragmental igneous rocks produced as lapilli or ash in the throats of volcanoes which dotted the late Mesozoic landscape.

Lonsdale (1927) described the igneous rocks of the Balcones fault region, Texas, which consist of peridotite, limburgite, olivine basalt, nepheline basalt, nepheline-melilite basalt and phonolite. The age of the alkaline rocks is Cretaceous(?) and early Tertiary

Closer to Magnet Cove pulaskite and fourchite occur to the northeast and peridotite to the southwest.

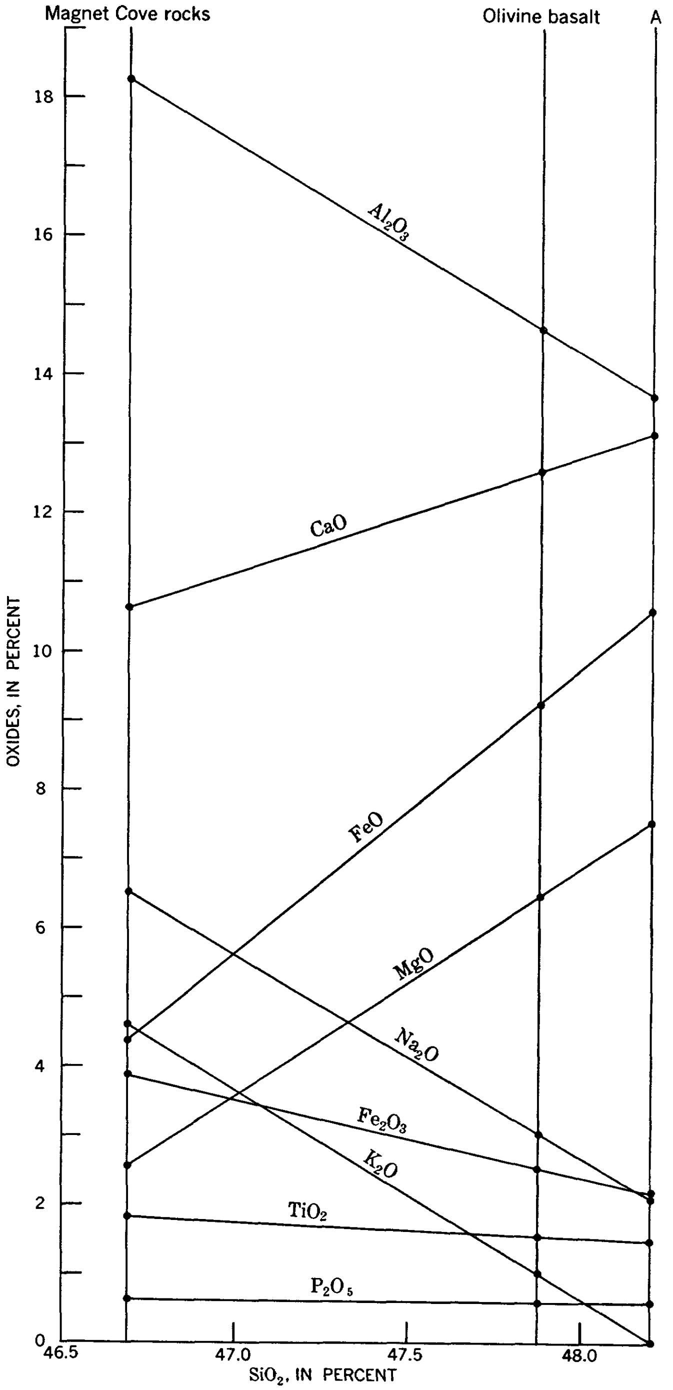

FIGURE 10.—Variation diagram showing composition of material (*A*) subtracted from an olivine basalt to produce magma of the weighted-average composition of the Magnet Cove complex.

We conclude that the regional magma generated in the Ouachita geosyncline was an undersaturated olivine basalt, and further, that fractionation of this magma produced peridotite and other ultrabasic rock on the one hand, and a highly alkaline undersaturated phonolitic end fraction on the other. Lonsdale (1927) concluded that the parent magma in the Balcones fault region was olivine basalt. Moody (1949) concluded that two different magmas appeared in the northern Gulf Coastal plain. The earlier was pre-Cretaceous basalt and the later was alkaline and basaltic and both reached to the surface in certain areas and gave rise to volcanic activity.

With this regional picture in mind we can now discuss the Magnet Cove igneous complex as a residual magma derived from a parental regional undersaturated olivine basalt.

The weighted average composition of the Magnet Cove igneous complex, table 46, is best described as that of a melanocratic phonolite. The graph (fig. 10) shows that a residual magma of this composition can be obtained by subtraction of 70 parts of an olivine melagabbro from 100 parts of parental olivine basalt. The parental olivine basalt used in these calculations is the average of four chemical analyses of olivine basalt given by Lonsdale (1927) for the Balcones fault region—a part of our regional belt of undersaturated rocks. Unfortunately these analyses did not include CO_2, F, Cl, and minor element concentrations. As may be seen from the graph (fig. 10) the composition of the subtracted olivine melagabbro (or material *A*) is very similar to the parent olivine basalt. MgO and CaO are slightly higher; Al_2O_3, Na_2O. and K_2O, are slightly lower. Thus the subtracted magma seems to have a very reasonable and predictable composition; no unique or unusual crystal separation need be made. Nepheline in the norm indicates that the parental olivine basalt is undersaturated and that differentiation of this undersaturated parental magma would produce a highly alkalic, silica-deficient end fraction even without crystal fractionation. Note that the end fraction would also be rich in titanium and phosphate.

As previously pointed out, no data were available for volatile and minor element content of the parent olivine

	Parent olivine basalt	*A (material subtracted)*	*End fraction Magnet Cove composition*
	Chemical analyses		
SiO_2	47.88	48.88	46.69
Al_2O_3	14.66	13.77	18.28
Fe_2O_3	2.51	2.16	3.88
FeO	9.24	10.63	4.37
MgO	6.96	7.58	2.55
CaO	12.60	13.22	10.64
Na_2O	3.03	2.09	6.54
K_2O	.99	.00	4.60
TiO_2	1.54	1.49	1.83
P_2O_5	.59	.58	.62
	Norm		
or	6.12	--------	25.58
ab	15.20	17.82	--------
an	22.80	28.08	6.95
lc	--------	--------	1.31
ne	5.40	--------	29.82
di	31.56	28.04	17.30
wo	--------	--------	8.58
hy	--------	14.57	--------
ol	9.98	4.11	--------
mt	3.71	3.25	5.57
il	2.89	2.89	3.50
ap	1.34	1.34	1.34

basalt. However, a perovskite concentrate from the peridotite near Murfreesboro, Ark., contained 2.5 percent columbium. Perovskite and sphene also occur in the basalts and nepheline basalts in the Balcones fault region of Texas (Lonsdale, 1927). Rankama and Sahama (1950) note that "remarkably much columbium is present in ultrabasic rocks." Carbon dioxide, water, and sulfur are common emanations from volcanic vents. Thus, it would appear the parental olivine basalt does contain all the essential typical elements of Magnet Cove rocks—Ti, P, Nb, CO_2, and S in particular.

We have now derived our Magnet Cove magma. The next question: how were the widely divergent rock types formed from this magma and in what sequence of intrusion?

Williams (1891) concluded the complex is the result of a series of intrusions: (1) ijolite, (2) lamprophyres, and (3) syenites. Washington (1900) concluded the complex is the result of a laccolith differentiated in place. Landes (1931) concluded the complex is the result of two injections: (1) ijolite as a stock differentiated in place with the carbonatite as an included block, and (2) syenites differentiated in place from a later intrusion of an acidic differentiate of the main magma. Washington and Landes followed Williams' terminology in calling the phonolite-trachyte ring metamorphosed sediments.

The present writers conclude that the Magnet Cove alkalic igneous complex is a series of ring dikes, intruded at different times with varying degrees of differentiation during individual intrusion phases. This conclusion is based upon the arcuate dike shape of the exposed rocks, the sequence of intrusion, the chemical relationships of the rocks, and striking similarity to ring complexes in other parts of the world (for details, see section on "Structure").

The sequence of intrusion is interpreted as: (1) trachyte-phonolite and breccia of the intermediate ring, (2) jacupirangite, (3) feldspathoidal syenites of the outer ring, (4) ijolite forming the central core, (5) carbonatite, pegmatite, tinguaite and similar late dike rocks. Backlund (1933), in his excellent review of the common denominators of alkalic rocks throughout the world, noted that

> the common principle governing the distribution of rocks seems to point to a gradual desilication of the rock suite from the wall inward and from the top downward: the core thus represents the most perfect grade of desilication.

Further he concludes that the

> general plan of rock sequence is that of increasing dominance of the undersaturated mineral association within the whole rock series, the most pronounced undersaturation being shown by the latest ones. This undersaturation proceeds step by step towards complete desilication of the rock suite, the carbonatic (Alno, Fen, Spitzkop), apatitic (Umptek, Palaboro, Spitzkop, Alno) and iron-ore (Spitzkop, Alno, Fen) rocks being in each case the last more or less independent member of a complete alkali suite.

The Magnet Cove rock suite closely fits this pattern of increasing undersaturation from the walls inward: syenites, phonolite, and trachyte in the outer and intermediate rings; ijolite core and almost complete desilication in very late carbonatite, apatite, and magnetite concentrations in the central part of the core.

Backlund (1933) points out that although there exists a certain sequence of more or less independent magmatic intrusions, no real time distinction can be made between the different rock groups. This problem is further complicated at Magnet Cove because of deep weathering and poor rock exposures. However, the phonolite-trachyte breccia of the intermediate ring gives sufficient evidence to indicate its early role in the sequence of intrusion at Magnet Cove. Further, we believe that the ring fracture occupied by these fine-grained rocks reached the surface and gave rise to explosive volcanic activity at Magnet Cove. This early period of explosive volcanic activity is suggested by the abundance of volatiles particularly CO_2, the presence of miarolitic cavities and amygdaloidal textures, and the absence of recognizable syenites or ijolite inclusions in the breccia. The chemical composition of the phonolites and breccia most closely approach the average composition of the igneous rocks (fig. 9)—a condition to be expected if this material was the first liquid to be suddenly released from the magma reservoir and extruded. That part of the magma trapped in the conduit at the end of explosive periods would react with CO_2, H_2O, and S to produce the altered phonolite. Most of the breccia pieces have the same composition as the groundmass which suggests repeated movement in the early ring fracture zone and repeated injections of heavily gas charged magma into this fracture zone.

About 29 percent of the igneous rocks were emplaced during this period, assuming that the area exposed is proportional to volume. Line *B* on fig. 11 shows the composition of the remaining magma after removal of the phonolite-trachyte to form the intermediate ring. Note that the remaining magma has not changed appreciably; SiO_2 and Al_2O_3 have depressed slightly and CaO and Fe_2O_3 have been increased. Further, note that throughout the diagram, the composition changes in the magma are much less severe than the composition changes in rocks formed from the magma.

The second recognizable period of intrusive activity was the emplacement of jacupirangite which comprises about 10 percent of the exposed igneous rocks. It is cut by swarms of narrow nepheline-syenite dikes and is, therefore, interpreted as older than the outer ring of feldspathoidal syenites. However, its appearance at this stage was probably accidental. The field evidence suggests that crystallization in the now slower cooling magma follows the agpaitic series of Ussing (1911)—early crystallization of feldspars and nepheline which because of their lower specific gravity than the residual liquids, are forced to rise. The mafic residue and volatile constituents accumulate downward. Backlund (1933) suggested that "agpaitic differentiation leads to decreasing viscosity of the cooling magma" whereas in the commoner granodioritic differentiation, increasing viscosity of the residual liquid is effected by the loss of volatiles that together with the more acid components have accumulated in the top portion of the the magma chamber.

In some exposures of garnet-pseudoleucite syenites, euhedral pseudoleucite phenocrysts are concentrated in a fine-grained groundmass; these crystals persist even in chilled border phases of the syenite. This suggests that pseudoleucite (nepheline and sodic orthoclase) formed early and were rising and collecting in the magma (agpaitic differentiation). Ijolite and melteigite segregations and inclusions in the same rock, however, were probably crystallizing and sinking and were carried along in the rising current of magma, when it was intruded. It seems probable then, that the lower part of the reservoir may have been tapped by fractures so that a part of the downward accumulating gas-charged mafic residue, with its pyroxene and magnetite crystals, streamed up the fractures and was emplaced as satellite bodies of jacupirangite. Line *C* of figure 11 shows the composition of the residual magma after removal of jacupirangite. As expected, SiO_2, Al_2O, and alkalies have increased slightly, and CaO, FeO, and MgO have decreased.

Emplacement of the feldspathoidal syenites of the outer ring, chiefly sphene-nepheline syenite and garnet-pseudoleucite syenite, formed the third period of intrusive activity. The "agpaitic" series is particularly well-demonstrated during this period. The lighter magma at the top of the magma reservoir with its early crystallized feldspar and nepheline is tapped by fractures and this magma rises to form the outer, almost complete ring dike of feldspathoidal syenites. About 30 percent of the rocks were emplaced during this period. The residual magma is now largely mafic but with ever increasing amounts of volatile constituents, P, Ti, Fe^{+3}, Zr, and rare earths. SiO_2 and Al_2O_3 have been depressed; CaO increases sharply; and the alkalies show minor change. The stage is now set for intrusion of most of the remaining magma as ijolite. The magma has been so desilicated that although the alkali content is high, not enough silica is present to form feldspar—only nepheline can crystallize. The pyroxene is now almost pure diopside; excess Fe,

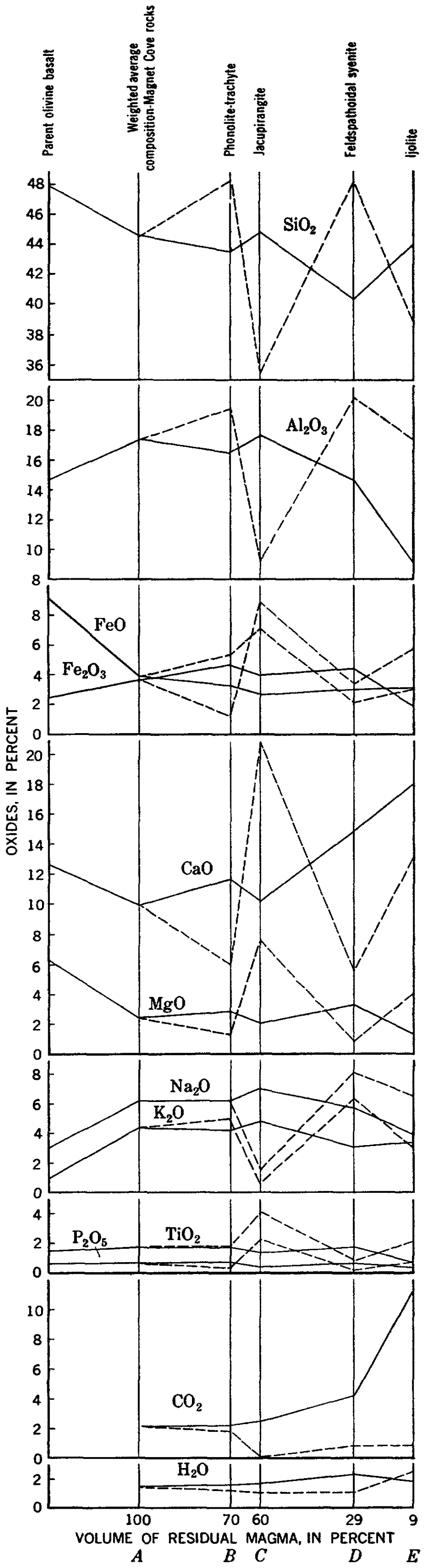

FIGURE 11.—Variation diagram showing composition of rocks (dashed line) and residual magmas (solid line) for main periods of intrusion.

Ti, and Ca must be used in the very low silica garnet; excess K_2O forms the silica-poor biotite. Effects of the high volatile content appear in the primary alteration of nepheline to cancrinite and sodalite. Much of the rock unit is pegmatitic and monomineralic segregations are common. Large masses of garnet, nepheline, magnetite, biotite (phlogopite) attest to the importance of the gas phase in prolonging fluidity of the magma and permitting development of giant crystals. Niobium content of perovskite crystals increases; beryllium concentrates in the zeolites. Thus the chemical analyses of the ijolites show a wide compositional range and a consequent wide scattering of points on any variation diagram.

The composition of the remaining end fraction (9 parts of the original 100, line *E*, fig. 11) appears unique. SiO_2 has increased again but CaO and CO_2 show very marked concentration and Al_2O_3 a very marked decrease. In this highly volatile end fraction, the elements are relatively free to move about and form even stronger monomineralic segregations than in the ijolite; this is the period of late magmatic, pneumatolytic and hydrothermal activity. Most of the alkali combines with remaining silica and alumina to form pegmatites rich in K-feldspar, nepheline, and giant aegirine crystals. Zirconium concentration is now great enough to form eudialyte. The CaO combines with P_2O_5 to make abundant apatite, with Ti to make perovskite, and with silica to make monticellite. Finally the CaO still in excess combines with CO_2 to form crystalline carbonatite bodies. Niobium concentrates in the perovskite up to 9 percent; rare earths and fluorine are concentrated in the apatite, zirconium forms kimzeyite and iron forms euhedral magnetite crystals. Probably much of the titanium and niobium is transported in the gas phase (fluorides?) or as hydrothermal solutions to form niobium-bearing rutile and brookite veins. Perhaps even small amounts of silica are transported in the gas phases to form the very rare occurrences of quartz-bearing veins.

We have now completed our picture of the petrogenesis at Magnet Cove. The derivation of rock types has no doubt been oversimplified. We stress the effect of gaseous phases without benefit of much supporting laboratory experimental data but certainly complex mineral assemblages may be expected to form in the presence of magmatic gases—particularly in an alkali-rich, undersaturated magma.

ECONOMIC GEOLOGY

Potentially commercial deposits of titanium, niobium, molybdenum, phosphate, agricultural lime, and iron ore occur in the igneous complex at Magnet Cove. The titanium deposits have been known for many years and through 1944, more than 5,000 tons of rutile (TiO_2) concentrate had been produced from the rutile pits in sec. 18. No production has come from the brookite (TiO_2) deposits in recrystallized novaculite along the northeast border of the complex. Detailed descriptions, and economic considerations of the titanium deposits have been given by Fryklund and Holbrook (1950).

Because of the association of niobium with titanium minerals, the U.S. Geological Survey in 1952 studied, sampled, and in part mapped the rutile, brookite, and perovskite ($CaTiO_3$) areas at Magnet Cove (Fryklund and others, 1954). Table 71 reproduced from the report of Fryklund and others summarizes the work of the U.S. Bureau of Mines, Fryklund and Holbrook (1950), and the U.S. Geological Survey.

Nieberlein and others (1954) reported that

> the ore reserves in the three columbium-bearing titania deposits investigated by the Bureau of Mines (Magnet Cove Titanium Corp. property, Christy brookite deposit, Hardy-Walsh property) are estimated to be at least 8 million tons containing 4 to 8 percent TiO_2 and 0.05 to 0.15 percent Cb. The columbium content of these reserves is estimated to be 12 million pounds.

TABLE 71.—*Summary of analytical data from the principal titanium deposits at Magnet Cove, Ark.*

[Data from Fryklund, Harner, and Kaiser, 1954, p. 49, table 10]

Locality	Mineral of possible value	Estimated average recoverable grade of known material (percent)			Estimated average grade of titanium concentrates (percent)		
		TiO_2	Nb	V_2O_5	TiO_2	Nb	V_2O_5
Magnet Cove Titanium Corp. property.	Rutile	3	0.04	0.09	92	1.2	0.5
Christy property	Brookite	5.9	.07	.35	92	2	.5
Kilpatrick (Hardy-Walsh) property.	do	5.9	.06	.21	92	2	.5(?)
Mo-Ti Corp. property	Rutile	------	------	------	------	------	------
Do	Perovskite	------	.03	------	------	------	------
Kimzey calcite quarry area	do	.20	.01	------	------	6	------

Milling tests on rutile and brookite ore from Magnet Cove have produced high-grade concentrates of about 92 percent TiO_2 but have given low overall titania recovery, due largely to the occurrence of TiO_2 in several unrecovered minerals such as ilmenite, leucoxene and silicates. Fryklund, Harner, and Kaiser (1954) point out, however, that "it is probable that processes for making metallic titanium from the rutile and brookite concentrates will allow separation and recovery of niobium and vanadium."

There has been no production of molybdenite ore from Magnet Cove.

Holbrook (1948) has described a small molybdenite vein deposit (Mo-Ti prospect) in fractured jacupirangite in the NW1/4 sec. 17. He states that the veins range in thickness from less than ½ inch to 5 feet, trend northwest, dip sharply northeast, and have a total strike length of about 400 feet. The most significant concentration of molybdenite is in an area about 225 feet long and from 10 to 35 feet wide. No tonnage estimates were made because of the unreliability of samples obtained by diamond drilling.

Other small molybdenite-bearing veins occur in the floor of the carbonatite quarry (NW1/4 sec. 19), in a stock pond in the western part of sec. 20, and with rutile veins about 500 feet south of the Mo-Ti prospect in sec. 17.

Weathering of the carbonatite produces a phosphate-rich residual material with a rare-earth content near 1 percent. Standard phosphate analyses (table 24) show that the grade is adequate for commercial phosphate. These residual phosphate areas are shown on the geologic map, but more drilling and sampling must be done to determine the size of the deposit. The parent carbonatite also offers possibilities for production of agricultural lime. Niobium-rich (4 to 8 percent) perovskite crystals in the carbonatite might be recovered as a byproduct.

Magnetite has been mined sporadically from the Kimzey magnetite pit in the NW1/4 sec. 20. It occurs as irregular rounded masses up to 1 foot across, some alined like beads on a string, in an idocrase-diopside matrix. No data are available on past production or estimated reserves. Geologic mapping and the aerial magnetometer survey, however, do not suggest an extensive magnetite ore body.

Low-grade uranium-bearing material and zeolite (thomsonite) with as much as 0.02 percent beryllium have been found but not in potentially commericial amounts.

REFERENCES CITED

Backlund, H. G., 1933, On the mode of intrusion of deep-seated alkaline bodies: Univ. Upsala Geol. Inst. Bull., v. 24, p. 1–24.

Barth, T. F. W., 1936, The crystallization process of basalt: Am. Jour. Sci., v. 31, no. 185, p. 321–351.

Borodin, L. S., 1957, Geochemistry of the Khibina alkalic rock massif: Akad. Nauk, SSSR Inst. Mineralogii, Geokhimii i Kristallografii Redkikh Elementov, Issue 1.

Bramlette, M. N., 1936, Geology of the Arkansas bauxite region: Arkansas Geol. Survey Inf. Circ. 8, 66 p.

Clarke, F. W., 1924, The data of geochemistry: 5th ed., U.S. Geol. Survey Bull. 770, 841 p.

Daly, R. A., 1910, Origin of the alkaline rocks: Geol. Soc. America Bull., v. 21, p. 87–118.

——— 1918, Genesis of the alkaline rocks: Jour. Geology, v. 26, p. 97–134.

——— 1933, Igneous rocks and the depths of the earth: New York, McGraw-Hill Book Co., 508 p.

Fersman, A. E., 1937, Mineralogy and geochemistry of the Khibine and Lovozero tundras: Guidebook, Northern Excursion, Kola Peninsula, Internat. Geol. Cong., 17th, Russia, 1937, p. 91–103.

Foshag, W. F., 1923, Catapleiite from Magnet Cove, Ark.: Am. Mineralogist, v. 8, p. 70–72.

Fryklund, V. C., Jr., 1949, The titanium ore deposits of Magnet Cove, Hot Spring County, Ark.: Minnesota Univ. Ph. D. thesis.

Fryklund, V. C., Jr., Harner, R. S., and Kaiser, E. P., 1954, Niobium (columbium) and titanium at Magnet Cove and Potash Sulphur Springs, Ark.: U.S. Geol. Survey Bull. 1015–B, p. 23–56.

Fryklund, V. C., Jr., and Holbrook, D. F., 1950, Titanium ore deposits of Hot Spring County, Ark.: Arkansas Resources and Devel. Comm., Div. Geology, Bull. 16, 173 p.

Glass, J. J., 1937, Sodalite from Magnet Cove, Ark. (abs.): Washington Acad. Sci. Jour., v. 27, no. 8, p. 358.

Gossner, B., and Reindl, E., 1934, Über die chemische Zusammensetzung titanhaltiger Silikate, insbesondere von Astrophyllit: Centralbl. für Mineralogie, Geologie, und Paleontologie, Abt. A, p. 161–167.

Harrington, B. J., 1907, Isomorphism as illustrated by certain varieties of magnetite: Mineralog. Mag., v. 14, p. 375–376.

Hess, H. H., 1941, Pyroxenes of common mafic magmas: Am. Mineralogist, v. 26, pt. 1, p. 515–535; pt. 2, p. 573–594.

——— 1949, Chemical composition and optical properties of common clinopyroxenes, pt. 1: Am. Mineralogist, v. 34, no. 9 and 10, p. 621–666.

Hey, M. H., 1932, Studies on the zeolites, pt. 2, Thomsonite; pt. 3, Natrolite and metanatrolite: Mineralog. Mag., v. 23, p. 62–63, 243–289.

Holbrook, D. F., 1947, A brookite deposit in Hot Spring County, Ark.: Arkansas Resources and Devel. Comm., Div. Geology, Bull. 11, 21 p.

——— 1948, Molybdenum in Magnet Cove, Ark.: Arkansas Resources and Devel. Comm., Div. Geology, Bull. 12, 16 p.

Holmes, Arthur, 1932, The origin of igneous rocks: Geol. Mag., v. 63, p. 543–558.

Holmes, Arthur, and Harwood, H. F., 1932, Petrology of the volcanic fields east and south-east of Ruwenzori, Uganda: Geol. Soc. London Quart. Jour., v. 88, p. 370–439.

Imlay, R. W., 1940, Lower Cretaceous and Jurassic formations of southern Arkansas and their oil and gas possibilities: Arkansas Geol. Survey Inf. Circ. 12, 64 p.

Jensen, H. I., 1908, The distribution, origin, and relationships of alkaline rocks: New South Wales Proc. Linn. Soc., v. 33, p. 585–586.

Johannsen, Albert, 1938, A descriptive petrography of the igneous rocks: v. 4: Chicago, Chicago Univ. Press, 523 p.

Keller, Fred, Jr., and Henderson, J. R., 1949, Total intensity aeromagnetic map of Magnet Cove area, Hot Springs County, Arkansas: U.S. Geol. Survey Geophys. Inv. Prelim. Map.

Kennedy, W. Q., 1933, Trends of differentiation in basaltic magmas: Am. Jour. Sci., v. 25, p. 239–256.

Kinney, D. M., 1949, The Magnet Cove Rutile Company mine, Hot Springs County, Ark.: U.S. Geol. Survey open-file report.

Kouvo, J. A. O., 1952, A variety of monticellite from Crestmore, Calif.: Finlande Comm. Géol. Bull., no. 157, p. 7–11.

Landes, K. K., 1931, A paragenetic classification of the Magnet Cove minerals: Am. Mineralogist, v. 16, p. 313–326.

Lonsdale, J. T., 1927, Igneous rocks of the Balcones fault region of Texas: Texas Univ. Bull. 2744, 178 p.

Macrery, J., 1806, A description of the Hot Springs and volcanic appearance in the country adjoining the river Ouachita in Louisiana: New York Medical Depository, v. 3, p. 47–50 (communicated in a letter to Dr. Miller, according to Williams (1891)).

McConnell, Duncan, 1942, Griphite, a hydrophosphate garnetoid: Am. Mineralogist, v. 27, no. 6, p. 452–461.

McConnell, Duncan, and Gruner, J. W., 1940, The problem of the carbonate-apatites. III. Carbonate-apatite from Magnet Cove, Arkansas: Am. Mineralogist, v. 25, no. 3, p. 157–167.

Melville, W. H., 1892, Mineralogical notes, Natrolite from Magnet Cove, Arkansas: U.S. Geol. Survey Bull. 90, p. 38.

Milton, Charles, and Blade, L. V., 1958, Preliminary note on kimzeyite, a new zirconium garnet: Science, v. 127, no.3310, p.1343.

Miser, H. D., 1912, New areas of diamond-bearing peridotite in Arkansas: U.S. Geol. Survey Bull. 540, p. 534–546.

——— 1934, Relation of Ouachita belt of Paleozoic rocks to oil and gas fields of midcontinent region: Am. Assoc. Petroleum Geologists Bull., v. 18, no. 8, p. 1059–1077.

Miser, H. D., and Glass, J. J., 1941, Fluorescent sodalite and hackmanite from Magnet Cove, Arkansas: Am. Mineralogist, v. 26, p. 437–445.

Miser, H. D., and Stevens, R. E., 1938, Taeniolite from Magnet Cove, Arkansas: Am. Mineralogist, v. 23, p. 104–110.

Moody, C. L., 1949, Mesozoic igneous rocks of northern Gulf Coastal Plain: Am. Assoc. Petroleum Geologists Bull., v. 33, no. 8, p. 1410–1428.

Moor, G., 1957, Alkalic basalt dikes from the northern margin of the Siberian platform (Norilsk region): Acad. of Sciences of the U.S.S.R., Proc. Geol. Sci. Sections (Consultants Bur., Inc.; Eng. trans.), v. 116, no. 1–6, p. 803–805.

Murata, K. J., Rose, H. J., Jr., Carron, M. K., and Glass, J. J., 1957, Systematic variation of rare-earth elements in cerium-earth minerals: Geochim. et Cosmochim. Acta, v. 11, no. 3, p. 141–161.

Murdoch, Joseph, 1951, Perovskite: Am. Mineralogist, v. 36, p. 573–580.

Nieberlein, V. A., Fine, M. M., Calhoun, W. A., and Parsons, E. W., 1954, Progress report on development of columbium in Arkansas for 1953: U.S. Bur. Mines Rept. Inv. 5064, 23 p.

Nockolds, S. R., 1954, Average chemical compositions of some igneous rocks: Geol. Soc. America Bull., v. 65, p. 1007–1032.

Parks, Bryan, and Branner, G. C., 1932, A barite deposit in Hot Spring County, Arkansas: Arkansas Geol. Survey Inf. Circ. 1.

Pecora, W. T., 1956, Carbonatites: A review: Geol. Soc. America Bull., v. 67, no. 11, p. 1537–1556.

Penfield, S. L., 1894, Anatase von Magnet Cove, Arkansas: Zeitschr. für Kristallographie, v. 23, p. 261.

Penfield, S. L., and Forbes, E. H., 1896, Optical characters of the olivine group: Am. Jour. Sci., 4th ser., v. 1, p. 129–135.

Purdue, A. H., and Miser, H. D., 1923, Description of the Hot Springs quadrangle, Arkansas: U.S. Geol. Survey Geol. Atlas, Folio 215.

Rankama, Kalervo, and Sahama, Th. G., 1950, Geochemistry: Chicago, Chicago Univ. Press, 912 p.

Reed, D. F., 1949a, Investigation of Christy titanium deposit, Hot Spring County, Arkansas: U.S. Bur. Mines Rept. Inv. 4592, 10 p.

——— 1949b, Investigation of Magnet Cove rutile deposit, Hot Spring County, Arkansas: U.S. Bur. Mines Rept. Inv. 4593, 9 p.

Ross, C. S., 1938, Volcanic activity at Magnet Cove, Arkansas: Am. Geophys. Union Trans. 19th Ann. Mtg., Pt. 1, Nat. Res. Council, p. 263–264.

——— 1941, Occurrence and origin of the titanium deposits of Nelson and Amherst Counties, Virginia: U.S. Geol. Survey Prof. Paper 198, 59 p.

Ross, C. S., and Hendricks, S. B., 1945, Minerals of the montmorillonite group; their origin and relation to soils and clays: U.S. Geol. Survey Prof. Paper 205–B, p. 23–79.

Ross, C. S., Miser, H. D., and Stephenson, L. W., 1929, Waterlaid volcanic rocks of early Upper Cretaceous age in southwestern Arkansas, southeastern Oklahoma, and northeastern Texas: U.S. Geol. Survey Prof. Paper 154–F, p. 175–202.

Shand, S. J., 1945, The present status of Daly's hypothesis of the alkaline rocks: Am. Jour. Sci., v. 243A, p. 495–507.

Sleight, V. G., 1941, Molybdenite at Magnet Cove, Arkansas: Am. Mineralogist, v. 26, p. 132–133.

Smyth, C. H., 1913, The chemical composition ot the alkaline rocks and its significance as to their origins: Am. Jour. Sci., 4th ser., v. 36, p. 33–46.

——— 1927, The genesis of alkaline rocks: Am. Philos. Soc. Proc., v. 66, p. 535–580.

Spencer, R. V., 1946, Exploration of the Magnet Cove Rutile Co., property, Magnet Cove area, Hot Spring County, Arkansas: U.S. Bur. Mines Rept. Inv. 3900, 23 p.

Strauss, C. A., and Truter, F. C., 1951, The alkali complex at Spitzkop: Geol. Soc. South Africa Trans. and Proc., v. 53, p. 81–130.

Turner, F. J., and Verhoogen, Jean, 1951, Igneous and metamorphic petrology: New York, McGraw-Hill Book Co., 602 p.

Ussing, N. V., 1912, Geology of the country around Julianehaab, Greenland: Meddel. Om Grönland, no. 38, 426 p.

Vacquier, V., Steenland, N. C., Henderson, R. G., and Zietz, Isidore, 1951, Interpretation of aeromagnetic maps: Geol. Soc. America Mem. 47, 151 p.

von Eckermann, H., 1948, The alkaline district of Alno island: Sveriges Geologiska Undersökning, Ser. Ca., no. 36.

Wahlstrom, E. E., 1947, Igneous minerals and rocks: New York, John Wiley and Sons, 367 p.

Washington, H. S., 1900, Igneous complex of Magnet Cove, Arkansas: Geol. Soc. America Bull., v. 11, p. 389–416.

——— 1901, The foyaite-ijolite series of Magnet Cove: Jour. Geology, v. 9, p. 607–622, 645–670.

Williams, Howel, 1941, Calderas and their origin: California Univ. Dept. Geol. Sci. Bull., v. 25, no. 6, p. 239–346.

Williams, J. F., 1891, The igneous rocks of Arkansas: Arkansas Geol. Survey Ann. Rept., 1890, v. 2, 457 p.

INDEX